MycoKeys 65: 1–24 (2020)
doi: 10.3897/mycokeys.65.48409
http://mycokeys.pensoft.net

RESEARCH ARTICLE

A peer-reviewed open-access journal
MycoKeys
Launched to accelerate biodiversity research

Phylogeography of post-Pleistocene population expansion in *Dasyscyphella longistipitata* (Leotiomycetes, Helotiales), an endemic fungal symbiont of *Fagus crenata* in Japan

Jaime Gasca-Pineda[1], Patricia Velez[2], Tsuyoshi Hosoya[3]

1 *UBIPRO, Facultad de Estudios Superiores Iztacala, Universidad Nacional Autónoma de México, 54090, Estado de México, Mexico* **2** *Departamento de Botánica, Instituto de Biología, Universidad Nacional Autónoma de México, Mexico City, 04510, Mexico* **3** *National Museum of Nature and Science, 4-1-1 Amakubo, Tsukuba, Ibaraki 305-0005 Japan*

Corresponding author: Tsuyoshi Hosoya (hosoya@kahaku.go.jp); Patricia Velez (pvelez@ib.unam.mx)

Academic editor: F. D. Grande | Received 12 November 2019 | Accepted 20 January 2020 | Published 10 March 2020

Citation: Gasca-Pineda J, Velez P, Hosoya T (2020) Phylogeography of post-Pleistocene population expansion in *Dasyscyphella longistipitata* (Leotiomycetes, Helotiales), an endemic fungal symbiont of *Fagus crenata* in Japan. MycoKeys 65: 1–24. https://doi.org/10.3897/mycokeys.65.48409

Abstract

During the Last Glacial Maximum (LGM), drastic environmental changes modified the topology of the Japanese Archipelago, impacting species distributions. An example is *Fagus crenata*, which has a present continuous distribution throughout Japan. However, by the end of the LGM it was restricted to southern refugia. Similarly, *Dasyscyphella longistipitata* (Leotiomycetes, Helotiales, Lachnaceae) occurs strictly on cupules of *F. crenata*, sharing currently an identical distribution. As the effects of the LGM remain poorly understood for saprobiotic microfungal species, herein we identified past structuring forces that shaped the current genetic diversity within *D. longistipitata* in relation to its host using a phylogeographic approach. We inferred present and past potential distributions through species distribution modeling, identifying environmental suitability areas in mid-southern Japan from which subsequent colonizations occurred. Our findings suggest that current high genetic diversity and lack of genetic structure within *D. longistipitata* are the result of recent multiple re-colonization events after the LGM.

Keywords

Divergence, gene flow, geographic information systems, haplotype network, host distribution, intraspecific variation, species distribution modeling

Introduction

Dramatic cyclical glacial advances and retreats characterize the Pleistocene (Bradley 1999). During this epoch the Japanese archipelago underwent important climate changes accompanied by the alternation of dry and wet conditions. Furthermore, by the end of the Pleistocene, during the Last Glacial Maximum (LGM), the advent of a strong cold dry period led to a significant sea level lowering that exposed the entire Seto Sea area (Tsukada 1983). Subsequently, during the Pleistocene-Holocene transition, a rapid warming trend led to an increment of sea level, transforming what had been a long appendage of the Asian continent into an entirely separated archipelago (Aikens and Akazawa 1996).

Strong evidence suggests that, during the LGM, Japan was extensively covered by coniferous forests of *Pinus*, *Picea*, *Abies*, and *Tsuga*. Small populations of *Fagus*, however, were limited to the Pacific coasts of Kyushu and Shikoku (Tsukada 1985). Pleistocene climate and geospatial changes modified the distribution of biomes in this region (Gotanda and Yasuda 2008), causing major migrations and extinctions (Kawamura 2007), and rearranging the geographic distribution of vegetation assemblages (Tsukada 1982b, c 1983).

The Japanese endemic canopy tree *Fagus crenata* has been extensively studied in this sense, representing an acknowledged model. Independent lines of evidence suggest that by the end of the LMG, the populations of *F. crenata* were restricted to environmentally stable southern areas (refugia) along the shoreline in southern areas of Japan, and then expanded northwards via two migration routes through the western and eastern shore of Japan (Tsukada 1982a; Tsukada 1982b; Tomaru et al. 1997, 1998; Koike et al. 1998; Fujii et al. 2002; Okaura and Harada 2002). Presently, *F. crenata* is widely distributed from the northern regions in Oshima Peninsula, Hokkaido to southern areas in the Osumi Peninsula, Kyushu, where it occurs sparsely in mountainous regions.

Although the LGM has long been a focal point for research in a wide range of plant and animal taxa, information on the microbial component remains lacking. Fungal phylogeographic analyses are recently increasing (e.g., to identify glacial refugia, recolonization routes, and interglacial population expansions; Marske et al. 2009, Geml et al. 2010, Leavitt et al. 2013), yet the numbers are still limited (Lumbsch et al. 2008). Several methodological reasons may explain this, including limited taxon sampling, impediments in identification (because of the existence of close relatives with similar morphologies), difficulties in obtaining DNA material (in the case of unculturable symbionts, e.g., Hongoh 2011) and genetically heterogeneous nuclei (such as in some Basidiomycota members e.g. Booth 2014). So, in this sense, culturable and clearly delimited fungal species with wide distribution ranges represent advantageous phylogeographic study models.

Dasyscyphella longistipitata Hosoya (Leotiomycetes, Helotiales, Lachnaceae) overcomes the above-mentioned impediments. This culturable ascomycete is highly specific to *F. crenata*, sharing an identical wide geographical distribution throughout Japan (Ono and Hosoya 2001, Hosoya et al. 2010), and so far only known from Japan. Previ-

ous ITS-based phylogeographic analyses revealed that *D. longistipitata* forms a genetic continuum comprising three kindred clusters dominated by a single haplotype (named as H12 in Hosoya et al. 2010), which may suggest a recent population expansion (Bandelt et al. 1995; Ferreri et al. 2011). However, the small population numbers, uneven sampling, and a single genetic marker-based analysis hampered the interpretation of the results, leaving unanswered questions as to whether this species occupied the same refugia as its host during the LGM.

In this study, we reconstructed the historical demography of *D. longistipitata* based on genetic variation data, in addition to information on the geographical distribution and ecological attributes for *D. longistipitata* as well as for its host *F. crenata*. The correspondence between both species in their response to major past climate changes was assessed in order to attain a better understanding of the impacts of glacial cycling on the Japanese biota and neglected fungal taxa.

Materials and methods

Fungal collection and isolation

A total of 270 fungal collections were sampled during 2010–2018 in 14 localities covering the entire geographical distribution of the host species *F. crenata* from Jogakura (Locality 1) in the northeast to Mt. Shibi (Locality 14) in the southwest (Fig. 1, Table 1). Sampling and isolation procedure followed Hosoya et al. (2010). Briefly, around 20 cupules with *D. longistipitata* apothecia were sampled. Each group of cupules was collectively regarded as a single specimen, and registered under a single number in the fungarium of the National Museum of Nature and Science (TNS) as voucher specimens. Single ascospore isolates were obtained from one of the apothecia occurring on each cupule using a Skerman's micromanipulator (Skerman 1968), and numbered with a prefix "DL-".

DNA extraction and sequencing

Culturing, DNA extraction and sequencing methods were conducted following Hosoya et al. (2010). Isolates were genotyped by the ITS1-5.8S-ITS2 region using the primer set ITS1 and ITS4 (White et al. 1990), as well as by the beta-tubulin gene using primer set Bt1a and Bt1b (Glass and Donaldson 1995). For the ITS1-5.8S-ITS2 region, PCR procedures were as reported in Hosoya et al. (2010). Whereas, beta-tubulin gene amplification was performed using the following protocol: initial denaturation for 2 min at 94 °C, 35 cycles of 94 °C for 30 s, 51 °C for 30 s and 72 °C for 30 s, and a final extension at 72 °C for 7 min. Total DNA samples were deposited in the Molecular Biodiversity Research Center in the National Museum of Nature and Science, and are available for research upon request. Only material leading to the successful sequencing of both ITS-5.8S and beta-tubulin regions was retained for the analysis (Suppl. material 4: Table S3).

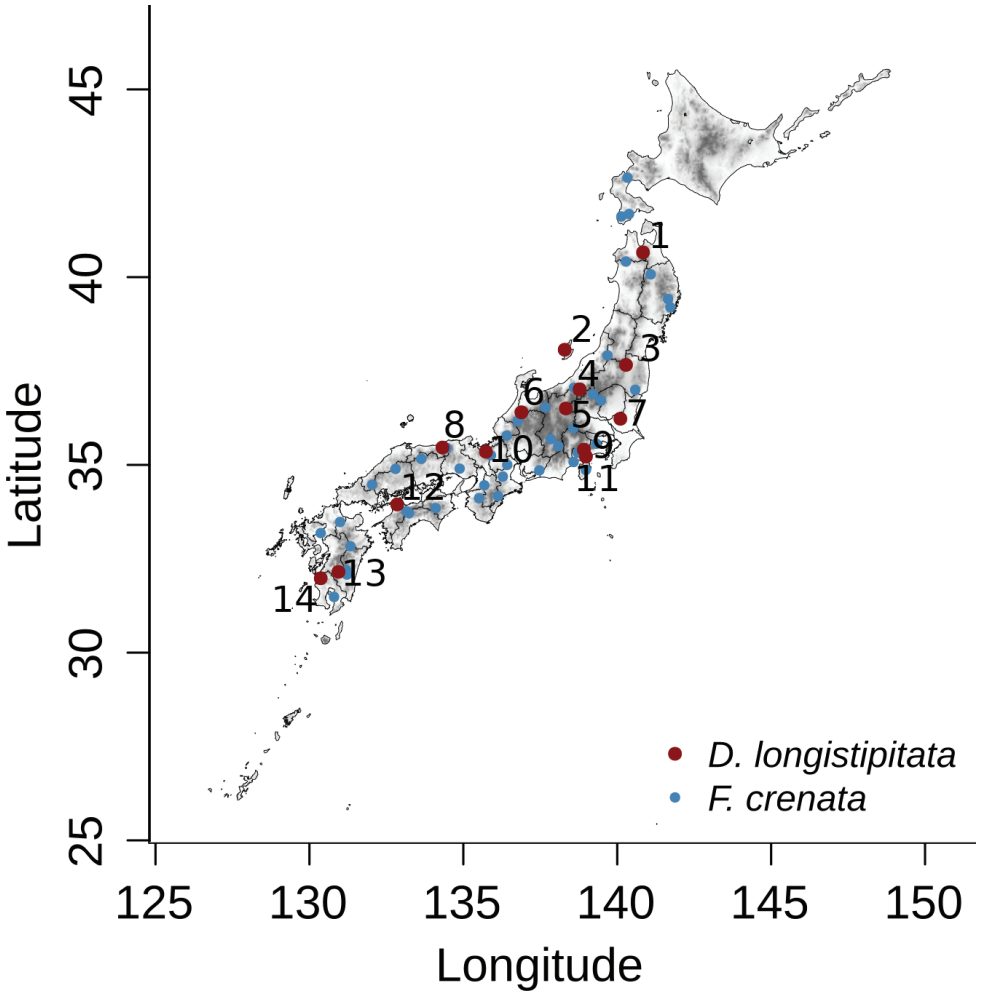

Figure 1. Geographical distribution of the sampling localities for *Dasyscyphella longistipitata* associated with cupules of *Fagus crenata* in Japan. Red dots and numbers correspond to *D. longistipitata*; whereas blue dots represent *F. crenata* study sites from Fujii et al. (2002). For sites nomenclature see Table 1.

Genetic diversity and structure

The following population genetics summary statistics were calculated to estimate the amount of genetic diversity: Number of polymorphic (segregating) sites (S), number of haplotypes (h), haplotype diversity (Hd), and nucleotide diversity (Pi). The Tajima's D neutrality test (Tajima 1989) was computed to infer possible demographic changes (population bottleneck or demographic growth). All statistics were performed using DNAsp v6.12.03 (Rozas et al. 2017). The ITS haplotype numbering followed criteria established by Hosoya et al. (2010), using the prefix "H" and previously reported haplotype numbers to maintain consistency with the previous results. Novel haplotypes

Table 1. Sampling localities, decimal geographic coordinates, and summary statistics for *Dasyscyphella longistipitata* across Japan based on the concatenated ITS and beta-tubulin markers. Significance at $p < 0.05$ in indicated by *. Latitude and Longitude are indicated in decimal following WGS84 datum; number of isolates analyzed (N), segregating sites (S), haplotype number (h), haplotype diversity (Hd), nucleotidic diversity (Pi), Tajima's D neutrality test parameter (D).

Number	Locality	Voucher specimen	Collection year	Latitude / Longitude	N	S	h	Hd	Pi	D
1	Jogakura	TNS-F-32166	2010	40.65806, 140.8378	14	56	14	1	0.0106	-1.6175
2	Sado Isl.	TNS-F-38439	2013	38.06667, 138.2928	21	60	21	1	0.0099	-1.3972*
3	Tsuchiyu	TNS-F-46835	2012	37.66302, 140.2851	24	103	23	0.996	0.0090	-1.5928*
4	Mt. Atema	TNS-F-35002	2010	37.01183, 138.7792	17	49	17	1	0.0086	-1.5025
5	Obora	TNS-F-32140	2010	36.50295, 138.3289	16	55	16	1	0.0105	-1.4934
6	Suganuma	TNS-F-32150	2010	36.401, 136.8891	21	70	21	1	0.0101	-1.7464*
7	Mt. Tsukuba	TNS-F-31635	2010	36.22789, 140.1017	20	51	18	0.984	0.0080	-1.5806*
8	Mt. Ougiyama	TNS-F-46830	2012	35.46278, 134.3214	20	63	20	1	0.0098	-1.6550*
9	Mikunitouge	TNS-F-35001	2010	35.40472, 138.9164	20	59	20	1	0.0102	-1.3855
10	Ashiu	TNS-F-46827	2012	35.35045, 135.7326	12	46	12	1	0.0096	-1.5862*
11	Yamakita	TNS-F-32167	2010	35.22131, 138.9831	20	50	20	1	0.0092	-1.1969
12	Mt. Takanawa	TNS-F-32168	2010	33.94556, 132.85	23	77	23	1	0.0111	-1.7589*
13	Mt. Shiragadake	TNS-F-54834	2018	32.15147, 130.9429	21	74	21	1	0.0097	-2.4506*
14	Mt. Shibi	TNS-F-54822	2018	31.98015, 130.3676	21	59	21	1	0.0093	-1.7216
Overall					270	270	255	0.999	0.0096	-2.4491*

were subsequently numbered. For beta-tubulin, prefix "B" was used to designate the sequences. All the haplotype sequences from representative isolates were registered to GenBank as indicated in Suppl. material 5: Table S4.

In addition, to compare our results with further fungal population-level genetic variation estimates, we analyzed ITS and beta-tubulin sequences from NCBI GenBank (by Douhan et al. 2008; Roe et al. 2011; Mo et al. 2018; Cho et al. 2019) for the widely-distributed Ascomycota species: *Colletotrichum scovillei* Damm, P.F. Cannon and Crous, *Aspergillus fumigatus* Fresen., *Ceratocystis montium* (Rumbold) J. Hunt, and *Claviceps purpurea* (Fr.) Tul. We concatenated ITS and beta-tubulin sequences, and calculated nucleotide diversity (Pi) using DNAsp v6.12.03 (Rozas et al. 2017).

To estimate the genetic structure among the 14 sampling localities of *D. longistipitata*, we calculated the AMOVA-based pairwise PhiST (Excoffier et al. 1992), using

the R-package haplotypes v1.1 (R Core Team 2018; Aktas 2019). Ten thousand permutations were performed to assess the PhiST statistical significance. The proportion of variance explained by the genetic differences among localities was calculated using the R-package poppr v2.8.3 (Kamvar et al. 2014). To evaluate differences in the genetic variation among localities, we computed a Principal Component Analysis (PCA) at the individual level (isolates), and a Principal Correspondence Analysis (PCoA) using the localities as a grouping factor as implemented in the R-package adegenet v2.1.1 (Jombart 2008). To explore the influence of geographic distance on the distribution of genetic variation, we performed isolation by distance analysis (IBD) using a Mantel test of an Edwards' distance-matrix against a geographic-distance matrix using R. Furthermore, a haplotype network based on statistical parsimony (Templeton et al. 1992, Clement et al. 2000) was constructed to explore the genetic relationships among haplotypes, using the R-package haplotypes v1.1 (Aktas 2019) with a cut-off probability threshold of 0.95.

Demographic inference and dispersion routes in *D. longistipitata* and *F. crenata*

We evaluated effective population size changes over time using the Bayesian Gaussian Markov Random Field (GMRF) Skyride Plots (Minin et al. 2008) implemented in BEAST v1.10.4 (Suchard et al. 2018). The best fitting model of sequence evolution was chosen by the Akaike Information Criterion (AIC) using jModelTest2 (Darriba et al. 2012). For this, the ITS and beta-tubulin markers of *D. longistipitata* were concatenated. In addition, we obtained the complete Matk gene sequences reported by Fujii et al. (2002) under the GenBank accession numbers AB046492–AB046523. We used the uncorrelated relaxed molecular clock model to allow rates to vary along branches, using the General Time Reversible (GTR) substitution model with invariable-site proportion and gamma distribution for *D. longistipitata*; and Hasegawa-Kishino-Yano (HKY)+I+G for *F. crenata*. Both analyses run for 500 million generations, and the MCMC convergence was checked using tracer v1.7.1 (Rambaut et al. 2018) discarding the 10% as burning step. Due to the lack of reliable substitution rates (or molecular calibration dates) for fungal ITS and beta-tubulin sequences, we employed the scaled units of effective size and time in the Skyride Plots (Minin et al. 2008). All runs were computed using the CIPRES Science Gateway server (http://www.phylo.org/; Miller et al. 2010).

Species distribution modeling and spatial phylogenetic analyses

We implemented the analysis of species distribution modeling (SDM) to evaluate the geographical areas of conserved environmental suitability using the BioClim environmental layers (BIO1–BIO19; http://worldclim.org/bioclim; Hijmans et al. 2005) for the present, Mid Holocene, LGM and Last interglacial (LIG; Otto-Bliesner et

al. 2008) periods. To avoid possible bias due to highly correlated variables (McCormack et al. 2010; Ortego et al. 2015), we extracted data from the 19 BioClim layers and conducted paired Pearson correlation tests considering a > 0.75 threshold. From each pair of correlated variables, the variable showing more than one significant correlation was discarded. Additionally, we estimated the variance inflation factor using the function "vifcor" of the R- package usdm (Naimi et al. 2014). We obtained 429 geo-referenced records for *D. longistipitata* from the Global Biodiversity Information Facility (http://data.gbif.org; https://doi.org/10.15468/dl.fnvbrv). To reduce bias due to autocorrelation caused by a local overrepresentation of records, we divided the sampling area for each species into cells of 1/10 degrees and selected one point at random from each cell using the R-package raster.

The present and past distribution models were generated using the R package biomod2 v 3.1 (Thuiller et al. 2016) by means of ensemble models (Araújo and New 2007; Qiao et al. 2015). Six standard modeling algorithms were computed: the generalized linear model (GLM; McCullagh and Nelder 1989), generalized boosted model (GBM; Friedman 2001), artificial neural networks (ANNs), random forest (RF; Breiman 2001), multivariate adaptive regression splines (MARS; Friedman 1991), and MAXENT (Phillips et al. 2006). Two independent pseudo-absence sets of 5,000 points were generated at random, and the species records were split into 70% for model training and 30% for model evaluation performance. Using this 70% – 30% criteria, five random replicates were run for all models. A total of 70 independent models (seven algorithms, two background sets and five random replicates) were run to achieve the final ensembles. Model performance was assessed using the area under the receiver operating characteristic curve (AUC; Swets 1988). Final ensembles were built selecting models with AUC > 0.9 and using the committee-averaging criteria.

Areas of conserved environmental suitability across time were delimited as follows: the ensemble layers were transformed to presence/absence considering a threshold of 90% of the distribution of suitability values, and the resulting layers were merged. The area of the resulting layer was classified as highly conserved (overlapping of four layers), medium (at least three overlapping layers), and low (two overlapping layers).

Finally, to estimate the ancestral locations and the spatial dynamics of the two species, we performed a continuous-space phylogeographic analysis using BEAST software. Runs were performed using the molecular clock rates, and substitution models above mentioned. The statistics for spatial traits (i.e., localities) were generated using the Cauchy RRW model. Also, to avoid noise due to duplicate location traits, a jitter window size of 0.01 was used. Posterior to convergence checking, the consensus discrete trait-annotated trees were obtained by means of treeAnnotator using the "Common Ancestor Heights" option and discarding the first 10% trees. Then, this information was used as an input in SPREAD3 v1.0.7 (Bielejec et al. 2011) to geographically visualize the ancestral localities and the possible dispersion routes across the geographic distribution of sampling sites. The KML outputs of the SPREAD3 analysis for *Dasyscyphella longistipitata* and *Fagus crenata* showing colonization trends are available upon request.

Results

Haplotype diversity

We analyzed a total of 270 isolates (12–24 per site). Overall, 85 ITS-based haplotypes were identified. The majority was represented by H12 (40.7%), followed by H28 (14.4 %), and H10 (10.7 %), and the 27.8 % were singletons. Both H12 and H28 were found in all the 14 sites, while H10 was found from 12 sites.

In contrast, the beta-tubulin sequences were remarkably diverse, with 224 recognized haplotype patterns. The most frequently observed haplotypes were B4 (3.7 %), B27 (2.2 %), and B75 (1.9 %), and the majority (74.8 %) was occupied by singletons. The ITS and beta-tubulin concatenated sequences ranged from 980–1022 bp, resulting in 255 haplotypes with 270 segregating sites (Table 1, detail for each marker is reported in Suppl. material 2: Table S1). The overall haplotype diversity was 0.999, and the nucleotide diversity ranged from 0.0080–0.0111 among populations. Moreover, overall Tajima's D parameter was -2.449, with values ranging from -1.3855 to -2.4506 at a population level (Table 1).

Genetic structure

The paired PhiST yielded low values, ranging from 0 to 0.0358 (Suppl. material 3: Table S2), yet, only three of 96 paired values were significantly different from zero (Fig. 2). Moreover, the AMOVA test showed that 99.99% of the variance was explained by differences between individuals within localities. The individual-level PCA (Fig. 3A) displayed a rambling distribution of individuals without a clear grouping by locality. Although most individuals were stacked around the center of the graph, some individuals with divergent haplotypes were scattered in the four quadrants of the graph; however, they did not belong to neighboring localities. In the case of the locality-level PCoA (Fig. 3B), localities did not show spatial grouping (i.e., neighboring localities were not genetically close). In agreement with the PCoA results, the Mantel test did not show significance ($p > 0.5$) in the correlation between genetic and geographic distances.

The haplotype network revealed intricate relationships among *D. longistipitata* haplotypes (Fig. 4), lacking spatial aggregation patterns. Consistently, haplotypes with furthermost geographic distribution were connected by one mutational step. Remarkably, the network displayed multiple star-shaped connections, where central haplotypes did not occur in high frequencies.

Past demographic inferences

The Skyride plots (Fig. 5) displayed changes in the historical effective size of *D. longistipitata* and *F. crenata*. While *D. longistipitata* showed a continuous and steady growth

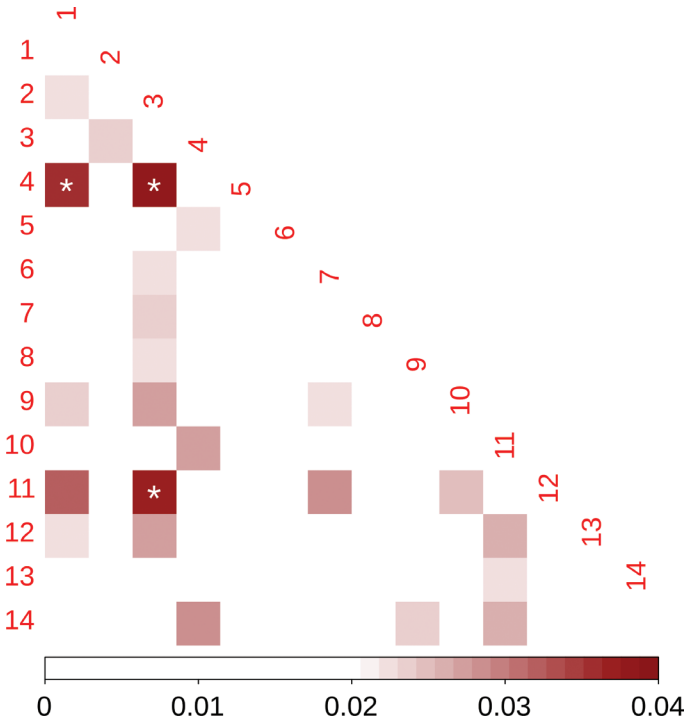

Figure 2. Paired PhiST values for *Dasyscyphella longistipitata* in the 14 studied localities. White asterisks indicate significance at $p \leq 0.05$.

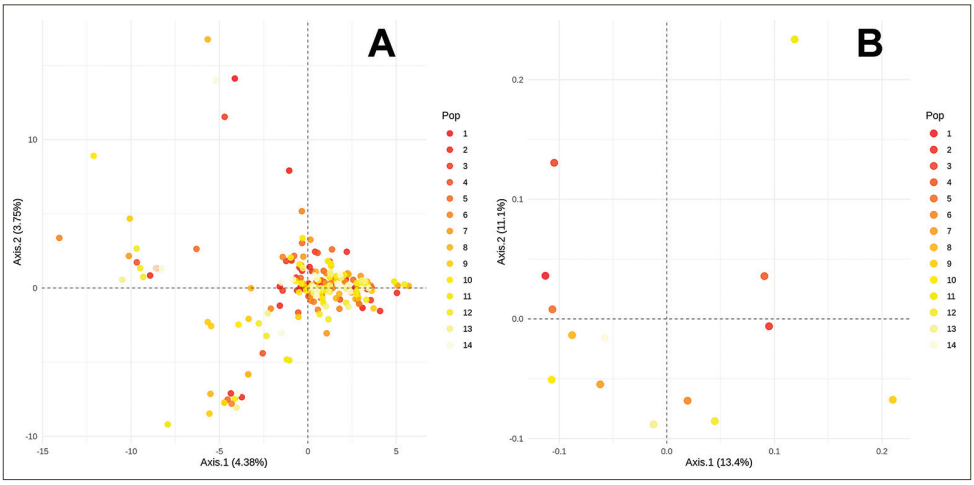

Figure 3. Multivariate analyses of the genetic diversity inferred from ITS and beta-tubulin concatenated sequences of *Dasyscyphella longistipitata.* **A** Principal Component Analysis (PCA) of genetic diversity at the individual level **B** principal Correspondence Analysis (PCoA) of genetic diversity using the localities as grouping factor. Colors represent the locality of origin arranged as a latitudinal gradient where red represents the further north site.

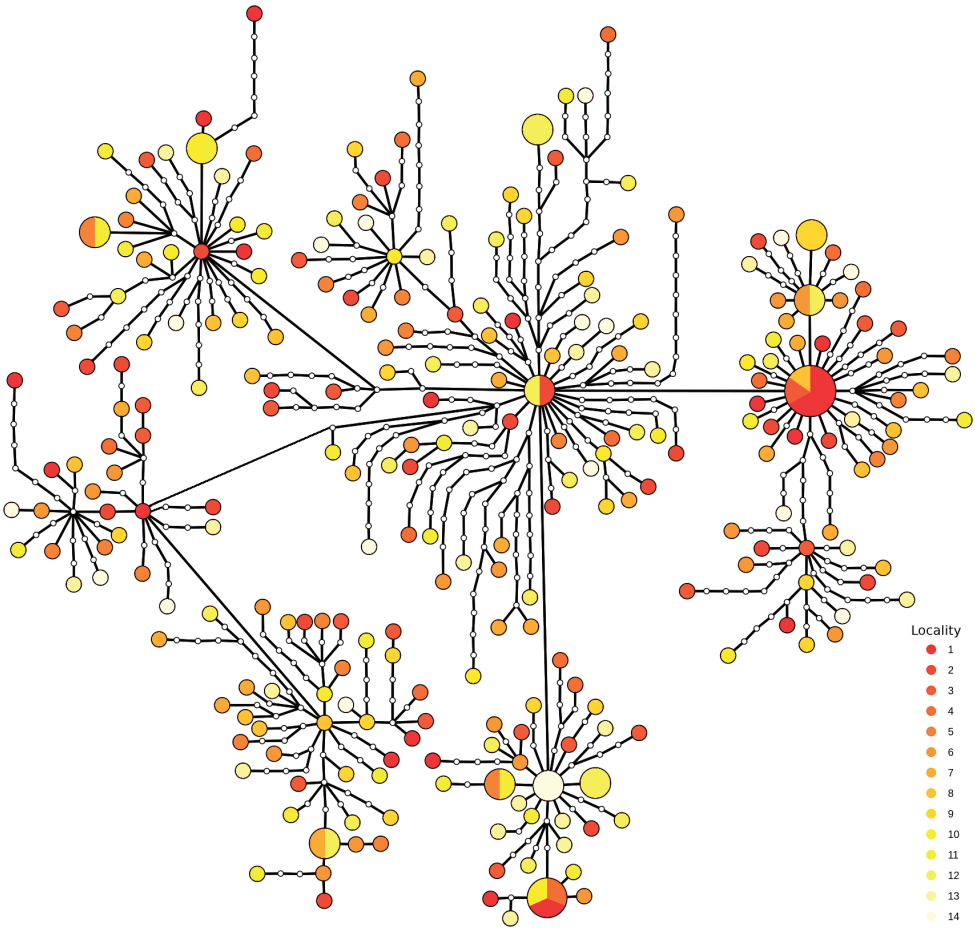

Figure 4. Haplotype network based on the concatenated sequences of ITS and beta-tubulin of *Dasyscyphella longistipitata.* The size of the circles represents the haplotype frequency; white dots represent mutational steps between haplotypes (note that the branches lengths do not correspond to genetic distances). Colors represent the locality of origin arranged as a latitudinal gradient where red represents the further north site.

of the past effective size, the plot of *F. crenata* displayed a three-fashion trend, showing a former stable size followed by a period of constant reduction, and a recent event of population growth. Because the effective size and time scales depend on mutation rates of the different markers, it is important to note that the observed events do not necessarily correspond to the same period in years, nor the actual effective sizes.

Species distribution modeling

The SDM of *D. longistipitata* resembles the current distribution of *F. crenata* (Nakao et al. 2013). In contrast to the broad area of suitable conditions displayed by present-time

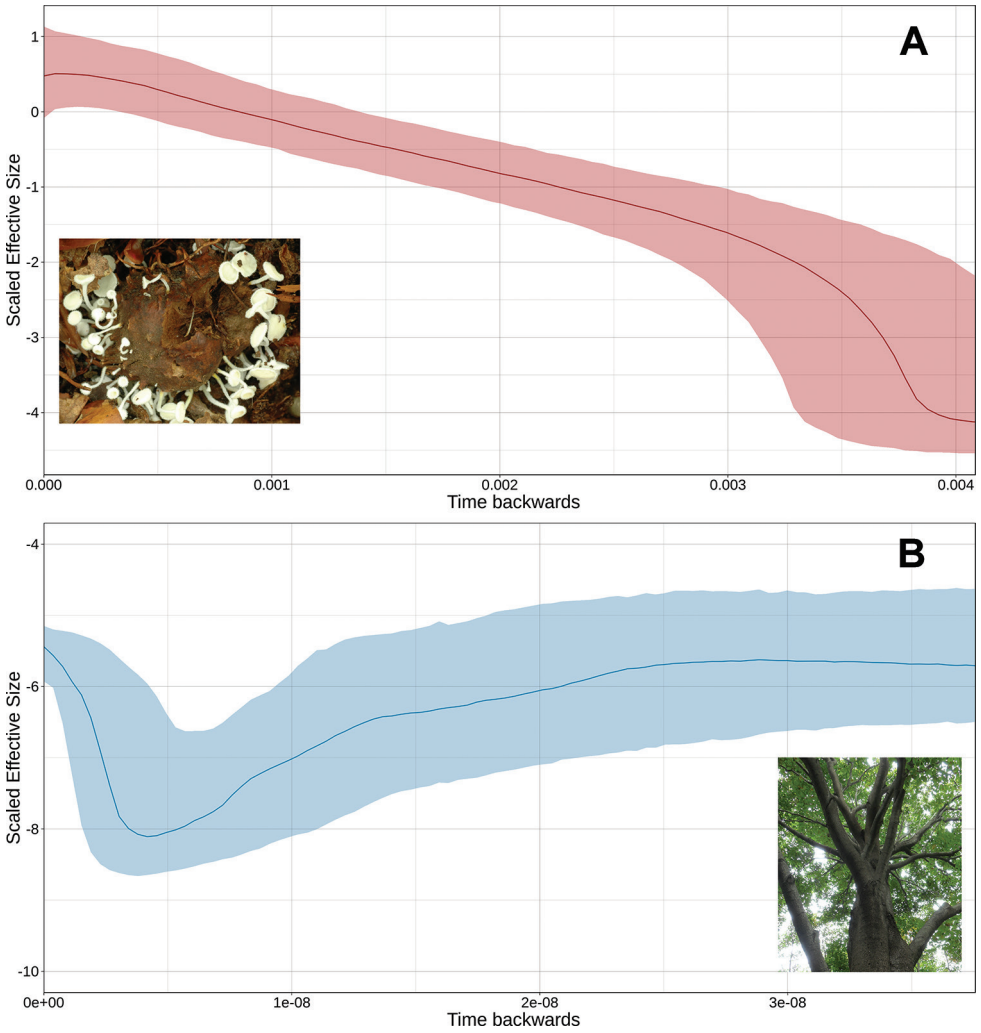

Figure 5. Bayesian Skyride Plot for **A** *Dasyscyphella longistipitata* using the concatenated ITS and beta-tubulin, and **B** *Fagus crenata*, using the reported sequences in Fujii et al. (2002). The y-axis represents the scaled effective population size (log_{10}(Ne*u)), and the x-axis represents time as substitutions per site. Shaded area shows the 95% HPD of the posterior distribution. Solid lines show the median value of effective population size. Dotted shades show the upper and lower 95% highest posterior density. Note that the x-axis in A and B are non-equivalent to each other.

projection (Suppl. material 1: Fig. S1A), the past projections revealed areas with non-overlapping geographic areas of environmental suitability (Suppl. material 1: Fig. S1A, B). Moreover, the overlapping geographic areas across periods (current, mid-holocene, LGM and LIG) yielded to limited areas of conserved environmental suitability (Fig. 6), revealing drastic changes in environmental conditions across Japan from the Interglacial period to the present.

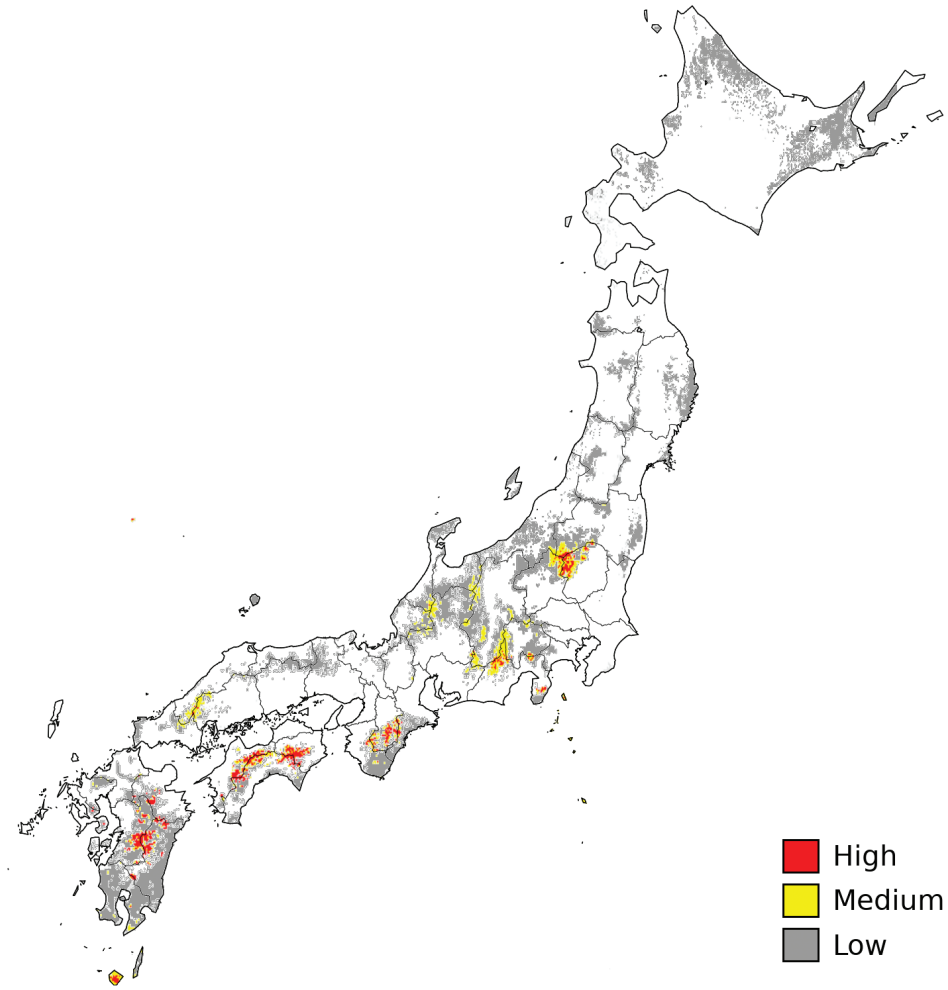

Figure 6. Areas of conserved environmental suitability for *Dasyscyphella longistipitata*, where red is high (overlapping of four layers), yellow medium (at least three overlapping layers), and gray low (two overlapping layers) suitability.

Dispersion trends

Our results on the ancestral localities and dispersion trends, suggested that *D. longistipitata* originated from Mt. Ougiyama (site 8), Obora (site 5), Ashiu (site 10), and Suganuma regions (site 6; Fig. 7, Time 1) in mid-southern Japan. The subsequent events of dispersion took place to the north and south, including the localities of Kyushu (Fig. 7, Time 2). In the specific case of *F. crenata* low genetic diversity (13 haplotypes within 45 sites; Fujii et al. 2002) hampered the colonization tracking at the locality level. However, in good accordance with *D. longistipitata*, the generated dispersion polygons revealed two principal regions for the origin dispersion in central Japan (Fig. 7 Time 1). Follow-

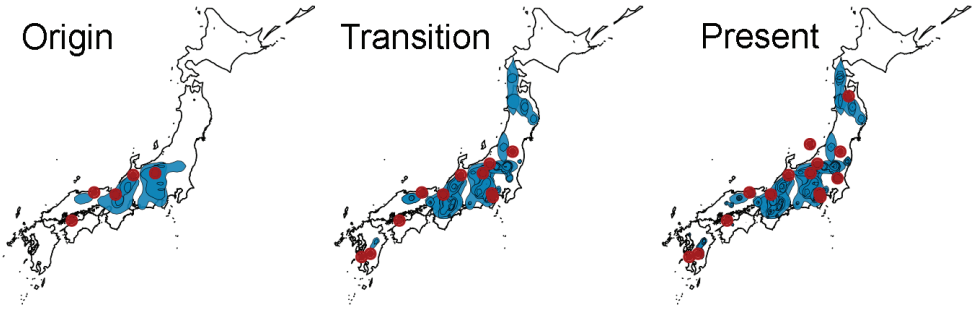

Figure 7. Bayesian continuous-space phylogeographic analyses for *Dasyscyphella longistipitata*, and *Fagus crenata* grouped in three consecutive times. Red dots represent *D. longistipitata* localities, and blue areas are polygons for the nodes of dispersion for *F. crenata*.

ing colonization, events were scattered to the north and expanded to the south (Fig. 7 Times 2 and 3). Overall, the SPREAD3 analyses mapped the originating localities for dispersion of both species *F. crenata* and *D. longistipitata* in mid-southern Japan (Fig. 7).

Discussion

Saprophytic fungi (those obtaining nutrients from dead organic matter) are critical to the dynamics and resilience of ecosystems (Meyer 1994). However, there is tremendous specificity with regard to the types of chemical structure that individual species are capable of degrading (Rodriguez and Redman 1997). To date, the fungal species *D. longistipitata* has been exclusively reported from *F. crenata* cupules, sharing an identical geographical distribution (Hosoya et al. 2010; Ono and Hosoya 2001). Field efforts to obtain material from the co-distributed species *Fagus japonica* as an alternative host (Fang and Lechowicz 2006) have been unsuccessful. In addition to the well-known host specificity in many species of Lachnaceae (e.g., Tochihara and Hosoya 2019), overall this provides further evidence of the strong ecological relationship between *D. longistipitata* and *F. crenata*.

One of the most remarkable results of this study was the unexpected high genetic diversity in *D. longistipitata* (pi = 0.0094; Table 1, Fig. 4). Few population level genetic analyses are available for non-model fungal species, with most of the literature focusing on species of public interest such as phytopathogens (Benne tt et al. 2019), human pathogens (Cogliati et al. 2019), insect pathogens (Tsui et al. 2019), and mycorrhiza (Savary et al. 2018). As a result, comparisons are difficult to obtain. Anyhow, the nucleotide diversity estimates for the concatenated ITS and beta-tubulin sequences of *D. longistipitata* were higher in relation to assorted pathogenic Ascomycota including *C. scovillei*, *A. fumigatus*, and *C. montium* (pi = 0.0027, 0.0003, and 0.0041, respectively). Considering that demographic history represents a determinant of genetic diversity, governing effective population size (Ellegren and Galtier 2016), the observed high genetic diversity

within *D. longistipitata* may be related to a large effective population size accompanied by a distribution range expansion, resembling what has been reported for its host.

The estimated nucleotide diversity in *D. longistipitata* was lower compared to *C. purpurea* (pi = 0.0101), which is reasonable, as *C. purpurea* comprises three divergent lineages (Douhan et al. 2008). In this context, our results confirmed that *D. longistipitata* represents a well-defined taxonomic entity, useful as a model for phylogeographic studies. This statement is also supported by the ITS-based average genetic divergence (0.99%), agreeing with the canonical 1–3% (–5% Schmidt et al. 2013) threshold for intraspecific variation in fungi (Kõljalg et al. 2013), and specifically 1.96 % SD 3.73 for Ascomycota (Nilsson et al. 2008). Besides, our results did not detect genetic clustering (Fig. 3a), confirming this species forms a single and widely distributed genetic assemblage across Japan (Hosoya et al. 2010).

Several factors influence the genetic structure in fungal populations, due in part to the diverse ecological roles of these osmotrophs. For instance, Prospero et al. (2008) reported high overall F_{ST} = 0.43 in populations of the pathogenic fungus *Armillaria ostoyae* (Romagn.) Herink throughout ~200 km. In this case, biological traits such as host infection ability and reproductive cycle shaped the genetic structure. Furthermore, Barrès et al. (2008) described low but significant genetic structure in *Melampsora populnea* (Pers.) P. Karst. within continental populations in a similar geographic range to the present study. The authors noted positive isolation by distance associated with dispersal constraints, and host preference. In contrast, Velez et al. (2016) described the lack of large-scale geographic structure among populations of the cosmopolitan marine species *Corollospora maritima* Werderm., perhaps as a result of high dispersal potential, or meteorological phenomena like hurricanes.

Even though the sampled localities are distributed across a broad geographic range covering ~1700 km, our genetic structure estimates were practically negligible (Fig. 2, and Suppl. material 3: Table S2). In addition, the lack of correlation between haplotypes relationships and the spatial distribution (Fig. 4), as well as the absence of isolation-by-distance patterns suggest that the lack of structure in *D. longistipitata* is a consequence of the homogeneous distribution of the genetic diversity, instead of a similar genetic composition among localities. Even though dispersion mechanisms remain unknown for *D. longistipitata*, based on its host specificity and field observations, its occurrence as an endophyte is feasible. Under this assumption, a joint seed-vectored dispersion may be possible, opening the opportunity for a broader animal-mediated dispersal (Magyar et al. 2016). This would agree with former reports for the host *F. crenata* (Akashi 1997), and rapid dispersion rates (~100 m/yr) in *Fagus* species under climate change scenario to cope with environmental stress (McLachlan et al. 2005). However, greenhouse experimental and field evidence is required to support this hypothesis.

According to the negative values of the neutrality tests and the star-shaped connections in the haplotype network, the Bayesian Skyride plots revealed that both *D. longistipitata* and *F. crenata* underwent important recent demographic growth events. However, the effective-size of *D. longistipitata* was several orders of magnitude larger than *F. crenata*. For instance, assuming a fixed mutation rate of 1×10^-10 for both species, we

would expect a current effective-size of ~36×10^9 for *D. longistipitata*, and 35,000 for *F. crenata*. Moreover, considering a generation time of 10 years for *F. crenata* along with a mutation rate range of 1×10^-11 to 1×10^-12 per site/year (which is feasible for the *matk* gene given the reported mutation rate and the slow evolution rates reported for *Fagaceae* family; Frascaria et al. 1993; Lavin et al. 2005; Barthet and Hilu 2007), the beginning of the demographic growth is estimated for 570 to 5,700 ya; hence stable population size for *F. crenata* would be dated within 2,700 to 27,000 ya. Nevertheless, approximating the time of demographic growth for *D. longistipitata* is problematic.

Aside from the lack of mutation rates for the genetic markers, and precise reports on the number of reproductive events per year (*i.e.*, the generation time), our rough calculations on the estimates for population growth agree with the hypothesis of post-glacial demographic expansion. Furthermore, the demographic increase trend in *D. longistipitata* may be related to a higher mutation rate and shorter generation times. So, growth trends for *D. longistipitata* in the Skyride plots could correspond to a fraction of the time scale in *F. crenata*. In this sense, the mast seeding (large, synchronic seed production) in *F. crenata* (Hiroki and Matsubara 1995), could promote a rapid demographic growth, and high effective size in *D. longistipitata*.

The SDM analyses revealed several restricted areas of climatic stability distributed in mid-southern Japan (Fig. 6). This suggests that *D. longistipitata* and *F. crenata* populations might have had a limited distribution range due to unfavorable past climate conditions in the Pleistocene-Holocene transition, followed by an expansion driven by climatic suitability. According to this hypothesis, the SPREAD3 analysis mapped the origin of dispersion for *D. longistipitata* and *F. crenata* around the predicted areas of climatic suitability in mid-southern Japan (Figs 6, 7), in accordance to former work on chloroplast data of *F. crenata* (Fujii et al. 2002). The statement is also supported by occurrence of the most abundant haplotype (H12B4) in Tsukuba (Site 7), Suganuma (Site 6), and Mt. Atema (Site 4), located in mid Japan among 36.2 to 37.0 N in latitude. However, consecutive dispersion patterns showed slight discrepancies between both species (Fig. 7, Times 2 and 3). This may be attributed to 1) sampling bias or 2) fungal environmental/physiological constraints during ascomata development (e.g., humidity and temperature) as previously suggested (Carré 1964; Fukasawa 2012).

Conclusions

Modifications in species distribution ranges result from the interaction between ecological and evolutionary processes (Sexton et al. 2009). Our data suggest that drastic past environmental changes marked the genetic diversity within populations of *D. longistipitata*, as exhibited by the magnitude and distribution of the genetic diversity, and historical effective population size fluctuations. Overall, these findings agree with previous reports on the close ecological relationship between the fungus and *F. crenata* (which share an ecological background during Pleistocene-Holocene transition), and the influence of past environmental changes on suitable areas for its distribution.

Dasyscyphella longistipitata has been recognized as a fine woody debris decomposer, in particular of cupule litter, an essential component of litterfall in beech forests (Fukasawa et al. 2012). Hence it potentially plays an important role in nutrients cycling and the resilience of the ecosystem. We provide genetic diversity evidence at the population level for this saprophytic fungal species, which is relevant for the conservation and management of forests. Moreover, we confirmed the validity of using host (substrate) data to formulate phylogeographic hypothesis for substrate-specific organisms, which represents an interesting model to explore symbiont relationships under past and future climatic scenarios.

Acknowledgments

This project was funded by Grant-in-Aid for scientific research (C) 17570088. We thank Dr. A. Yabe for his valuable discussion about past distribution of *Fagus crenata* in Japan. We also appreciate sampling assistance by Kazuaki Tanaka, Harue Abe, Makoto Hashiya, Etsuko Kurokawa, Kentaro Hosaka, Takashi Shirouzu, Hideji Ushijima, Konomi Yanaga, Yoko Kimura, Daisuke Sakuma, Tomio Okino, Miyuki Kobayashi. This paper was written during a research stay of PV at the National Museum of Nature and Science, Tsukuba, with support of FY2018 JSPS Invitational Fellowship for Research in Japan (ID No. S18062). We acknowledge anonymous reviewers for constructive comments on earlier versions of the manuscript.

References

Aikens CM, Akazawa T (1996) The Pleistocene-Holocene transition in Japan and adjacent northeast Asia. In: Straus LG, Eriksen BV, Erlandson JM, Yesner DR (Eds) Humans at the end of the ice age. Springer, Boston, 215–227. https://doi.org/10.1007/978-1-4613-1145-4_11

Akashi N (1997) Dispersion pattern and mortality of seeds and seedlings of *Fagus crenata* Blume in a cool temperate forest in western Japan. Ecological Research 12: 159–165. https://doi.org/10.1007/BF02523781

Aktas C (2019) Haplotypes: manipulating DNA sequences and estimating unambiguous haplotype network with statistical parsimony. R package version 1.1. https://CRAN.R-project.org/package=haplotypes

Araújo MB, New M (2007) Ensemble forecasting of species distributions. Trends in Ecology and Evolution 22: 42–47. https://doi.org/10.1016/j.tree.2006.09.010

Bandelt PJ, Forster P, Sykes BC, Richards MB (1995) Mitochondrial portraits of human populations using median networks. Genetics 141: 743–753.

Barrès B, Halkett F, Dutech C, Andrieux A, Pinon J, Frey P (2008) Genetic structure of the poplar rust fungus *Melampsora larici-populina*: evidence for isolation by distance in Europe and recent founder effects overseas. Infection, Genetics and Evolution 8: 577–587. https://doi.org/10.1016/j.meegid.2008.04.005

Barthet MM, Hilu KW (2007) Expression of *matK*: functional and evolutionary implications. American Journal of Botany 94: 1402–1412. https://doi.org/10.3732/ajb.94.8.1402

Bennett PI, Hood IA, Stone JK (2019) The genetic structure of populations of the Douglas-fir Swiss needle cast fungus *Nothophaeocryptopus gaeumannii* in New Zealand. Phytopathology 109: 446–455. https://doi.org/10.1094/PHYTO-06-18-0195-R

Bielejec F, Rambaut A, Suchard MA, Lemey P (2011) SPREAD: Spatial Phylogenetic Reconstruction of Evolutionary Dynamics. Bioinformatics 27: 2910–2912. https://doi.org/10.1093/bioinformatics/btr481

Booth A (2014) Populations and individuals in heterokaryotic fungi: a multilevel perspective. Philosophy of Science 81: 612–632. https://doi.org/10.1086/677953

Bradley RS (1999) Paleoclimatology: Reconstructing Climates of the Quaternary. Academic Press, San Diego, 1–610. https://doi.org/10.1016/S0074-6142(99)80003-5

Breiman L (2001) Random forests. Machine Learning 45: 5–32. https://doi.org/10.1023/A:1010933404324

Carré CG (1964) Fungus decomposition of beech cupules. Transactions of the British Mycological Society 47: 437–444. https://doi.org/10.1016/S0007-1536(64)80015-2

Cho S, Lee D, Kim W, Chun H, Park C, Myong J, Park Y, Choi J, Lee Y, Kim S, Park S, Choi S, Choi J, Yoo J (2019) Epidemiology and antifungal susceptibility profile of *Aspergillus* species: comparison between environmental and clinical isolates from patients with hematologic malignancies. Journal of Clinical Microbiology 57: e02023–18. https://doi.org/10.1128/JCM.02023-18

Clement M, Posada DCKA, Crandall KA (2000) TCS: a computer program to estimate gene genealogies. Molecular Ecology 9: 1657–1659. https://doi.org/10.1046/j.1365-294x.2000.01020.x

Cogliati M, Desnos-Ollivier M, McCormick-Smith I, Rickerts V, Ferreira-Paim K, Meyer W, et al. (2019) Genotypes and population genetics of *Cryptococcus neoformans* and *Cryptococcus gattii* species complexes in Europe and the Mediterranean area. Fungal Genetics and Biology 129: 16–29. https://doi.org/10.1016/j.fgb.2019.04.001

Darriba D, Taboada GL, Doallo R, Posada D (2012) jModelTest 2: more models, new heuristics and parallel computing. Nature Methods 9: 772. https://doi.org/10.1038/nmeth.2109

Douhan GW, Smith ME, Huyrn KL, Westbrook A, Beerli P, Fisher AJ (2008) Multigene analysis suggests ecological speciation in the fungal pathogen *Claviceps purpurea*. Molecular Ecology, 17: 2276–2286. https://doi.org/10.1111/j.1365-294X.2008.03753.x

Ellegren H, Galtier N (2016) Determinants of genetic diversity. Nature Reviews Genetics 17: 422–433. https://doi.org/10.1038/nrg.2016.58

Excoffier L, Smouse PE, Quattro JM (1992) Analysis of molecular variance inferred from metric distances among DNA haplotypes: application to human mitochondrial DNA restriction data. Genetics 131: 479–491.

Fang J, Lechowicz MJ (2006) Climatic limits for the present distribution of beech (*Fagus* L.) species in the world. Journal of Biogeography 33: 1804–1819. https://doi.org/10.1111/j.1365-2699.2006.01533.x

Ferreri M, Qu W, Han B (2011) Phylogenetic networks: a tool to display character conflict and demographic history. African Journal of Biotechnology 10: 12799–12803. https://doi.org/10.5897/AJB11.010

Frascaria N, Maggia L, Michaud M, Bousquet J (1993) The *rbcL* gene sequence from chestnut indicates a slow rate of evolution in the *Fagaceae*. Genome 36: 668–671. https://doi.org/10.1139/g93-089

Friedman, JH (1991) Multivariate adaptive regression splines. The Annals of Statistics 19: 1–67. https://doi.org/10.1214/aos/1176347963

Friedman JH (2001) Greedy function approximation: a gradient boosting machine. Annals of Statistics 29: 1189–1232. https://doi.org/10.1214/aos/1013203451

Fujii N, Tomaru N, Okuyama K, Koike T, Mikami T, Ueda K (2002) Chloroplast DNA phylogeography of *Fagus crenata* (*Fagaceae*) in Japan. Plant Systematics and Evolution 232: 21–33. https://doi.org/10.1007/s006060200024

Fukasawa Y (2012) Effects of wood decomposer fungi on tree seedling establishment on coarse woody debris. Forest Ecology and Management 266: 232–238. https://doi.org/10.1016/j.foreco.2011.11.027

Fukasawa Y, Tateno O, Hagiwara Y, Hirose D, Osono T (2012) Fungal succession and decomposition of beech cupule litter. Ecological Research 27: 735–743. https://doi.org/10.1007/s11284-012-0947-3

Global Biodiversity Information Facility (2019) GBIF Occurrence Download. http://data.gbif.org [accessed September 2, 2019]

Geml J, Tulloss RE, Laursen GA, Sazanova NA, Taylor DL (2010) Phylogeographic analyses of a boreal-temperate ectomycorrhizal basidiomycete, *Amanita muscaria*, suggest forest refugia in Alaska during the last glacial maximum. In: Habel JC, Assmann T (Eds) Relict Species – Phylogeography and Conservation Biology. Springer, Berlin, 173–186. https://doi.org/10.1007/978-3-540-92160-8_9

Glass NL, Donaldson GC (1995) Development of primer sets designed for use with the PCR to amplify conserved genes from filamentous ascomycetes. Applied and Environmental Microbiology 61: 1323–1330. https://doi.org/10.1128/AEM.61.4.1323-1330.1995

Gotanda, K, Yasuda Y (2008) Spatial biome changes in southwestern Japan since the Last Glacial Maximum. Quaternary International 184: 84–93. https://doi.org/10.1016/j.quaint.2007.09.029

Hijmans RJ, Cameron SE, Parra JL, Jones PG, Jarvis A (2005) Very high resolution interpolated climate surfaces for global land areas. International Journal of Climatology 25: 1965–1978. https://doi.org/10.1002/joc.1276

Hiroki S, Matsubara T (1995) Fluctuation of nut production and seedling appearance of a Japanese beech (*Fagus crenata* Blume). Ecological Research 10: 161–169. https://doi.org/10.1007/BF02347938

Hongoh Y (2011) Toward the functional analysis of uncultivable, symbiotic microorganisms in the termite gut. Cellular and Molecular Life Sciences 68: 1311–1325. https://doi.org/10.1007/s00018-011-0648-z

Hosoya T, Hirose D, Fujisaki M, Osono T, Kubono T, Tokumasu S, Kakishima M (2010) Internal transcribed spacer haplotype diversity and their geographical distribution in *Dasyscyphella longistipitata* (Hyaloscyphaceae, Helotiales) occurring on *Fagus crenata* cupules in Japan. Mycoscience 51: 116–122. https://doi.org/10.1007/S10267-009-0020-4

Jombart T (2008) adegenet: a R package for the multivariate analysis of genetic markers. Bioinformatics 24: 1403–1405. https://doi.org/10.1093/bioinformatics/btn129

Kamvar ZN, Tabima JF, Grünwald NJ (2014) Poppr: an R package for genetic analysis of populations with clonal, partially clonal, and/or sexual reproduction. PeerJ 2: e281. https://doi.org/10.7717/peerj.281

Kawamura Y (2007) Last Glacial and Holocene lad mammas of the Japanese islands: their fauna, extinction and immigration. The Quaternary Research 46: 171–177. https://doi.org/10.4116/jaqua.46.171

Koike T, Kato S, Shimamoto Y, Kitamura K, Kawano S, Ueda K, et al. (1998) Mitochondrial DNA variation follows a geographic pattern in Japanese beech species. Botanica Acta 111: 87–92. https://doi.org/10.1111/j.1438-8677.1998.tb00682.x

Kõljalg U, Nilsson RH, Abarenkov K, Tedersoo L, Taylor AF, Bahram M, et al. (2013) Towards a unified paradigm for sequence-based identification of fungi. Molecular Ecology, 22: 5271–5277. https://doi.org/10.1111/mec.12481

Lavin M, Herendeen PS, Wojciechowski MF (2005) Evolutionary rates analysis of Leguminosae implicates a rapid diversification of lineages during the tertiary. Systematic Biology 54: 575–594. https://doi.org/10.1080/10635150590947131

Leavitt SD, Lumbsch HT, Stenroos S, Clair LLS (2013) Pleistocene speciation in North American lichenized fungi and the impact of alternative species circumscriptions and rates of molecular evolution on divergence estimates. PLoS One 8: e85240. https://doi.org/10.1371/journal.pone.0085240

Lumbsch HT, Buchanan PK, May TW, Mueller GM (2008) Phylogeography and biogeography of fungi. Mycological Research 112: 423–424. https://doi.org/10.1016/j.mycres.2008.02.002

Magyar D, Vass M, Li DW (2016) Dispersal strategies of microfungi. In: Li D (Ed) Biology of microfungi. Springer, Cham, 315–371. https://doi.org/10.1007/978-3-319-29137-6_14

Marske KA, Leschen RA, Barker GM, Buckley TR (2009) Phylogeography and ecological niche modelling implicate coastal refugia and trans-alpine dispersal of a New Zealand fungus beetle. Molecular Ecology 18: 5126–5142. https://doi.org/10.1111/j.1365-294X.2009.04418.x

McCormack JE, Zellmer AJ, Knowles LL (2010) Does niche divergence accompany allopatric divergence in *Aphelocoma jays* as predicted under ecological speciation?: insights from tests with niche models. Evolution 64: 1231–1244. https://doi.org/10.1111/j.1558-5646.2009.00900.x

McCullagh P, Nelder JA (1989) Generalized Linear Models. Chapman and Hall, 1–511. https://doi.org/10.1007/978-1-4899-3242-6

McLachlan JS, Clark JS, Manos PS (2005) Molecular indicators of tree migration capacity under rapid climate change. Ecology 86: 2088–2098. https://doi.org/10.1890/04-1036

Meyer O (1994) Functional groups of microorganisms. In: Schulze E, Mooney HA (Eds) Biodiversity and ecosystem function. Springer, Berlin, Heidelberg, 67–96. https://doi.org/10.1007/978-3-642-58001-7_4

Miller MA, Pfeiffer W, Schwartz T (2010) Creating the CIPRES Science Gateway for inference of large phylogenetic trees. Proceedings of the Gateway Computing Environments Workshop (GCE), 14 Nov. 2010, New Orleans, 1–8. https://doi.org/10.1109/GCE.2010.5676129

Minin VN, Bloomquist EW, Suchard MA (2008) Smooth Skyride through a rough Skyline: Bayesian coalescent-based inference of population dynamics. Molecular Biology and Evolution 25: 1459–1471. https://doi.org/10.1093/molbev/msn090

Mo J, Zhao G, Li Q, Solangi GS, Tang L, Guo T, et al. (2018) Identification and characterization of *Colletotrichum* species associated with mango anthracnose in Guangxi, China. Plant Disease 102: 1283–1289. https://doi.org/10.1094/PDIS-09-17-1516-RE

Naimi B, Hamm Na, Groen TA, Skidmore AK, Toxopeus AG (2014) Where is positional uncertainty a problem for species distribution modelling. Ecography 37: 191–203. https://doi.org/10.1111/j.1600-0587.2013.00205.x

Nakao K, Higa M, Tsuyama I, Matsui T, Horikawa M, Tanaka N (2013) Spatial conservation planning under climate change: Using species distribution modeling to assess priority for adaptive management of *Fagus crenata* in Japan. Journal for Nature Conservation 2: 406–413. https://doi.org/10.1016/j.jnc.2013.06.003

Nilsson RH, Kristiansson E, Ryberg M, Hallenberg N, Larsson K-H (2008) Intraspecific ITS variability in the kingdom Fungi as expressed in the international sequence databases and its implications for molecular species identification. Evolutionary Bioinformatics 4: 193–201. https://doi.org/10.4137/EBO.S653

Okaura T, Harada K (2002) Phylogeographical structure revealed by chloroplast DNA variation in Japanese beech (*Fagus crenata* Blume). Heredity 88: 322–329. https://doi.org/10.1038/sj.hdy.6800048

Ono Y, Hosoya T (2001) Hyaloscyphaceae in Japan (5): Some *Lachum*-like members. Mycoscience 42: 611–622. https://doi.org/10.1007/BF02460960

Ortego J, Gugger PF, Sork VL (2015) Climatically stable landscapes predict patternsof genetic structure and admixture in the Californian canyon live oak. Journal of Biogeography 42: 328–338. https://doi.org/10.1111/jbi.12419

Otto-Bliesner BL, Marshall SJ, Overpeck JT, Miller GH, Hu A (2006) Simulating Arctic climate warmth and icefield retreat in the last interglaciation. Science 311: 1751–1753. https://doi.org/10.1126/science.1120808

Phillips SJ, Anderson RP, Schapire RE (2006) Maximum entropy modeling of species geographic distributions. Ecological Modelling 190: 231–259. https://doi.org/10.1016/j.ecolmodel.2005.03.026

Prospero S, Lung-Escarmant B, Dutech C (2008) Genetic structure of an expanding *Armillaria* root rot fungus (*Armillaria ostoyae*) population in a managed pine forest in southwestern France. Molecular Ecology 17: 3366–3378. https://doi.org/10.1111/j.1365-294X.2007.03829.x

Qiao H, Soberón J, Peterson AT (2015) No silver bullets in correlative ecological niche modelling: insights from testing among many potential algorithms for niche estimation. Methods in Ecology and Evolution 6: 1126–1136. https://doi.org/10.1111/2041-210X.12397

R Core Team (2018) R: A language and environment for statistical computing. R Foundation for Statistical Computing, Vienna, Austria. URL https://www.R-project.org/ [Accessed on Nov 2018]

Rambaut A, Drummond AJ, Xie D, Baele G and Suchard MA (2018) Posterior summarisation in Bayesian phylogenetics using Tracer 1.7. Systematic Biology 5: 901–904. https://doi.org/10.1093/sysbio/syy032

Rodriguez RJ, Redman RS (1997) Fungal life-styles and ecosystem dynamics: biological aspects of plant pathogens, plant endophytes and saprophytes. Advances in Botanical Research 24: 169–193. https://doi.org/10.1016/S0065-2296(08)60073-7

Roe AD, Rice AV, Coltman DW, Cooke JE, Sperling FA (2011) Comparative phylogeography, genetic differentiation and contrasting reproductive modes in three fungal symbionts of a multipartite bark beetle symbiosis. Molecular Ecology 20: 584–600. https://doi.org/10.1111/j.1365-294X.2010.04953.x

Rozas J, Ferrer-Mata A, Sánchez-DelBarrio JC, Guirao-Rico S, Librado P, Ramos-Onsins SE, Sánchez-Gracia A (2017) DnaSP 6: DNA Sequence Polymorphism Analysis of Large Datasets. Molecular Biology and Evolution 34: 3299–3302. https://doi.org/10.1093/molbev/msx248

Savary R, Masclaux FG, Wyss T, Droh G, Corella JC, Machado AP, et al. (2018) A population genomics approach shows widespread geographical distribution of cryptic genomic forms of the symbiotic fungus *Rhizophagus irregularis*. The ISME Journal 12: 17–30. https://doi.org/10.1038/ismej.2017.153

Schmidt PA, Bálint M, Greshake B, Bandow C, Römbke J, Schmitt I (2013) Illumina metabarcoding of a soil fungal community. Soil Biology and Biochemistry 65: 128–132. https://doi.org/10.1016/j.soilbio.2013.05.014

Sexton JP, McIntyre PJ, Angert AL, Rice KJ (2009) Evolution and ecology of species range limits. Annual Review of Ecology Evolution and Systematics 40: 415–436. https://doi.org/10.1146/annurev.ecolsys.110308.120317

Skerman VBD (1968) A new type of micromanipulator and microforge. Journal of General Microbiology 54: 287–297. https://doi.org/10.1099/00221287-54-2-287

Suchard MA, Lemey P, Baele G, Ayres DL, Drummond AJ, Rambaut A (2018) Bayesian phylogenetic and phylodynamic data integration using BEAST 1.10. Virus Evolution 4: vey016. https://doi.org/10.1093/ve/vey016

Swets JA (1988) Measuring the accuracy of diagnostic systems. Science 240: 1285–1293. https://doi.org/10.1126/science.3287615

Tajima F (1989) Statistical method for testing the neutral mutation hypothesis by DNA polymorphism. Genetics 123: 585–595.

Templeton AR, Crandall KA, Sing CF (1992) A cladistic analysis of phenotypic associations with haplotypes inferred from restriction endonuclease mapping and DNA sequence data. III. Cladogram estimation. Genetics 132: 619–635.

Thuiller W, Georges D, Engler R, Breiner F (2019) biomod2: Ensemble Platform for Species Distribution Modeling. R package version 3.3-7.1. https://CRAN.R-project.org/package=biomod2

Tochihara Y, Hosoya T (2019) Three new species of *Incrucipulum* (Lachnaceae, Helotiales, Ascomycota) from Japan. Phytotaxa 403: 25–38. https://doi.org/10.11646/phytotaxa.403.1.2

Tomaru N, Mitsutsuji T, Takahashi M, Tsumura Y, Uchida K, Ohba K (1997) Genetic diversity in *Fagus crenata* (Japanese beech): influence of the distributional shift during the late-Quaternary. Heredity 78: 241–251. https://doi.org/10.1038/hdy.1997.38

Tomaru N, Takahashi M, Tsumura Y, Takahashi M, Ohba K (1998) Intraspecific variation and phylogeographic patterns of *Fagus crenata* (*Fagaceae*) mitochondrial DNA. American Journal of Botany 85: 629–636. https://doi.org/10.2307/2446531

Tsui CK, Beauseigle S, Ojeda DI, Rice A, Cooke JE, Sperling FA, et al. (2019) Fine-scale genetic structure and relatedness in fungi associated with the mountain pine beetle. Canadian Journal of Forest Research 48: 933–941. https://doi.org/10.1139/cjfr-2018-0418

Tsukada M (1982a) *Cryptomeria japonica*: Glacial refugia and late-glacial and postglacial migration. Ecology 63: 1091–1105. https://doi.org/10.2307/1937247

Tsukada M (1982b) Late-Quaternary shift of *Fagus* distribution. Botanical Magazine= Shokubutsu-Gaku-Zasshi 95: 203–217. https://doi.org/10.1007/BF02488586

Tsukada M (1982c) Late-Quaternary development of the *Fagus* forest in the Japanese Archipelago. Japanese Journal of Ecology 32: 113–118.

Tsukada M (1983) Vegetation and climate during the last glacial maximum in Japan. Quaternary Research 19: 212–235. https://doi.org/10.1016/0033-5894(83)90006-6

Tsukada M (1985) Map of vegetation during the last glacial maximum in Japan. Quaternary Research 23: 369–381. https://doi.org/10.1016/0033-5894(85)90041-9

Velez P, Gasca-Pineda J, Nakagiri A, Hanlin RT, González MC (2016) Genetic diversity and population structure of *Corollospora maritima sensu lato*: new insights from population genetics. Botanica Marina 59: 307–320. https://doi.org/10.1515/bot-2016-0058

White TJ, Bruns T, Lee S, Taylor J (1990) Amplification and direct sequencing of fungal ribosomal RNA genes for phylogenetics. In: Innis MA, Gelfand DH, Sninsky JJ, White TJ (Eds) PCR protocols: a guide to methods and applications. Academic Press, San Diego, 315–322. https://doi.org/10.1016/B978-0-12-372180-8.50042-1

Supplementary material 1

Figure S1. Species distribution modeling (SDM) for *Dasyscyphella longistipitata*.
Authors: Jaime Gasca-Pineda, Patricia Velez, Tsuyoshi Hosoya
Data type: occurrence
Explanation note: **A** Projection for the current major environmental conditions. Color bar represents environmental suitability values, where warmer colors indicate higher suitability, **B** projections for the four time periods analyzed in this study. LGM = Last Glacial Maximum, LIG = Last Interglacial period. The areas represent the upper 90% of the distribution of the suitability values for each period of time.

Link: https://doi.org/10.3897/mycokeys.65.48409.suppl1

Supplementary material 2

Table S1

Authors: Jaime Gasca-Pineda, Patricia Velez, Tsuyoshi Hosoya

Data type: statistical data

Explanation note: Summary statistics for ITS and beta-tubulin markers, showing the sample size (N), number of polymorphic sites (S), number of haplotypes (h), haplotype diversity (Hd), and nucleotide diversity (Pi).

Link: https://doi.org/10.3897/mycokeys.65.48409.suppl2

Supplementary material 3

Table S2

Authors: Jaime Gasca-Pineda, Patricia Velez, Tsuyoshi Hosoya

Data type: statistical data

Explanation note: Paired PhiST values between *D. longistipitata* localities (1–14). Bold numbers denote significance at $p < 0.05$. For nomenclature on sampling localities please refer to Table 1.

Link: https://doi.org/10.3897/mycokeys.65.48409.suppl3

Supplementary material 4

Table S3. List of isolates and their haplotype properties

Authors: Jaime Gasca-Pineda, Patricia Velez, Tsuyoshi Hosoya

Data type: molecular data

Explanation note: All the isolates obtained were numbered with a suffix "DL-", and their ITS-5.8S and beta-tubulin regions were sequenced. Only isolates that were successful sequenced in both regions were used. In total, 270 isolates were used.

Link: https://doi.org/10.3897/mycokeys.65.48409.suppl4

Supplementary material 5

Table S4. List of accession numbers for ITS-5.8S and beta-tubulin haplotypes

Authors: Jaime Gasca-Pineda, Patricia Velez, Tsuyoshi Hosoya

Data type: molecular data

Explanation note: When a haplotype was obtained from multiple isolate, one isolate was randomly chosen and its sequence was registered. SeqID is for the authors' private use, and indicated for convenience.

Link: https://doi.org/10.3897/mycokeys.65.48409.suppl5

MycoKeys 65: 25–47 (2020)
doi: 10.3897/mycokeys.65.47574
http://mycokeys.pensoft.net

RESEARCH ARTICLE

A peer-reviewed open-access journal
MycoKeys
Launched to accelerate biodiversity research

Diversity of *Trametes* (Polyporales, Basidiomycota) in tropical Benin and description of new species *Trametes parvispora*

Boris Armel Olou[1,2,3], Franz-Sebastian Krah[4,5], Meike Piepenbring[6], Nourou Soulemane Yorou[2], Ewald Langer[1]

1 *Department of Ecology, Universität Kassel, Heinrich-Plett-Str. 40, Kassel, Germany* **2** *Research Unit Tropical Mycology and Plant-Soil Fungi Interactions (MyTIPS), University of Parakou BP 123, Parakou, Benin* **3** *Laboratory of Applied Ecology, University of Abomey-Calavi (LEA/UAC), Benin* **4** *Animal Ecology, Department of Ecology, Faculty of Biology, Philipps-Universität Marburg, Marburg, Germany* **5** *Bavarian Forest National Park, Freyunger Str. 2, 94481 Grafenau, Germany* **6** *Department of Mycology, Biologicum, Goethe Universität, Max-von-Laue-Str. 13, 60438 Frankfurt am Main, Germany*

Corresponding author: Boris Armel Olou (borisolou@yahoo.fr)

Academic editor: M.-A. Neves | Received 28 October 2019 | Accepted 22 December 2019 | Published 10 March 2020

Citation: Olou BA, Krah F-S, Piepenbring M, Yorou NS, Langer E (2020) Diversity of *Trametes* (Polyporales, Basidiomycota) in tropical Benin and description of new species *Trametes parvispora*. MycoKeys 65: 25–47. https://doi.org/10.3897/mycokeys.65.47574

Abstract

Trametes is a globally distributed genus of white-rot polypores and well sampled in temperate and boreal areas. However, the diversity, taxonomy, and phylogenetic positions of *Trametes* spp. are poorly known in tropical Africa. This study aims at documenting the diversity of *Trametes* species in Benin (tropical Africa) and their phylogenetic positions with a focus on the *T. elegans* species complex. Therefore, we collected specimens of *Trametes* from different forest types across Benin. To infer phylogenetic relationships between *Trametes* species, we investigated sequences of five gene regions and added available sequences from GenBank. Using Maximum likelihood and Bayesian phylogeny inference methods, we found eight supported species clades. For the *T. elegans* species complex, we re-establish the name *Trametes palisotii* for species previously known as *T. elegans* in tropical Africa. Furthermore, we propose *Trametes parvispora* as a species new to science and provide the description of this species. Our molecular phylogeny of *Trametes* with a focus on tropical Benin contributes to taxonomic clarity of an important wood-decay fungal genus, which is the basis for biodiversity assessments of *Trametes* in the tropics.

Keywords

Africa, morphology, new taxa, phylogeny, Polyporales, taxonomy, tropics, white rot

Introduction

The genus *Trametes* Fr. (Polyporales, Basidiomycota) consists of wood-decay fungi with a distribution covering all continents and all major climatic zones (Gilbertson and Ryvarden 1987; Ryvarden 1991). Species of *Trametes* are characterized by a combination of a pileate basidioma, a poroid hymenophore, a trimitic hyphal system, and non-amyloid, thin-walled basidiospores (Gilbertson and Ryvarden 1987). They are saprotrophs causing white rot during the decay of woody substrates (Wong and Wilkes 1988). Species of the genus *Trametes* have a long ethnomycological history as medicinal fungi in many cultures (Cui et al. 2011; Ss and Pandey 2012; Ueitele et al. 2017) and some species are studied in the context of cancer research (Zmitrovich et al. 2012; Cruz et al. 2016; Blagodatski et al. 2018). Despite the global-scale distribution, importance for wood decomposition, and medicinal properties, the taxonomic and phylogenetic knowledge of *Trametes* spp. worldwide is still incomplete (Carlson et al. 2014).

Since the first formal description of the genus *Trametes* by Fries (1835), based on the type species *Trametes suaveolens* (L.) Fr., the concept of this genus was interpreted in different ways, resulting in different numbers of species attributed to the genus (Karsten 1881; Murrill 1905; Kavina and Pilát 1936; Kotlaba and Pouzar 1957; Gilbertson and Ryvarden 1987; Corner 1989). Recently, based on phylogenetic analyses, the concept of *Trametes* was re-delimited and circumscribed (Justo and Hibbett 2011). Here, we apply the broad concept of *Trametes* as proposed by Justo and Hibbett (2011). This concept includes in addition to species of *Trametes* sensu stricto, species of *Artolenzites* Falck, *Coriolopsis* Murrill, *Lenzites* Fr., and *Pycnoporus* P. Karst.

Previous studies on *Trametes* spp. mainly concentrated on specimens from temperate and boreal regions (David 1967; Gilbertson and Ryvarden 1987; Hattori 2005; Tomšovský et al. 2006; Pieri and Rivoire 2007; Ryvarden et al. 2009; Gomes-Silva et al. 2010; Hattori and Sotome 2013), and thus most *Trametes* spp. have been described from these regions. By contrast, little is known on *Trametes* spp. in tropical Africa (Fig. 1A), and most known specimens of *Trametes* spp. from this area are missing in most phylogenetic analyses.

For Benin, seven species of *Trametes*, namely *T. cingulata* Berk., *T. elegans* (Spreng.) Fr., *T. flavida* (Lév.) Zmitr., Wasser & Ezhov (cited as *Leiotrametes flavida*), *T. polyzona* (Pers.) Justo, *T. sanguinea* (L.) Lloyd (cited as *Pycnoporus sanguineus*), and *T. socotrana* Cooke were reported by Olou et al. (2019). Taking a closer look at these species, we noticed that sequence data are lacking for specimens from tropical Africa and that the knowledge on taxonomical and phylogenetic placements is incomplete.

Additional to these known species in Benin, we recently found a putatively new species of *Trametes* (Olou et al. 2019), but morphological and phylogenetic analyses were outstanding. In the same study, we reported the occurrence of *T. elegans* in Benin.

Trametes elegans was found to be a species complex and has therefore recently been split into three distinct species, namely *T. aesculi* (Fr.) Justo, *T. elegans* s.str., and *T. repanda* (Pers.) Justo (Carlson et al. 2014). However, this study did not include tropical African specimens although *T. elegans* exists in this area.

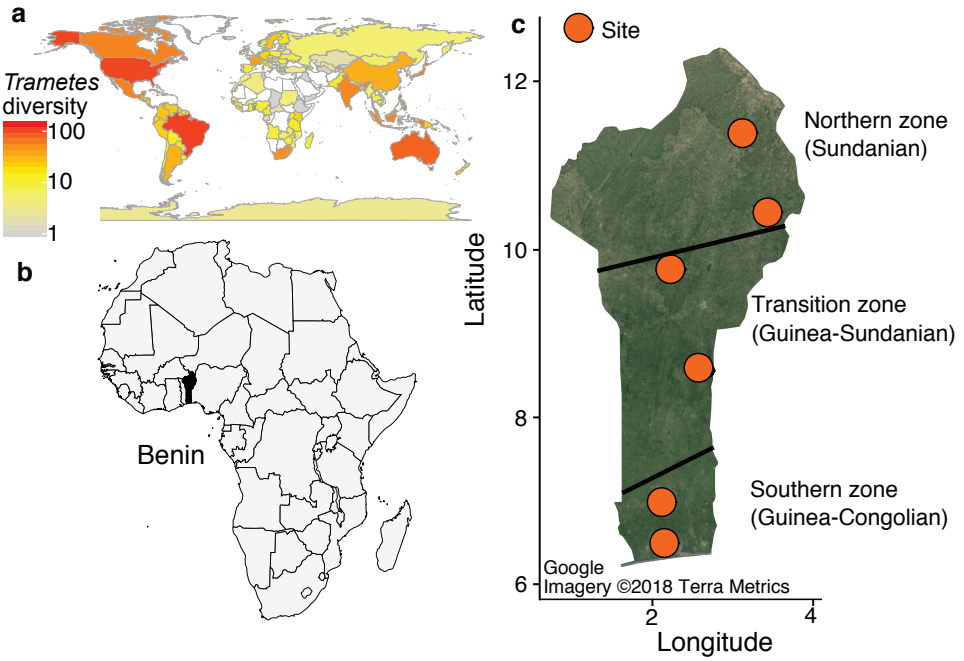

Figure 1. a Observations of *Trametes* spp. retrieved from MyCoPortal and GBIF, based on herbarium specimens and citizen science observations **b** The study area (Benin) in the western part of Africa (highlighted in black) **c** Locations of the sampling sites within macroclimatic zones, which are delimited by black lines. The circles in orange indicate respectively from bottom to top the sampling sites: dry dense forest of Pahou, dense semi-deciduous forest of Lama, woodlands of Kilibo, woodlands of Ouémé Superieur, Trois Rivières woodland, and savanna ecosystems of the national park W.

Our study thus aims to report the diversity of *Trametes* species in Benin and their phylogenetic positions, with a focus on a new species of *Trametes* and the *T. elegans* species complex.

Material and methods

Specimens sampling and preservation

A total of 37 specimens of *Trametes* were collected in three different macroclimatic zones and different forests of Benin (Fig. 1A, C) from July to September in 2017 (Olou et al. 2019) and in 2018 (another series of surveys). Small pieces of fresh fruit bodies were placed in plastic bags half-filled with silica gel for DNA extraction. The rest of fruit bodies were air- or oven-dried at 45–50 °C for 1–2 days depending on the consistency of the fruit body. The dried fruit bodies were then preserved in plastic bags for morphological investigation. Specimens are deposited at the mycological herbaria of the University of Parakou (UNIPAR; Thiers 2019) and the University of Kassel (KAS).

DNA extraction, amplification, sequencing and alignment

DNA extraction. Genomic DNA of all specimens classified into nine morphotypes was extracted using the microwave DNA extraction method (Dörnte and Kües 2013) or the NucleoSpin Plant II DNA extraction kit (Macherey, Nagel, Germany).

Amplifications and sequencing. The extracted genomic DNA was amplified targeting two nuclear ribosomal DNA (*nr*DNA) regions, internal transcribed spacer (ITS) and ribosomal large subunit-coding DNA (28S rRNA) for all specimens. Additionally, three protein-coding genes, RNA polymerase II largest subunit (RPB1), RNA polymerase II second largest subunit (RPB2), and translation elongation factor 1-alpha (TEF1) were amplified for specimens forming part of the *T. elegans* species complex and specimens of *Trametes* sp. The amplification of the 5.8S rRNA gene region, including ITS were performed in Mastercycler nexus gradient (Eppendorf, Germany), using the primer pair ITS-1F/ITS4 (White et al. 1990; Gardes and Bruns 1993). The Polymerase Chain Reaction (PCR) procedure for the ITS region, was as follows: initial denaturation at 95 °C for 3 min, followed by 35 cycles at 95 °C for 30 s, 52 °C for 30 s and 68 °C for 1 min, and a final extension at 68 °C for 3 min. Amplifications of LSU and three protein-coding genes were performed in 96-well TGradient Thermocycler (Biometra, Göttingen, Germany). PCR procedure for amplifying partial LSU rDNA using the primer pair LR0R/LR5 (Vilgalys and Hester 1990) approximately 964 bp differed to the ITS only by the annealing temperature (55 °C instead of 52 °C) and increased cycle extension time (90 s per cycle). The primer pairs EF1-983F/EF1-1567R (Rehner and Buckley 2005), RPB1-Af/RPB1-Cr (Stiller and Hall 1997; Matheny et al. 2002), and RPB2-b6F/RPB2-b7.1R (Liu et al. 1999; Matheny 2005) were used to amplify approximately 500 bp of TEF1, 1000 bp of RPB1, and 800 bp of RPB2. To amplify the protein-coding genes RPB1 and RPB2, the touchdown PCR protocol following Justo and Hibbett (2011) was used. PCR products were checked on 1% agarose gel stained with GelRed fluorescence dye (Biotium, Hayward, California, USA) in the Transilluminator Biometra Ti5 equipped with BioDocAnalyze software (Biometra GmbH, Göttingen, Germany). They were further cleaned up with QIAquick PCR Purification Kit according to manufacturer's instructions (QIAGEN GmbH, Hilden, Germany). Thereafter, Sanger sequenced at GATC Biotech in Germany.

At least one sequence per specimen was generated for each morphotype except for the morphotype named *T.* aff. *versicolor* (Fig. 2N; Suppl. material 1). All newly generated sequences composed of 25 ITS, 20 LSU, two RPB1, four RPB2, and three TEF1 were deposited in GenBank (for accession numbers, see Table 1).

Sequence alignment and phylogenetic analyses. To place all the 25 generated ITS sequences of specimens of *Trametes* spp. in a phylogenetic context, we aligned them in addition to 66 ITS sequences retrieved from GenBank (Benson et al. 2011). Further, 48 LSU sequences were aligned with 20 LSU sequences generated here. For the

Table 1. Taxa names with collection details and GenBank accession numbers of all sequences of *Trametes* spp.

Species name	Voucher or strain	Origin	GenBank N°					Reference
			ITS	LSU	RPB1	RPB2	TEF1	
Dentocorticium sulphurellum	FP11801		JN165018	JN164815	JN164841	JN164876		Justo and Hibbett 2011
Lopharia cinerascens	FP105043sp	USA: Mississippi	JN165019	JN164813	JN164840	JN164874		Justo and Hibbett 2011
T. aesculi (*T. elegans* species complex)	HHB4626sp	USA	JN164950		KF573173	KF573134	KF573083	Justo and Hibbett 2011, Carlson et al. 2014
	FP105679sp	USA/Georgia	JN164944	JN164799	JN164833	JN164861	JN164899	
	HHB6551	USA/Florida	JN164938		KF573172	KF573136	KF573082	
	FP105038sp	USA: Mississippi	JN164951		KF573174	KF573135	KF573081	
T. betulina (*Lenzites betulinus*)	HHB9942sp	USA	JN164983	JN164794		JN164860		Justo and Hibbett 2011
	Dai6847		KC848305	KC848390				unpublished
T. cingulata	MUCL:40167	Malawi	JN645075					Welti et al. 2012
	Dollinger 629	USA/Florida	KY264043					unpublished
	DMC814	Cameroon	KC589133	KC589159				unpublished
	OAB0135	**Benin**	**MK736973**					**this study**
	OAB0117	**Benin**	**MK736972**					
	OAB0093	**Benin**	**MK736970**					
	OAB0114	**Benin**	**MK736971**	**MK736950**				
	OAB0161	**Benin**	**MK736975**	**MK736951**				
	OAB0155	**Benin**	**MK736974**					
	OAB0171	**Benin**	**MK736976**	**MK736952**				
	OAB0173	**Benin**	**MK736977**	**MK736953**				
	OAB0178	**Benin**	**MK736978**	**MK736954**				
	OAB0231	**Benin**	**MK736979**	**MK736955**				
T. cinnabarina (cited as *Pycnoporus cinnabarinus*)	Dai 14386	China	KX880629	KX880667	KX880818	KX880854		unpublished
T. coccinea (cited as *Pycnoporus coccineus*)	Cui-7096		KC848330	KC848414				unpublished
T. conchifer	FP106793sp	USA/ Mississippi	JN164924	JN164797	JN164823	JN164849		Justo and Hibbett 2011
T. cubensis	TJV93_213sp	USA/ Mississippi	JN164923	JN164798	JN164834	JN164865		Justo and Hibbett 2011
	AJ177	USA: Florida	JN164905					
	UZ526_17	Malaysia	MF363158					unpublished
T. ectypa	FP103976sp	USA: FLorida	JN164961					Justo and Hibbett 2011
	FP106037T	USA	JN164929	JN164803	JN164824	JN164848		
T. elegans (*T. elegans* species complex)	PR1133	Puerto Rico	JN164937		KF573178	KF573139	KF573075	Justo and Hibbett 2011, Carlson et al. 2014
	FPRI10	Philippines	JN164973			KF573138	KF573074	
	FP150762	Belize	JN164928			KF573137	KF573076	
T. flavida	**OAB0047**	**Benin**	**MK736966**	**MK736946**				**this study**
	OAB0090	**Benin**	**MK736967**					
	OAB0196	**Benin**	**MK736968**	**MK736947**				
T. flavida (cited as *Leiotrametes flavida*)	DMC811	Cameroon	KC589130	KC589156				unpublished
	CBS 158.35		MH855616	MH867126				Vu et al. 2019
T. gibbosa	DMC815	Cameroon	KC589144	KC589164				unpublished
	L11664sp	England	JN164943	JN164800	JN164831	JN164859		Justo and Hibbett 2011
T. hirsuta	DMC341	Cameroon	KC589146	KC589166				unpublished
	RLG5133T	USA: New York	JN164941	JN164801	JN164829	JN164854		Justo and Hibbett 2011
T. junipericola	145295(O)		KC017758	KC017763				unpublished
T. lactinea	DMC346	Cameroon	KC589126	KC589152				unpublished

Species name	Voucher or strain	Origin	GenBank N°					Reference
			ITS	LSU	RPB1	RPB2	TEF1	
T. lactinea (cited as Leiotrametes lactinea)	CBS 109427	Taiwan	MH862825					Vu et al. 2019
T. lactinea	LIP:GUY09-110	French Guiana	JN645069					Welti et al. 2012
	Dai6865		KC848327	KC848411				unpublished
	OAB0232	**Benin**	**MK736983**	**MK736948**				**this study**
	BCC 33266	Thailand	GQ982888	GQ982881				unpublished
	Yuan5493		KC848320	KC848404				
T. ljubarskyi	Wei1653		KC848332	KC848416				unpublished
	Li286		KC848331	KC848415				
T. maxima	OH189sp	Venezuela	JN164957	JN164804	JN164816	JN164864		Justo and Hibbett 2011
T. membranacea	PRSC82	Puerto Rico	JN164945	JN164805	JN164832	JN164857		Justo and Hibbett 2011
T. menziesii	BRFM<FRA>:1368	Martinique	JN645103					Welti et al. 2012
	Dai6782		KC848289	KC848374				unpublished
T. meyenii		Philippines	JN164933		KF573179	KF573145		Justo and Hibbett 2011
T. meyenii	CBS:453.76	India	MH860991	MH872762				Vu et al. 2019
T. ochracea	HHB13445sp	USA/Michigan	JN164954	JN164812	JN164826	JN164852		Justo and Hibbett 2011
	Dai2005	China	KC848272	KC848357				unpublished
T. palisotii (*T. elegans* species complex)	**OAB0118**	**Benin**	**MK736980**	**MK736956**	**MK802884**	**MK802882**	**MK802886**	**this study**
	OAB0153	**Benin**	**MK736981**	**MK736957**	**MK802885**	**MK802883**	**MK802887**	
	OAB0198	**Benin**	**MK736982**	**MK736958**			**MK802888**	
T. palisotii	DMC360	Cameroon	KC589139	KC589160				unpublished
	DMC817	Cameroon	KC589142	KC589163				
	DMC816	Cameroon	KC589141	KC589162				
T. parvispora	**OAB0022**	**Benin**	**MK736989**	**MK736964**		**MN127965**		**this study**
	OAB0023	**Benin**	**MK736990**	**MK736965**		**MN127964**		
T. pavonia	FP103050sp	USA/Florida	JN164958	JN164806	JN164835	JN164862		Justo and Hibbett 2011
T. polyzona	DMC370	Cameroon	KC589125	KC589151				unpublished
	Cui 11040	China	KX880647	KX880689	KX880836	KR610849		
	BKW004	Ghana	JN164978	JN164790				Justo and Hibbett 2011
	OAB0092	**Benin**	**MK736984**	**MK736959**				**this study**
	OAB0128	**Benin**	**MK736985**	**MK736960**				
	OAB0195	**Benin**	**MK736986**	**MK736961**				
T. pubescens	FP101414sp	USA/Wisconsin	JN164963	JN164811	JN164827	JN164851		Justo and Hibbett 2011
T. pucinea (cited as *Pycnoporus puniceus*)	BCC26408	Thailand	FJ372685	FJ372707				unpublished
T. punicea	BCC27595		FJ372686	FJ372708				unpublished
T. rependa (*T. elegans* species complex)	FRI437T		JN164985		KF573177	KF573142	KF573080	Justo and Hibbett 2011, Carlson et al. 2014
	FPRI390	Philippines	JN164921		KF573175	KF573141	KF573077	
	OH271sp	Venezuela	JN164936		KF573176	KF573143	KF573079	
	M0138339	Papua New Guinea	KF573029			KF573140	KF573078	
T. sanguinea	**OAB0088**	**Benin**	**MK736969**	**MK736949**				**this study**
T. sanguinea (cited as *Pycnoporus sanguineus*)	PRSC95	Puerto Rico	JN164982	JN164795	JN164842	JN164858		Justo and Hibbett 2011
	BCC 36861	Thailand	GQ982885	GQ982878				unpublished
	8R_1_2	Thailand	FJ372672	FJ372694				
	CBS:614.73	Sri Lanka	MH860781	MH872513				
T. socotrana	BJFC12724	China	KC848313	KC848397				unpublished
	OAB0131	**Benin**	**MK736987**	**MK736962**				**this study**
	OAB0162	**Benin**	**MK736988**	**MK736963**				
Trametes sp. (cited as *Leiotrametes* sp.)	LIP:GUY08-156	French Guiana	JN645062					Welti et al. 2012

Species name	Voucher or strain	Origin	GenBank N°					Reference
			ITS	LSU	RPB1	RPB2	TEF1	
Trametes sp.	BC1	Finland	KT896651					Linnakoski et al. 2016
*Trametes*sp. (cited as *Leiotrametes* sp.)	LIP:GUY08-167	French Guiana	JN645063					Welti et al. 2012
T. suaveolens	FP102529sp	USA/Wisconsin	JN164966	JN164807	JN164828	JN164853		Justo and Hibbett 2011
	Dai 10729	China	JN048770	JN048789				unpublished
T. versicolor	FP135156sp	USA/New York	JN164919	JN164809	JN164825	JN164850		Justo and Hibbett 2011
T. villosa	FP71974R	USA/Tennessee	JN164969	JN164810	JN164830	JN164855		Justo and Hibbett 2011

The rows referring to sequences generated in this study are written in bold.

T. elegans species complex, seven newly generated sequences of protein-coding genes were aligned in addition to sequences used by Carlson et al. (2014). Each marker was aligned separately using MAFFT version 7, with the algorithm L-INS-i (Katoh et al. 2017) and standard settings as default. The resulting multiple species alignments were slightly adjusted and trimmed at both ends a bit from incomplete sequences in Geneious 5.6.7 (Kearse et al. 2012). Eight different datasets were assembled for the phylogenetic analyses: (i) ITS dataset with 91 sequences of *Trametes* spp., (ii) combined ITS-LSU dataset with 91 sequences *Trametes* spp., (iii) combined RPB1-RPB2 dataset with 23 sequences of *Trametes* spp., (iv) ITS dataset with 17 sequences of *T. elegans* species complex, (v) RPB1 dataset with ten sequences of the *T. elegans* species complex, (vi) RPB2 dataset with 12 sequences of *T. elegans* species complex, (vii) TEF1 dataset with 14 sequences of *T. elegans* species complex, and (viii) combined dataset of four genes (ITS, RPB1, RPB2, TEF1) of *T. elegans* species complex. The combined datasets were concatenated using Geneious 5.6.7 (Kearse et al. 2012). For the phylogenetic analyses, the partitioning of the combined datasets of *Trametes* spp. was considered. *Lopharia cinerascens* (Schwein.) G. Cunn., and *Dentocorticium sulphurellum* (Peck) M.J. Larsen & Gilb., were chosen as the outgroup in all datasets (Justo and Hibbett 2011). Two phylogenetic tree inference methods, Maximum likelihood (ML) and Bayesian (BY) were performed in each dataset. The ML of all datasets were performed using RAxML 8.2.10 (Stamatakis 2014) and the BY of all individual genes and combined dataset of *T. elegans* species complex were performed using MrBayes 3.2.6 (Ronquist et al. 2012) at the Cipres Science Gateway V.3.3. (Miller et al. 2010). The BY of the partitioned datasets of *Trametes* spp. were run independently using MrBayes 3.2.7 (Ronquist et al. 2012). The parameters in BY inference were set as follows: lset applyto = (all), nst = 6, rates = invgamma, ngammacat = 4, sampling frequency = 1000, and the command "unlink" was used to unlink parameters across characters on partitioned datasets. Two independent Markov Chain Monte Carlo (MCMC) processes were run, each in 4 chains, for 5 million generations, and 0.2 fraction were discarded as burn-in. The Phylogenetic Tree Summarization (SumTrees) program within DendroPy 4.3.0. (Sukumaran and Holder 2010) was used to build the consensus tree with branch supports (posterior probabilities). Further, by using IQ-Tree (Trifinopoulos et al. 2016), we assigned the bootstrap values (BS) of ML to the consensus tree of BY. The resulting phyloge-

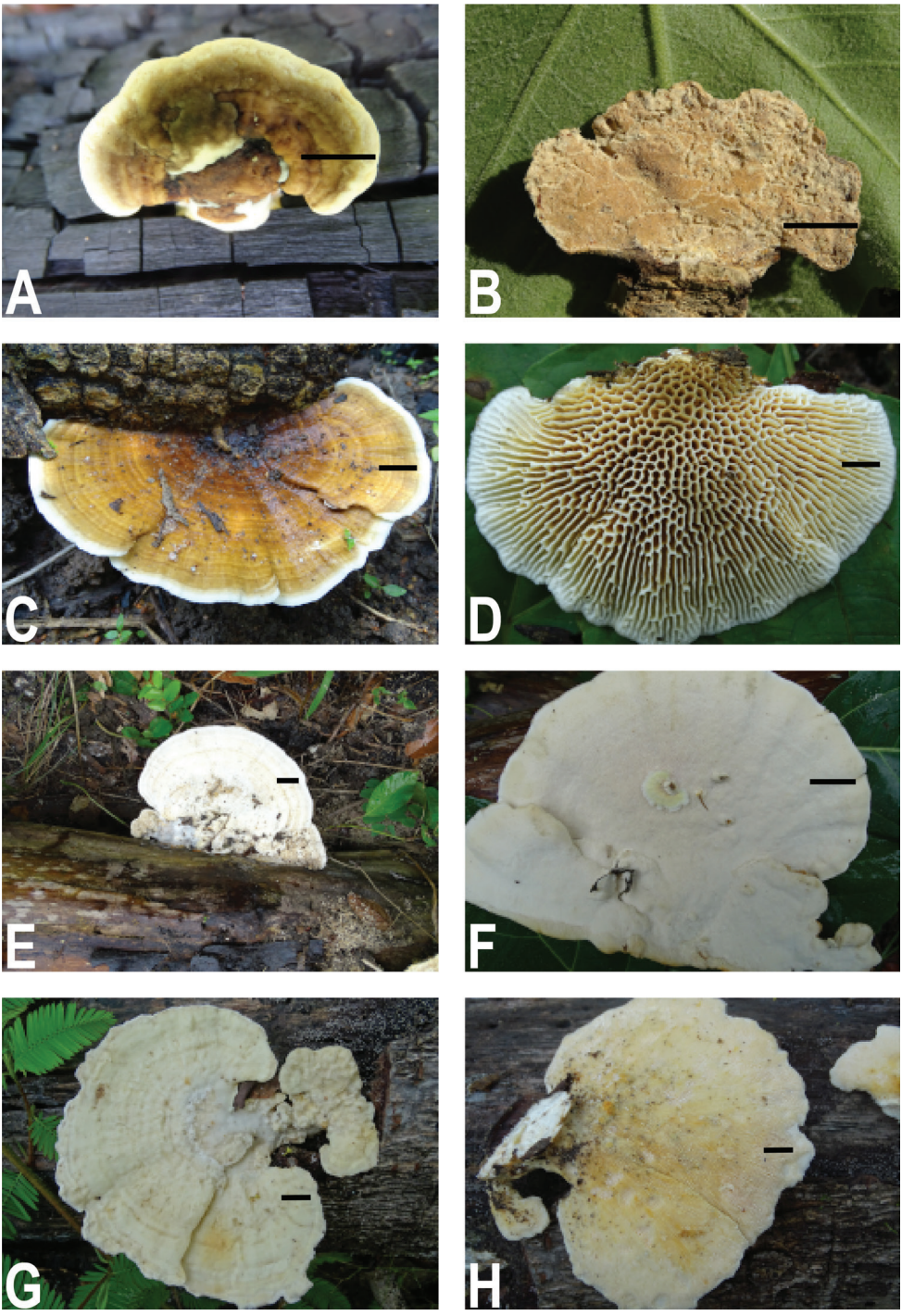

Figure 2. Macromorphology of *Trametes* species in Benin and specimen numbers in parentheses. **A** *Trametes cingulata* **B** hymenophore of *Trametes cingulata* (10) **C** *Trametes flavida* **D** hymenophore of *Trametes flavida* (05) **E** *Trametes lactinea* **F** hymenophore of *Trametes lactinea* (01) **G** *Trametes palisotii* **H** hymenophore of *Trametes palisotii* (04)

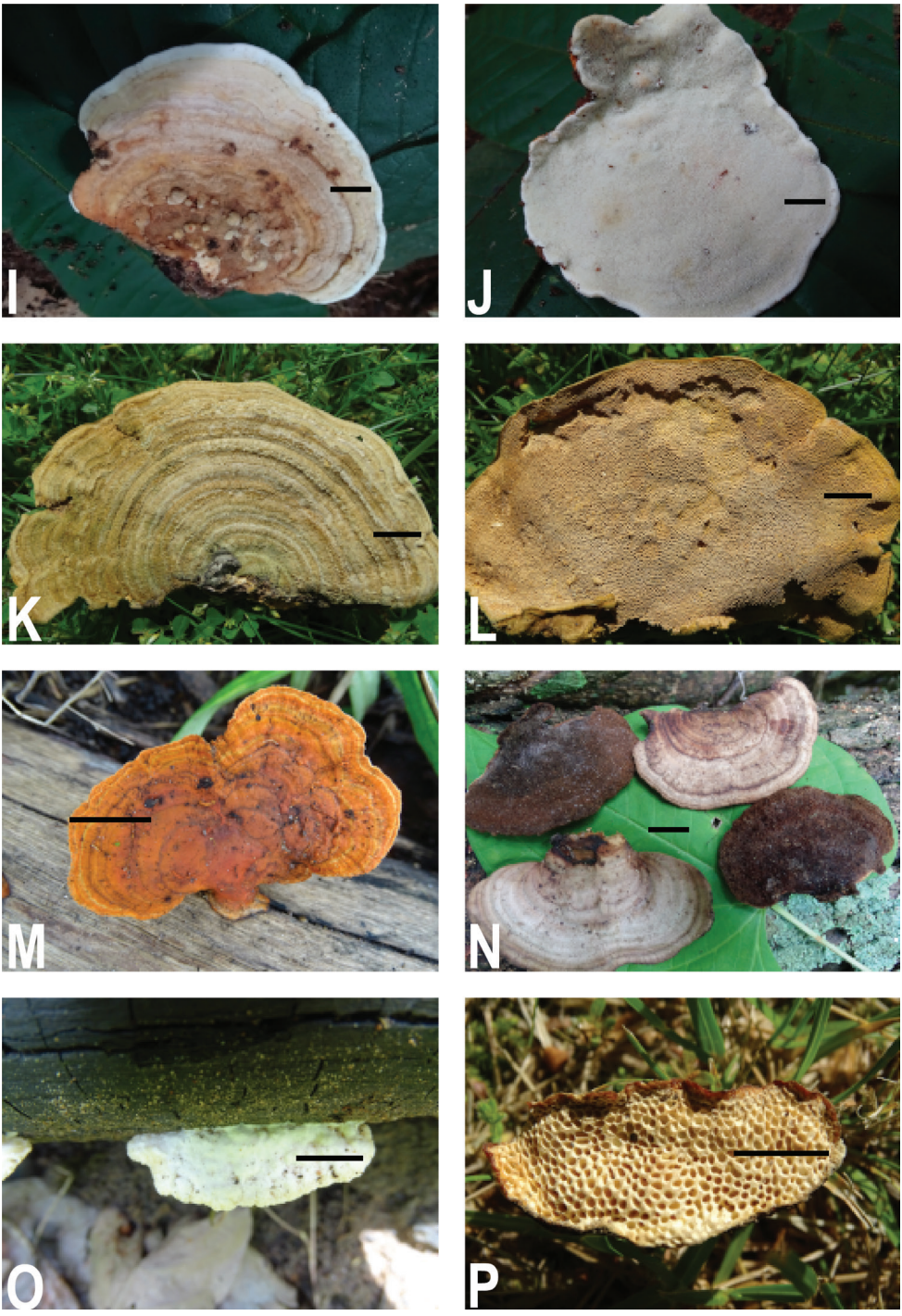

Figure 2. (Continued) **I** *Trametes parvispora* **J** hymenophore of *Trametes parvispora* (04) **K** *Trametes polyzona* **L** hymenophore of *Trametes polyzona* (06) **M** *Trametes sanguinea* (04) **N** *Trametes* aff. *versicolor* (01) **O** *Trametes socotrana* **P** hymenophore of *Trametes socotrana* (02). Scale bar corresponds to 1cm except in **E**, **F** where it corresponds to 2 cm.

netic trees were inspected in FigTree v. 1.4.2 (Rambaut 2014). All sequence alignments and phylogenetic trees generated in the study were deposited in TreeBASE: http://purl.org/phylo/treebase/phylows/study/TB2:S24354. The topologies of the consensus trees obtained from BY are presented in all figures throughout the document. Posterior probabilities (PP) and bootstrap values (BS) on or below branches as followed (PP/BS).

Microscopic analyses of specimens of the new species of *Trametes*

Macro-morphological descriptions were based on fresh and dried herbarium specimens. Microstructures are described using dried herbarium specimens. Fine sections through the basidiomata were prepared for observation using a razor blade under a stereomicroscope Leica EZ4 and mounted in 5% aqueous solution of potassium hydroxide (KOH) mixed with 1% aqueous solution of Phloxine. Melzer's reagent (to test for dextrinoid or amyloid reactions), Cotton Blue (to test for cyanophilic reaction) were used and then examined at a magnification of 1000× using a Leica DM500 light microscope. Measurements were done with the software "Makroaufmaßprogramm" from Jens Rüdigs (https://ruedig.de/tmp/messprogramm.htm) and analysed with the software "Smaff" version 3.2 (Wilk 2012). In total, 135 basidiospores were measured from the sequenced specimen OAB0022 and additional examined specimen OAB0268. The basidiospore size is given as length and width of the spore. As measurements we present the mean with standard deviation and minimum and maximum values in parentheses (see below). The length (L), arithmetic average of all spore lengths, and the width (W), arithmetic average of all spore widths, were calculated. In addition, the ratio of length/width (Q) was calculated.

Availability of data and materials

All alignments and phylogenetic trees generated in this study are available in TreeBASE under this link: http://purl.org/phylo/treebase/phylows/study/TB2:S24354. Newly generated sequences are available in GenBank, and the accession numbers are given in Table 1. Alignments, phylogenetic trees, and accession numbers of newly generated sequences will be public after the paper is published. Collected specimens are available at the mycological herbarium of the University of Parakou (UNIPAR). The new species was registered in mycoBank, and the registration number is given in the taxonomy section of this paper.

Abbreviations

a.s.l.	above sea level
BS	Bootstrap values
BY	Bayesian

ITS	Internal Transcribed Spacer
KAS	Mycological herbarium of the University of Kassel
L	Length
LSU	Large Subunit
MCMC	Markov chain Monte Carlo
ML	Maximum likelihood
*nr*DNA	nuclear ribosomal DNA
PP	Posterior probabilities
Q	Length to width ratio
RPB1	RNA polymerase II largest subunit
RPB2	RNA polymerase II second largest subunit
TEF1	Translation elongation factor 1-alpha
UNIPAR	Mycological herbarium of the University of Parakou

Results

Phylogenetic analyses of sequences of *Trametes* species from Benin

ITS dataset. The 25 ITS sequences obtained from *Trametes* spp. from Benin clustered in eight distinct clades (Suppl. material 2). All sequences of *Trametes* spp. from Benin fell into the monophyletic corresponding clades except the clade of *Trametes lactinea* (Berk.) Sacc., which, besides sequences of *T. lactinea*, accommodated also sequences of *Trametes cubensis* (Mont.) Sacc. with a very high support (BP = 1.00/BS = 100). Sequences of specimens of *Trametes* sp. (OAB0022 and OAB0023) from Benin formed a separated and well-supported clade within the *Trametes* clade (BP = 0.73/BS = 66).

ITS-LSU dataset. Results of ML and of BY show higher congruency, higher support values, and a higher number of resolved nodes than the results obtained with ITS data only. As evident by the ITS dataset, the sequence of *T. lactinea* from Benin clustered in addition to other sequences of *T. lactinea* retrieved from GenBank with sequences of *T. cubensis* with high support (BP = 1.00/BS = 92). Like in the analysis of the ITS dataset, sequences of *Trametes* sp. from Benin formed a distinct clade (Fig. 3). The two sequences of the new species of *Trametes* from Benin clustered in a distinct lineage within the *Trametes* clade (Figs 2I, J; 4). The clade of the *T. elegans* species complex is presented in the section below.

Phylogenetic placement of *Trametes elegans* from tropical Africa within the *Trametes elegans* species complex

The phylogenetic trees generated from individual gene regions ITS, RPB1, RPB2, and TEF1 (Suppl. material 3) and the combined datasets (Fig. 5) show similar results for phylogenetic relationships within the *T. elegans* species complex. Four distinct and

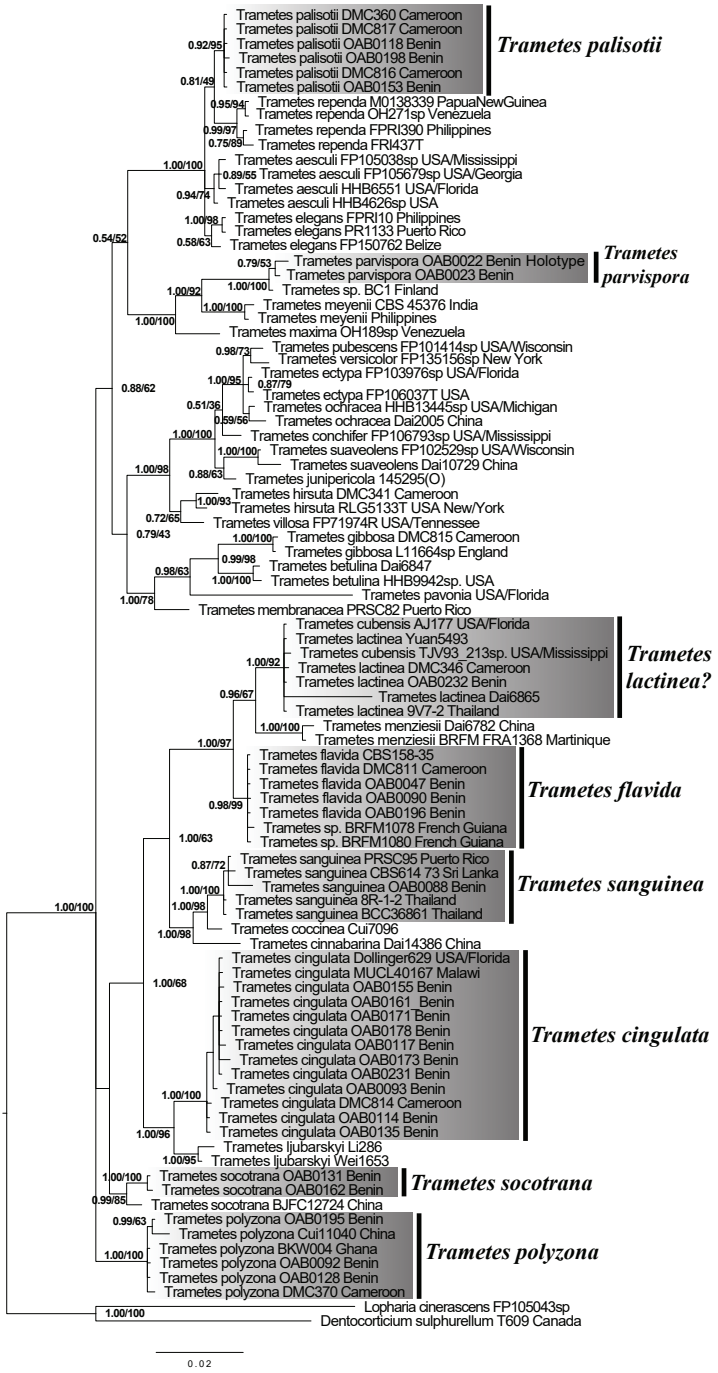

Figure 3. ML phylogeny of *Trametes* spp. based on combined ITS-LSU dataset. Branch support values given as PP/BS. All clades where newly generated sequences clustered are highlighted in grey and bars with names are given beside for more readability. Taxon names are followed by voucher or stain number and country of origin.

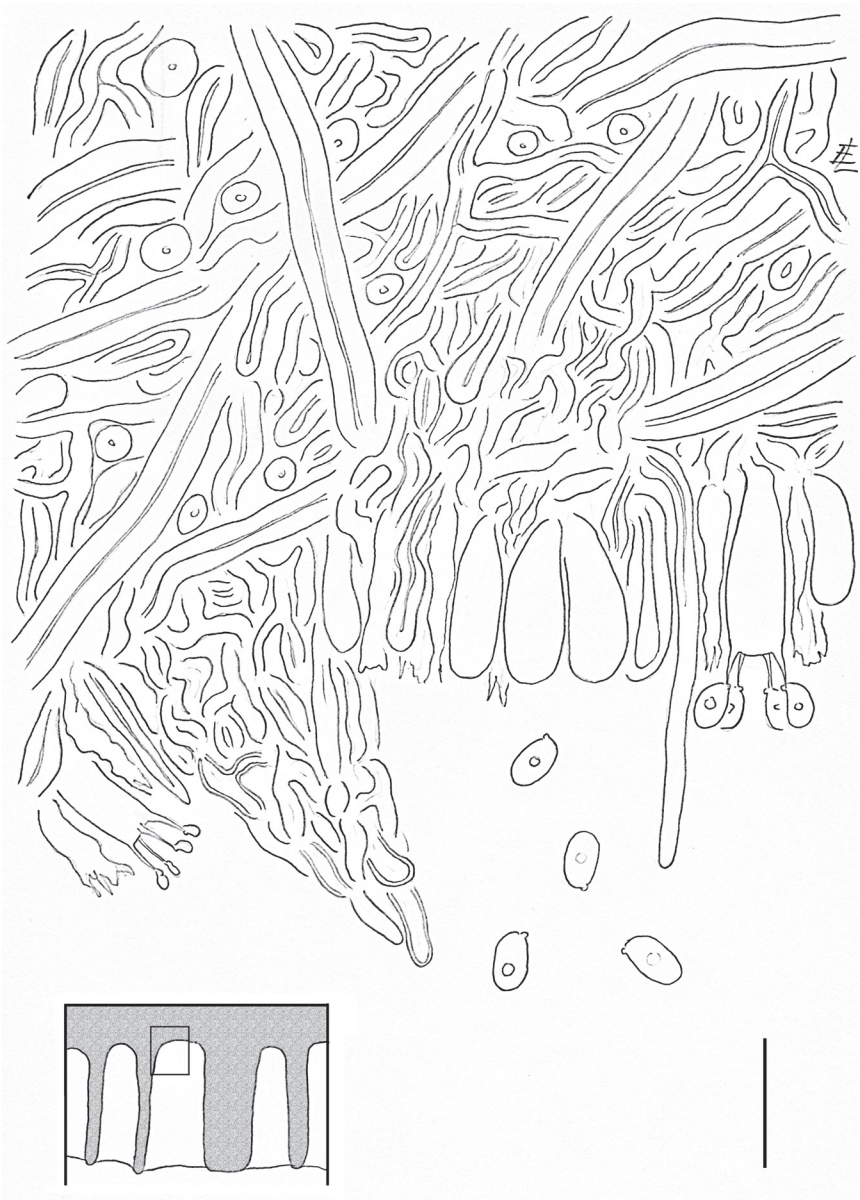

Figure 4. Crossection of the hymenium at the base of a pore of *Trametes parvispora*. Basidiospores, hyphae, basidia, basidioles, and a hyphal peg are showing. The box (lower left corner) shows the location (small rectangle) of the line drawing in the cross-section of the hymenophore. Scale bar = 10 μm

well-supported clades were evident in all datasets. The clade highlighted in grey (Fig. 5; Suppl. material 3) is distinct from all other clades within *T. elegans* species complex and highly supported in all individual gene and combined dataset. This clade contains only sequences of *T. elegans* from Benin and Cameroon.

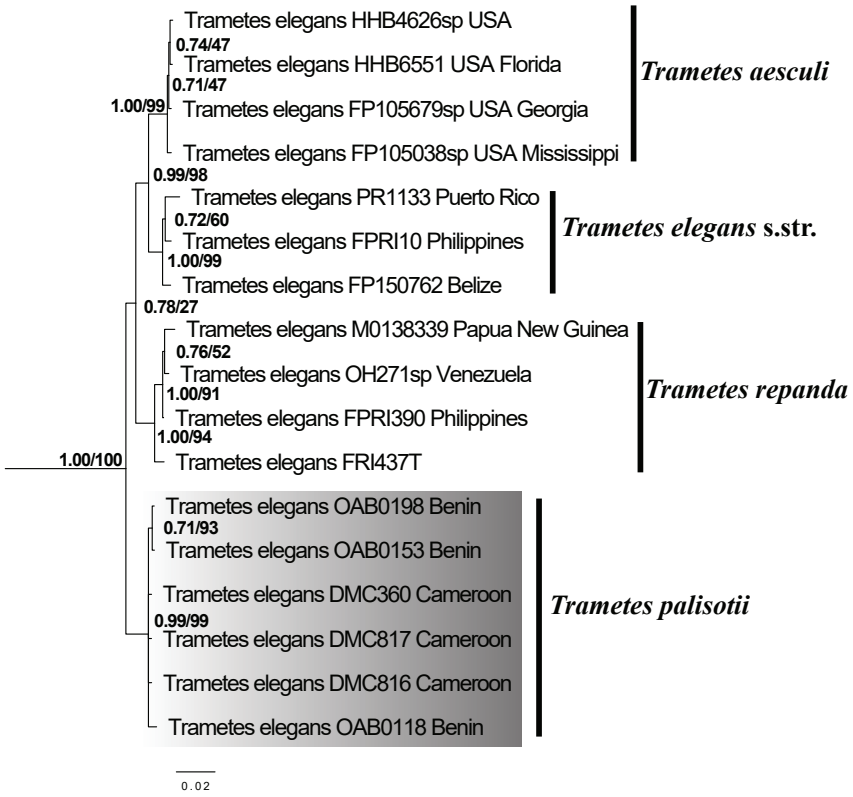

Figure 5. ML phylogeny of *Trametes elegans* species complex based on combined dataset of four-gene regions (ITS, RPB1, RPB2, TEF1). Branch support values given as PP/BS. Sequences of *T. elegans* from tropical Africa investigated in this study are highlighted in grey.

Taxonomy

Trametes parvispora **Olou, Yorou & Langer, sp. nov.**
MycoBank No: 830395
Figures 2I, J, 4

Diagnosis. *Trametes parvispora* differs from known species of *Trametes* in the combination of the following characteristics: daedaleoid hymenophore, context whitish, thin 1–1.5 mm, homogeneous, without black lines, small spores 3.2–4.6 × 2.1–2.8 µm, regular hyphal pegs 25–30 µm long, cystidia absent, abundance of basidioles, and basidia 12–15 × 3–5 µm.

Type. BENIN. Atlantic province, dry dense forest of Pahou in Ouidah, 6°23'2.97"N, 2°9'15.90"E, altitude: 33.1 m, on dead part of living tree of *Dialium guineense* Willd., leg. Boris A. Olou, sampling date: 21.07.2017, OAB0022 (dried specimen, holotype in UNIPAR and isotype in KAS). Holotype Sequences: ITS MK736989, LSU MK736964, and RPB2 MN127965

Etymology. *parvispora* (Lat.): referring to the small size of the spores.

Description. Basidiomata probably perennial, sessile, pileate, applanate, semicircular, up to 13 cm long and 8 cm wide, up to 2.5 cm thick at the base, coriaceous to woody and hard when dry, without odour or taste when fresh. Pileus surface dull, glabrous, and whitish, zonate, margin thick, obtuse. Pore surface whitish, daedaleoid**.** Context whitish, thin (1–1.5 mm), homogeneous, without black lines.

Hyphal system trimitic, generative hyphae hyaline branched with clamp connections, thin-walled, 1.5–2.0 µm in diameter, acyanophilous; skeletal hyphae solid to thick-walled, hyaline, non-septate, 3–4 µm in diameter, totally dominating in the context, acyanophilous, tissues unchanged in KOH, unbranched; binding hyphae very common in both the context and trama, hyaline, thick-walled, acyanophilous, and much branched.

Cystidia absent, but the branches of the binding hyphae may easily be mistaken for thick-walled cystidia in the hymenium unless a careful examination is undertaken. Hyphal pegs present, especially at the base of pores, and regular, 25–30 µm long.

Basidia 12–15 × 3–5 µm, clavate, tetrasterigmatic, sterigmata 3 µm long; Basidioles numerous, similar in shape to basidia but slightly smaller than basidia, up to 4 µm in diameter.

Basidiospores broadly ellipsoid, hyaline, thin-walled, smooth, usually with one guttule each, negative in Melzer's reagent, acyanophilous, (2.9)3.2–4.6(4.9) × 2.1–2.8(2.9) µm, L = 3.88 µm, W = 2.48 µm; Q = (1.17)1.24–1.91(2.05), Q = 1.57.

Ecology and distribution. Saprotrophic, on dead part of living tree *Dialium guineense* and only known from dry dense forest of Pahou in southern Benin.

Additional materials examined. BENIN. Atlantic province, dry dense forest of Pahou/ Ouidah, leg. Boris A. Olou, on dead wood of *D. guineense*, 21.07.2017, 6°23'3.07"N, 2°9'16.32"E, altitude 18.4 m a.s.l., OAB0023 (UNIPAR); on dead part of living tree of *D. guineense*, 6°23'2.49"N, 2°9'16.27"E, altitude 33.1 m a.s.l., 20.07.2018, OAB0267 (UNIPAR); at the same locality, 26.09.2018, OAB0268 (UNIPAR).

Discussion

Trametes spp. diversity in Benin

In Benin, seven species of *Trametes* were previously reported (Olou et al. 2019). By the present, study two additional species, namely *T. lactinea* and *T.* aff. *versicolor* (Fig. 2E, F, N), were recorded in addition to previous species. Thus, to our knowledge, nine species of *Trametes* are currently known for Benin. Of these nine species, only two species, *T. elegans* and *T. sanguinea*, were reported in Benin until 2002 (Yorou and De Kesel 2002). The remaining seven species, namely *T. cingulata*, *T. flavida*, *T. lactinea*, *T. parvispora*, *T. polyzona*, *T. socotrana*, and *T.* aff. *versicolor*, were recorded between 2017 and 2018. Given this history, it is most likely that more species will be found. Nonetheless, this number is significant when compared to the total diversity of 9–14 species of *Trametes* reported for Europe (Ryvarden and Gilbertson 1994; Ryvarden and Melo 2014). Further studies are needed to document the overall diversity of species of *Trametes* in Benin.

Phylogenetic positions of *Trametes* species of Benin

To place specimens of *Trametes* spp. from Benin in a larger phylogenetic context, we generated sequences of several genes. Generated sequences were placed into the phylogeny of the genus *Trametes* as established by Justo and Hibbett (2011). Eight distinct clades corresponding to eight different species were obtained from these sequences.

Our phylogenetic analyses from ITS and combined ITS-LSU datasets reveal sequence similarities and taxonomic misplacement within the clades of *T. flavida* and *T. lactinea* (Fig. 3; Suppl. material 2). The clade of *T. flavida* accommodated, in addition to sequences of *T. flavida*, sequences of *Trametes* sp. from French Guiana which is known as *Leiotrametes* sp. (Welti et al. 2012). This species was proposed as a new species by Welti et al. (2012). Here, *Trametes* sp. clustered together with *T. flavida* with high support in the ITS dataset (PP = 0.84/BS = 89) and the combined ITS-LSU datasets (PP = 0.98/BS = 99). Both species share also high morphological similarity (Welti et al. 2012; Fig. 2C, D) and a tropical distribution. We therefore suggest that *Trametes* sp. from French Guiana should not be considered as a new species but should be referred to as *T. flavida*. In addition to the *T. flavida* clade, our phylogenetic analyses showed that the *T. lactinea* clade contains not only sequences of *T. lactinea*, but also sequences of *T. cubensis* with high support in the ITS and ITS-LSU datasets (Fig. 3; Suppl. material 2). This result is similar to previous phylogenetic analyses on *Trametes* using the ITS marker (Justo and Hibbett 2011; Carlson et al. 2014). *Trametes lactinea* and *T. cubensis* are still valid names and both species share quite similar morphological characters. They are characterized by an applanate, broadly attached to dimidiate, white to cream basidiomata and a white to cream pore surface (Ryvarden and Johansen 1980; Gilbertson and Ryvarden 1987). Nevertheless, although both species are sharing quite similar morphological characters, they also differ in some characters. *Trametes. cubensis* is characterized by an annual basidioma, small pores, almost invisible to the naked eye, 5–7 per mm, and cylindrical basidiospores 7–9 × 3–3.5 µm (Gilbertson and Ryvarden 1987), while *T. lactinea* has an annual to perennial basidioma and large pores, which are visible to the naked eye, mostly 1.5–2 per mm, but can reach up to 3–4 (5) per mm in some specimens with cylindrical-ellipsoid basidiospores 4–7.5 × 2.2–3 µm (Ryvarden and Johansen 1980). Our specimen of *T. lactinea* (Fig. 2E, F) matches the morphological description of *T. lactinea* with 3–4 pores per mm, but we did not observe any spore despite numerous attempts. Thus, considering the result of our phylogenetic analyses, absence of spores in our *T. lactinea* specimen, and the high morphological similarity between species within *Trametes* (Gilbertson and Ryvarden 1987), we cannot reasonably distinguish *T. lactinea* from *T. cubensis*. Further morphological, chemotaxonomic, and molecular studies integrating proteins coding genes (e.g. RPB1, RPB2, and TEF1) are therefore needed to confirm whether *T. lactinea* and *T. cubensis* refer to the same species.

Previously the phylogenetic resolution of *T. cingulata* was problematic due to low sequence availability. Here we generated a total of 17 de novo sequences and show that *T. cingulata* appears as a monophyletic group within *Trametes* with high support in ITS

and combined ITS-LSU datasets respectively (PP = 1.00/BS = 97) and (PP = 1.00/BS = 100) (Fig. 3; Suppl. material 2). Thus, contrary to the uncertain position of *T. cingulata* within the genus *Trametes* (Welti et al. 2012), our results revealed that the latter does not belong to *Trametes* sensu stricto in the sense of Justo and Hibbett (2011) and Welti et al. (2012) (Fig. 3; Suppl. material 2) but rather to *Trametes* sensu lato.

Species diversity in the *Trametes elegans* species complex

The specimens from Benin identified as members of the *T. elegans* species complex correspond to the morphological descriptions of *T. elegans* by Gilbertson and Ryvarden (1987) and Ryvarden and Johansen (1980). The clades evident in all datasets within the *T. elegans* complex (Figs 3, 5; Suppl. material 2, 3) represent three clades previously attributed to three different species by Carlson et al. (2014), and a new clade highlighted in grey (Fig. 5; Suppl. material 3) represents specimens of *T. elegans* from Benin and Cameroon (Tropical Africa). This new clade contains only sequences of *T. elegans* from Benin and Cameroon due to the non-publication of most *T. elegans* sequences from tropical Africa (Olusegun 2015; Awala and Oyetayo 2016; Ueitele et al. 2018). Thus, prior to this study, only sequences of *T. elegans* from Cameroon and Gabon are available in GenBank for Africa. However, the sequences of *T. elegans* from Gabon (GenBank accession number: KY449397, KY449398) were not considered because they fell outside the *T. elegans* species complex and were instead closely related to *T. lactinea*. We, therefore, excluded these sequences from our analyses. All in all, since the sequences of *T. elegans* from tropical Africa investigated in this study are demarcated from sequences of *T. elegans* s. str., the adoption of another correct name for specimens of *T. elegans* from this area is necessary.

Specimens belonging to the *T. elegans* species complex have been reported in the past for tropical African countries (Ryvarden and Johansen 1980), with the first name applied to such specimens being *Daedalea amanitoides* P. Beauv., which was based on a specimen from Nigeria (cited as kingdom of Oware) (Palisot-Beauvois 1804). The morphological characteristics evident in the very short description and illustration of a fruiting body of *D. amanitoides* match the characteristics of the specimens examined in this study. However, for reasons that we ignore, Fries (1821) replaced this name (*D. amanitoides)* by the name *Daedalea palisotii* Fr., which is sanctioned and therefore must be used. The combination *Trametes palisotii* (Fr.) Imazeki (Imazeki 1952) is available and must be used for African specimens known previously as *T. elegans* (Fig. 5).

Phylogenetic position and taxonomy of the new species *Trametes parvispora*

The sequences belonging to the new species named *T. parvispora* form a distinct and well-supported clade in the ITS and the combined ITS-LSU datasets (Fig. 3; Suppl. material 2). This species forms a sister clade with the still formally undescribed *Tram-*

etes sp. (KT896651) from Finland. However, unlike *T. parvispora* where fruiting bodies were available for morphological characterization (Fig. 2I, J), the Finnish specimen was isolated as mycelium from the bark beetle *Ips typographus* L. (Linnakoski et al. 2016). Thus, anatomical and morphological comparisons are currently not possible. Furthermore, both sequences of *T. parvispora* share a clade with *Trametes meyenii* (Klotzsch) Lloyd. This clade was confirmed by phylogenetic analyses including two additional markers RPB1 and RPB2 (Suppl. material 4). *Trametes meyenii* has hispid and cream-yellow pilei, irpicoid and white to ochraceous hymenophore, pores 1–3 per mm, 4.5–6 × 2–2.5 µm basidiospores (Zmitrovich et al. 2012), whereas *T. parvispora* has glabrous and whitish pilei, a daedaleoid and white hymenophore, 3.2–4.6 × 2.1–2.8 µm basidiospores, and the presence of regular hyphal pegs (Figs 2I, J, 4). These morphological differences confirm that *T. parvispora* and *T. meyenii* are distinct species as shown by the phylogenetic analyses (Fig. 3; Suppl. material 2, 4). However, some species lacking DNA sequences, namely *Trametes barbulata* Corner, *Trametes daedaleoides* Corner, and *Trametes rugosituba* Corner (Corner 1989; Hattori 2005; Hattori and Sotome 2013), share with *T. parvispora* a quite similar spore size range. But the latter species differs from each other species by the combination of macro- and microscopic characteristics outlined above. Thus, the rare anatomic features of the regular hyphal pegs and the small size of the basidiospores together with the phylogenetic placement within the *Trametes* clade, provide enough evidence for *T. parvispora* as a distinct new species.

Acknowledgements

The research grant "Bi-nationally Supervised Doctoral Degrees" from the German Academic Exchange Services (DAAD) allowed for the stay of Boris Armel Olou in Germany while carrying out this study.

References

Awala SI, Oyetayo VO (2016) The Phytochemical and Antimicrobial Properties of the Extracts Obtained from Trametes Elegans Collected from Osengere in Ibadan, Nigeria. Jordan Journal of Biological Sciences 8(4): 289–99. https://doi.org/10.12816/0027065

Benson DA, Karsch-Mizrachi I, Clark K, Lipman DJ, Ostell J, Sayers EW (2011) GenBank. Nucleic Acids Research 40(D1): D48–D53. https://doi.org/10.1093/nar/gkq1079

Blagodatski A, Yatsunskaya M, MikhailovaV, Tiasto V, Kagansky A, Katanaev VL (2018) Medicinal mushrooms as an attractive new source of natural compounds for future cancer therapy. Oncotarget 9(49): 29259–29274. https://doi.org/10.18632/oncotarget.25660

Carlson A, Justo A, Hibbett DS (2014) Species delimitation in *Trametes*: a comparison of ITS, RPB1, RPB2 and TEF1 Gene Phylogenies. Mycologia 106(4): 735–745. https://doi.org/10.3852/13-275

Corner EJH (1989) Ad Polyporaceas VI. The genus *Trametes*. Beihefte zur Nova Hedwigia 97: 1–197.

Cruz A, Pimentel L, Rodríguez-Alcalá LM, Fernandes T, Pintado M (2016) Health benefits of edible mushrooms focused on *Coriolus versicolor*: a review. Journal of Food and Nutrition Research 4(12): 773–781. https://doi.org/10.1155/2016/9827369

Cui DZ, Zhao M, Yang HY, Wang Cl, Dai HB (2011) Molecular phylogeny of *Trametes* and related genera based on Internal Transcribed Spacer (ITS) and Nearly Complete Mitochondrial Small Subunit Ribosomal DNA (Mt SSU RDNA) sequences." African Journal of Biotechnology 10(79): 18111–18121. https://doi.org/10.5897/AJB10.1830

David A (1967) Caractères mycéliens de quelques *Trametes* (Polyporacées). Les Naturalistes Canadiens 94: 557–572.

Dörnte B, Kües U (2013) Fast microwave-based DNA extraction from vegetative mycelium and fruiting body tissues of Agaricomycetes for PCR amplification. Current Trends in Biotechnology and Pharmacy 7(4): 825–836.

Fries EM (1821) Systema Mycologicum, sistens Fungorum ordines, genera et species huc usque cognitas quas ad normas methodi naturalis deter- minavit, dispoduit atque descripsit. vol. 1: Vol. 1. Ex Officina Berlingiana, Greifswald, 520 pp. https://doi.org/10.5962/bhl.title.5378

Fries EM (1835) Corpus Florarum provincialium Sueciae I. Floram Scanicam. Typis Palmblad, Upsala, 349 pp. https://doi.org/10.5962/bhl.title.47083

Gardes M, Bruns TD (1993) ITS primers with enhanced specificity for Basidiomycetes—application to the identification of mycorrhizae and rusts. Molecular Ecology 2(2): 113–118. https://doi.org/10.1111/j.1365-294X.1993.tb00005.x

Gilbertson RL, Ryvarden L (1987) North American polypores: Megasporoporia – Wrightoporia. Vol. 2. Fungiflora, Oslo, 434–885.

Gomes-Silva AC, Ryvarden L, Gibertoni TB (2010). Notes on *Trametes* from the Brazilian Amazonia. Mycotaxon 113(1): 61–71. https://doi.org/10.5248/113.61

Hattori T (2005) Type studies of the polypores described by E.J.H. Corner from Asia and West Pacific areas. VII. Species described in *Trametes* (1). Mycoscience 46(5): 303–312. https://doi.org/10.1016/j.myc.2012.10.008

Hattori T, Sotome K (2013) Type studies of the polypores described by E.J.H. Corner from Asia and West Pacific areas VIII. Species described in *Trametes* (2). Mycoscience 54(4): 297–308. https://doi.org/10.1016/j.myc.2012.10.008

Imazeki R (1952) A contribution to the fungous flora of Dutch New Guinea. Bulletin of the Government Forest Experimental Station Meguro 57: 87–128.

Justo A, Hibbett DS (2011) Phylogenetic classification of *Trametes* (Basidiomycota, Polyporales) based on a five-marker dataset. Taxon 60(6): 1567–1583. https://doi.org/10.1002/tax.606003

Karsten PA (1881) Enumeratio Boletinearum et Polyporearum Fennicarum, systemate novo dispositarum. Revue mycologique, Toulouse 3(9): 16–19.

Katoh K, Rozewicki J, Yamada KD (2017) MAFFT online service: multiple sequence alignment, interactive sequence choice and visualization. Briefings in Bioinformatics 20(4): 1160–1166. https://doi.org/10.1093/bib/bbx108

Kavina C, Pilát A (1936) Atlas des champignons de l'Europe. Tome III, Polyporaceae I. Chez les éditeurs, Praha, 624 pp.

Kearse M, Moir R, Wilson A, Stones-Havas S, Cheung M, Sturrock S, Buxton S, Cooper A, Markowitz S, Duran C, Thierer T, Ashton B, Meintjes P, Drummond A (2012) Geneious

Basic: an integrated and extendable desktop software platform for the organization and analysis of sequence data. Bioinformatics 28 (12): 1647–1649.https://doi.org/10.1093/bioinformatics/bts199

Kotlaba F, Pouzar Z (1957) On the classification of European pore fungi. Ceska Mycol 11: 152–170.

Linnakoski R, Mahilainen S, Harrington A, Vanhanen H, Eriksson M, Mehtatalo L, Pappinen A, Wingfield MJ (2016) Seasonal succession of fungi associated with *Ips typographus* beetles and their phoretic mites in an outbreak region of Finland. PLoS ONE 11(5): 1–14. https://doi.org/10.1371/journal.pone.0155622

Liu YJ, Whelen S, Hall BD (1999) Phylogenetic relationships among ascomycetes: evidence from an RNA polymerse II subunit. Molecular Biology and Evolution 16: 1799–1808. https://doi.org/10.1093/oxfordjournals.molbev.a026092

Matheny PB (2005) Improving phylogenetic inference of mushrooms with RPB1 and RPB2 nucleotide sequences (*Inocybe*; Agaricales). Molecular Phylogenetics and Evolution 35: 1–20. https://doi.org/10.1016/j.ympev.2004.11.014

Matheny PB, Liu YJ, Ammirati JF, Hall BD (2002) Using RPB1 sequences to improve phylogenetic inference among mushrooms (*Inocybe*, Agaricales). American Journal of Botany 89: 688–698. https://doi.org/10.3732/ajb.89.4.688

Miller MA, Pfeiffer W, Schwartz T (2010) Creating the CIPRES Science Gateway for inference of large phylogenetic trees. In: 2010 Gateway Computing Environments Workshop, GCE 2010, IEEE, 1–8. https://doi.org/10.1109/GCE.2010.5676129

Murrill WA (1905) The Polyporaceae of North America: XI. A synopsis of the brown pileate species. Bulletin of the Torrey Botanical Club 32: 353–371. https://doi.org/10.2307/2478499

Olou BA, Yorou NS, Striegel M, Bässler C, Krah FS (2019) Effects of macroclimate and resource on the diversity of tropical wood-inhabiting fungi. Forest Ecology and Management 436: 79–87. https://doi.org/10.1016/j.foreco.2019.01.016

Olusegun OV. (2015) Molecular identification of *Trametes* species collected from Ondo and Oyo states, Nigeria. Jordan Journal of Biological Sciences 7: 165–169. https://doi.org/10.12816/0008234

Palisot-Beauvois AMFJ (1804) Flore d'Oware et de Benin en Afrique (2nd edn). Imprimerie de Fain et Compagnie, Paris, 464 pp. https://doi.org/10.5962/bhl.title.101798

Pieri M, Rivoire B (2007) Autour du genre *Trametes*. Bulletin de la Société Mycologique de France 123(1): 49–66.

Rambaut A (2014) FigTree, a graphical viewer of phylogenetic trees. http://tree.bio.ed.ac.uk/software/figtree

Rehner SA, Buckley E (2008) A *Beauveria* phylogeny inferred from nuclear ITS and EF1- sequences: evidence for cryptic diversification and links to *Cordyceps* teleomorphs. Mycologia 97: 84–98. https://doi.org/10.3852/mycologia.97.1.84

Ronquist F, Teslenko M, Van Der Mark P, Ayres DL, Darling A, Höhna S, Larget B, Liu L, Suchard MA, Huelsenbeck JP (2012) Mrbayes 3.2: efficient bayesian phylogenetic inference and model choice across a large model space. Systematic Biology 61: 539–542. https://doi.org/10.1093/sysbio/sys029

Ryvarden L (1991) Genera of polypores, nomenclature and taxonomy. Synopsis Fungorum. 5: 1–373.

Ryvarden L, Johansen I (1980) A preliminary polypore flora of East Africa. Fungiflora, Oslo, 636 pp.
Ryvarden L, Gilbertson RL (1994) European polypores. Part 2. Synopsis Fungorum 7: 394–743 pp.
Ryvarden L, Melo I (2014) Poroid Fungi of Europe. Fungiflora, Oslo, 431 pp.
Ryvarden L, Aime MC, Baroni TJ (2009) Studies in neotropical polypores 26. A new species of *Trametes* and revisitation of an old. Synopsis Fungorum 26: 27–32.
Stiller JW, Hall BD (1997) The origin of red algae: Implications for plastid evolution. Proceedings of the National Academy of Sciences 94: 4520–4525. https://doi.org/10.1073/pnas.94.9.4520
Ss V, Pandey M (2012) Physiological and cultivation requirements of *Trametes versicolor*, a medicinal mushroom to diversify Indian mushroom industry. Indian Journal of Agricultural Sciences 82: 672–675.
Stamatakis A (2014) RAxML Version 8: A tool for phylogenetic analysis and post-analysis of large phylogenies. Bioinformatics 30(9): 1312–1313. https://doi.org/10.1093/bioinformatics/btu033
Sukumaran J, Holder MT (2010) DendroPy: a python library for phylogenetic computing. Bioinformatics 26(12): 1569–1571. https://doi.org/10.1093/bioinformatics/btq228
Thiers B (2019) Index Herbariorum: a global directory of public herbaria and associated staff. New York Botanical Garden's Virtual Herbarium. http://sweetgum.nybg.org/ih [Accessed on: 2019-03-14; continuously updated]
Tomšovský M, Kolařík M, Pažoutová S, Homolka L (2006) Molecular phylogeny of European *Trametes* (Basidiomycetes, Polyporales) species based on LSU and ITS (nrDNA) sequences. Nova Hedwigia 82: 269–280. https://doi.org/10.1127/0029-5035/2006/0082-0269
Trifinopoulos J, Nguyen LT, von Haeseler A, Minh BQ (2016) W-IQ-TREE: a fast online phylogenetic tool for maximum likelihood analysis. Nucleic Acids Research 44: W232–W235. https://doi.org/10.1093/nar/gkw256
Ueitele IS, Kadhila-Muandingi NP, Chimwamurombe PM (2017) Ethnomycology of indigenous trametes mushrooms from northern Namibia. International Science Technology Journal of Namibia 9: 26–36.
Ueitele ISE, Chimwamurombe PM, Kadhila NP (2018) Molecular phylogeny of trametes and related genera from Northern Namibia. Jordan Journal of Biological Sciences 11: 99–105.
Vilgalys R, Hester M (1990) Rapid genetic identification and mapping of enzymatically amplified ribosomal DNA from several *Cryptococcus* species. Journal of bacteriology 172: 4238–4246. https://doi.org/10.1128/JB.172.8.4238-4246.1990
Vu D, Groenewald M, de Vries M, Gehrmann T, Stielow B, Eberhardt U, Al-Hatmi A, Groenewald JZ, Cardinali G, Houbraken J, Boekhout T, Crous PW, Robert V, Verkley GJM (2019) Large-scale generation and analysis of filamentous fungal DNA barcodes boosts coverage for kingdom fungi and reveals thresholds for fungal species and higher taxon delimitation. Studies in Mycology 92: 135–154. https://doi.org/10.1016/j.simyco.2018.05.001
Welti S, Moreau PA, Favel A, Courtecuisse R, Haon M, Navarro D, Taussac S, Lesage-Meessen L (2012) Molecular phylogeny of *Trametes* and related genera, and description of a new genus *Leiotrametes*. Fungal Diversity 55: 47–64. https://doi.org/10.1007/s13225-011-0149-2
White TJ, Bruns S, Lee S, JT (1990) Amplification and direct sequencing of fungal ribosomal RNA genes for phylogenetics. In: Innis MA, Gelfand DH, Sninsky JJ, White TJ (Eds) PCR Protocols: A Guide to Methods and Applications. Academic Press, New York: 315–322. https://doi.org/10.1016/B978-0-12-372180-8.50042-1

Wilk J (2012) Smaff – "Statistische Messreihen-Auswertung für Fungi v3.1." Südwestdeutsche Pilzrundschau 48: 49–56.

Wong AHH, Wilkes J (1988) Progressive changes in cell wall components of *Pinus radiata* during decay. International Biodeterioration 24: 481–487. https://doi.org/10.1016/0265-3036(88)90036-X

Zmitrovich IV., Ezhov ON, Wasser SP (2012) A survey of species of genus *Trametes* Fr. (Higher Basidiomycetes) with estimation of their medicinal source potential. International Journal of Medicinal Mushrooms 14: 307–319. https://doi.org/10.1615/IntJMedMushr.v14.i3.70

Yorou SN, De Kesel A (2002) Connaissances ethnomycologiques des peuples Nagot du centre du Bénin (Afrique de l'Ouest). Proceedings of XVI the AETFAT congress, Brussels 2000. Systematic and Geographic of Plants 71: 627–637. https://doi.org/10.2307/3668707

Supplementary material 1

Names, voucher numbers, and substrates of specimens of *Trametes* spp. collected in Benin

Authors: Boris Armel Olou, Franz-Sebastian Krah, Meike Piepenbring, Nourou Soulemane Yorou, Ewald Langer

Data type: species data

Link: https://doi.org/10.3897/mycokeys.65.47574.suppl1

Supplementary material 2

ML phylogeny of *Trametes* spp. based on a single gene region ITS

Authors: Boris Armel Olou, Franz-Sebastian Krah, Meike Piepenbring, Nourou Soulemane Yorou, Ewald Langer

Data type: phylogeny data

Explanation note: Support values are given as PP/BS. Newly generated sequences are highlighted in bold italic. Taxon names are followed by the voucher or stain numbers and the country of origin.

Link: https://doi.org/10.3897/mycokeys.65.47574.suppl2

Supplementary material 3

ML phylogeny of *Trametes elegans* species complex as recovered from four individual gene regions

Authors: Boris Armel Olou, Franz-Sebastian Krah, Meike Piepenbring, Nourou Soulemane Yorou, Ewald Langer

Data type: phylogeny data

Explanation note: Support values are given as PP/BS. Taxon names are followed by the voucher or stain numbers and the country of origin. The clade formed by the sequences of *T. elegans* from tropical Africa are highlighted in grey.

Link: https://doi.org/10.3897/mycokeys.65.47574.suppl3

Supplementary material 4

ML phylogeny of *Trametes parvispora*, based on two-gene dataset (RPB1, RPB2)

Authors: Boris Armel Olou, Franz-Sebastian Krah, Meike Piepenbring, Nourou Soulemane Yorou, Ewald Langer

Data type: phylogeny data

Explanation note: Support values given as PP/BS. Taxon names are followed by the voucher or stain numbers and the country of origin.

Link: https://doi.org/10.3897/mycokeys.65.47574.suppl4

MycoKeys 65: 49–99 (2020)
doi: 10.3897/mycokeys.65.47704
http://mycokeys.pensoft.net

RESEARCH ARTICLE

A peer-reviewed open-access journal
MycoKeys
Launched to accelerate biodiversity research

Citizen science project reveals high diversity in Didymellaceae (Pleosporales, Dothideomycetes)

Lingwei Hou[1,2*], Margarita Hernández-Restrepo[3*], Johannes Zacharias Groenewald[3], Lei Cai[1,2], Pedro W. Crous[3,4]

1 *State Key Laboratory of Mycology, Institute of Microbiology, Chinese Academy of Sciences, Beijing 100101, China* **2** *University of Chinese Academy of Sciences, Beijing 100049, China* **3** *Westerdijk Fungal Biodiversity Institute, Uppsalalaan 8, 3584 CT Utrecht, The Netherlands* **4** *Microbiology, Department of Biology, Utrecht University, Padualaan 8, 3584 CH Utrecht, The Netherlands*

Corresponding author: Lei Cai (cail@im.ac.cn); Pedro W. Crous (p.crous@wi.knaw.nl)

Academic editor: T. Lumbsch | Received 29 October 2019 | Accepted 17 December 2019 | Published 10 March 2020

Citation: Hou L, Hernández-Restrepo M, Groenewald JZ, Cai L, Crous PW (2020) Citizen science project reveals high diversity in Didymellaceae (Pleosporales, Dothideomycetes). MycoKeys 65: 49–99. https://doi.org/10.3897/mycokeys.65.47704

Abstract

Fungal communities play a crucial role in maintaining the health of managed and natural soil environments, which directly or indirectly affect the properties of plants and other soil inhabitants. As part of a Citizen Science Project initiated by the Westerdijk Fungal Biodiversity Institute and the Utrecht University Museum, which aimed to describe novel fungal species from Dutch garden soil, the diversity of Didymellaceae, which is one of the largest families in the Dothideomycetes was investigated. A preliminary analysis of the ITS and LSU sequences from the obtained isolates allowed the identification of 148 strains belonging to the family. Based on a multi-locus phylogeny of a combined ITS, LSU, *rpb2* and *tub2* alignment, and morphological characteristics, 20 different species were identified in nine genera, namely *Ascochyta*, *Calophoma*, *Didymella*, *Juxtiphoma*, *Nothophoma*, *Paraboeremia*, *Phomatodes*, *Stagonosporopsis*, and *Xenodidymella*. Several isolates confirmed to be ubiquitous plant pathogens or endophytes were for the first time identified from soil, such as *Ascochyta syringae*, *Calophoma clematidis-rectae*, and *Paraboeremia litseae*. Furthermore, one new genus and 12 novel species were described from soil: *Ascochyta benningiorum* **sp. nov.**, *Didymella degraaffiae* **sp. nov.**, *D. kooimaniorum* **sp. nov.**, *Juxtiphoma kolkmaniorum* **sp. nov.**, *Nothophoma brennandiae* **sp. nov.**, *Paraboeremia rekkeri* **sp. nov.**, *P. truiniorum* **sp. nov.**, *Stagonosporopsis stuijvenbergii* **sp. nov.**, *S. weymaniae* **sp. nov.**, *Vandijckomycella joseae* **gen. nov. et sp. nov.**, *V. snoekiae* **sp. nov.**, and *Xenodidymella weymaniae* **sp. nov**. From the results of this study, soil was revealed to be a rich substrate for members of Didymellaceae, several of which were previously known only from diseased or apparently healthy plant hosts.

* Contributed equally as the first authors

Keywords
biodiversity, new taxa, *Phoma*, phylogeny, soil-borne fungi

Introduction

Due to high plasticity and the capacity to adapt and survive in adverse or unfavourable conditions, fungi are exceedingly successful soil inhabitants (Frąc et al. 2018). The majority of the fungal species presently known can survive in, or directly adapt to, the soil environment (Bridge and Spooner 2001; Botha 2011). Soil-borne fungi play essential roles in nutrient cycling in terrestrial ecosystems and are able to break down all kinds of organic matter, decompose soil components or act as effective biosorbents of toxic metals, thereby helping to maintain soil health (Anderson and Domsch 1973; Bender et al. 2013; Rudgers et al. 2014; Tedersoo et al. 2014; Yang et al. 2017; Frąc et al. 2018). Soil fungal communities also form symbiotic associations with plants, thereby improving nutrient absorption (Voøíšková and Baldrian 2012). Most fungal taxa found in the soil are continuously present in the environment as harmless saprobic organisms, but some also play a negative role. For instance, plant pathogenic fungi in soil could infect seedlings or other plant tissues when conditions are suitable, resulting in significant damage (van Agtmaal et al. 2017). In addition, some fungi reside in soil in the form of propagules to survive in an unsuitable environment, posing a long-term threat to other inhabitants (Maryani et al. 2019).

Didymellaceae is a ubiquitous fungal family including saprobic, endophytic and pathogenic species (Aveskamp et al. 2008, 2010; Marin-Felix et al. 2017). More than 50% of the species in this family have been reported as plant pathogens, causing great losses to a wide range of economic crops (Aveskamp et al. 2008). Other species are found in different substrates, including soil, air, and water or cyst nematodes (Dorenbosch 1970; Chen et al. 1996; Boerema et al. 2004; Aveskamp et al. 2010; Porras-Alfaro et al. 2011; Chen et al. 2015, 2017; Grishkan 2018; Valenzuela-Lopez et al. 2018), and even in some extreme environments such as deep-sea sediments, or soils in Antarctica, deserts, and karst caves (Ruisi et al. 2007; Li et al. 2016; Zhang et al. 2016a, 2016b, 2017; Chen et al. 2017; Nagano et al. 2017; Grishkan 2018). Although recent research has suggested that the soil environment represents an important niche for the discovery of novel phoma-like species (Chen et al. 2017, van Agtmaal et al. 2017), very few studies have investigated the diversity of Didymellaceae in soil, which is a massive reservoir for plant, animal and human pathogens.

The first paper systematically investigating Didymellaceae species from soil was published by Dorenbosch (1970), who provided diagnostic characteristics and a usable identification method (keys) for nine ubiquitous phoma-like fungi from soil, including *Pyrenochaeta acicola*, *Phoma chrysanthemicola*, *Ph. eupyrena*, *Ph. exigua*, *Ph. fimeti*, *Ph. glomerata*, *Ph. herbarum*, *Ph. medicaginis* var. *pinodella*, and *Ph. prunicola* (names used at that time). Later, Boerema et al. (2004) and Domsch et al. (2007) illustrated several Didymellaceae species from soil and provided their ecological distributions. Since then,

a few species have been reported sporadically, along with the research of root and seed diseases, but studies of Didymellaceae from soil are still rare, with even fewer describing new taxa from soil. Most species in previous studies have been reallocated to other genera in this family based on their DNA phylogeny (Chen et al. 2015, 2017; Valenzuela-Lopez et al. 2018). To date, only approximately 30 species from eight genera in Didymellaceae have been recorded from soil, namely *Ascochyta*, *Phoma*, *Didymella*, *Neodidymelliopsis*, *Epicoccum*, *Cumuliphoma*, *Ectophoma* and *Juxtiphoma* (Dorenbosch 1970; Boerema et al. 2004; Domsch et al. 2007; Chen et al. 2017; Valenzuela-Lopez et al. 2018). Although most of the species documented from soil are plant-associated (pathogens and endophytes), some species, such as *Ph. herbarum* and *J. eupyrena*, are characterised as soil-borne (Dorenbosch 1970; Boerema et al. 2004).

Didymellaceae species from soil always produce diverse metabolites, some of which can be cytotoxic, including cytochalasin A and B, deoxaphomin, proxiphomin and tenuazonic acid (Bennett et al. 2018). Currently, most Didymellaceae species thus far found in the soil environment were originally described from plant substrates, such as leaves, seedlings, wood, stem bases or roots, some of which are even capable of wood decay (Boerema et al. 2004; Aveskamp et al. 2008, 2010; Chen et al. 2015). On the contrary, crops that are grown in close proximity to infected soil appear to be more contaminated, given that soil is a known source of plant pathogenic fungi (Paterson and Lima 2017). Besides, some species have also been reported to be opportunistic pathogens in animals and humans, such as *J. eupyrena* (= *Phoma eupyrena*) and *Phoma herbarum* (Bakerspigel et al. 1981; Tullio et al. 2010). Considering the potential threat and great losses caused by soil-borne pathogens, and the application in the biotechnological or pharmaceutical industries, knowledge of the diversity of Didymellaceae in soil is urgently needed to better understand the functions, interactions and ecosystem feedback of fungi in the terrestrial environment.

The present Citizen Science Project was initiated by the Westerdijk Fungal Biodiversity Institute (WI) and the Utrecht University Museum, aiming to investigate the diversity of fungi in Dutch garden soil collected by children in their home gardens from different regions in the Netherlands (Groenewald et al. 2018). During the course of this project thousands of isolates were obtained from 293 soil samples. Of these, 148 isolates were found to belong to Didymellaceae, and subsequently selected for study. The aim of the present study was to investigate the diversity of Didymellaceae from Dutch garden soil, describe and illustrate novel species, and compare them with known and related species.

Materials and methods

Sampling and isolation

Protocols for the collection and processing of soil samples are described in Groenewald et al. (2018) and Giraldo et al. (2019). Isolates are maintained in the Johanna Wester-

dijk (**JW**) working collection housed at the **WI** in Utrecht, the Netherlands. New and interesting strains were also deposited in the **CBS** fungal collection and holotypes in the fungarium at the **WI**, respectively.

DNA extraction, PCR amplification and sequencing

Genomic DNA was extracted using the Wizard® Genomic DNA Purification Kit (Promega, Madison, USA) following the manufacturer's protocols. Initially, the internal transcribed spacer regions 1 and 2 and 5.8S nuclear ribosomal RNA gene (ITS) and partial large subunit nrDNA (LSU) were amplified using primer pairs ITS5/ITS4 (White et al. 1990) and LR0R/LR5 (Vilgalys and Hester 1990; Vilgalys and Sun 1994), respectively. For members of Didymellaceae two extra loci were amplified, the partial beta-tubulin (*tub2*) and the partial RNA polymerase II second largest subunit (*rpb2*), using the primer pairs Tub2Fd/Tub4Rd (Woudenberg et al. 2009) and Rpb2-5F2/Rpb2-7cR (Liu et al. 1999; Sung et al. 2007), respectively. The PCR amplifications were performed following Chen et al. (2015), except for *rpb2*, which was amplified in a total volume of 12.5 µL containing 1.25 µL of 10× EasyTaq Buffer (Bioline, Luckenwalde, Germany), 0.5 µL of dNTPs (40 µM), 0.5 µL of $MgCl_2$ (2 mM), 0.5 µL of bovine berum albumin (BSA, 1 µg/µL), 0.5 µL of each primer (0.2 µM), 0.1 µL of Taq DNA polymerase (Bioline) and 1 µL of genomic DNA. PCR conditions for *rpb2* were set as follows: an initial denaturation at 94 °C for 5 min; 35 cycles of denaturation at 95 °C for 45 s, annealing at 55 °C for 80 s and extension at 72 °C for 2 min; and a final extension step at 72 °C for 10 min. The PCR products were sequenced according to the methods of Crous et al. (2013). Consensus sequences were assembled from forward and reverse sequences using Seqman Pro v.12.1.0 (DNASTAR, Madison, WI, USA). All sequences generated in this study were deposited in GenBank (Table 1).

Selection of Didymellaceae strains

A preliminary species identification of the strains was carried-out by a BLASTn search performed with each ITS and/or LSU sequence against the NCBI (http://blast.ncbi.nlm.nih.gov) and WI (http://www.westerdijkinstitute.nl/Collections) databases. The ITS and/or LSU sequences generated in this study with more than 98 % similarity with reference sequences for Didymellaceae were selected for further study (Table 1).

Sequence alignment and molecular phylogenetic analysis

To further study the phylogenetic relationships, reference sequences of Didymellaceae were downloaded from GenBank (Table 1). Sequences of single loci were aligned with MAFFT v.7 using default settings (Katoh et al. 2017), and manually edited in MEGA

v.6.0 when necessary (Tamura et al. 2013). MrModeltest v.2.3 (Nylander 2004) was used to select the best-fit models of evolution for the four data partitions according to the Akaike information criterion. Bayesian inference (BI), maximum-likelihood (ML) and maximum parsimony (MP) methods were implemented for phylogenetic analysis of individual gene regions and the combined dataset. The multi-locus gene dataset was generated using SequenceMatrix v.1.8 (Vaidya et al. 2011).

Bayesian analyses were performed using MrBayes v.3.2.6 (Ronquist et al. 2012) as described by Chen et al. (2015). The burn-in fraction was set to 0.25, after which the 50 % majority rule consensus trees and posterior probability (PP) values were calculated. The ML analyses including 1000 bootstrap replicates were conducted using RAxML v.7.2.6 (Stamatakis and Alachiotis et al. 2010) as described by Chen et al. (2015). Statistical support for the branches was evaluated using a bootstrap analysis (BS) of 1000 replicates. MP analyses were carried out using PAUP v.4.0b10 (Swofford 2003) as described by Braun et al. (2018). Statistical support for the branches was evaluated using a bootstrap analysis (PBS) of 1000 replicates. Trees were visualised in FigTree v.1.4.0 (Rambaut 2014) and the layout was created in Adobe Illustrator. Alignments and phylogenetic trees derived from this study were uploaded to TreeBASE (www.treebase.org) and sequences deposited in GenBank (Table 1).

Morphological characterisation

Isolates of Didymellaceae were transferred to fresh oatmeal agar (OA), 2 % malt extract agar (MEA) and potato dextrose agar (PDA) (Crous et al. 2019) plates and incubated at 25 °C under near-ultraviolet (UV) light (12 h light/12 h dark) to induce sporulation. Colony diameters were measured after 7 d of incubation (Boerema et al. 2004), and macroscopic characters and colony colours were described after 14 days of incubation and rated according to the colour charts of Rayner (1970). Preparations were mounted in distilled water to study the micro-morphological structures of mature conidiomata, conidiogenous cells and conidia from OA cultures (Aveskamp et al. 2010; Chen et al. 2015). Morphological observations included the general characteristics of the conidiomata, shape, presence of mycelium/setae on conidiomata, number of ostioles, thickness and texture of the pycnidial wall, length and width of the conidiogenous cells and conidia. To study the pycnidial wall, sections of mature conidiomata were generated using a Leica CM 1900 freezing microtome (Aveskamp et al. 2010; Chen et al. 2015). Observations of micro-morphological characteristics were processed with a Nikon Eclipse 80i compound microscope with differential interference contrast (DIC) optics and a Nikon AZ100 dissecting microscope, both equipped with a Nikon DS-Ri2 high-definition colour digital camera (Nikon, Tokyo, Japan) using NIS-elements imaging software v.4.3. The NaOH spot test was carried out using a drop of concentrated NaOH to determine the secretion of metabolite E on OA cultures (Boerema et al. 2004). Morphological descriptions and taxonomic information for the new taxa were deposited in MycoBank (Crous et al. 2004).

Table 1. Taxa used in this study and their GenBank accession numbers.

Taxon name[1]	Strain number[2]	Substrate	Country	GenBank Accession numbers[3]			
				rpb2	***tub2***	**ITS**	**LSU**
Allophoma cylindrispora	CBS 142453^{T}; FMR 13723	Human superficial tissue	USA	LT593058	LT592989	LN907376	LT592920
Al. nicaraguensis	CBS 506.91^{T}; IMI 215229; PD 91/876	*Coffea* sp.	Nicaragua	KT389551	GU237596	GU238058	GU237876
Al. piperis	CBS 268.93^{T}; PD 88/720	*Peperomia pereskifolia*	The Netherlands	KT389554	GU237644	GU238129	GU237816
Al. tropica	CBS 436.75^{T}	*Saintpaulia ionantha*	Germany	KT389556	GU237663	GU238149	GU237864
Ascochyta benningiorum	**CBS 144957^{T}; JW 196005**	Garden soil	The Netherlands	**MN824606**	**MN824755**	**MN823432**	**MN823581**
	CBS 144958; JW 196023	Garden soil	The Netherlands	**MN824607**	**MN824756**	**MN823433**	**MN823582**
	JW 196013	Garden soil	The Netherlands	**MN824608**	**MN824757**	**MN823434**	**MN823583**
A. boeremae	CBS 372.84^{T}; PD 80/1246	*Pisum sativum*	Australia	–	KT389774	KT389697	KT389480
	CBS 373.84; PD 80/1247	*Pisum sativum*	Australia	KT389560	KT389775	KT389698	KT389481
A. fabae	CBS 649.71	*Vicia faba*	The Netherlands	–	GU237527	GU237964	GU237902
	CBS 524.77	*Phaseolus vulgaris*	Belgium	–	GU237526	GU237963	GU237880
	PD 83/492	*Phaseolus vulgaris*	The Netherlands	–	GU237528	GU237965	GU237917
A. herbicola	CBS 629.97^{R}; PD 76/1017	Water	USA	KP330421	GU237614	GU238083	GU237898
A. lentis	CBS 370.84; PD 81/783	*Lens culinaris*	Unknown	–	KT389768	KT389691	KT389474
A. medicaginicola var. *macrospora*	CBS 112.53^{T}	*Medicago sativa*	USA	–	GU237628	GU238101	GU237749
	CBS 404.65^{R}; IMI 116999	*Medicago sativa*	Canada	KP330423	GU237629	GU238102	GU237859
A. nigripycnidia	CBS 116.96^{T}; PD 95/7930	*Vicia cracca*	Russia	–	GU237637	GU238118	GU237756
A. phacae	CBS 184.55^{T}	*Phaca alpina*	Switzerland	–	KT389769	KT389692	KT389475
A. pisi	CBS 126.54	*Pisum sativum*	The Netherlands	DQ677967	GU237531	EU754137	GU237772
	CBS 122785^{T}; PD 78/517	*Pisum sativum*	The Netherlands	–	GU237532	GU237969	GU237763
	CBS 122751; ATCC 201620	*Pisum sativum*	Canada	EU874867	KP330388	KP330444	KP330432
A. rabiei	CBS 534.65	*Cicer arietinum*	India	KP330405	GU237533	GU237970	GU237886
	CBS 237.37^{T}	*Cicer arietinum*	Bulgaria	–	KT389773	KT389696	KT389479
A. syringae	CBS 545.72	*Syringa vulgaris*	The Netherlands	–	KT389777	KT389700	KT389483
	JW 1074	Garden soil	The Netherlands	**MN824605**	**MN824754**	**MN823431**	**MN823580**
A. versabilis	CBS 876.97^{R}	*Silene* sp.	The Netherlands	KT389561	GU237664	GU238152	GU237909
A. viciae	CBS 451.68	*Vicia sepium*	The Netherlands	KT389562	KT389778	KT389701	KT389484
A. viciae-pannonicae	CBS 254.92	*Vicia pannonica*	Czech Republic	–	KT389779	KT389702	KT389485
Boeremia exigua var. *heteromorpha*	CBS 443.94^{T}	*Nerium oleander*	Italy	KT389573	GU237497	GU237935	GU237866

Taxon name[1]	Strain number[2]	Substrate	Country	GenBank Accession numbers[3]			
				rpb2	*tub2*	ITS	LSU
B. exigua var. *populi*	CBS 100167^{T}; PD 93/217	*Populus*(×)*euramericana*	The Netherlands	–	GU237501	GU237939	GU237707
Briansuttonomyces eucalypti	CBS 114879^{T}	*Eucalyptus* sp.	South Africa	–	KU728595	KU728519	KU728479
	CBS 114887	*Eucalyptus* sp.	South Africa	–	KU728596	KU728520	KU728480
Calophoma clematidina	CBS 102.66	*Clematis* sp.	UK	KT389587	FJ427099	FJ515630	FJ426988
	CBS 108.79^{T}; PD 78/522	*Clematis* sp.	The Netherlands	KT389588	FJ427100	FJ515632	FJ426989
C. clematidis-rectae	JW 179007	Garden soil	The Netherlands	**MN824612**	**MN824761**	**MN823438**	**MN823587**
	CBS 507.63	*Clematis* sp.	The Netherlands	KT389589	FJ515624	FJ515647	FJ515606
C. vodakii	CBS 173.53^{T}	*Hepatica triloba*	Switzerland	–	KT389791	KT389714	KT389497
Coniothyrium palmarum	CBS 400.71	*Chamaerops humilis*	Italy	KT389592	KT389792	EU754153	AY720708
Cumuliphoma indica	CBS 654.77^{T}; FMR 15341	Unknown	India	LT623261	FJ427153	GU238122	FJ427043
Cu. omnivirens	CBS 341.86^{T}; FMR 14915	*Phaseolus vulgaris*	Belgium	LT62326	FJ427152	LT623214	FJ427042
Cu. pneumoniae	CBS 142454^{T}; FMR13739	Human respiratory tract	USA	LT593063	LT592994	LN907392	LT592925
Didymella aeria	CGMCC 3.18353^{T}; LC 7441	Air	China	KY742137	KY742293	KY742205	KY742051
D. aliena	LC 8121	*Pyrus calleryana*	Italy	–	KY742295	KY742207	KY742053
	CBS 379.93; PD 82/945	*Berberis* sp.	The Netherlands	KP330416	GU237578	GU238037	GU237851
D. americana	CBS 185.85^{R}; PD 80/1191	*Zea mays*	USA	KT389594	FJ427088	GU237990	FJ426972
D. anserina	CBS 360.84^{R}	Potato flour	The Netherlands	KT389596	GU237551	GU237993	GU237839
D. aquatica	CGMCC 3.18349^{T}; LC 5556	Water	China	KY742140	KY742297	KY742209	KY742055
D. arachidicola	CBS 333.75^{T}; ATCC 28333; IMI 386092	*Arachis hypogaea*	South Africa	KT389598	GU237554	GU237996	GU237833
D. aurea	CBS 269.93^{T}; PD 78/1087	*Medicago polymorpha*	New Zealand	KT389599	GU237557	GU237999	GU237818
D. bellidis	CBS 714.85^{R}; PD 74/265	*Bellis perennis*	The Netherlands	KP330417	GU237586	GU238046	GU237904
D. boeremae	CBS 109942^{T}; PD 84/402	*Medicago littoralis* cv. *harbi*	Australia	KT389600	FJ427097	GU238048	FJ426982
D. brunneospora	CBS 115.58^{T}; FMR 15745	*Chrysanthemum roseum*	Germany	KT389625	KT389802	KT389723	KT389505
D. calidophila	CBS 448.83^{T}	Desert soil	Egypt	–	FJ427168	GU238052	FJ427059
D. chenopodii	CBS 128.93^{R}; PD 79/140	*Chenopodium quinoa* cv. *sajana*	Peru	KT389602	GU237591	GU238055	GU237775
D. chloroguttulata	CGMCC 3.18351^{T}; LC 7435	Air	China	KY742142	KY742299	KY742211	KY742057
D. coffeae-arabicae	CBS 123380^{T}; PD 84/1013	*Coffea arabica*	Ethiopia	KT389603	FJ427104	GU238005	FJ426993
D. dactylidis	CBS 124513^{T}; PD 73/1414	*Dactylis glomerata*	USA	–	GU237599	GU238061	GU237766
D. degraaffiae	**CBS 144956^{T}; JW 195004**	Garden soil	The Netherlands	**MN824470**	**MN824618**	**MN823295**	**MN823444**
D. dimorpha	CBS 346.82^{T}	*Opuntia phyllocladium*	Spain	–	GU237606	GU238068	GU237835
D. ellipsoidea	CGMCC 3.18350^{T}; LC 7434	Air	China	KY742145	KY742302	KY742214	KY742060

Taxon name[1]	Strain number[2]	Substrate	Country	GenBank Accession numbers[3]			
				rpb2	***tub2***	**ITS**	**LSU**
D. eucalyptica	CBS 377.91^{R}; PD 79/210	*Eucalyptus* sp.	Australia	KT389605	GU237562	GU238007	GU237846
D. exigua	CBS 183.55^{T}	*Rumex arifolius*	France	EU874850	GU237525	EU754155	GU237794
D. gardeniae	CBS 626.68^{T}; IMI 108771	*Gardenia jasminoides*	India	KT389606	FJ427114	GQ387595	FJ427003
D. glomerata	CBS 528.66^{R}; PD 63/590	*Chrysanthemum* sp.	The Netherlands	GU371781	FJ427124	EU754184	FJ427013
D. heteroderae	CBS 109.92^{T}; PD 73/1405	Undefined food material	The Netherlands	KT389601	FJ427098	GU238002	FJ426983
D. ilicicola	CGMCC 3.18355^{T}; LC 8126	*Ilex chinensis*	Italy	KY742150	KY742307	KY742219	KY742065
D. infuscatispora	CGMCC 3.18356^{T}; LC 8128	*Chrysanthemum indicum*	China	KY742152	KY742309	KY742221	KY742067
D. keratinophila	CBS 143032^{T}; FMR 13690	Human superficial tissue	USA	LT593039	LT592970	LN907343	LT592901
D. kooimaniorum	**CBS 144951^{T}; JW 27006**	Garden soil	The Netherlands	**MN824474**	**MN824622**	**MN823299**	**MN823448**
D. lethalis	CBS 103.25	Unknown	Unknown	KT389607	GU237564	GU238010	GU237729
D. macrophylla	CGMCC 3.18357^{T}; LC 8131	*Hydrangea macrophylla*	Italy	KY742154	KY742312	KY742224	KY742070
D. macrostoma	JW 57015	Garden soil	The Netherlands	**MN824472**	**MN824620**	**MN823297**	**MN823446**
	CBS 223.69^{R}	*Acer pseudoplatanus*	Switzerland	KT389608	GU237623	GU238096	GU237801
	JW 149014	Garden soil	The Netherlands	**MN824473**	**MN824621**	**MN823298**	**MN823447**
	CBS 482.95	*Larix decidua*	Germany	KT389609	GU237626	GU238099	GU237869
D. maydis	CBS 588.69^{T}	*Zea mays*	USA	GU371782	FJ427190	EU754192	FJ427086
D. microchlamydospora	CBS 105.95^{T}	*Eucalyptus* sp.	UK	KP330424	FJ427138	GU238104	FJ427028
D. molleriana	CBS 229.79^{R}	*Digitalis purpurea*	New Zealand	KP330418	GU237605	GU238067	GU237802
D. negriana	CBS 358.71^{R}	*Vitis vinifera*	Germany	KT389610	GU237635	GU238116	GU237838
D. nigricans	CBS 444.81^{T}; PDDCC 6546	*Actinidia chinensis*	New Zealand	–	GU237558	GU238000	GU237867
	PD 77/919	*Actinidea chinensis*	Unknown	–	GU237559	GU238001	GU237915
D. ocimicola	CGMCC 3.18358^{T}; LC 8137	*Ocimum* sp.	China	–	KY742320	KY742232	KY742078
D. pedeiae	CBS 124517^{T}; PD 92/612A	*Schefflera elegantissima*	The Netherlands	KT389612	GU237642	GU238127	GU237770
D. pinodella	LC 8139	*Acer palmatum*	Japan	KY742161	KY742322	KY742234	KY742080
	CBS 531.66	*Trifolium pratense*	USA	KT389613	FJ427162	GU238017	FJ427052
D. pinodes	CBS 525.77^{T}	*Pisum sativum*	Belgium	KT389614	GU237572	GU238023	GU237883
D. pomorum	JW 196022	Garden soil	The Netherlands	**MN824469**	**MN824617**	**MN823294**	**MN823443**
	CBS 539.66^{R}; IMI 122266; PD 64/914	*Polygonum tataricum*	The Netherlands	KT389618	FJ427166	GU238028	FJ427056
D. protuberans	CBS 381.96^{T}; PD 71/706	*Lycium halifolium*	The Netherlands	KT389620	GU237574	GU238029	GU237853
D. pteridis	CBS 379.96^{T}	*Pteris* sp.	The Netherlands	KT389624	KT389801	KT389722	KT389504
D. rhei	CBS 109177^{R}; PD 2000/9941	*Rheum rhaponticum*	New Zealand	KP330428	GU237653	GU238139	GU237743

Taxon name[1]	Strain number[2]	Substrate	Country	GenBank Accession numbers[3]			
				rpb2	***tub2***	**ITS**	**LSU**
D. rumicicola	CBS 683.79^{T}	*Rumex obtusifolius*	New Zealand	KT389622	KT389800	KT389721	KT389503
	CBS 179.97	*Rumex hydrolapathum*	The Netherlands	KP330415	GU237575	GU238034	GU237793
	CBS 539.77	*Rumex obtusifolius*	New Zealand	**MN824471**	**MN824619**	**MN823296**	**MN823445**
D. sancta	CBS 281.83^{T}	*Ailanthus altissima*	South Africa	KT389623	FJ427170	GU238030	FJ427063
D. segeticola	CGMCC 3.17489^{T}; LC 1636	*Cirsium segetum*	China	KP330414	KP330399	KP330455	KP330443
D. senecionicola	CBS 160.78^{R}	*Senecio jacobaea*	New Zealand	–	GU237657	GU238143	GU237787
D. subglomerata	CBS 110.92^{R}; PD 76/1010	*Triticum* sp.	USA	KT389626	FJ427186	GU238032	FJ427080
D. subherbarum	CBS 250.92^{T}; PD 92/371	*Zea mays*	Canada	–	GU237659	GU238145	GU237809
D. suiyangensis	CGMCC 3.18352^{T}; LC 7439	Air	China	KY742169	KY742332	KY742244	KY742090
D. viburnicola	CBS 523.73^{R}; PD 69/800	*Viburnum cassioides*	The Netherlands	KP330430	GU237667	GU238155	GU237879
Ectophoma multirostrata	CBS 274.60^{T}; FMR 15335; IMI 081598	Soil	India	LT623265	FJ427141	GU238111	FJ427031
Ec. pomi	CBS 267.92^{T}; FMR 15346; PD 76/1014	*Coffea arabica*	India	LT623263	GU237643	GU238128	GU237814
Epicoccum nigrum	CBS 173.73^{T}; IMI 164070	*Dactylis glomerata*	USA	KT389632	FJ427107	GU237975	FJ426996
	LC 8157	*Ocimum* sp.	China	KY742179	KY742352	KY742264	KY742110
	LC 5180	*Lonicera japonica*	China	KY742178	KY742351	KY742263	KY742109
	LC 8158	*Poa annua*	USA	KY742180	KY742353	KY742265	KY742111
Ep. pimprinum	CBS 246.60^{T}; IMI 081601	Soil	India	–	FJ427159	GU237976	FJ427049
	PD 77/1028	Unknown	Unknown	KT389633	FJ427160	GU237977	FJ427050
Heterophoma sylvatica	CBS 874.97^{T}; PD 93/764	*Melampyrum pratense*	The Netherlands	–	GU237662	GU238148	GU237907
H. verbascicola	CGMCC 3.18364^{T}; LC 8163	*Verbascum thapsus*	China	KY742187	KY742361	KY742273	KY742119
Juxtiphoma eupyrena	JW 164001	Garden soil	The Netherlands	**MN824541**	**MN824689**	**MN823366**	**MN823515**
	JW 263011	Garden soil	The Netherlands	**MN824542**	**MN824690**	**MN823367**	**MN823516**
	JW 158007	Garden soil	The Netherlands	**MN824543**	**MN824691**	**MN823368**	**MN823517**
	JW 201014	Garden soil	The Netherlands	**MN824544**	**MN824692**	**MN823369**	**MN823518**
	JW 213001	Garden soil	The Netherlands	**MN824545**	**MN824693**	**MN823370**	**MN823519**
	JW 201009	Garden soil	The Netherlands	**MN824546**	**MN824694**	**MN823371**	**MN823520**
	JW 4005	Garden soil	The Netherlands	**MN824547**	**MN824695**	**MN823372**	**MN823521**
	JW 4017	Garden soil	The Netherlands	**MN824548**	**MN824696**	**MN823373**	**MN823522**
	JW 3015	Garden soil	The Netherlands	**MN824549**	**MN824697**	**MN823374**	**MN823523**
	JW 224006	Garden soil	The Netherlands	**MN824550**	**MN824698**	**MN823375**	**MN823524**
	JW 132015	Garden soil	The Netherlands	**MN824551**	**MN824699**	**MN823376**	**MN823525**

Taxon name[1]	Strain number[2]	Substrate	Country	GenBank Accession numbers[3]			
				rpb2	*tub2*	ITS	LSU
Juxtiphoma eupyrena	JW 146002	Garden soil	The Netherlands	–	**MN824700**	**MN823377**	**MN823526**
	JW 160021	Garden soil	The Netherlands	**MN824552**	**MN824701**	**MN823378**	**MN823527**
	JW 18016	Garden soil	The Netherlands	**MN824553**	**MN824702**	**MN823379**	**MN823528**
	JW 40009	Garden soil	The Netherlands	**MN824554**	**MN824703**	**MN823380**	**MN823529**
	JW 40019	Garden soil	The Netherlands	**MN824555**	**MN824704**	**MN823381**	**MN823530**
	JW 97009	Garden soil	The Netherlands	**MN824556**	**MN824705**	**MN823382**	**MN823531**
	JW 96020	Garden soil	The Netherlands	**MN824557**	**MN824706**	**MN823383**	**MN823532**
	JW 57007	Garden soil	The Netherlands	**MN824558**	**MN824707**	**MN823384**	**MN823533**
	JW 149010	Garden soil	The Netherlands	**MN824559**	**MN824708**	**MN823385**	**MN823534**
	JW 74008	Garden soil	The Netherlands	**MN824560**	**MN824709**	**MN823386**	**MN823535**
	JW 247003	Garden soil	The Netherlands	**MN824561**	**MN824710**	**MN823387**	**MN823536**
	JW 267005	Garden soil	The Netherlands	**MN824562**	**MN824711**	**MN823388**	**MN823537**
	JW 261008	Garden soil	The Netherlands	**MN824563**	**MN824712**	**MN823389**	**MN823538**
	JW 30012	Garden soil	The Netherlands	**MN824564**	**MN824713**	**MN823390**	**MN823539**
	JW 167015	Garden soil	The Netherlands	**MN824565**	**MN824714**	**MN823391**	**MN823540**
	JW 221022B	Garden soil	The Netherlands	**MN824566**	**MN824715**	**MN823392**	**MN823541**
	JW 259004	Garden soil	The Netherlands	**MN824567**	**MN824716**	**MN823393**	**MN823542**
	JW 73004	Garden soil	The Netherlands	**MN824568**	**MN824717**	**MN823394**	**MN823543**
	JW 170018	Garden soil	The Netherlands	**MN824569**	**MN824718**	**MN823395**	**MN823544**
	JW 141018	Garden soil	The Netherlands	**MN824570**	**MN824719**	**MN823396**	**MN823545**
	JW 181003	Garden soil	The Netherlands	**MN824571**	**MN824720**	**MN823397**	**MN823546**
	JW 289013	Garden soil	The Netherlands	**MN824572**	**MN824721**	**MN823398**	**MN823547**
	JW 127004	Garden soil	The Netherlands	**MN824573**	**MN824722**	**MN823399**	**MN823548**
	JW 81007	Garden soil	The Netherlands	**MN824574**	**MN824723**	**MN823400**	**MN823549**
	JW 182002	Garden soil	The Netherlands	**MN824575**	**MN824724**	**MN823401**	**MN823550**
	JW 212001	Garden soil	The Netherlands	**MN824576**	**MN824725**	**MN823402**	**MN823551**
	JW 191036	Garden soil	The Netherlands	**MN824577**	**MN824726**	**MN823403**	**MN823552**
	JW 221020	Garden soil	The Netherlands	**MN824578**	**MN824727**	**MN823404**	**MN823553**
	JW 96002	Garden soil	The Netherlands	**MN824579**	**MN824728**	**MN823405**	**MN823554**
	JW 52011	Garden soil	The Netherlands	**MN824580**	**MN824729**	**MN823406**	**MN823555**
	JW 38012	Garden soil	The Netherlands	**MN824581**	**MN824730**	**MN823407**	**MN823556**
	JW 40007	Garden soil	The Netherlands	**MN824582**	**MN824731**	**MN823408**	**MN823557**
	JW 43007	Garden soil	The Netherlands	**MN824583**	**MN824732**	**MN823409**	**MN823558**

Taxon name[1]	Strain number[2]	Substrate	Country	GenBank Accession numbers[3]			
				rpb2	*tub2*	ITS	LSU
Juxtiphoma eupyrena	JW 75002	Garden soil	The Netherlands	**MN824584**	**MN824733**	**MN823410**	**MN823559**
	JW 116017	Garden soil	The Netherlands	**MN824585**	**MN824734**	**MN823411**	**MN823560**
	JW 170013	Garden soil	The Netherlands	**MN824586**	**MN824735**	**MN823412**	**MN823561**
	JW 79016	Garden soil	The Netherlands	**MN824587**	**MN824736**	**MN823413**	**MN823562**
	CBS 374.91; FMR 15329	*Solanum tuberosum*	The Netherlands	LT623268	FJ427110	GU238072	FJ426999
	JW 125024	Garden soil	The Netherlands	**MN824588**	**MN824737**	**MN823414**	**MN823563**
	JW 158014	Garden soil	The Netherlands	**MN824589**	**MN824738**	**MN823415**	**MN823564**
	JW 4010	Garden soil	The Netherlands	**MN824590**	**MN824739**	**MN823416**	**MN823565**
	JW 202020	Garden soil	The Netherlands	**MN824591**	**MN824740**	**MN823417**	**MN823566**
J. kolkmaniorum	JW 125028	Garden soil	The Netherlands	**MN824592**	**MN824741**	**MN823418**	**MN823567**
	CBS 146005^{T}; JW 185006	Garden soil	The Netherlands	**MN824593**	**MN824742**	**MN823419**	**MN823568**
	JW 191004	Garden soil	The Netherlands	**MN824594**	**MN824743**	**MN823420**	**MN823569**
	JW 23021	Garden soil	The Netherlands	**MN824595**	**MN824744**	**MN823421**	**MN823570**
	JW 167004	Garden soil	The Netherlands	**MN824596**	**MN824745**	**MN823422**	**MN823571**
	JW 221010	Garden soil	The Netherlands	**MN824597**	**MN824746**	**MN823423**	**MN823572**
	JW 220011	Garden soil	The Netherlands	**MN824598**	**MN824747**	**MN823424**	**MN823573**
	JW 241011	Garden soil	The Netherlands	**MN824599**	**MN824748**	**MN823425**	**MN823574**
	JW 94009	Garden soil	The Netherlands	**MN824600**	**MN824749**	**MN823426**	**MN823575**
	CBS 527.66; FMR 15337	Wheat field soil	Germany	LT623269	FJ427111	GU238073	FJ427000
	JW 63001	Garden soil	The Netherlands	**MN824601**	**MN824750**	**MN823427**	**MN823576**
	JW 168007	Garden soil	The Netherlands	**MN824602**	**MN824751**	**MN823428**	**MN823577**
Leptosphaeria doliolum	CBS 505.75^{T}	*Urtica dioica*	The Netherlands	KT389640	JF740144	GQ387576	JF740205
Leptosphaerulina australis	CBS 311.51	Lawn	Switzerland	–	–	FJ795508	–
L. saccharicola	CBS 939.69	Soil	The Netherlands	–	GU237541	JX681098	GU237911
L. trifolii	CBS 235.58	*Trifolium* sp.	The Netherlands	–	GU237542	GU237982	GU237806
Macroventuria anomochaeta	CBS 525.71^{T}	Decayed canvas	South Africa	GU456346	GU237544	GU237984	GU237881
Ma. wentii	CBS 526.71^{T}	Plant litter	USA	KT389642	GU237546	GU237986	GU237884
Microsphaeropsis olivacea	CBS 233.77	*Pinus laricio*	France	KT389643	GU237549	GU237988	GU237803
	CBS 442.83	*Taxus baccata*	The Netherlands	–	GU237547	EU754171	GU237865
Mi. proteae	CBS 111319^{T}; CPC 1425	*Protea nitida*	Unknown	–	JN712650	JN712563	JN712497
Neoascochyta argentina	CBS 112524^{T}	*Triticum aestivum*	Argentina	–	KT389822	KT389742	KT389524
Neoa. desmazieri	CBS 297.69^{T}	*Lolium perenne*	Germany	KT389644	KT389806	KT389726	KT389508

Taxon name[1]	Strain number[2]	Substrate	Country	GenBank Accession numbers[3]			
				rpb2	***tub2***	**ITS**	**LSU**
Neoa. paspali	CBS 560.81^{T}; PDDCC 6614	*Paspalum dilatatum*	New Zealand	KP330426	FJ427158	GU238124	FJ427048
Neoa. tardicrebrescens	CBS 689.97^{T}	Hay	Norway	KT389654	KT389824	KT389744	KT389526
Neoa. triticicola	CBS 544.74^{T}	*Triticum aestivum*	South Africa	KT389652	GU237488	EU754134	GU237887
Neodidymelliopsis cannabis	CBS 234.37	*Cannabis sativa*	Unknown	KP330403	GU237523	GU237961	GU237804
	CBS 121.75^{T}; IMI 194767; PD 73/584	*Urtica dioica*	The Netherlands	–	GU237535	GU237972	GU237761
Neod. polemonii	CBS 109181^{T}; PD 83/757	*Polemonium caeruleum*	The Netherlands	KP330427	GU237648	GU238133	GU237746
Neod. xanthina	CBS 383.68^{T}	*Delphinium* sp.	The Netherlands	KP330431	GU237668	GU238157	GU237855
Neomicrosphaeropsis italica	MFLUCC 16-0284	*Tamarix* sp.	Italy	KU714604	–	KU900296	KU900321
	MFLUCC 15-0484	*Tamarix* sp.	Italy	KU695539	–	KU729853	KU900319
	MFLUCC 15-0485^{T}	*Tamarix* sp.	Italy	KU674820	–	KU729854	KU900318
Nothophoma anigozanthi	CBS 381.91^{T}; FMR 14914	*Anigozanthus maugleisii*	The Netherlands	KT389655	GU237580	GU238039	GU237852
N. arachidis-hypogaeae	CBS 125.93^{R}; PD 77/1029	*Arachis hypogaea*	India	KT389656	GU237583	GU238043	GU237771
N. brennandiae	**JW 1066**	Garden soil	The Netherlands	**MN824603**	**MN824752**	**MN823429**	**MN823578**
	CBS 145912^{T}; JW 53011	Garden soil	The Netherlands	**MN824604**	**MN824753**	**MN823430**	**MN823579**
	MFLUCC 16-1392	*Ulmus* (×) *hollandica*	Italy	KY053898	KY053899	KY053897	KY053896
N. gossypiicola	CBS 377.67; FMR 14912	*Gossypium* sp.	USA	KT389658	GU237611	GU238079	GU237845
	UTHSC:DI16-294	Human deep tissue/ fluids	USA	LT593082	LT593012	LN907437	LT592943
N. infossa	CBS 123395^{T}	*Fraxinus pennsylvanica*	Argentina	KT389659	FJ427135	GU238089	FJ427025
	CBS 123394	*Fraxinus pennsylvanica*	Argentina	–	FJ427134	GU238088	FJ427024
N. macrospora	CBS 140674^{T}; FMR 13767	Human respiratory tract	USA	LT593073	LN880539	LN880537	LN880536
N. pruni	MFLUCC 18-1600^{T}	*Prunus avium*	China	MH853664	MH853671	MH827028	MH827007
N. quercina	MFLUCC 18-1588	*Prunus avium*	China	MH853665	MH853672	MH827029	MH827008
	CBS 633.92^{R}; ATCC 36786	*Microsphaera alphitoides* from *Quercus* sp.	Ukraine	KT389657	GU237609	EU754127	GU237900
	UTHSC:DI16-270; FMR 13761	Human superficial tissue	USA	LT593067	LT592998	LN907413	LT592929
N. variabilis	CBS 142457^{T}; FMR 13777	Human respiratory tract	USA	LT593078	LT593008	LN907428	LT592939
Paraboeremia adianticola	CBS 260.92; PD 86/1103	*Pteris ensiformis*	Unknown	–	KT389832	KT389752	KT389534
P. adianticola	CBS 187.83; PD 82/128; FMR 15344	*Polystichum adiantiforme*	USA	KP330401	GU237576	GU238035	GU237796
P. camelliae	CGMCC 3.18108	*Camellia* sp.	China	KX829052	KX829060	KX829044	KX829036
	CGMCC 3.18106^{T}	*Camellia* sp.	China	KX829050	KX829058	KX829042	KX829034
	CGMCC 3.18107	*Camellia* sp.	China	KX829051	KX829059	KX829043	KX829035

Taxon name[1]	Strain number[2]	Substrate	Country	GenBank Accession numbers[3]			
				rpb2	*tub2*	ITS	LSU
P. litseae	CGMCC 3.18110; LC 5030	*Litsea* sp.	China	KX829046	KX829054	KX829038	KX829030
	JW 157001	Garden soil	The Netherlands	**MN824519**	**MN824667**	**MN823344**	**MN823493**
	CGMCC 3.18109[T]; LC 5028	*Litsea* sp.	China	KX829045	KX829053	KX829037	KX829029
P. putaminum	JW 110005	Garden soil	The Netherlands	**MN824480**	**MN824628**	**MN823305**	**MN823454**
	JW 126003	Garden soil	The Netherlands	**MN824481**	**MN824629**	**MN823306**	**MN823455**
	JW 265009	Garden soil	The Netherlands	**MN824482**	**MN824630**	**MN823307**	**MN823456**
	JW 221011	Garden soil	The Netherlands	**MN824483**	**MN824631**	**MN823308**	**MN823457**
	JW 165006	Garden soil	The Netherlands	**MN824484**	**MN824632**	**MN823309**	**MN823458**
	JW 232004	Garden soil	The Netherlands	**MN824485**	**MN824633**	**MN823310**	**MN823459**
	JW 192007	Garden soil	The Netherlands	**MN824486**	**MN824634**	**MN823311**	**MN823460**
	JW 125011	Garden soil	The Netherlands	**MN824487**	**MN824635**	**MN823312**	**MN823461**
	JW 18014	Garden soil	The Netherlands	**MN824488**	**MN824636**	**MN823313**	**MN823462**
	JW 142002	Garden soil	The Netherlands	**MN824489**	**MN824637**	**MN823314**	**MN823463**
	JW 221018	Garden soil	The Netherlands	**MN824490**	**MN824638**	**MN823315**	**MN823464**
	JW 238003	Garden soil	The Netherlands	**MN824491**	**MN824639**	**MN823316**	**MN823465**
	JW 192019	Garden soil	The Netherlands	**MN824492**	**MN824640**	**MN823317**	**MN823466**
	JW 213009	Garden soil	The Netherlands	**MN824493**	**MN824641**	**MN823318**	**MN823467**
	JW 226017	Garden soil	The Netherlands	**MN824494**	**MN824642**	**MN823319**	**MN823468**
	JW 109022	Garden soil	The Netherlands	**MN824495**	**MN824643**	**MN823320**	**MN823469**
	JW 4002	Garden soil	The Netherlands	**MN824496**	**MN824644**	**MN823321**	**MN823470**
	CBS 130.69[R]; IMI 331916	*Malus sylvestris*	Denmark	–	GU237652	GU238138	GU237777
	JW 16015	Garden soil	The Netherlands	**MN824497**	**MN824645**	**MN823322**	**MN823471**
	JW 16001	Garden soil	The Netherlands	**MN824498**	**MN824646**	**MN823323**	**MN823472**
	JW 25002	Garden soil	The Netherlands	**MN824499**	**MN824647**	**MN823324**	**MN823473**
	JW 276009	Garden soil	The Netherlands	**MN824500**	**MN824648**	**MN823325**	**MN823474**
	JW 48011	Garden soil	The Netherlands	**MN824501**	**MN824649**	**MN823326**	**MN823475**
	JW 4011	Garden soil	The Netherlands	**MN824502**	**MN824650**	**MN823327**	**MN823476**
	JW 276008	Garden soil	The Netherlands	**MN824503**	**MN824651**	**MN823328**	**MN823477**
	JW 65008	Garden soil	The Netherlands	**MN824505**	**MN824653**	**MN823330**	**MN823479**
	JW 132016	Garden soil	The Netherlands	**MN824506**	**MN824654**	**MN823331**	**MN823480**
	JW 226014	Garden soil	The Netherlands	**MN824507**	**MN824655**	**MN823332**	**MN823481**
	JW 226015	Garden soil	The Netherlands	**MN824508**	**MN824656**	**MN823333**	**MN823482**
	JW 25012	Garden soil	The Netherlands	**MN824509**	**MN824657**	**MN823334**	**MN823483**

Taxon name[1]	Strain number[2]	Substrate	Country	GenBank Accession numbers[3]			
				rpb2	*tub2*	ITS	LSU
P. putaminum	JW 11007	Garden soil	The Netherlands	**MN824510**	**MN824658**	**MN823335**	**MN823484**
	JW 129005	Garden soil	The Netherlands	**MN824511**	**MN824659**	**MN823336**	**MN823485**
	CBS 372.91[R]; PD 75/690	*Ceratocystis ulmi*	The Netherlands	–	GU237651	GU238137	GU237843
	JW 145026	Garden soil	The Netherlands	**MN824504**	**MN824652**	**MN823329**	**MN823478**
	JW 4006	Garden soil	The Netherlands	**MN824512**	**MN824660**	**MN823337**	**MN823486**
	JW 191017	Garden soil	The Netherlands	**MN824513**	**MN824661**	**MN823338**	**MN823487**
	JW 161002	Garden soil	The Netherlands	**MN824514**	**MN824662**	**MN823339**	**MN823488**
	JW 116031	Garden soil	The Netherlands	**MN824515**	**MN824663**	**MN823340**	**MN823489**
	JW 1008	Garden soil	The Netherlands	**MN824516**	**MN824664**	**MN823341**	**MN823490**
	JW 1020	Garden soil	The Netherlands	**MN824517**	**MN824665**	**MN823342**	**MN823491**
	JW 1046	Garden soil	The Netherlands	**MN824518**	**MN824666**	**MN823343**	**MN823492**
P. rekkeri	**JW 13016**	Garden soil	The Netherlands	**MN824526**	**MN824674**	**MN823351**	**MN823500**
	JW 13030	Garden soil	The Netherlands	**MN824527**	**MN824675**	**MN823352**	**MN823501**
	JW 79024	Garden soil	The Netherlands	**MN824528**	**MN824676**	**MN823353**	**MN823502**
	JW 25013	Garden soil	The Netherlands	**MN824529**	**MN824677**	**MN823354**	**MN823503**
	JW 167006	Garden soil	The Netherlands	**MN824530**	**MN824678**	**MN823355**	**MN823504**
	JW 132004	Garden soil	The Netherlands	**MN824531**	**MN824679**	**MN823356**	**MN823505**
	CBS 144949; JW 4024	Garden soil	The Netherlands	**MN824532**	**MN824680**	**MN823357**	**MN823506**
	JW 13017	Garden soil	The Netherlands	**MN824533**	**MN824681**	**MN823358**	**MN823507**
	JW 91008	Garden soil	The Netherlands	**MN824534**	**MN824682**	**MN823359**	**MN823508**
	JW 226002	Garden soil	The Netherlands	**MN824535**	**MN824683**	**MN823360**	**MN823509**
	JW 3018	Garden soil	The Netherlands	**MN824536**	**MN824684**	**MN823361**	**MN823510**
	CBS 144955[T]; JW 172002	Garden soil	The Netherlands	**MN824537**	**MN824685**	**MN823362**	**MN823511**
	JW 51014	Garden soil	The Netherlands	**MN824538**	**MN824686**	**MN823363**	**MN823512**
	JW 196020	Garden soil	The Netherlands	**MN824539**	**MN824687**	**MN823364**	**MN823513**
	CBS 144950; JW 6005	Garden soil	The Netherlands	**MN824540**	**MN824688**	**MN823365**	**MN823514**
P. selaginellae	CBS 122.93[T]; PD 77/1049	*Selaginella* sp.	The Netherlands	–	GU237656	GU238142	GU237762
P. truiniorum	**JW 270002**	Garden soil	The Netherlands	**MN824520**	**MN824668**	**MN823345**	**MN823494**
	CBS 144952[T]; JW 47002	Garden soil	The Netherlands	**MN824521**	**MN824669**	**MN823346**	**MN823495**
	JW 147025	Garden soil	The Netherlands	**MN824522**	**MN824670**	**MN823347**	**MN823496**
	JW 182014	Garden soil	The Netherlands	**MN824523**	**MN824671**	**MN823348**	**MN823497**
	JW 192003	Garden soil	The Netherlands	**MN824524**	**MN824672**	**MN823349**	**MN823498**
	CBS 144961; JW 203021	Garden soil	The Netherlands	**MN824525**	**MN824673**	**MN823350**	**MN823499**

Taxon name[1]	Strain number[2]	Substrate	Country	GenBank Accession numbers[3]			
				rpb2	***tub2***	**ITS**	**LSU**
Phoma herbarum	CBS 274.37	*Picea excelsa*	UK	KT389662	KT389835	KT389754	KT389537
	CBS 615.75^{R}; IMI 199779; PD 73/655	*Rosa multiflora* cv. *cathayensis*	The Netherlands	KP330420	FJ427133	EU754186	FJ427022
Phomatodes aubrietiae	CBS 627.97^{T}; PD 70/714	*Aubrietia* sp.	The Netherlands	KT389665	GU237585	GU238045	GU237895
Phomat. nebulosa	JW 166004	Garden soil	The Netherlands	**MN824609**	**MN824758**	**MN823435**	**MN823584**
	JW 166006	Garden soil	The Netherlands	**MN824610**	**MN824759**	**MN823436**	**MN823585**
	JW 166013	Garden soil	The Netherlands	**MN824611**	**MN824760**	**MN823437**	**MN823586**
	CBS 100191	*Thlapsi arvense*	Poland	KT389666	KP330390	KP330446	KP330434
	CBS 117.93; PD 83/90	*Mercurialis perennis*	The Netherlands	KP330425	GU237633	GU238114	GU237757
Pseudoascochyta novae-zelandiae	CBS 141689^{T}; FMR 15110	*Cordyline australis*	New Zealand	LT592895	LT592894	LT592893	LT592892
Pse. pratensis	CBS 141688^{T}; FMR 14524	Soil	Spain	LT223133	LT223132	LT223131	LT223130
Remotididymella anthropophylica	CBS 142462^{T}; FMR 13770	Human respiratory tract	USA	LT593075	LT593005	LN907421	LT592936
R. destructiva	CBS 378.73^{T}; FMR 15328	*Lycopersicon esculentum*	Tonga	LT623258	GU237601	GU238063	GU237849
Stagonosporopsis andigena	CBS 269.80; PD 75/914	*Solanum* sp.	Peru	–	GU237675	GU238170	GU237817
S. astragali	CBS 178.25^{R}; MUCL 9915	*Astragalus* sp.	Unknown	–	GU237677	GU238172	GU237792
S. bomiensis	LC 8168	Boraginaceae	China	KY742190	KY742366	KY742278	KY742124
	CGMCC 3.18366^{T}; LC 8167	Boraginaceae	China	KY742189	KY742365	KY742277	KY742123
S. crystalliniformis	CBS 713.85^{T}; ATCC 76027; PD 83/826	*Lycopersicon esculentum*	Colombia	KT389675	GU237683	GU238178	GU237903
S. dorenboschii	CBS 426.90^{T}; IMI 386093; PD 86/551	*Physostegia virginiana*	The Netherlands	KT389678	GU237690	GU238185	GU237862
S. hortensis	CBS 104.42^{R}	–	The Netherlands	KT389680	GU237703	GU238198	GU237730
	CBS 572.85; PD 79/269	*Phaseolus vulgaris*	The Netherlands	KT389681	GU237704	GU238199	GU237893
S. loticola	CBS 562.81^{T}; PDDCC 6884	*Lotus pedunculatus*	New Zealand	KT389684	GU237697	GU238192	GU237890
S. papillata	LC 8170	*Rumex nepalensis*	China	KY742192	KY742368	KY742280	KY742126
	CGMCC 3.18367^{T}; LC 8169	*Rumex nepalensis*	China	KY742191	KY742367	KY742279	KY742125
S. stuijvenbergii	**CBS 144953^{T}; JW 132011**	Garden soil	The Netherlands	**MN824475**	**MN824623**	**MN823300**	**MN823449**
	JW 33021	Garden soil	The Netherlands	**MN824476**	**MN824624**	**MN823301**	**MN823450**
	JW 14003	Garden soil	The Netherlands	**MN824477**	**MN824625**	**MN823302**	**MN823451**
	JW 44014	Garden soil	The Netherlands	**MN824478**	**MN824626**	**MN823303**	**MN823452**
S. weymaniae	**CBS 144959^{T}; JW 201003**	Garden soil	The Netherlands	**MN824479**	**MN824627**	**MN823304**	**MN823453**

Taxon name[1]	Strain number[2]	Substrate	Country	GenBank Accession numbers[3]			
				rpb2	***tub2***	**ITS**	**LSU**
Vacuiphoma bulgarica	CBS 357.84^{T}	*Trachystemon orientale*	Bulgaria	LT623256	GU237589	GU238050	GU237837
Vac. oculihominis	UTHSC:DI16-308^{T}; FMR 13801	Human superficial tissue	USA	LT593093	LT593023	LN907451	LT592954
Vandijckomycella joseae	**CBS 144948; JW 1068**	Garden soil	The Netherlands	**MN824614**	**MN824763**	**MN823440**	**MN823589**
Van. joseae	**CBS 143011^{T}; JW 1073**	Garden soil	The Netherlands	**MN824615**	**MN824764**	**MN823441**	**MN823590**
Van. snoekiae	**CBS 144954^{T}; JW 149017**	Garden soil	The Netherlands	**MN824616**	**MN824765**	**MN823442**	**MN823591**
Xenodidymella applanata	CBS 115577	*Rubus idaeus*	Sweden	KT389688	KT389850	KT389762	KT389546
	CBS 195.36^{T}	*Rubus idaeus*	The Netherlands	–	KT389852	KT389764	KT389548
	CBS 205.63	*Rubus idaeus*	The Netherlands	KP330402	GU237556	GU237998	GU237798
	CBS 115578	*Rubus arcticus* nothossp. *stellarcticus*	Sweden	–	KT389851	KT389763	KT389547
X. asphodeli	CBS 375.62^{T}	*Asphodelus albus*	France	KT389689	KT389853	KT389765	KT389549
	CBS 499.72	*Asphodelus ramosus*	Italy	–	KT389853	KT389766	KT389550
X. catariae	CBS 102635; PD 77/1131	*Nepeta catenaria*	The Netherlands	KP330404	GU237524	GU237962	GU237727
X. humicola	CBS 220.85^{R}; PD 71/1030	*Franseria* sp.	USA	KP330422	GU237617	GU238086	GU237800
X. weymaniae	**CBS 144960^{T}; JW 201005**	Garden soil	The Netherlands	**MN824613**	**MN824762**	**MN823439**	**MN823588**

[1] New species are marked in **bold**. [2]ATCC = American Type Culture Collection, Virginia, USA; CBS = Westerdijk Fungal Biodiversity Institute, Utrecht, The Netherlands; CGMCC = China General Microbiological Culture Collection, Beijing, China; CPC = Culture collection of Pedro Crous, housed at the Westerdijk Fungal Biodiversity Institute, Utrecht, The Netherlands; FMR = Facultat de Medicina, Universitat Rovira i Virgili, Reus, Spain; JW = Johanna Westerdijk working collection housed at the Westerdijk Fungal Biodiversity Institute, Utrecht, The Netherlands; LC = Personal culture collection of Lei Cai, housed at CAS, China; MFLUCC = Mae Fah Luang University Culture Collection, Chiang Rai, Thailand; PD = Plant Protection Service, Wageningen, the Netherlands; PDDCC = Plant Diseases Division Culture Collection, Auckland, New Zealand; UTHSC = Fungus Testing Laboratory at the University of Texas Health Science Center, San Antonio, Texas, USA. ^{T} and ^{R} indicate ex-type and representative strains, respectively. [3] *rpb2*: partial RNA polymerase II second largest subunit gene; *tub2*: partial β-tubulin gene; ITS: internal transcribed spacers and intervening 5.8S nrDNA; LSU: partial large subunit nrDNA. Strains representing new species are marked in **bold**. Sequences generated in this study are marked in **bold**.

Results

A total of 293 soil samples were analysed, and nearly 3000 fungal strains were obtained. Among them, 148 Didymellaceae isolates were identified from 89 different garden soil samples, representing several locations in the Netherlands (Table 1).

Phylogenetic identification

A multi-locus phylogeny comprising 325 strains, including the JW soil isolates and reference strains from GenBank, was used to infer the relationships among species in Didymellaceae (Figure 1, Table 1). *Coniothyrium palmarum* (CBS 400.71) and *Leptosphaeria doliolum* (CBS 505.75) were used as outgroups. The final combined ITS, LSU, *rpb2* and *tub2* alignment comprised 2317 characters including gaps (500 for ITS; 859 for LSU; 602 for *rpb2*; 356 for *tub2*), of which 1563 characters were constant, 106 parsimony-uninformative, and 618 were parsimony-informative. For the Bayesian analysis, SYM+I+G was selected as the best-fit model for the ITS dataset, and GTR+I+G was selected as the best model for the LSU, *tub2* and *rpb2* datasets. The phylogenetic trees obtained with three analyses showed a similar topology and were congruent with each other, and only the ML tree is presented herein with BS, PP, and PBS values plotted on the branches (Figure 1).

In the phylogenetic analysis, the 148 isolates from Dutch soil were distributed in 10 clades (Figure 1). The majority of the isolates clustered in *Juxtiphoma* (n=63) which were recovered from 48 soil samples and 28 cities, followed by *Paraboeremia* (n=61) from 29 soil samples and 19 cities. Other isolates belonged to *Didymella* spp. (n=5), *Stagonosporopsis* spp. (n=5), *Ascochyta* spp. (n=4), *Phomatodes nebulosa* (n=3), *Nothophoma* spp. (n=2), *Calophoma clematidis* (n=1), and *Xenodidymella applanata* (n=1), and three isolates clustered in an unknown clade (Figure 1, Table 1).

In the *Juxtiphoma* clade species clustered in two lineages, one corresponding to *J. eupyrena* (77/1/-) and the other representing a potentially new species (100/1/99). In the *Paraboeremia* clade, the soil isolates clustered in *P. putaminum* (86/0.99/67) and *P. litseae* (98/1/97). However, 21 isolates were distributed in two different lineages (with 6 and 15 isolates, respectively) that were phylogenetically distant from other species, representing two potentially new taxa. The soil isolates belonging to *Stagonosporopsis* clustered in a clade (100/1/99) that was phylogenetically distant from the other species, representing two potentially new species. In *Didymella*, the species were distributed in *D. macrostoma* (100/1/100) and *D. pomorum* (100/1/100), while isolates JW 195004 and JW 27006 were placed in two different branches, representing two putative new species. In *Ascochyta* one isolate grouped with *A. syringae* (93/1/86), whereas three isolates grouped in a different clade distant from previously known species, representing a potentially new species (100/1/100). The other three isolates grouped together at the bottom of the tree in a distant unknown lineage, which is introduced herein as a new genus with two species (100/1/90). All the new taxa are introduced in the taxonomy section based on the phylogenetic analysis and supported by morphological data. Descriptions and illustrations of the new taxa are provided in the taxonomy section below.

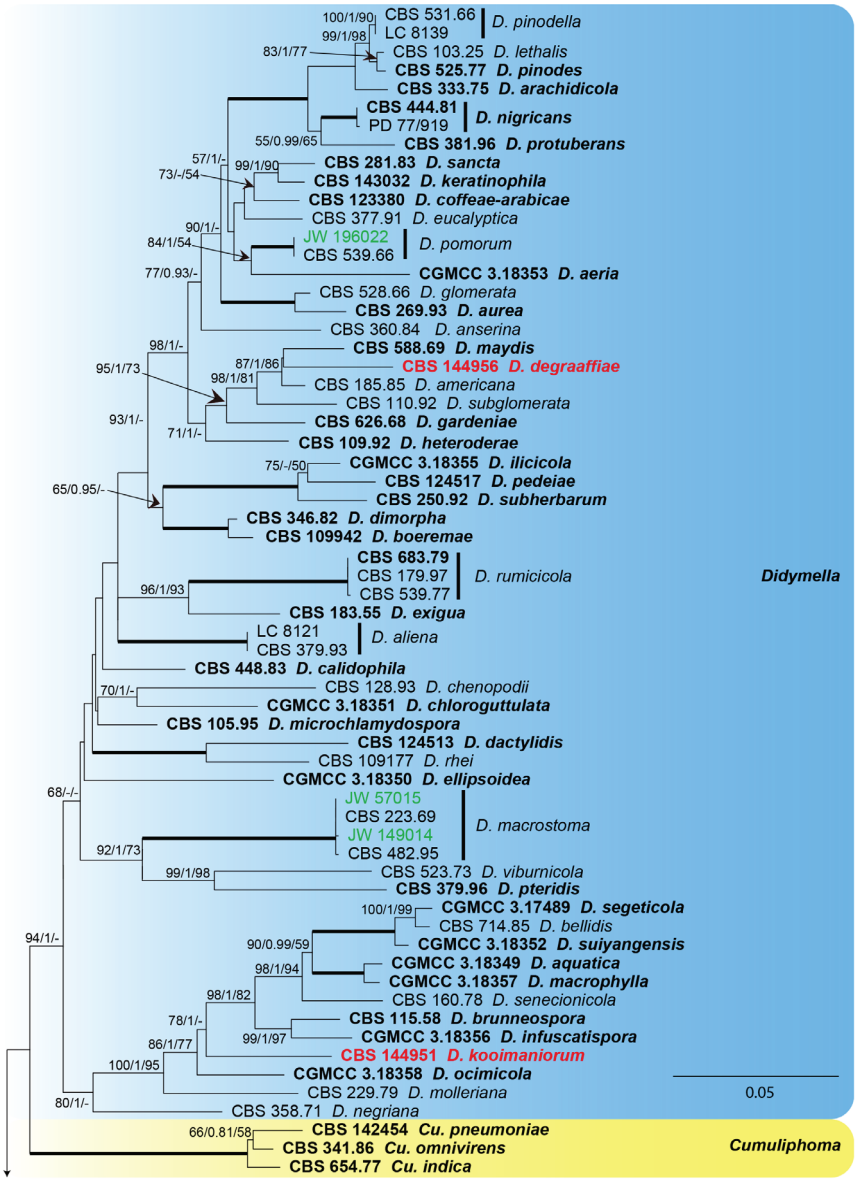

Figure 1. Phylogenetic tree generated from the maximum-likelihood analysis based on the combined ITS, LSU, *tub2* and *rpb2* sequence alignment of Didymellaceae members. The RAxML bootstrap support values (BS), Bayesian posterior probabilities (PP), and parsimony bootstrap support values (PBS) are given at the nodes (BS/PP/PBS). BS and PBS values represent parsimony bootstrap support values >50 %. Full supported branches are indicated in bold. The scale bar represents the expected number of changes per site. Ex-type strains are represented in bold. Strains obtained in the current study are printed in green; among them, whilst strains that represent new taxa are printed in red. Some of the basal branches were shortened to facilitate layout (the fraction in round parentheses refers to the presented length compared to the actual length of the branch). The tree was rooted to *Coniothyrium palmarum* CBS 400.71 and *Leptosphaeria doliolum* CBS 505.75.

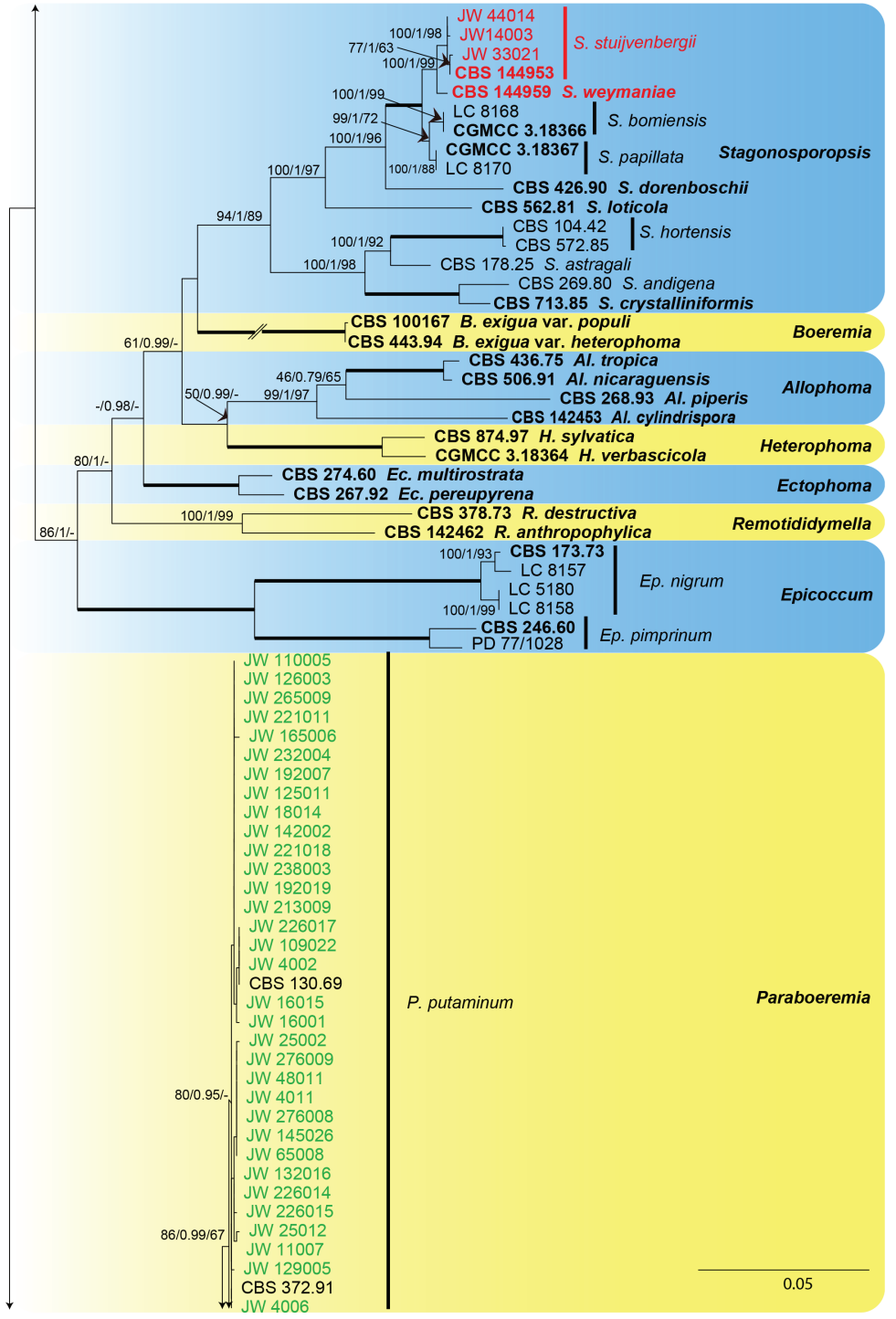

Figure 1. Continued.

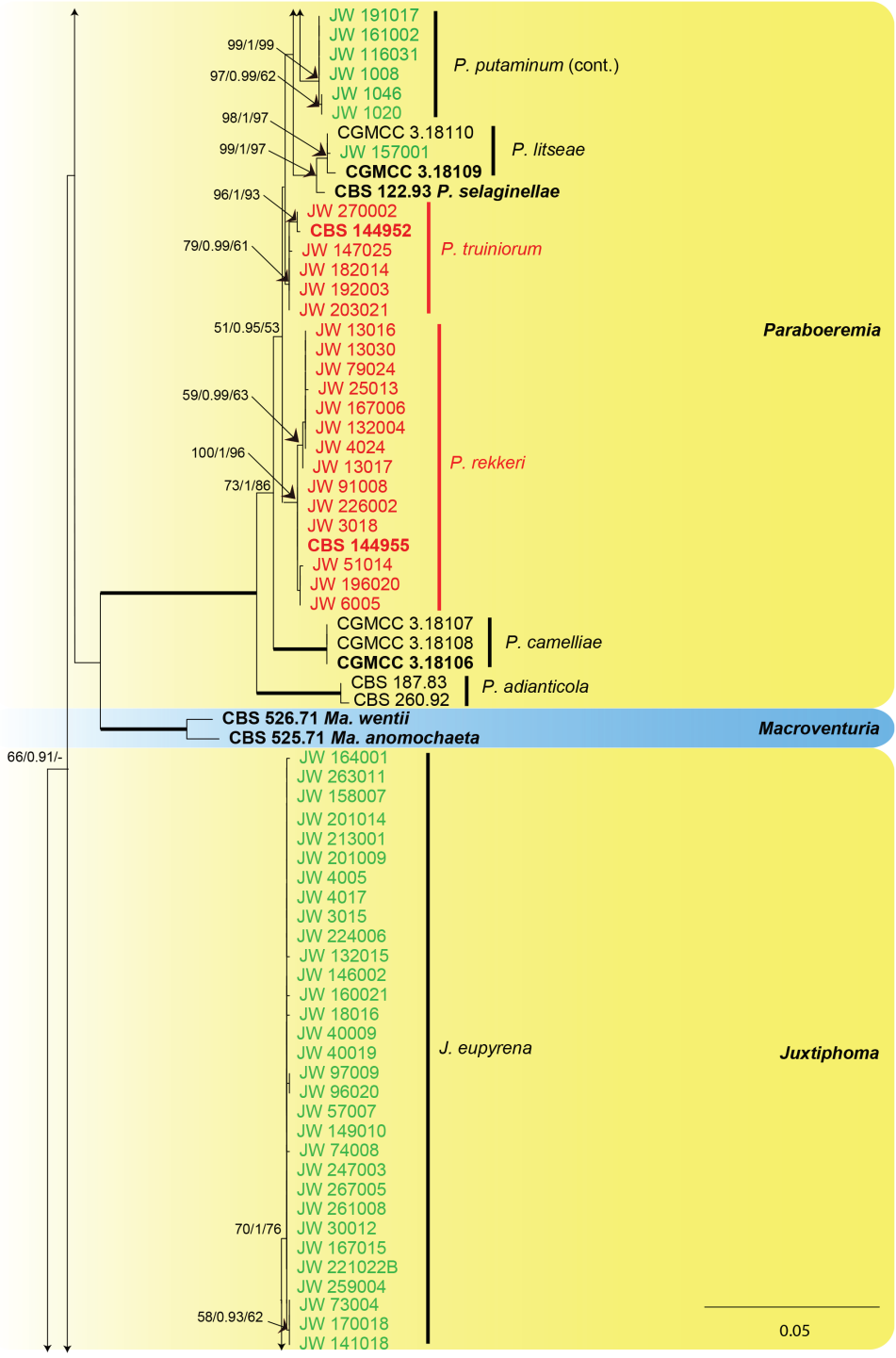

Figure 1. Continued.

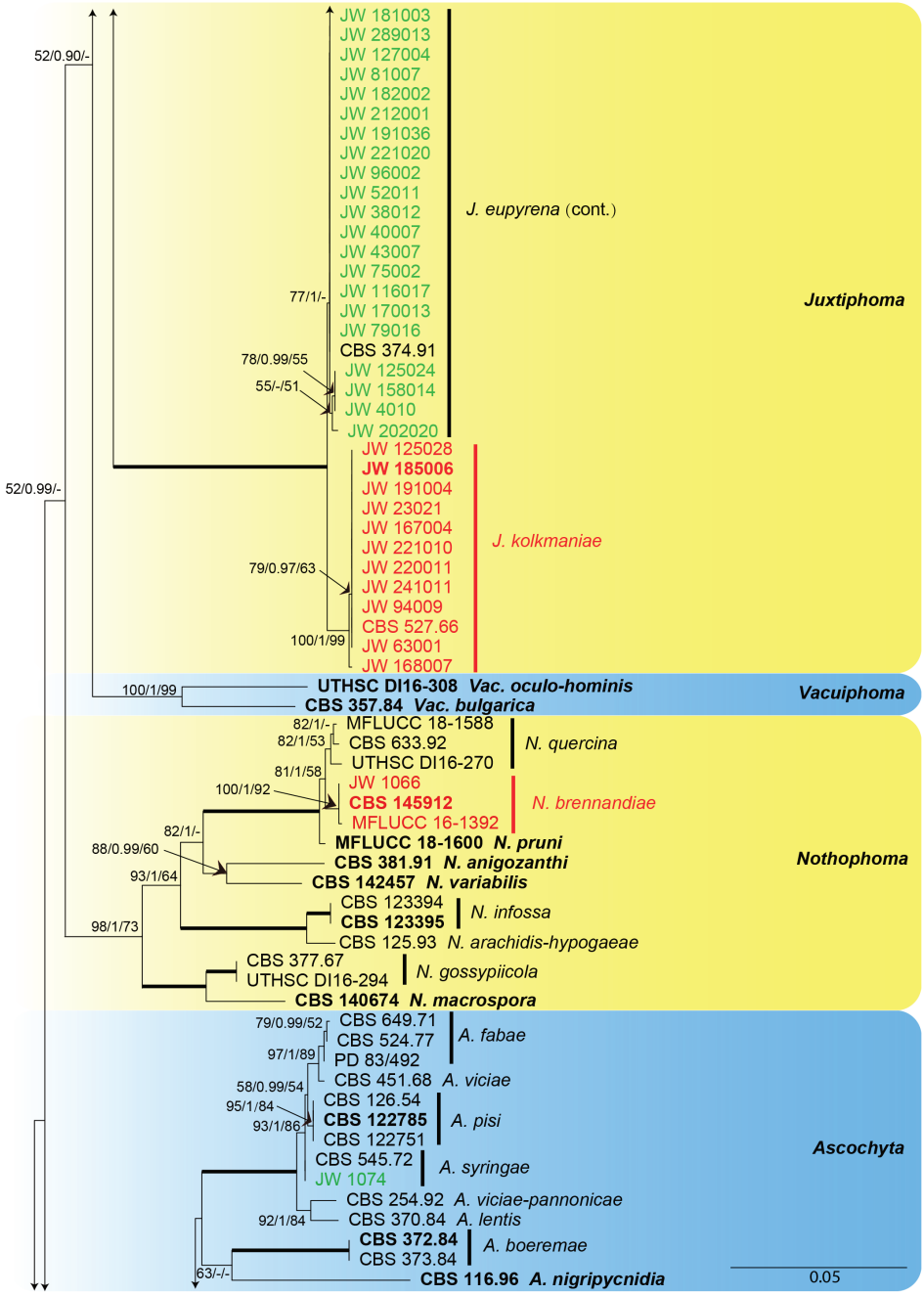

Figure 1. Continued.

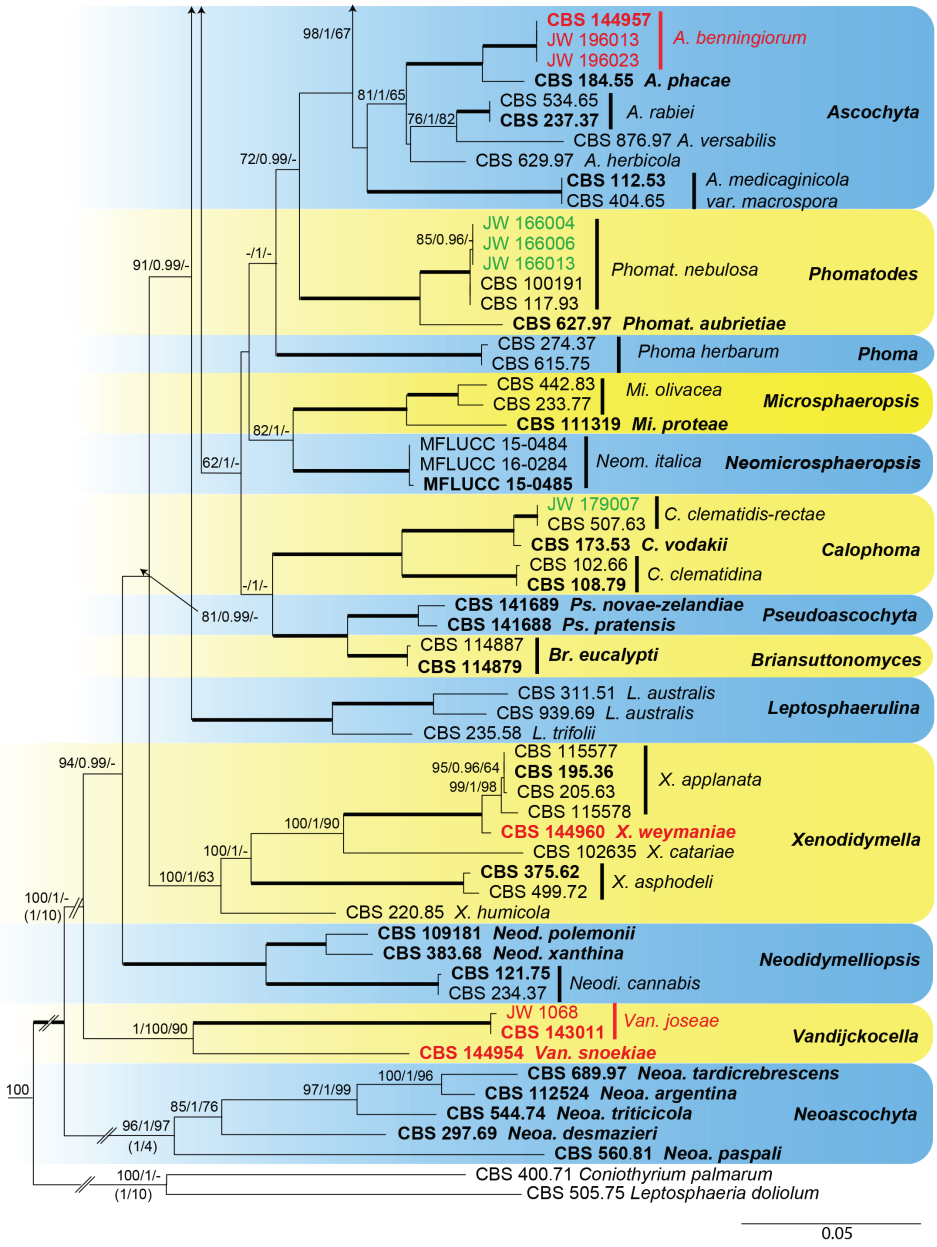

Figure 1. Continued.

Loci resolution

The single locus phylogenies of *rpb2* and *tub2* performed quite well at both generic and species levels. The *rpb2* phylogeny was able to discriminate all 27 generic clades included in the phylogeny (Figure 1), with good resolution of species among these genera (140 of 143 species). The *tub2* phylogeny was able to distinguish 26 of 27 generic clades recognising 134 of 143 species, but proved unsuccessful for *Vacuiphoma* and *Ascochyta*, mainly because species of these genera did not cluster into monophyletic lineages, but were sometimes intermixed or formed separate lineages. However, the LSU phylogeny displayed a low resolution at both generic and species levels, being able to distinguish only 12 of 27 genera and 50 of 143 species. The ITS phylogeny was able to distinguish 17 of the 27 generic clades and 44 of the 143 species.

Taxonomy

Ascochyta benningiorum **Hern.-Restr., L. W. Hou, L. Cai & Crous, sp. nov.**
MycoBank No: 833194
Figure 2

Etymology. *benningiorum* refers to Eva, Bas & Anne Benning who collected the soil sample from which the ex-type strain was isolated.

Typus. The Netherlands. Gelderland province, Wijchen, isolated from garden soil, Mar. 2017, E. Benning, B. Benning & A. Benning (***holotype*** designated here CBS H-24104, living ex-type culture CBS 144957 = JW 196005).

Conidiomata pycnidial, mostly solitary, sometimes confluent, globose or subglobose, irregularly-shaped with age, brown to dark brown, glabrous, mostly produced on the agar surface and some immersed, 140–480(–580) × 100–370(–440) µm; with 1–6(–10) slightly papillate ostioles; pycnidial wall pseudoparenchymatous, 4–8 layers, 14.5–65 µm thick, outer layers composed of brown, flattened polygonal cells of 11–28 µm diam. *Conidiogenous cells* phialidic, hyaline, smooth, globose, ampulliform to lageniform, 5.5–9 × 4–6.5 µm. *Conidia* cylindrical, hyaline, smooth- and thin-walled, mostly straight, occasionally curved, aseptate, (3.5–)4.5–7 × 1.5–2.5 µm, 2-guttulate, small. *Conidia matrix* whitish.

Culture characteristics. Colonies after 7 d at 25 °C, on OA reaching 50–55 mm diam, aerial mycelium floccose, olivaceous to olivaceous black, buff towards the periphery, abundant production of pycnidia, margin irregular; reverse concolorous with the surface. On MEA reaching 40–45 mm diam, aerial mycelium floccose, concentric circles, centre pink, grey olivaceous, mouse grey, rosy buff toward periphery, moderate production of pycnidia, margin irregular; reverse orange, olivaceous black toward periphery. On PDA reaching 45–50 mm diam, aerial mycelium floccose, dark brick to olivaceous grey, buff towards periphery, abundant production of pycnidia, margin irregular; reverse concolorous with the surface. NaOH spot test negative on OA.

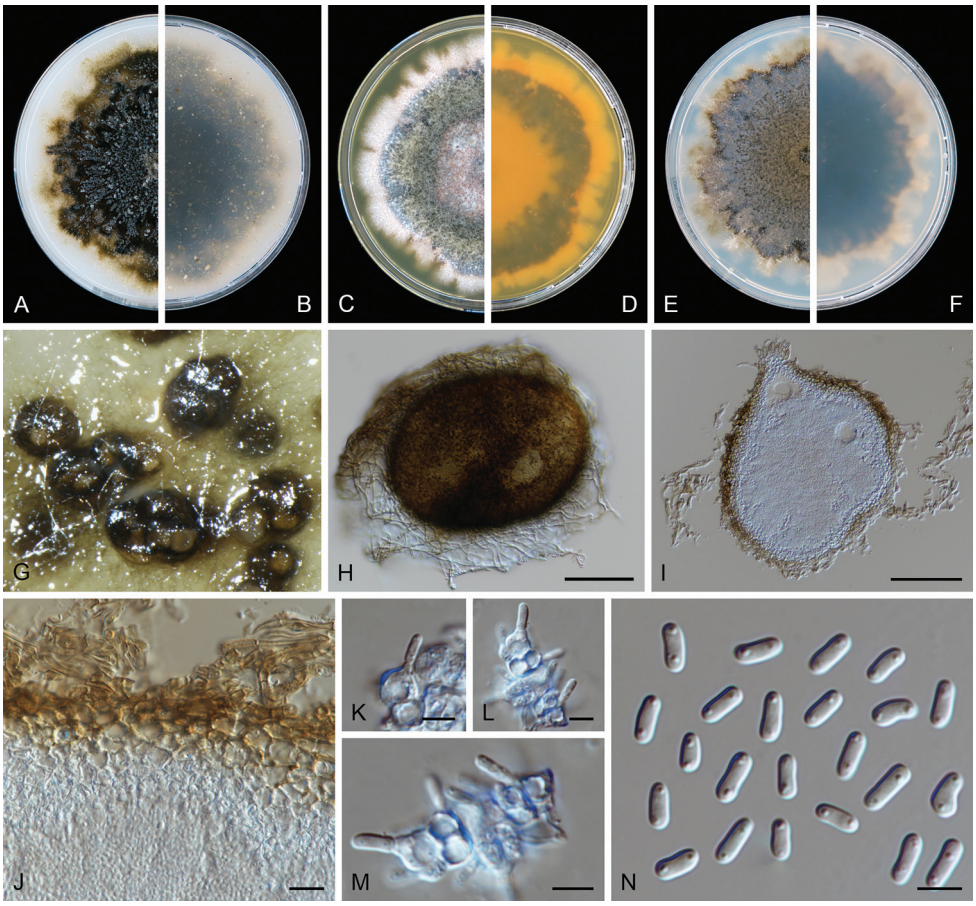

Figure 2. *Ascochyta benningiorum* (CBS 144957). **A, B** Colony on OA (front and reverse) **C, D** colony on MEA (front and reverse) **E, F** colony on PDA (front and reverse) **G** pycnidia forming on OA **H** pycnidium **I** section of pycnidium **J** section of pycnidial wall **K–M** conidiogenous cells **N** conidia. Scale bars: 100 µm (**H, I**); 10 µm (**J**); 5 µm (**K–N**).

Additional specimens examined. The Netherlands. Gelderland province, Wijchen, isolated from garden soil, Mar. 2017, E. Benning, B. Benning & A. Benning, JW 196023 = CBS 144958; ibid. JW 196013.

Notes. *Ascochyta benningiorum* is represented in the phylogenetic tree by three isolates (CBS 144957, CBS 144958 and JW 196013) from the same soil sample collected in Wijchen (Gelderland province). *Ascochyta benningiorum* grouped in a distinct clade close to *A. phacae* (Figure 1). However, it morphologically differs from *A. phacae* by having smaller (3.5–7 × 1.5–2.5 µm) and aseptate conidia. In *A. phacae* the conidia are 7–10 × 2–4 µm and 0–1-septate (Corbaz 1955).

Species in *Ascochyta* are commonly regarded as plant pathogens, especially of cereal crops and legumes (Davidson and Kimber 2007; Tivoli and Banniza 2007), and only a few species were reported from soil, namely *A. fabae*, *A. lentis*, *A. pisi*, *A. rabiei* (Gossen and Morrall 1986; Tivoli and Banniza 2007) and *A. syringae* in the current study.

Nevertheless, *A. benningiorum* is phylogenetically and morphologically distinct from these species (Figure 1; Chen et al. 2015).

Didymella degraaffiae **Hern.-Restr., L. W. Hou, L. Cai & Crous, sp. nov.**
MycoBank No: 833195
Figure 3

Etymology. *degraaffiae* refers to Janne de Graaff who collected the soil sample from which the ex-type strain was isolated.

Typus. The Netherlands. Limburg province, Weert, isolated from garden soil, Mar. 2017, J. de Graaff (***holotype*** designated here CBS H-24105, living ex-type culture CBS 144956 = JW 195004).

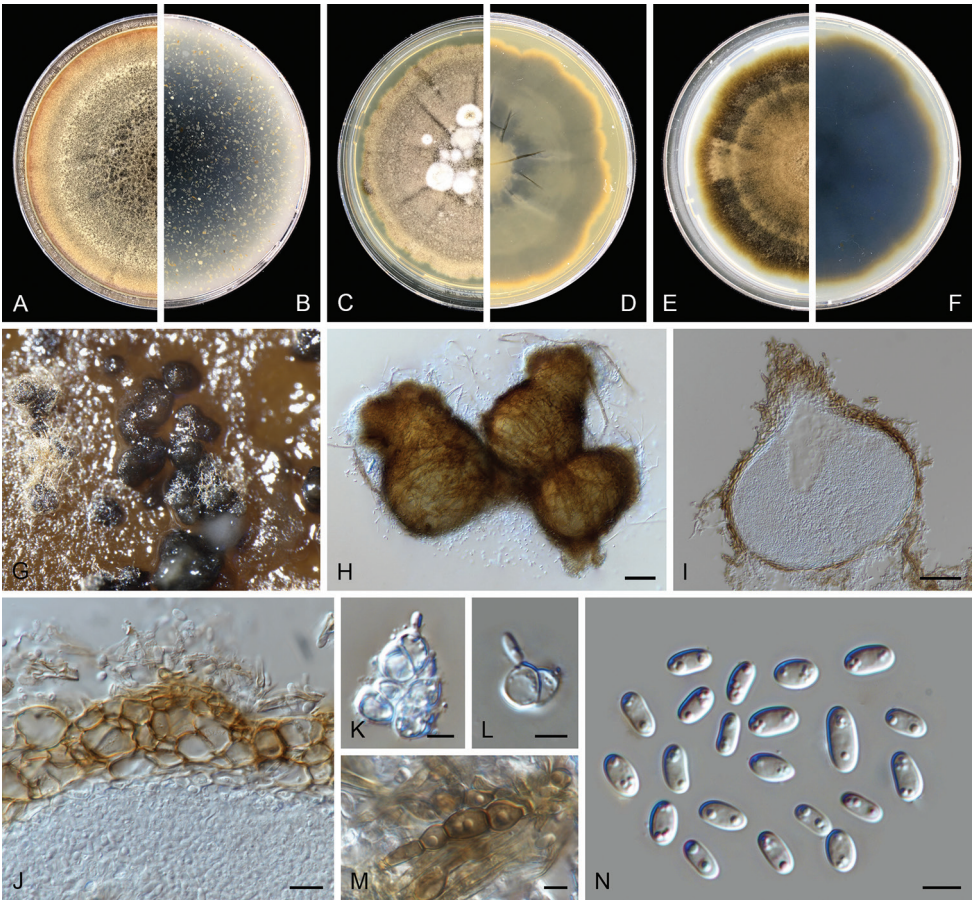

Figure 3. *Didymella degraaffiae* (CBS 144956). **A, B** Colony on OA (front and reverse) **C, D** colony on MEA (front and reverse) **E, F** colony on PDA (front and reverse) **G, H** pycnidia on OA **I** section of pycnidium **J** section of pycnidial wall **K, L** conidiogenous cells **M** chlamydospores **N** conidia. Scale bars: 50 µm (**H, I**); 10 µm (**J**); 5 µm (**K–N**).

Conidiomata pycnidial, superficial on the agar or semi-immersed in the agar, scattered or aggregated, mostly confluent, globose, subglobose, lageniform to irregularly-shaped with age, brown to dark brown, ostiolate, covered by hyphal outgrowths, especially near the ostiole, 150–485 × 120–330 µm; non-papillate or with up to two papillate ostioles; pycnidial wall pseudoparenchymatous, 3–6 layers, 10–55 µm thick, outer layers composed of brown, isodiametric cells, 16–33 µm diam. *Conidiogenous cells* phialidic, hyaline, smooth, ampulliform, lageniform, pyriform or globose, 5.5–8.5 × 5–8 µm. *Conidia* ellipsoidal, oblong or oval, thin- and smooth-walled, hyaline, aseptate, 4.5–9(–11) × 3–4.5 µm, 2–6-guttulate, small. *Conidial matrix* milky white.

Culture characteristics. Colonies after 7 d at 25 °C, on OA reaching 65–70 mm diam, aerial mycelium floccose, orange to olivaceous, margin regular; reverse black near the centre, pale grey towards the periphery. On MEA reaching 55–60 mm diam, aerial mycelium floccose, buff to pale olivaceous, with white mycelium pellet and radially furrowed zones near the centre, margin regular; reverse buff near the centre, olivaceous to yellow towards the periphery. On PDA reaching 50–55 mm diam, aerial mycelium floccose, concentric circles pale brown, pale olivaceous grey, dark olivaceous, honey, margin irregular; reverse black with a pale olivaceous edge. NaOH spot test negative on OA.

Notes. In our phylogenetic analysis, *D. degraaffiae* grouped with *D. americana* and *D. maydis* (Figure 1). However, morphologically, *D. americana* differs by its smaller conidiogenous cells (3–5 × 3–4 µm) and conidia (5–7 × 2–2.5 µm) (Boerema 1993); while *D. maydis* differs in having larger conidia (15–17 × 3.5–5 µm) (de Gruyter 2002). Furthermore, *D. americana* and *D. maydis* occasionally produced 1-septate conidia, while septate conidia were not observed in *D. degraaffiae*.

Didymella kooimaniorum **Hern.-Restr., L. W. Hou, L. Cai & Crous, sp. nov.**
MycoBank No: 833196
Figure 4

Etymology. *kooimaniorum* refers to Noud & Robin Kooiman who collected the soil sample from which the ex-type strain was isolated.

Typus. The Netherlands. Utrecht province, Vleuten, isolated from garden soil, Mar. 2017, N. Kooiman & R. Kooiman (***holotype*** designated here CBS H-24106, living ex-type culture CBS 144951 = JW 27006).

Conidiomata pycnidial, superficial or semi-immersed, scattered or solitary, sometimes confluent, globose to subglobose, irregularly-shaped with age, pale brown to brown, covered by hyphal outgrowths, especially near the ostioles, 200–375 × 195–280 µm; with 1–3(–6) papillate ostioles; pycnidial wall pseudoparenchymatous, 3–5 layers, 10–35 µm thick, outer layers composed of pale brown, flattened polygonal cells of 16–32 µm diam. *Conidiogenous cells* phialidic, hyaline, smooth, ampulliform, lageniform or somewhat isodiametric, (4.5–)5.5–10 × 3.5–9 µm. *Conidia* ellipsoidal to oblong, straight, thin- and smooth-walled, hyaline, aseptate, 3.5–7 × 2–3 µm, 2-guttulate, big. *Conidial matrix* buff.

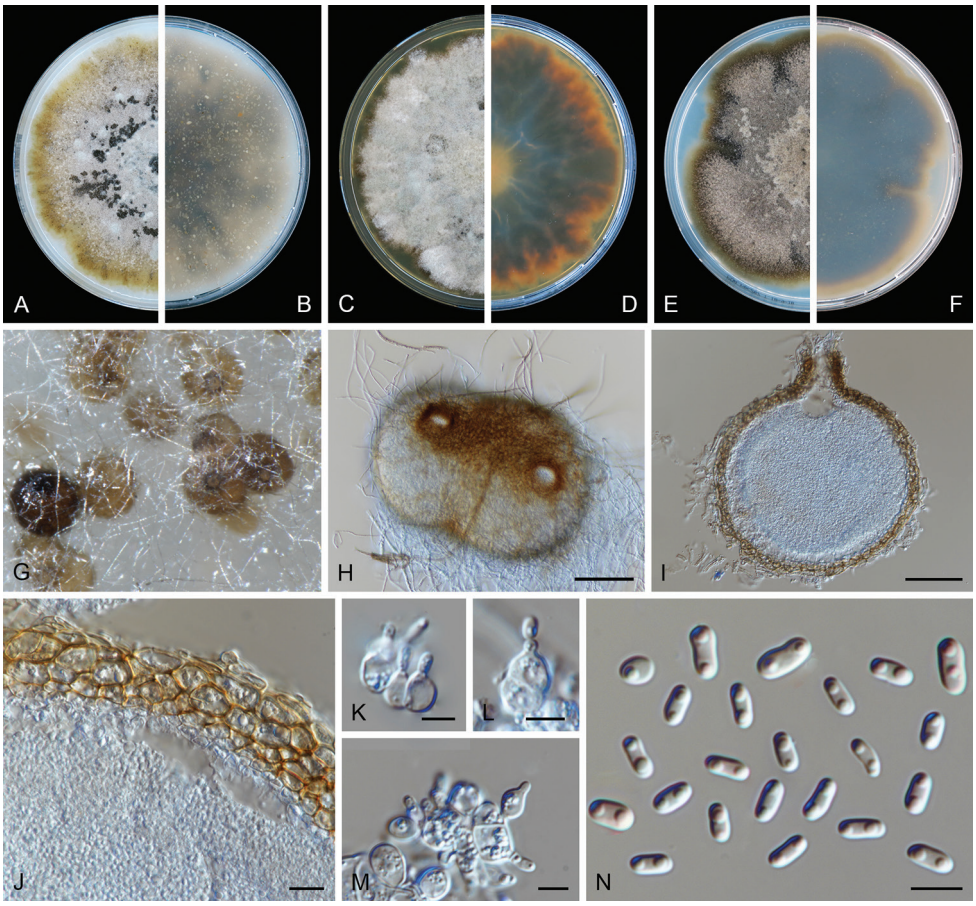

Figure 4. *Didymella kooimaniorum* (CBS 144951). **A, B** Colony on OA (front and reverse) **C, D** colony on MEA (front and reverse) **E, F** colony on PDA (front and reverse) **G** pycnidia forming on OA **H** pycnidia **I** section of pycnidium **J** section of pycnidial wall **K–M** conidiogenous cells **N** conidia. Scale bars: 100 µm (**H**); 50 µm (**I**); 10 µm (**J**); 5 µm (**K–N**).

Culture characteristics. Colonies after 7 d at 25 °C, on OA reaching 55–60 mm diam, aerial mycelium floccose, pale smoke grey, pale brown towards periphery, abundant production of confluent pycnidia, margin regular; reverse pale olivaceous, with some olivaceous black zones. On MEA reaching 50–55 mm diam, aerial mycelium woolly, pale olivaceous grey, margin irregular; reverse buff near the centre, dark brown with orange edge. On PDA reaching 50–55 mm diam, aerial mycelium floccose, pale mouse grey with olivaceous edge, margin irregular; reverse dark brown with pale brown edge. NaOH spot test negative on OA.

Notes. Based on the multi-gene phylogenetic analyses, *D. kooimaniorum* forms an independent branch, clearly separated from other species in *Didymella* (Figure 1). Morphologically, *D. kooimaniorum* is characterised by pale brown pycnidia densely covered by long hairs, and ostioles with up to six papillae with a darker neck.

Juxtiphoma kolkmaniorum **Hern.-Restr., L. W. Hou, L. Cai & Crous, sp. nov.**
MycoBank No: 833197
Figure 5

Etymology. *kolkmaniorum* refers to Linde & Mette Kolkman who collected the soil sample from which the ex-type strain was isolated.

Typus. The Netherlands. Ophemert, isolated from garden soil, Mar. 2017, L. & M. Kolkman (***holotype*** designated here CBS H-24214, living ex-type culture CBS 146005 = JW 185006).

Conidiomata pycnidial, superficial, solitary or confluent, globose to subglobose, brown to dark brown, glabrous, covered by dark hyphae and chlamydospores, 100–350 µm; uniostiolate papillate; pycnidial wall pseudoparenchymatous, 2–4 layers, 7.5–12.5 µm thick, outer layer composed of brown, flattened polygonal cells. *Conidiogenous cells* mono- or

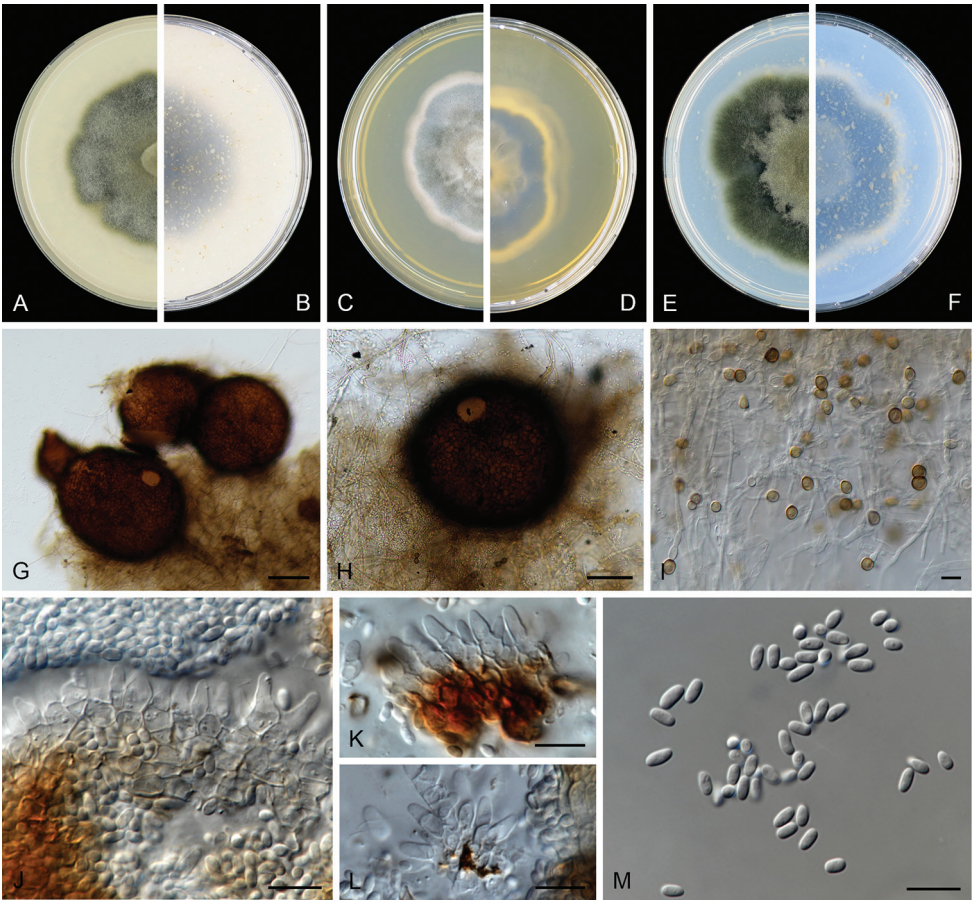

Figure 5. *Juxtiphoma kolkmaniorum* (CBS 146005). **A, B** Colony on OA (front and reverse) **C, D** colony on MEA (front and reverse) **E, F** colony on PDA (front and reverse) **G, H** pycnidium forming on OA **I** chlamydospores **J–L** conidiogenous cells **M** conidia. Scale bars: 100 µm (**G, H**); 10 µm (**I–M**).

polyphialidic, hyaline, smooth, subcylindrical, ampulliform or somewhat isodiametric, 5.5–11.5 × 2.5–5.5 µm. *Conidia* ellipsoidal to oblong, straight or curved, thin- and smooth-walled, hyaline, aseptate, 3.5–7.5 × 2–3 µm, 1–3-guttulate, medium. *Conidial matrix* white to buff. *Chlamydospores* terminal or intercalary, solitary, or in simple or branched chains, barrel-shaped, subglobose or ellipsoidal, pale brown to brown, guttulate, 5.5–12 × 4–8 µm.

Culture characteristics. Colonies after 7 d at 25 °C, on OA reaching 45–60 mm diam, aerial mycelium cottony to floccose, isabelline to olivaceous, margin irregular; reverse concolorous. On MEA reaching 45–55 mm diam, aerial mycelium cottony to floccose, smoke grey to pale olivaceous grey with white edge, margin entire; reverse buff to smoke grey near the centre, olivaceous black with buff edge. On PDA reaching 45–50 mm diam, aerial mycelium cottony to floccose, olivaceous buff, dull green to buff, margin irregular; reverse smoke grey near the centre, olivaceous black with buff edge. NaOH spot test negative on OA.

Additional specimens examined. Germany. Kiel-Kitzeberg, from wheat field soil, 1966, W. Gams, living cultures CBS 527.66 = FMR 15337 = ATCC 22238; The Netherlands. North Brabant province, Breda, isolated from garden soil, Mar. 2017, F. Versantvoort, JW 167004; ibid. JW 168007; Rijen, isolated from garden soil, Mar. 2017, G. & L. Schijvenaars, JW 94009. North Holland province, Hilversum, isolated from garden soil, Mar. 2017, S. Nieuwenhuijsen, JW 23021. Utrecht province, Amersfoort, isolated from garden soil, Mar. 2017, M. Kerssen, JW 125028; Amersfoort, isolated from garden soil, Mar. 2017, E., K. & O. de Jong Verpaalen, JW 241011; Amersfoort, isolated from garden soil, Mar. 2017, F. Wiegerinck, specimen CBS H-24102, culture CBS 145911 = JW 4017; Amersfoort, isolated from garden soil, Mar. 2017, T. & K. Wesselink, JW 191004; Bilthoven, isolated from garden soil, Mar. 2017, Y. El Ghazi, JW 220011; Utrecht, isolated from garden soil, Mar. 2017, J. Kooijmans, JW 63001.

Notes. *Juxtiphoma kolkmaniorum* is very similar and phylogenetically close to *J. eupyrena*. However, based on the multi-gene phylogenetic analyses, *J. kolkmaniorum* forms a separate clade (Figure 1). Morphologically, *J. kolkmaniorum* has conidia slightly larger and with more guttules than those of *J. eupyrena* (3.5–7.5 × 2–3 µm, 1–3-guttulate vs. 4.2–5.6 × 1.8–2.4 µm, 2-guttulate, de Gruyter and Noordeloos 1992) and smaller chlamydospores (5.5–12 × 4–8 µm vs. 8–20 × 6–15 µm, de Gruyter and Noordeloos 1992).

Nothophoma brennandiae **Hern.-Restr., L. W. Hou, L. Cai & Crous, sp. nov.**
MycoBank No: 833198
Figure 6

Etymology. *brennandiae* refers to Kristel Brennand who collected the soil sample from which the ex-type strain was isolated.

Typus. The Netherlands. Limburg province, Ell, isolated from garden soil, Mar. 2017, K. Brennand (***holotype*** designated here CBS H-24103, living ex-type culture CBS 145912 = JW 53011).

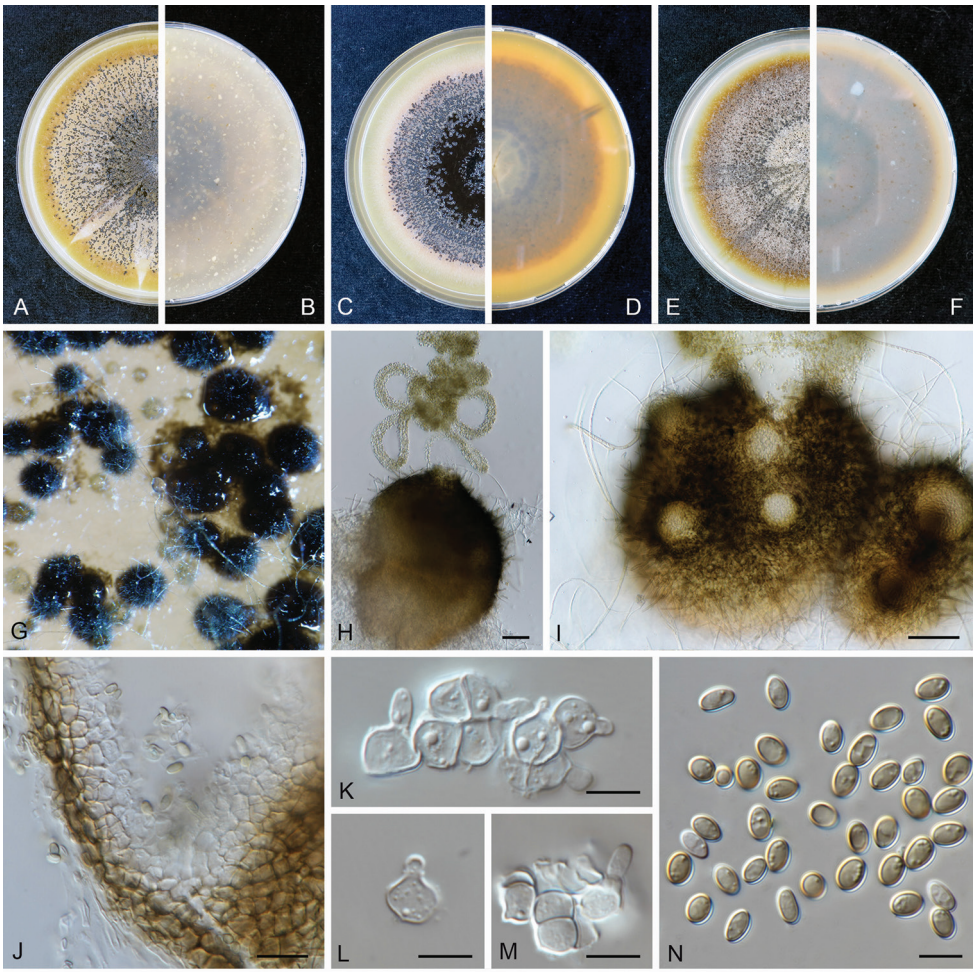

Figure 6. *Nothophoma brennandiae* (CBS 145912). **A, B** Colony on OA (front and reverse) **C, D** colony on MEA (front and reverse) **E, F** colony on PDA (front and reverse) **G** pycnidia forming on OA. **H, I** pycnidia **J** section of pycnidial wall **K–M** conidiogenous cells **N** conidia. Scale bars: 50 µm (**H, I**); 10 µm (**J**); 5 µm (**K–N**).

Conidiomata pycnidial, superficial to semi-immersed, solitary to confluent, globose to subglobose, irregularly-shaped with age, brown, setose, especially near the ostioles, 155–350 × 100–300 µm; with 1–4 papillate ostioles; pycnidial wall pseudoparenchymatous, 3–6 layers, 13.5–21.5 µm thick, outer layers composed of brown, flattened polygonal cells. *Conidiogenous cells* phialidic, hyaline, smooth, ampulliform or somewhat isodiametric, 3–5 × 5–8 µm. *Conidia* ellipsoidal, broadly ellipsoidal to oblong, straight, thick- and smooth-walled, hyaline becoming brown, aseptate, 3–8.5 × 1.5–3 µm, 1–6-guttulate, minute. *Conidial matrix* sepia to brown vinaceous.

Culture characteristics. Colonies after 7 d at 25 °C, on OA reaching 50–55 mm diam, aerial mycelium scarce, spore mass with grease-like appearance, dark brick to sepia, cinnamon to the edge, abundant production of confluent pycnidia, margin en-

tire; reverse concentric rings umber to cinnamon. On MEA reaching 47–50 mm diam, aerial mycelium scarce, spore mass with grease-like appearance, dark brick to sepia, cinnamon to the edge, abundant production of confluent pycnidia, margin entire; reverse concentric rings umber to cinnamon. On PDA reaching 50–55 mm diam, aerial mycelium moderate to scarce, cottony, buff, spore mass with grease-like appearance, dark brick, ochreous to the edge, margin entire; reverse concentric rings dark brick to cinnamon. NaOH spot test negative on OA.

Additional specimen examined. The Netherlands. North Holland province, Amsterdam, isolated from garden soil, Mar. 2017, J. van Dijk, JW 1066.

Notes. In the phylogenetic tree *N. brennandiae* was close to *N. quercina* and *N. pruni* (Figure 1). Morphologically, *N. brennandiae* can be distinguished from *N. quercina* by having setose conidiomata with up to 4 ostioles, while in *N. quercina* conidiomata are glabrous with a single ostiole (Sydow and Sydow 1915; Aveskamp et al. 2010). Furthermore, conidia in *N. quercina* are larger and have less guttules (5.5–9 × 2.5–5 µm, 0–2(–3) guttules) (Sydow and Sydow 1915; Aveskamp et al. 2010). On the other hand, *N. pruni* is characterised by hyaline conidia (Chethana et al. 2019), while *N. brennandiae* produces conidia that turn brown with age.

Paraboeremia rekkeri **Hern.-Restr., L. W. Hou, L. Cai & Crous, sp. nov.**
MycoBank No: 833199
Figure 7

Etymology. *rekkeri* refers to Daan Rekker who collected the soil sample from which the ex-type strain was isolated.

Typus. The Netherlands. Gelderland province, Geldermalsen, isolated from garden soil, Mar. 2017, D. Rekker (***holotype*** designated here CBS H-24107, living ex-type culture CBS 144955 = JW 172002).

Conidiomata pycnidial, superficial, scattered or aggregated, solitary or confluent, globose or subglobose, irregularly-shaped with age, buff to brown, covered with abundant mycelial outgrowths especially when young, 150–390 × 120–320 µm; 1–2 papillate or non-papillate ostioles; pycnidial wall pseudoparenchymatous, 3–7 layers, 17.5–37 µm thick, outer layers composed of brown, flattened polygonal cells, 10–21 µm diam. *Conidiogenous cells* phialidic, hyaline, smooth, globose, subglobose or ampulliform, 5–10 × 4.5–7.5 µm. *Conidia* ellipsoidal to oblong, thin- and smooth-walled, hyaline, aseptate, 3.5–5 × 2.5–3 µm, with 2(–3) large guttules. *Conidial matrix* pink.

Culture characteristics. Colonies after 7 d at 25 °C, on OA reaching 75–80 mm diam, aerial mycelium floccose, saffron, vinaceous buff, pale olivaceous, margin regular; reverse concentric circles saffron, grey, olivaceous grey. On MEA reaching 55–60 mm diam, aerial mycelium floccose, margin irregular, pale olivaceous grey to whitish, orange near edge; reverse brown to dark brown, orange towards the periphery. On PDA reaching 70–75 mm diam, margin irregular, covered by felty aerial mycelium, buff, olivaceous grey towards periphery; reverse mouse, olivaceous towards periphery. NaOH spot test negative on OA.

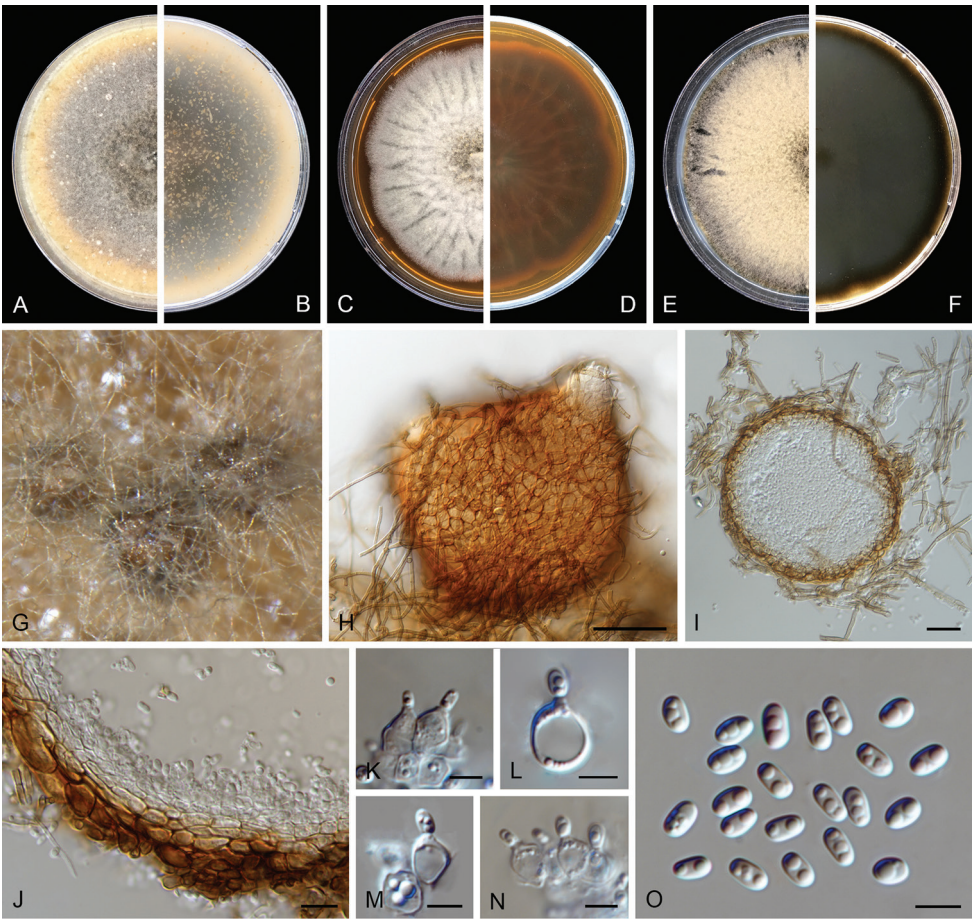

Figure 7. *Paraboeremia rekkeri* (CBS 144955). **A, B** Colony on OA (front and reverse) **C, D** colony on MEA (front and reverse) **E, F** colony on PDA (front and reverse) **G** pycnidia forming on OA **H** pycnidium **I** section of pycnidium **J** section of pycnidial wall **K–N** conidiogenous cells **O** conidia. Scale bars: 100 µm (**H**); 20 µm (**I**); 10 µm (**J**); 5 µm (**K–O**).

Additional specimens examined. Gelderland province, Culemborg, isolated from garden soil, Mar. 2017, H. van de Warenburg, JW 3018; Kapel-Avezaath, isolated from garden soil, Mar. 2017, A. Panneman, JW 79024; Meteren, isolated from garden soil, S. van Stuijvenberg, JW 132004; North Brabant province, Breda, isolated from garden soil, Mar. 2017, F. Wiegerinck, CBS 144949 = JW 4024; Breda, isolated from garden soil, Mar. 2017, F. Versantvoort, JW 167006; Zwanenburg, isolated from garden soil, Mar. 2017, J. Rebergen, JW 91008; North Holland province, Alkmaar, Mar. 2017, B. Verschoor, JW 13016, ibid. JW 13017 and JW13030; Utrecht province, Bilthoven, isolated from garden soil, Mar. 2017, H. Vos & S. Vos, JW 51014; Eemnes, isolated from garden soil, Mar. 2017, H.W. Vos, CBS 144950 = JW 6005; Hooglanderveen, isolated from garden soil, Mar. 2017, F. Rijpma, JW 25013; Utrecht, isolated from garden soil, R. van Zijl, JW 226002.

Notes. *Paraboeremia rekkeri* formed a well-supported (1.0/100/96) distinct lineage in *Paraboeremia* (Figure 1). It is most closely related with *P. truiniorum*, another novel species collected from Dutch soil and described in the present study. However, *P. rekkeri* is distinguished by producing larger pycnidia (150–390 × 120–320 µm), with a thinner pycnidial wall (3–7 layers and 17.5–37 µm thick). Pycnidia in *P. truiniorum* are 160–420 × 135–430 µm, and have a wall of 7–11 layers and 40–70 µm thick.

Paraboeremia truiniorum **Hern.-Restr., L. W. Hou, L. Cai & Crous, sp. nov.**
MycoBank No: 833201
Figure 8

Etymology. *truiniorum* refers to Cuno & Tygo Truin who collected the soil sample from which the ex-type strain was isolated.

Typus. The Netherlands. Gelderland province, Barneveld, Voorthuizen, isolated from garden soil, Mar. 2017, C. Truin & T. Truin (***holotype*** designated here CBS H-24108, living ex-type culture CBS 144952 = JW 47002).

Conidiomata pycnidial, superficial, scattered or aggregated, most solitary, globose or subglobose, confluent and irregularly-shaped with age, pale brown, thick-walled, covered with abundant mycelial outgrowths, 160–420 × 135–430 µm; 1-papillate or non-papillate ostioles, sometimes elongated to a short neck; pycnidial wall pseudoparenchymatous, 7–11 layers, 40–70 µm thick, outer layers composed of brown, flattened polygonal cells of 22–45.5 µm diam. *Conidiogenous cells* phialidic, hyaline, smooth, globose, subglobose, ampulliform or doliiform, 4.5–8.5 × 4–7 µm. *Conidia* ellipsoidal to oblong, thin- and smooth-walled, hyaline, aseptate, 3.5–5 × 2–3 µm, with (1–)2 large guttules. *Conidial matrix* whitish.

Culture characteristics. Colonies after 7 d at 25 °C, on OA reaching 70–75 mm diam, aerial mycelium floccose, vinaceous buff to hazel, margin regular; reverse buff to olivaceous. On MEA reaching 65–70 mm diam, aerial mycelium felty, whitish, pale mouse grey toward periphery, margin regular; reverse dark brick to dark brown, with pale brown edge. On PDA reaching 75–80 mm diam, aerial mycelium felty, olivaceous buff to pale mouse grey, olivaceous toward periphery, margin irregular; reverse mouse grey, olivaceous toward periphery. NaOH spot test negative on OA.

Additional specimens examined. The Netherlands, Gelderland province, Culemborg, isolated from garden soil, Mar. 2017, R. Fuld, JW 182014; The Netherlands. South Holland province, Alphen aan den Rijn, isolated from garden soil, Mar. 2017, K. Boutwell, CBS 144961 = JW 203021; The Netherlands. South Holland province, Gorinchem, isolated from garden soil, Mar. 2017, L. van Rosmalen, JW 270002; The Netherlands. Utrecht province, Utrecht, isolated from garden soil, Mar. 2017, L. van Rijnberk, JW 147025; The Netherlands. Utrecht province, Woerden, isolated from garden soil, Mar. 2017, L. Borsboom, JW 192003.

Notes. Based on the phylogenetic analyses, *P. truiniorum* is represented by six isolates, forming a distinct lineage (Figure 1). *Paraboeremia truiniorum* is charac-

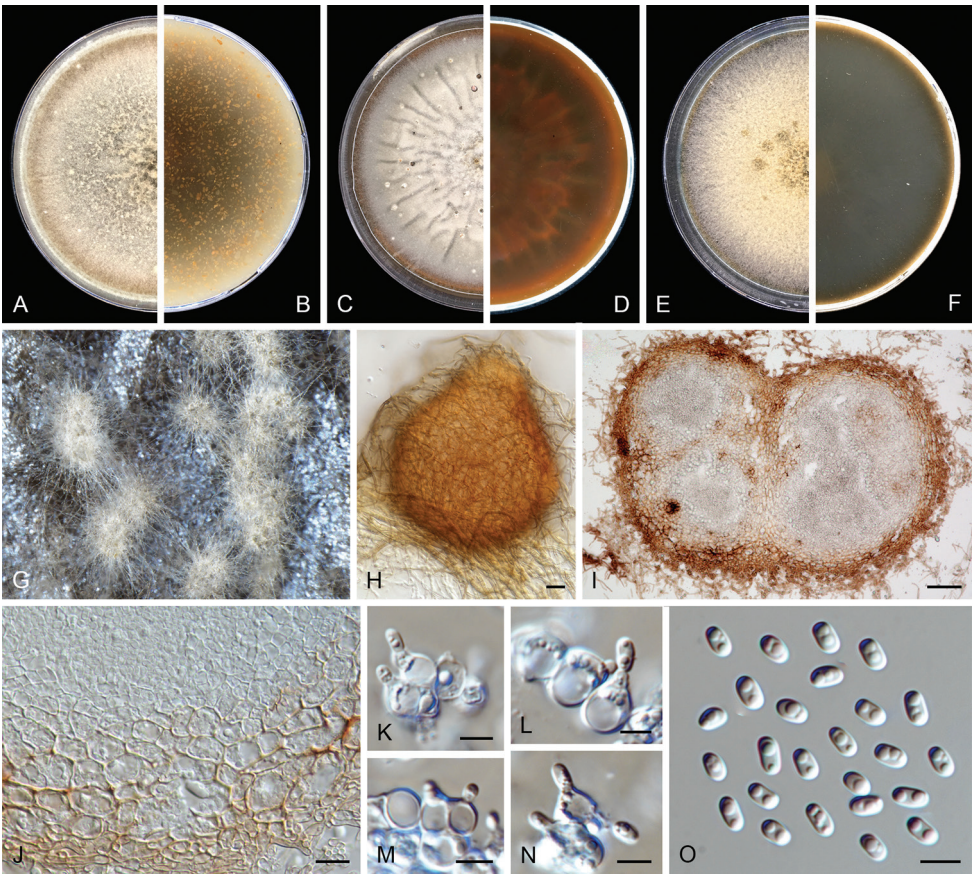

Figure 8. *Paraboeremia truiniorum* (CBS 144952). **A, B** Colony on OA (front and reverse) **C, D** colony on MEA (front and reverse) **E, F** colony on PDA (front and reverse) **G** pycnidia forming on OA **H** pycnidium **I** section of pycnidium **J** section of pycnidial wall **K–N** conidiogenous cells **O** conidia. Scale bars: 20 µm (**H**); 50 µm (**I**); 5 µm (**J–O**).

terised by the dense mycelial outgrowths on its pycnidia. Both *P. truiniorum* and *P. rekkeri* are phylogenetically close to the well-known soil-borne species, *P. putaminum*. However, *P. putaminum* is distinguished from these two new species by producing smaller conidia (3.2–4.2 × 2–2.6 µm) with greenish guttules (Boerema et al 2004).

Stagonosporopsis stuijvenbergii **Hern.-Restr., L. W. Hou, L. Cai & Crous, sp. nov.**
MycoBank No: 833203
Figure 9

Etymology. *stuijvenbergii* refers to Simon van Stuijvenberg, who collected the soil sample from which the ex-type strain was isolated.

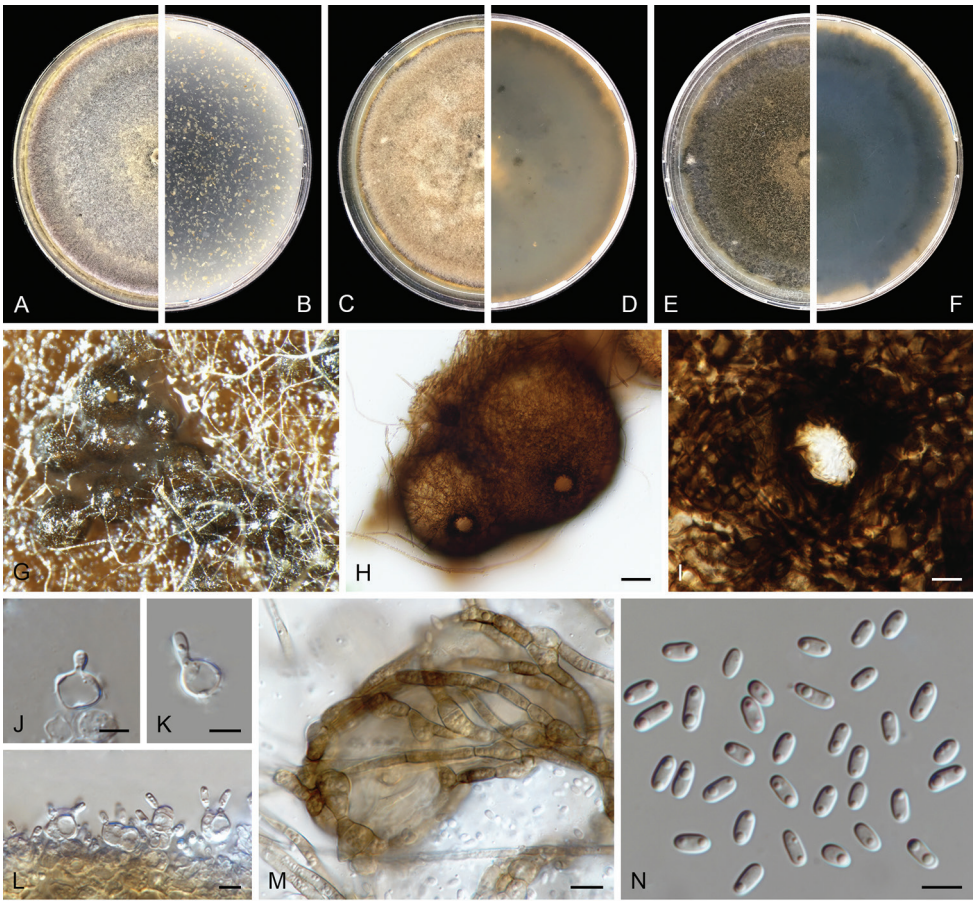

Figure 9. *Stagonosporopsis stuijvenbergii* (CBS 144953). **A, B** Colony on OA (front and reverse) **C, D** colony on MEA (front and reverse) **E, F** colony on PDA (front and reverse) **G** pycnidia forming on OA **H** pycnidia **I** ostiole **J–L** conidiogenous cells **M** stromatic hyphal aggregations **N** conidia. Scale bars: 50 µm (**H**); 10 µm (**I, M**); 5 µm (**J–L, N**).

Typus. The Netherlands. Gelderland province, Meteren, from garden soil, Mar. 2017, S. van Stuijvenberg (***holotype*** designated here CBS H-24109; living ex-type culture CBS 144953 = JW 132011).

Conidiomata pycnidial, produced on the agar surface, scattered or aggregated, solitary globose to subglobose, or 4–7(–10) confluent and irregularly-shaped, brownish, glabrous, ostiolate, 200–1000 × 195–930 µm; with 1–2 slightly papillate ostioles, sometimes elongated to a short neck; pycnidial wall pseudoparenchymatous, 4–5 layers, 6.5–35 µm thick, outer layers composed of brown, flattened polygonal cells, 9.5–33 µm diam. *Conidiogenous cells* phialidic, hyaline, smooth, globose, ampulliform or lageniform, 4.5–9 × 4–8 µm. *Conidia* ellipsoidal to oblong, smooth- and thin-walled, hyaline, aseptate, 3.5–6.5 × 2–3 µm, 1–2-guttulate. *Conidial matrix* whitish.

Culture characteristics. Colonies after 7 d at 25 °C, on OA reaching 75–80 mm diam, floccose aerial mycelium, olivaceous to pale olivaceous, whitish to pink near the edge, margin regular; reverse iron grey. On MEA reaching 65–70 mm diam, margin regular, aerial mycelium floccose, vinaceous buff with olivaceous edge; reverse darker brown with olivaceous black edge, buff near the centre. On PDA reaching 70–75 mm diam, margin regular, covered by floccose aerial mycelium, olivaceous, olivaceous black towards periphery, with pinkish to pale brown edge; reverse iron-grey, buff towards periphery. NaOH spot test negative on OA.

Additional specimens examined. The Netherlands, Gelderland province, Arnhem, from garden soil, Mar. 2017, D. Peters, JW 14003; Utrecht province, Utrecht, from garden soil, Mar. 2017, N. Francisca, JW 44014; Utrecht, from garden soil, Mar. 2017, P. de Koff, JW 33021.

Notes. Phylogenetically, *S. stuijvenbergii* is most closely related to *S. weymaniae*, another novel species collected from Dutch soil in this study (Figure 1). However, *S. stuijvenbergii* is distinguishable from *S. weymaniae* by the colour and the size of its pycnidia, being brown and measuring 200–1000 × 195–930 µm in *S. stuijvenbergii*, whereas *S. weymaniae* produces whitish pycnidia, measuring 330–650 × 250–550 µm. Furthermore, *S. weymaniae* produces microconidia and chlamydospores, which were not observed in *S. stuijvenbergii*. Although there are several reports that *Stagonosporopsis* spp. could survive in soil for a short time (Vaghefi et al. 2016), this is the first record of a *Stagonosporopsis* species only known from soil (Domsch et al. 2007). *Stagonosporopsis stuijvenbergii* is represented by four strains isolated from different samples collected in Utrecht and Gelderland provinces.

Stagonosporopsis weymaniae **Hern.-Restr., L. W. Hou, L. Cai & Crous, sp. nov.**
MycoBank No: 833204
Figure 10

Etymology. *weymaniae* refers to Anna Weyman, who collected the soil sample from which the ex-type strain was isolated.

Typus. The Netherlands. Utrecht province, Baarn, isolated from garden soil, Mar. 2017, A. Weyman (***holotype*** designated here CBS H-24110; living ex-type culture CBS 144959 = JW 201003).

Conidiomata pycnidial, semi-immersed or immersed, mostly solitary, scattered or aggregated, (sub-)globose, whitish to buff, glabrous, 330–650 × 250–550 µm; non-ostiolate or with a single, inconspicuous ostiole; pycnidial wall pseudoparenchymatous, 2–9 layers, 20–60 µm thick, outer layers composed of hyaline, flattened polygonal cells. *Conidiogenous cells* phialidic, hyaline, smooth, (sub-)globose to ampulliform, 4.5–7.5 × 4–7.5 µm. *Macroconidia* oblong, smooth- and thin-walled, hyaline, aseptate, 4–6.5(–8) × 2–3 µm, 1–3(–4)-guttulate, with one large central guttule or two large polar guttules. *Microconidia* produced in the same pycnidia with macroconidia, globose to subglobose, smooth, hyaline, aseptate, 3–4 × 2.5–3.5

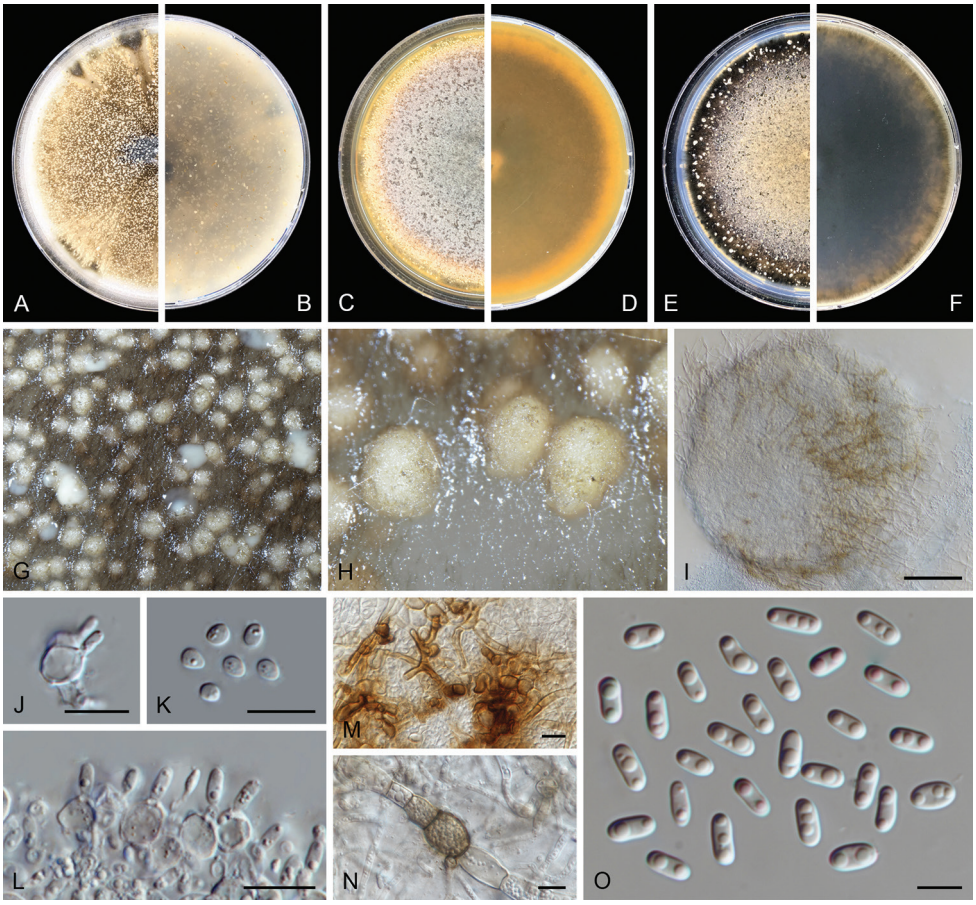

Figure 10. *Stagonosporopsis weymaniae* (CBS 144959). **A, B** Colony on OA (front and reverse) **C, D** colony on MEA (front and reverse) **E, F** colony on PDA (front and reverse) **G–I** pycnidia forming on OA **J, L** conidiogenous cells **K** subglobose conidia **M** stromatic hyphal aggregations **N** chlamydospores **O** oblong conidia. Scale bars: 100 µm (**I**); 10 µm (**J–N**); 5 µm (**O**).

µm, with a single, small guttule. *Conidial matrix* whitish. *Chlamydospores* unicellular, intercalary in chains, barrel-shaped, thick-walled, pale brown to green brown, guttulate, 9.5–14 × 11–16 µm diam.

Culture characteristics. Colonies after 7 d at 25 °C, on OA reaching 70–75 mm diam, sparse aerial mycelium, buff to pale olivaceous with sparse olivaceous zones, darker grey near the centre, abundant production of buff pycnidia, margin regular; reverse pale olivaceous, olivaceous black near the centre. On MEA reaching 80–85 mm diam, margin regular, aerial mycelium floccose, yellow to vinaceous buff; reverse orange to olivaceous. On PDA reaching 75–80 mm diam, margin regular, covered by floccose aerial mycelium, centre vinaceous buff, dark olivaceous towards the periphery with production of buff pycnidia; reverse olivaceous black, olivaceous towards the periphery. NaOH spot test: pale reddish discolouration on OA plate.

Notes. *Stagonosporopsis weymaniae* is phylogenetically closely related to *S. stuijvenbergii* (Figure 1). Morphological differences between *S. weymaniae* and *S. stuijvenbergii* are discussed under the latter species. *Stagonosporopsis weymaniae* together with *S. stuijvenbergii* formed a sister group with *S. bomiensis* and *S. papillata*, two plant pathogens from China (Chen et al. 2017). However, *S. weymaniae* differs from them by producing larger pycnidia [330–650 × 250–550 µm vs. 100–200 × 100–180 µm in *S. bomiensis* and (130–)200–280 × (100–)150–250 µm in *S. papillata*] and microconidia which are absent in *S. papillata* and *S. bomiensis* (Chen et al. 2017).

Vandijckomycella **Hern.-Restr., L. W. Hou, L. Cai & Crous, gen. nov.**
MycoBank No: 833205

Etymology. Named in honour of José F.T.M. van Dijck, who was elected as the first female President (2015–2018) of the Royal Dutch Academy of Arts and Sciences (KNAW).

Type species. *Vandijckomycella joseae* Hern.-Restr., L.W. Hou, L. Cai & Crous.

Conidiomata pycnidial, superficial on the surface of the agar, solitary or confluent, globose to lageniform, covered by hyphal outgrowths, ostiolate, pycnidial wall pseudoparenchymatous, with 3–9 layers. *Conidiogenous cells* phialidic, hyaline, smooth, globose or ampulliform. *Conidia* hyaline, smooth- and thin-walled, aseptate, ovoid, oblong or ellipsoidal, with 2–4 polar guttules.

Vandijckomycella joseae **Hern.-Restr., L. W. Hou, L. Cai & Crous, sp. nov.**
MycoBank No: 833208
Figure 11

Etymology. Named in honour of the first female President (2015–2018) of the Royal Dutch Academy of Arts and Sciences (KNAW), José F.T.M. van Dijck, who collected the soil sample from which the ex-type strain was isolated.

Typus. The Netherlands. North Holland province, Amsterdam, isolated from garden soil, Mar. 2017, J.F.T.M. van Dijk (***holotype*** designated here CBS H-24112; living ex-type culture CBS 143011 = JW 1073).

Conidiomata pycnidial, produced on the agar surface, scattered or aggregated, solitary, (sub-)globose, confluent and irregularly-shaped with age, pale brown, covered in abundant long and thin mycelium hair, 150–340 × 130–250 µm; with 1–2 slightly papillate or non-papillate ostioles, sometimes elongated to a short neck; pycnidial wall pseudoparenchymatous, 3–5 layers, 13–25 µm thick, outer layers composed of brown, flattened, polygonal cells of 10–23 µm diam. *Conidiogenous cells* phialidic, hyaline, smooth, globose, ampulliform, lageniform or subglobose, 5–8(–9.5) × 4–8 µm. *Conidia* ellipsoidal to oblong, smooth- and thin-walled, hyaline, aseptate, 3.5–5.5 × 2–2.5 µm, (1–)2(–3)-guttulate. *Conidial matrix* whitish.

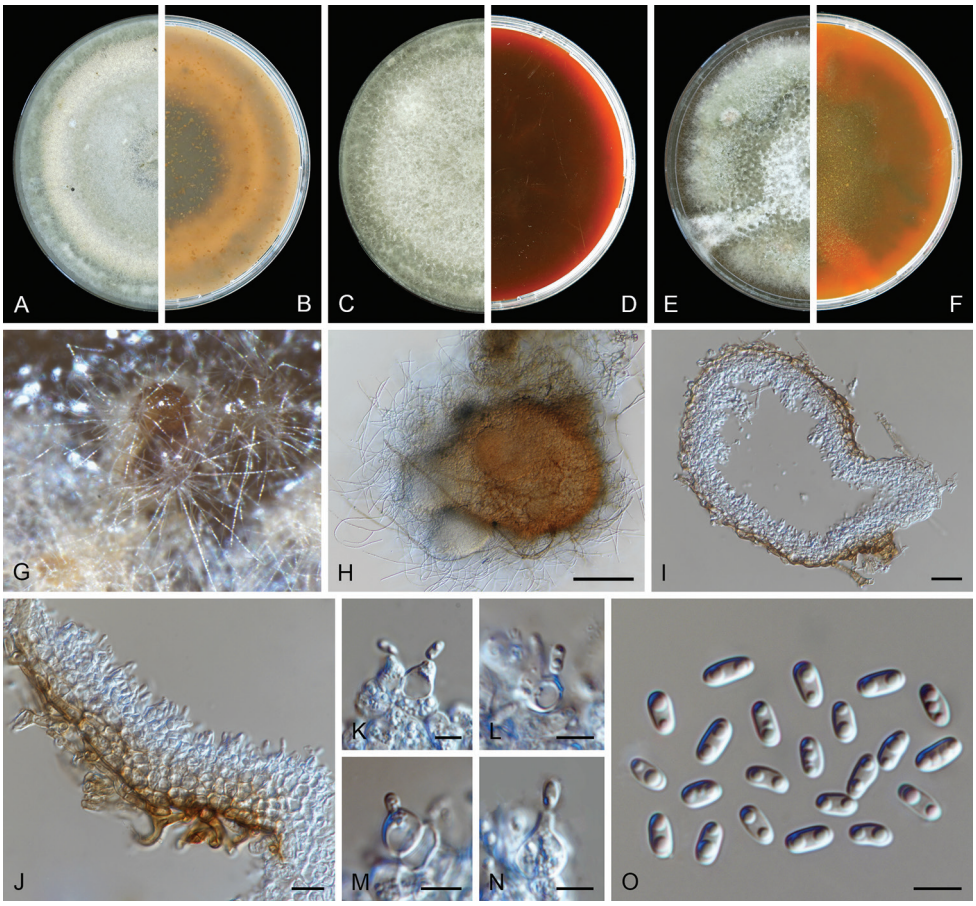

Figure 11. *Vandijckomycella joseae* (CBS 143011). **A, B** Colony on OA (front and reverse) **C, D** colony on MEA (front and reverse) **E, F** colony on PDA (front and reverse) **G, H** pycnidia forming on OA **I, J** section of pycnidial wall **K–N** conidiogenous cells **O** conidia. Scale bars: 100 µm (**H**); 20 µm (**I**); 10 µm (**J**); 5 µm (**K–O**).

Culture characteristics. Colonies after 7 d at 25 °C, on OA reaching 75–80 mm diam after 7 d, covered by woolly aerial mycelium, concentric circles, pale olivaceous grey, pink, pale greenish grey, whitish near the edge, margin regular; reverse concentric circles dark brown, pale brown, orange, and pale olivaceous. On MEA reaching 75–80 mm diam, aerial mycelium woolly, margin regular, pale olivaceous grey; reverse dark brown, reddish towards the periphery. On PDA reaching 75–80 mm diam, margin regular, covered by felty aerial mycelium, pale olivaceous grey or olivaceous grey, with whitish parts near the centre or through the plate; reverse zonate, orange to reddish, brown and yellow. NaOH spot test: a coral discolouration on OA.

Additional specimen examined. The Netherlands. North Holland province, Amsterdam, isolated from garden soil, Mar. 2017, J.F.T.M. van Dijk, CBS 144948 = JW 1068.

Notes. The new genus *Vandijckomycella* is introduced to accommodate two new species isolated from soil samples which form an independent lineage in Didymellaceae, being clearly separated from other genera (Figure 1). Based on the phylogenetic analysis, *V. joseae* forms a distinct lineage which is distant from the nearest species *V. snoekiae*, and chiefly differs on *tub2* and *rpb2* sequences. Morphological differences between *V. joseae* and *V. snoekiae* are discussed under the latter species. *Vandijckomycella joseae* is characterised by producing pycnidia with longer whitish hyphal outgrowths, and with elongated necks.

Vandijckomycella snoekiae **Hern.-Restr., L. W. Hou, L. Cai & Crous, sp. nov.**
MycoBank No: 833207
Figure 12

Etymology. *snoekiae* refers to Rana Marit Ida Snoek who collected the soil sample from which the ex-type strain was isolated.

Typus. The Netherlands. Utrecht province, Utrecht, isolated from garden soil, Mar. 2017, R.M.I. Snoek (***holotype*** designated here CBS H-24111, living ex-type culture CBS 144954 = JW 149017).

Conidiomata pycnidial, superficial on the agar or covered under a thick mycelial layer, scattered or aggregated, mostly solitary, globose to subglobose, sometimes confluent, ellipsoidal, dark brown, covered by abundant long hyphal outgrowths, 150–650(–850) × 145–600(–730) µm; ostioles inconspicuous; pycnidial wall pseudoparenchymatous, 5–9 layers, 37–58.5 µm thick, outer layers composed of brown, flattened polygonal cells, 10–23 µm diam. *Conidiogenous cells* phialidic, hyaline, smooth, globose, ampulliform or lageniform, 5–8.5 × 5–7.5 µm. *Conidia* oblong, smooth- and thin-walled, hyaline, aseptate, 4–6.5 × 2–2.5 µm, with two small polar guttules. *Conidial matrix* whitish.

Culture characteristics. Colonies after 7 d at 25 °C, on OA reaching 50–55 mm diam after 7 d, covered by floccose aerial mycelium, pink to grey, darker grey near the centre, margin regular; reverse black near the centre, yellow towards the periphery. On MEA reaching 50–55 mm diam, aerial mycelium floccose to cottony, buff with some mouse grey zones, margin regular; reverse orange with some radial yellow lines and some black zones. On PDA, reaching 45–50 mm diam, covered by floccose aerial mycelium, vinaceous grey to pale olivaceous, olivaceous grey near the centre, margin irregular; reverse buff to orange, black near the centre. NaOH spot test on OA: pale reddish discolouration.

Notes. Morphologically, *V. snoekiae* differs from its closest phylogenetic neighbour *V. joseae* in the size of its pycnidia and the number of ostioles. *Vandijckomycella snoekiae* produces larger pycnidia with inconspicuous ostioles, measuring 150–650(–850) × 145–600(–730) µm, while *V. joseae* produces pycnidia with 1–2 ostioles, measuring 150–340 × 130–250 µm. In addition, *V. snoekiae* produces conidia with less and smaller guttules than *V. joseae* (2 guttules, vs. 1–3 large guttules).

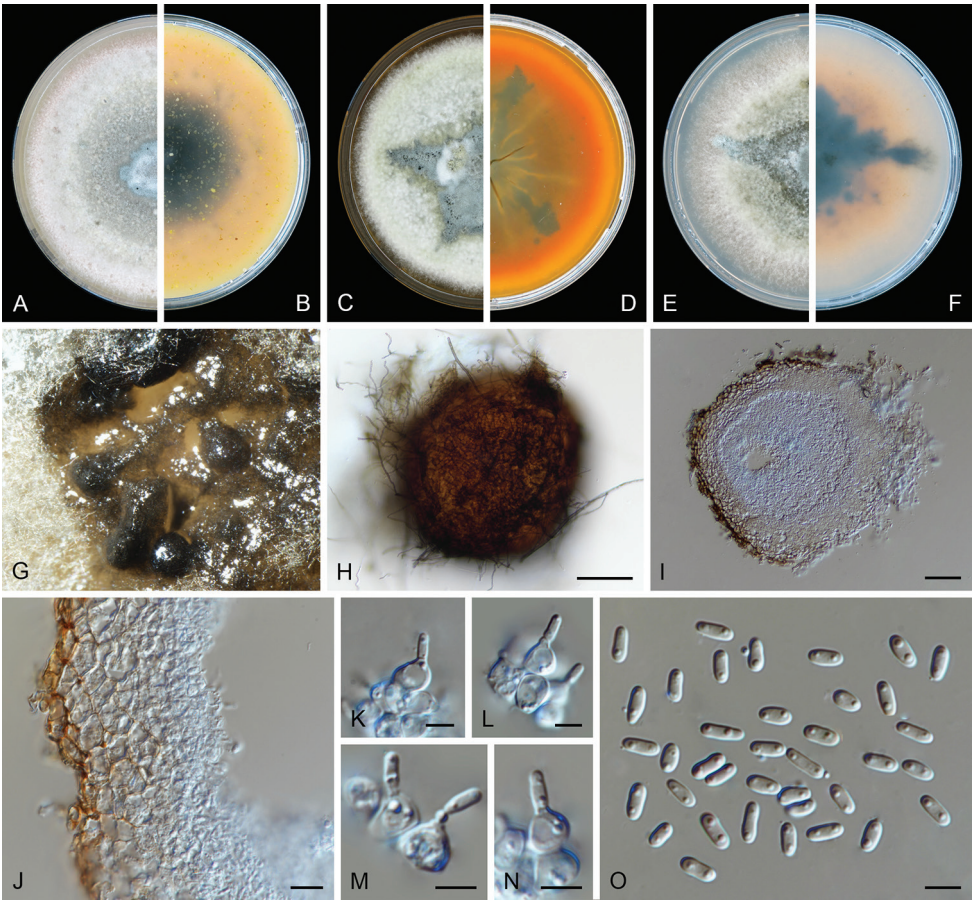

Figure 12. *Vandijckomycella snoekiae* (CBS 144954). **A, B** Colony on OA (front and reverse) **C, D** colony on MEA (front and reverse) **E, F** colony on PDA (front and reverse) **G, H** pycnidia forming on OA **I, J** section of pycnidial wall **K–N** conidiogenous cells **O** conidia. Scale bars: 100 µm (**H**); 50 µm (**I**); 10 µm (**J**); 5 µm (**K–O**).

Xenodidymella weymaniae **Hern.-Restr., L. W. Hou, L. Cai & Crous, sp. nov.**
MycoBank No: 833209
Figure 13

Etymology. *weymaniae* refers to Anna Weyman who collected the soil sample from which the ex-type strain was isolated.

Typus. The Netherlands. Utrecht province, Baarn, isolated from garden soil, Mar. 2017, A. Weyman (***holotype*** designated here CBS H-24113; living ex-type culture CBS 144960 = JW 201005).

Conidiomata pycnidial, semi-immersed on the agar, mostly confluent, sometimes solitary, scattered or aggregated, subglobose or ellipsoidal, irregularly-shaped when confluent, dark brown, ostiolate, glabrous or with long hyphal outgrowths around the

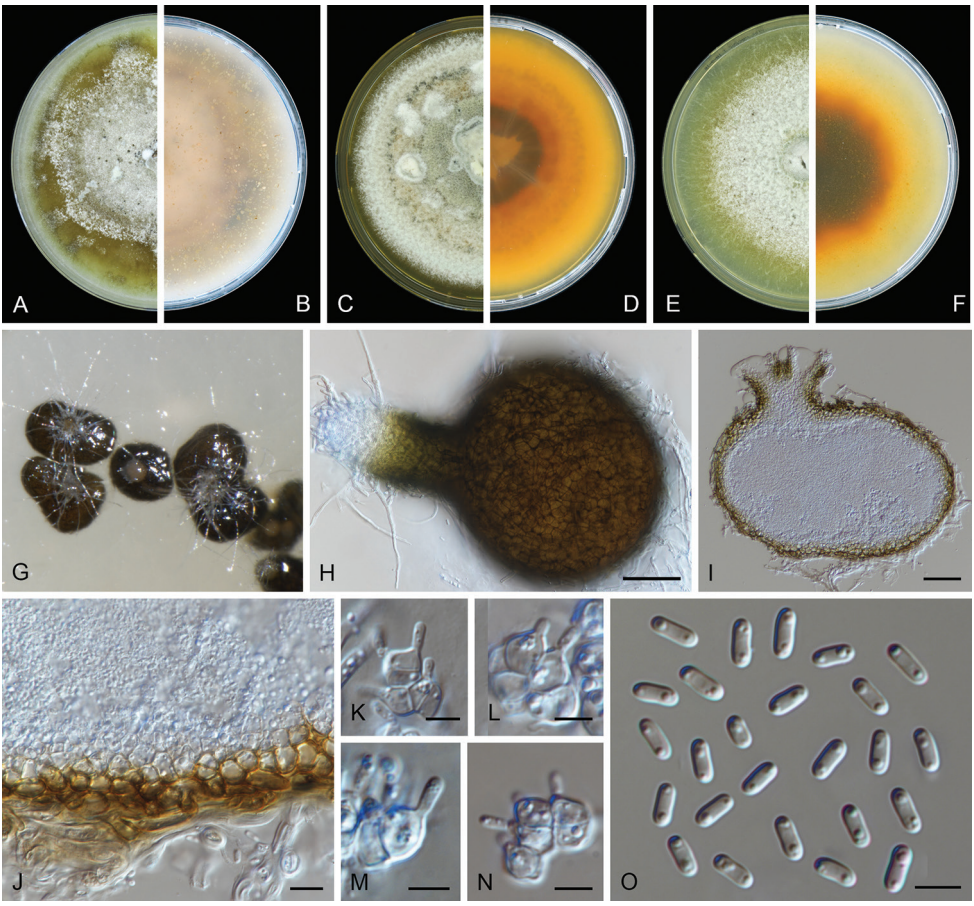

Figure 13. *Xenodidymella weymaniae* (CBS 144960). **A, B** Colony on OA (front and reverse) **C, D** colony on MEA (front and reverse) **E, F** colony on PDA (front and reverse) **G, H** pycnidia forming on OA **I, J** section of pycnidial wall **K–N** conidiogenous cells **O** conidia. Scale bars: 50 µm (**H**); 20 µm (**I**); 10 µm (**J**); 5 µm (**K–O**).

ostiole, 100–700 × 100–400(–590) µm; with 1–2(–6) ostioles, papillate or elongated into a long neck, up to 113 µm in length; pycnidial wall pseudoparenchymatous, 3–5 layers, 17–45 µm thick, outer layers composed of pale brown to brown, flattened polygonal cells of 10–35 µm diam. *Conidiogenous cells* phialidic, hyaline, smooth, subglobose, ampulliform or lageniform, 4.5–8 × 4–6.5 µm. *Conidia* oblong, smooth- and thin-walled, hyaline, aseptate, 4–6(–8) × 2–2.5 µm, with two small, polar guttules. *Conidial matrix* whitish.

Culture characteristics. Colonies after 7 d at 25 °C, on OA reaching 55–60 mm diam, aerial mycelium floccose near the centre, flat towards the periphery, pale olivaceous to whitish, black pycnidia visible near the centre, margin regular; reverse buff to salmon, pale olivaceous towards the periphery. On MEA reaching 40–45 mm diam, aerial mycelium felty, sectors with cottony mycelium, white, buff to pale olivaceous,

margin regular; reverse yellow to orange, dark brown and pale grey near the centre. On PDA reaching 45–60 mm, aerial mycelium floccose, whitish in the centre, honey towards the periphery, margin regular; reverse concentric circles dark brown in centre, orange, yellow, buff towards the periphery. NaOH spot test negative on OA.

Notes. *Xenodidymella weymaniae* formed a distinct branch basal to *X. applanata* (Figure 1). Morphologically, *X. weymaniae* could be clearly differentiated from *X. applanata* in pycnidial and conidial characteristics. In *X. weymaniae* pycnidia are dark brown, ostioles have elongated necks, 100–700 × 100–400(–590) µm, and conidia are oblong, with 2 small polar guttules. In *X. applanata* pycnidia are pale brown, with single, slightly papillate ostioles, 85–175 × 60–145 µm, and ellipsoidal to ovoid conidia, with several guttules (Chen et al. 2015). Furthermore, the two species can also be distinguished from the NaOH spot test on OA medium (negative vs. pale reddish discoloration). This is the first record of a *Xenodidymella* species isolated from soil (Boerema et al. 2004; Chen et al. 2015, 2017).

Discussion

During the present Citizen Science project which focused on Dutch soil fungi, numerous unknown species of filamentous and yeast fungi were described (Crous et al. 2017, 2018; Groenewald et al. 2018; Giraldo et al. 2019). As part of the project, we focused on investigating species diversity of Didymellaceae from soil samples obtained in the Netherlands.

As one of the largest families in the fungal kingdom, at least 26 genera are accepted in Didymellaceae (Chen et al. 2015, 2017; Valenzuela-Lopez et al. 2018) and more than 5400 species names are recorded in MycoBank to date (Crous et al. 2004), representing 4.2 % of the 120000 accepted fungal species. However, only around 30 ubiquitous species have been found in the soil environment as saprophytes, mainly in *Ascochyta*, *Boeremia*, *Didymella*, *Epicoccum* and *Phoma* (Boerema et al. 2004; Aveskamp et al. 2008, 2010; Chen et al. 2015, 2017). In our set of samples, we found 20 species distributed in 10 genera i.e. *Ascochyta*, *Calophoma*, *Didymella*, *Juxtiphoma*, *Nothophoma*, *Paraboeremia*, *Phomatodes*, *Stagonosporopsis*, *Vandijckomycella* and *Xenodidymella*. However, we did not find any species of *Phoma* and *Epicoccum*, probably due to the media used for primary isolation, and also because of the taxonomical changes that have been suffered by many species of both genera in recent years (Aveskamp et al. 2010, Chen et al. 2015)

Paraboeremia and *Juxtiphoma* were the most dominant genera. Species of *Paraboeremia* are more common on plants than in soil, except for *P. putaminum*, which is regarded as a widespread soil-borne fungus isolated from the subterranean parts of various herbaceous and woody plants (de Gruyter and Noordeloos 1992; Boerema et al. 2004). In the present study this species was the most abundant species, being recovered from 29 soil samples from 19 cities. Besides *P. putaminum*, one isolate was identified as *P. litseae*, which was previously only known on diseased leaves of *Litsea* from China (Jiang et al. 2016). In addition, two new species were described, namely

P. rekkeri found in Gelderland, North Brabant, North Holland and Utrecht provinces and *P. truiniorum* found in South Holland and Utrecht provinces.

The second most abundant species was *Juxtiphoma eupyrena*. The monotypic genus *Juxtiphoma* was recently introduced to accommodate *Phoma eupyrena* (Valenzuela-Lopez et al. 2018), a cosmopolitan soil-inhabiting fungus, which may cause damping-off of seedlings of herbaceous and woody plants (de Gruyter and Noordeloos 1992; Boerema et al. 2004; Morgan-Jones and Burch 1988), but was also reported as an opportunistic human pathogen (Bakerspigel et al. 1981). Furthermore, a new species was introduced in this genus as *Juxtiphoma kolkmaniorum* which includes 12 of our soil isolates (JW) and one strain (CBS 527.66) isolated from soil in a wheat field in Germany.

Among our isolates we found *Phomatodes nebulosa*, *Didymella macrostoma* and *D. pomorum* which are plurivorous and cosmopolitan species often isolated from soil (Boerema 1993; de Gruyter et al. 1993; Farr and Rossman 2019). Interestingly, we found two species identified as plant pathogens that had not been previously reported from soil, including *Ascochyta syringae* and *Calophoma clematidis-rectae*. *Ascochyta syringae* causes ascochyta blight of Lilac (*Syringa vulgaris*) in America, Australia and Europe (Farr and Rossman 2019), while *Calophoma clematidis-rectae* is known on *Clematidis* spp. in the Netherlands (Aveskamp et al. 2010). In addition, *Stagonosporopsis* is recognised mainly as a phytopathogenic genus on different plant hosts (Marin-Felix et al. 2019). However, we found two new species from soil, namely *S. stuijvenbergii* and *S. weymaniae*. Other new species described include *A. benningiorum*, *D. degraaffiae*, *D. kooimaniorum*, *N. brennandiae*, *V. joseae*, *V. snoekiae*, and *X. weymaniae*.

These findings suggest that species of Didymellaceae are also widely distributed in soil. Previous studies have revealed that many pathogens survive in soil by producing resting bodies (Dorenbosch 1970; Aveskamp et al. 2008), such as *A. pinodes* (currently: *Didymella pinodes*) and *Phoma medicaginis* var. *pinodella* (currently: *Didymella pinodella*) that produce chlamydospores or brown, thick-walled, swollen hyphae associated with sporocarps, which allow these species to survive in the soil for several years after the decay of their host tissues (Tivoli and Banniza 2007). On the other hand, some harmless saprobes in this family have also been observed to switch from an opportunistic to pathogenic lifestyle once in contact with the appropriate host (Aveskamp et al. 2008). Therefore, it is probable that the described new taxa are dormant in soil, remaining able to infect hosts under favourable conditions, especially species from phytopathogenic genera such as *S. stuijvenbergii*, *S. weymaniae*, *N. brennandiae* and *X. weymaniae*. However, considering that soil is a dynamic and multifunctional system and that the fungal community and its distribution are closely related to various living organisms such as plants, animals and insects, it was difficult to establish whether the species found in this study were true soil inhabitants or transferred to the soil via external vectors (such as worms, nematodes, etc.). Whether these new taxa originate from other habitats, or could change to pathogenic or endophytic lifestyles given the right conditions, remains to be determined. Furthermore, as the soil ecosystem is very complex and each type of soil and location may possess its own unique species diversity, the true diversity of Didymellaceae and their role in soil remains to be elucidated.

Recently, additional research based on cultivation-independent and cultivation-dependent methods has revealed that Didymellaceae species present in various soil environments are more diverse than one might have expected (Bell et al. 2014; Nallanchakravarthula et al. 2014; Li et al. 2016; Miao et al. 2016; Zhang et al. 2016a, 2016b; Chen et al. 2017; Nagano et al. 2017). Although recent high-throughput methods have detected a higher diversity of soil fungi compared with those based on culture-dependent methods, it is not possible to identify these taxa to species or even to genus level, as ITS sequence data alone are insufficient for species delimitation in most fungal families including Didymellaceae. Therefore, cultivation-dependent methods are still indispensable in the investigation of true species diversity of Didymellaceae based on additional loci such as *rpb2* and *tub2* obtained from cultivated isolates.

In summary, results of our study revealed the presence of a large number of unknown species and even a novel genus in soil, illustrating that this substrate is an important source for the discovery of novel taxa, and demonstrating that species diversity of Didymellaceae in soil is considerably greater than current estimates.

Acknowledgements

This study was financially supported by the Utrecht University Museum and the Royal Dutch Academy of Arts and Sciences for promoting the Citizen Science project, and for providing a platform to facilitate interaction with various Dutch primary schools. Lingwei Hou acknowledges CAS QYZDB-SSW-SMC044 for supporting her postgraduate studentship.

We are grateful to all the children and parents who participated in this project, collecting samples in their gardens and submitting them to the Westerdijk Institute for analyses; to José F.T.M. van Dijck, the first female President (2015–2018) of the Royal Dutch Academy of Arts and Sciences, who enthusiastically took part in this project and submitted the first soil sample in the Citizen Science Project. We are thankful to the staff from the Westerdijk Institute: Manon Verweij, Karin Schagen and Mariëtte Oosterwegel for promoting the project and establishing communication with the collectors and schools; to Trix Merkx and Arien van Iperen for depositing the isolates and specimens in the culture collection and fungarium.

References

Anderson JPE, Domsch KH (1973) Quantification of bacterial and fungal contributions to soil respiration. Archives of Microbiology 93: 113–127. https://doi.org/10.1007/BF00424942

Aveskamp MM, de Gruyter J, Crous PW (2008) Biology and recent developments in the systematics of *Phoma*, a complex genus of major quarantine significance. Fungal Diversity 31: 1–18.

Aveskamp MM, de Gruyter J, Woudenberg JHC, Verkley GJM, Crous PW (2010) Highlights of the Didymellaceae: a polyphasic approach to characterise *Phoma* and related pleosporalean genera. Studies in Mycology 65: 1–60. https://doi.org/10.3114/sim.2010.65.01

Aveskamp MM, Verkley GJM, de Gruyter J, Murace MA, Perelló A, Woudenberg JHC, Groenewald JZ, Crous PW (2009) DNA phylogeny reveals polyphyly of *Phoma* section *Peyronellaea* and multiple taxonomic novelties. Mycologia 101: 363–382. https://doi.org/10.3852/08-199

Bakerspigel A, Lowe D, Rostas A (1981) The isolation of *Phoma eupyrena* from a human lesion. Archives of Dermatology 117: 362–363. https://doi.org/10.1001/archderm.1981.01650060052024

Bell TH, Hassan SED, Lauron-Moreau A, Al-Otaibi F, Hijri M, Yergeau E, St-Arnaud M (2014) Linkage between bacterial and fungal rhizosphere communities in hydrocarbon-contaminated soils is related to plant phylogeny. The International Society for Microbial Ecology Journal 8: 331. https://doi.org/10.1038/ismej.2013.149

Bender SF, Plantenga F, Neftel A, Jocher M, Oberholzer HR, Kohl L, Giles M, Daniell TJ, van der Heijden MAG (2013) Symbiotic relationships between soil fungi and plants reduce N_2O emissions from soil. The International Society for Microbial Ecology Journal 8: 1336–1345. https://doi.org/10.1038/ismej.2013.224

Bennett A, Ponder MM, Garcia-Diaz J (2018) *Phoma* infections: classification, potential food sources, and their clinical impact. Microorganisms 6: 58. https://doi.org/10.3390/microorganisms6030058

Boerema GH (1993) Contributions towards a monograph of *Phoma* (Coelomycetes) – II. Section *Peyronellaea*. Persoonia 15: 197–221.

Boerema GH, de Gruyter J, Noordeloos ME, Hamers MEC (2004) *Phoma* identification manual. Differentiation of specific and infra-specific taxa in culture. CABI Publishing, 1–467. https://doi.org/10.1079/9780851997438.0000

Botha A (2011) The importance and ecology of yeasts in soil. Soil Biology and Biochemistry 43: 1–8. https://doi.org/10.1016/j.soilbio.2010.10.001

Braun U, Nakashima C, Crous PW, Groenewald JZ, Moreno-Rico O, Rooney-Latham S, Blomquist CL, Haas J, Marmolejo J (2018) Phylogeny and taxonomy of the genus *Tubakia* s. lat. Fungal Systematics and Evolution 1: 41–99. https://doi.org/10.3114/fuse.2018.01.04

Bridge P, Spooner B (2001) Soil fungi: diversity and detection. Plant and Soil 232: 147–154. https://doi.org/10.1023/A:1010346305799

Chen Q, Hou LW, Duan WJ, Crous PW, Cai L (2017) Didymellaceae revisited. Studies in Mycology 87: 105–159. https://doi.org/10.1016/j.simyco.2017.06.002

Chen Q, Jiang JR, Zhang GZ, Cai L, Crous PW (2015) Resolving the *Phoma* enigma. Studies in Mycology 82: 137–217. https://doi.org/10.1016/j.simyco.2015.10.003

Chen SY, Dickson DW, Kimbrough JW (1996) *Phoma heteroderae* sp. nov. isolated from eggs of *Heteroderae glycines*. Mycologia 88: 885–891. https://doi.org/10.2307/3761050

Chethana KWT, Jayawardene RS, Zhang W, Zhou YY, Liu M, Hyde KD, Li XH, Wang J, Zhang KC, Yan JY (2019) Molecular characterization and pathogenicity of fungal taxa associated with cherry leaf spot disease. Mycosphere 10: 490–530. https://doi.org/10.5943/mycosphere/10/1/8

Corbaz R (1955) Sur *Didymella phacae* Corbaz. Sydowia 9: 229–230.

Crous PW, Wingfield MJ, Burgess TI, Carnegie AJ, Hardy GEStJ, Smith D, Summerell BA, Cano-Lira JF, Guarro J, Houbraken J, Lombard L, Martín MP, Sandoval-Denis M, Alexandrova AV, Barnes CW, Baseia IG, Bezerra JDP, Guarnaccia V, May TW, Hernández-

Restrepo M, Stchigel AM, Miller AN, Ordoñez ME, Abreu VP, Accioly T, Agnello C, Agustin Colmán A, Albuquerque CC, Alfredo DS, Alvarado P, Araújo-Magalhães GR, Arauzo S, Atkinson, Thomas, Barili A, Barreto RW, Bezerra JL, Cabral TS, Camello Rodríguez F, Cruz RHSF, Daniëls PP, da Silva BDB, de Almeida DAC, de Carvalho Júnior AA, Decock CA, Delgat L, Denman S, Dimitrov RA, Edwards J, Fedosova AG, Ferreira RJ, Firmino AL, Flores JA, Garcia D, Gené J, Giraldo A, Góis JS, Gomes AAM, Gonçalves CM, Gouliamova DE, Groenewald M, Guéorguiev BV, Guevara-Suarez M, Gusmao LFP, Hosaka K, Hubka V, Huhndorf SM, Jadan M, Jurjević Ž, Kraak B, Kučera V, Kumar TKA, Kušan I, Lacerda SR, Lamlertthon S, Lisboa WS, Loizides M, Luangsa-ard JJ, Lysková P, Mac Cormack WP, Macedo DM, Machado AR, Malysheva EF, Marinho P, Matočec N, Meijer M, Mešić A, Mongkolsamrit S, Moreira KA, Morozova OV, Nair KU, Nakamura N, Noisripoom W, Olariaga I, Oliveira RJV, Paiva LM, Pawar P, Pereira OL, Peterson SW, Prieto M, Rodríguez-Andrade E, Rojo De Blas C, Roy M, Santos ES, Sharma R, Silva GA, Souza-Motta CM, Takeuchi-Kaneko Y, Tanaka C, Thakur A, Smith MTH, Tkalčec Z, Valenzuela-Lopez N, van der Kleij P, Verbeken A, Viana MG, Wang XW, Groenewald JZ (2017) Fungal Planet description sheets: 625–715. Persoonia 39: 270–467. https://doi.org/10.3767/persoonia.2017.39.11

Crous PW, Braun U, Hunter GC, Wingfield MJ, Verkley GJM, Shin HD, Nakashima C, Groenewald JZ (2013) Phylogenetic lineages in *Pseudocercospora*. Studies in Mycology 75: 37–114. https://doi.org/10.3114/sim0005

Crous PW, Verkleij GJM, Groenewald JZ, Houbraken J (2019) Fungal Biodiversity. [Westerdijk Laboratory Manual Series No. 1] Westerdijk Fungal Biodiversity Institute publishing, Utrecht, Netherlands.

Crous PW, Gams W, Stalpers JA, Robert V, Stegehuis G (2004) MycoBank: an online initiative to launch mycology into the 21st century. Studies in Mycology 50: 19–22.

Crous PW, Luangsa-ard JJ, Wingfield MJ, Carnegie AJ, Hernandez-Restrepo M, Lombard L, Roux, J, Barreto RW, Baseia IG, Cano-Lira JF, Martin MP, Morozova OV, Stchigel AM, Summerell BA, Brandrud TE, Dima B, Garcia D, Giraldo A, Guarro J, Gusmao LFP, Khamsuntorn P, Noordeloos ME, Nuankaew S, Pinruan U, Rodriguez-Andrade E, Souza-Motta CM, Thangavel R, Iperen AL, Abreu VP, Accioly T, Alves JL, Andrade JP, Bahram M, Baral HO, Barbier E, Barnes CW, Bendiksen E, Bernard E, Bezerra JDP, Bezerra JL, Bizio E, Blair JE, Bulyonkova TM, Cabral TS, Caiafa MV, Cantillo T, Colman AA, Conceicao LB, Cruz S, Cunha AOB, Darveaux BA, Silva AL, da Silva GA, da Silva GM, da Silva RMF, de Oliveira RJV, Oliveira RL, De Souza JT, Duenas M, Evans HC, Epifani F, Felipe MTC, Fernandez-Lopez J, Ferreira BW, Figueiredo CN, Filippova NV, Flores JA, Gene J, Ghorbani G, Gibertoni TB, Glushakova AM, Healy R, Huhndorf SM, Iturrieta-Gonzalez I, Javan-Nikkhah M, Juciano RF, Jurjevic Z, Kachalkin AV, Keochanpheng K, Krisai-Greilhuber I, Li YC, Lima AA, Machado AR, Madrid H, Magalhaes OMC, Marbach PAS, Melanda GCS, Miller AN, Mongkolsamrit S, Nascimento RP, Oliveira TGL, Ordonez ME, Orzes R, Palma MA, Pearce CJ, Pereira OL, Perrone G, Peterson SW, Pham THG, Piontelli E, Pordel A, Quijada L, Raja HA, de Paz ER, Ryvarden L, Saitta A, Salcedo SS, Sandoval-Denis M, Santos TAB, Seifert KA, Silva BDB, Smith ME, Soares AM, Sommai S, Sousa JO, Suetrong S, Susca A, Tedersoo L, Telleria MT, Thanakitpipattana D, Valen-

zuela-Lopez N, Visagie CM, Zapata M, Groenewald JZ (2018) Fungal planet description sheets: 785–867. Persoonia 41: 238–417. https://doi.org/10.3767/persoonia.2018.41.12

Davidson JA, Kimber RBE (2007) Integrated disease management of ascochyta blight in pulse crops. European Journal of Plant Pathology 119: 99–110. https://doi.org/10.1007/s10658-007-9132-x

De Gruyter J (2002) Contributions towards a monograph of *Phoma* (Coelomycetes) – IX Section *Macrospora*. Persoonia 18: 85–102.

De Gruyter J, Noordeloos ME (1992) Contributions towards a monograph of *Phoma* (Coelomycetes) – I. 1. Section *Phoma*: Taxa with very small conidia in vitro. Persoonia 15: 71–92.

De Gruyter J, Noordeloos ME, Boerema GH (1993) Contributions towards a monograph of *Phoma* (Coelomycetes) – I. 2. Section *Phoma*: Additional taxa with very small conidia and taxa with conidia up to 7 um long. Persoonia 15: 369–400.

Domsch KH, Gams W, Anderson TH (2007) Compendium of soil fungi, 2nd edition. IHW, Eching, Germany.

Dorenbosch MM (1970) Key to nine ubiquitous soil-borne *Phoma*-like fungi. Persoonia 6: 1–14.

Farr DF, Rossman AY (2019) Fungal databases, systematic mycology and microbiology laboratory. ARS, USDA. http://nt.ars-grin.gov/fungaldatabases/

Frąc M, Hannula SE, Bełka M, Jedryczka M (2018) Fungal biodiversity and their role in soil health. Frontiers in Microbiology 9: 707. https://doi.org/10.3389/fmicb.2018.00707

Giraldo A, Hernández-Restrepo M, Crous PW (2019) New plectosphaerellaceous species from Dutch garden soil. Mycological Progress 18: 1135–1154. https://doi.org/10.1007/s11557-019-01511-4

Gossen BD, Morrall RAA (1986) Transmission of *Ascochyta lentis* from infected lentil seed and plant residue. Canadian Journal of Plant Pathology 8: 28–32. https://doi.org/10.1080/07060668609501837

Grishkan I (2018) Spatio temporal variations in soil cultivable mycobiota at the Arava desert (Israel) along latitudinal and elevational gradients. AIMS Microbiology 4: 502–521. https://doi.org/10.3934/microbiol.2018.3.502

Groenewald M, Lombard L, de Vries M, Lopez AG, Smith M, Crous PW (2018) Diversity of yeast species from Dutch garden soil and the description of six novel Ascomycetes. Federation of European Microbiological Societies Yeast Research 18: foy076. https://doi.org/10.1093/femsyr/foy076

Jiang JR, Chen Q, Cai L (2016) Polyphasic characterisation of three novel species of *Paraboeremia*. Mycological Progress 16: 285–295. https://doi.org/10.1007/s11557-016-1253-1

Katoh K, Rozewicki J, Yamada KD (2017) MAFFT online service: multiple sequence alignment, interactive sequence choice and visualization. Brief Bioinformatics: 1–7. https://doi.org/10.1093/bib/bbx108

Li W, Wang MM, Wang XG, Cheng XL, Guo JJ, Bian XM, Cai L (2016) Fungal communities in sediments of subtropical Chinese seas as estimated by DNA metabarcoding. Scientific Reports 6: 26528. https://doi.org/10.1038/srep26528

Liu YJ, Whelen S, Hall BD (1999) Phylogenetic relationships among ascomycetes: evidence from an RNA polymerase II subunit. Molecular Biology and Evolution 16: 1799–1808. https://doi.org/10.1093/oxfordjournals.molbev.a026092

Marin-Felix Y, Groenewald JZ, Cai L, Chen Q, Marincowitz S, Barnes I, Bensch K, Braun U, Camporesi E, Damm U, de Beer ZW, Dissanayake A, Edwards J, Giraldo A, Hernandez-Restrepo M, Hyde KD, Jayawardena RS, Lombard L, Luangsa-Ard J, McTaggart AR, Rossman AY, Sandoval-Denis M, Shen M, Shivas RG, Tan YP, van der Linde EJ, Wingfield MJ, Wood AR, Zhang JQ, Zhang Y, Crous PW (2017) Genera of phytopathogenic fungi: GOPHY 1. Studies in Mycology 86: 99–216. https://doi.org/10.1016/j.simyco.2017.04.002

Marin-Felix Y, Hernández-Restrepo M, Wingfield MJ, Akulov A, Carnegie AJ, Cheewangkoon R, Gramaje D, Groenewald JZ, Guarnaccia V, Halleen F, Lombard L, Luangsa-Ard J, Marincowitz S, Moslemi A, Mostert L, Quaedvlieg W, Schumacher RK, Spies CFJ, Thangavel R, Taylor PWJ, Wilson AM, Wingfield BD, Wood AR, Crous PW (2019) Genera of phytopathogenic fungi: GOPHY 2. Studies in Mycology 92: 43–133. https://doi.org/10.1016/j.simyco.2018.04.002

Maryani N, Lombard L, Poerba YS, Subandiyah S, Crous PW, Kema GHJ (2019) Phylogeny and genetic diversity of the banana *Fusarium* wilt pathogen *Fusarium oxysporum* f. sp. *cubense* in the Indonesian centre of origin. Studies in Mycology 92: 155–194. https://doi.org/10.1016/j.simyco.2018.06.003

Miao CP, Mi QL, Qiao XG, Zheng YK, Chen YW, Xu LH, Guan HL, Zhao LX (2016) Rhizospheric fungi of *Panax notoginseng*: diversity and antagonism to host phytopathogens. Journal of Ginseng Research 40: 127–134. https://doi.org/10.1016/j.jgr.2015.06.004

Morgan-Jones G, Burch KB (1988) Studies in the genus *Phoma*. X. Concerning *Phoma eupyrena*, an ubiquitous, soil-borne species. Mycotaxon 31: 427–434.

Nagano Y, Miura T, Nishi S, Lima AO, Nakayama C, Pellizari VH, Fujikura K (2017) Fungal diversity in deep-sea sediments associated with asphalt seeps at the Sao Paulo Plateau. Deep Sea Research Part II: Topical Studies in Oceanography 146: 59–67. https://doi.org/10.1016/j.dsr2.2017.05.012

Nallanchakravarthula S, Mahmood S, Alström S, Finlay RD (2014) Influence of soil type, cultivar and *Verticillium dahliae* on the structure of the root and rhizosphere soil fungal microbiome of strawberry. PLoS ONE 9: e111455. https://doi.org/10.1371/journal.pone.0111455

Nylander JAA (2004) MrModeltest v2. Program distributed by the author. Evolutionary Biology Centre, Uppsala University.

Porras-Alfaro A, Herrera J, Natvig DO, Lipinski K, Sinsabaugh RL (2011) Diversity and distribution of soil fungal communities in a semiarid grassland. Mycologia 103: 10–21. https://doi.org/10.3852/09-297

Paterson RRM, Lima N (2017) Filamentous fungal human pathogens from food emphasising *Aspergillus*, *Fusarium* and *Mucor*. Microorganisms 5: 44. https://doi.org/10.3390/microorganisms5030044

Rayner RW (1970) A mycological colour chart. Commonwealth Mycological Institute and British Mycological Society, Kew Publishing, 1–34.

Rambaut A (2014) FigTree 1.4.2. http://tree.bio.ed.ac.uk/software/figtree

Ronquist F, Teslenko M, van der Mark P, Ayres DL, Darling A, Hohna S, Larget B, Liu L, Suchard MA, Huelsenbeck JP (2012) MrBayes 3.2: efficient Bayesian phylogenetic in-

ference and model choice across a large model space. Systematic Biology 61: 539–542. https://doi.org/10.1093/sysbio/sys029

Rudgers JA, Kivlin SN, Whitney KD, Price MV, Waser NM, Harte J (2014) Responses of high-altitude graminoids and soil fungi to 20 years of experimental warming. Ecology 95: 1918–1928. https://doi.org/10.1890/13-1454.1

Ruisi S, Barreca D, Selbmann L, Zucconi L, Onofri S (2007) Fungi in Antarctica. Reviews in Environmental Science and Bio/Technology 6: 127–141. https://doi.org/10.1007/s11157-006-9107-y

Stamatakis A, Alachiotis N (2010) Time and memory efficient likelihood-based tree searched on phylogenomic alignments with missing data. Bioinformatics 26: i132–i139. https://doi.org/10.1093/bioinformatics/btq205

Sung GH, Sung JM, Hywel-Jones NL, Spatafora JW (2007) A multi-gene phylogeny of Clavicipitaceae (Ascomycota, Fungi): identification of localized incongruence using a combinational bootstrap approach. Molecular Phylogenetics and Evolution 44: 1204–1223. https://doi.org/10.1016/j.ympev.2007.03.011

Swofford DL (2003) PAUP*. Phylogenetic Analysis Using Parsimony (*and other methods). Version 4. Sinauer Associates, Sunderland, Massachusetts, USA.

Sydow H, Sydow P (1915) Novae fungorum species. Annales Mycologici 13: 35–43.

Tamura K, Stecher G, Peterson D, Filipski A, Kumar S (2013) MEGA6: molecular evolutionary genetics analysis version 6.0. Molecular Biology and Evolution 30: 2725–2729. https://doi.org/10.1093/molbev/mst197

Tedersoo L, Bahram M, Põlme S, Koljalg U, Yorou NS, Wijesundera R, Ruiz LV, Vasco-Palacios AM, Thu PQ, Suija A, Smith ME, Sharp C, Saluveer E, Saitta A, Rosas M, Riit T, Ratkowsky D, Pritsch K, Poldmaa K, Piepenbring M, Phosri C, Peterson M, Parts K, Partel K, Otsing E, Nouhra E, Njouonkou AL, Nilsson RH, Morgado LN, Mayor J, May TW, Majuakim L, Lodge DJ, Lee SS, Larsson KH, Kohout P, Hosaka K, Hiiesalu I, Henkel TW, Harend H, Guo LD, Greslebin A, Grelet G, Geml J, Gates G, Dunstan W, Dunk C, Drenkhan R, Dearnaley J, De Kesel A, Dang T, Chen X, Buegger F, Brearley FQ, Bonito G, Anslan S, Abell S, Abarenkov K (2014) Global diversity and geography of soil fungi. Science 346: 125688. https://doi.org/10.1126/science.1256688

Tivoli B, Banniza S (2007) Comparison of the epidemiology of ascochyta blights on grain legumes. European Journal of Plant Pathology 119: 59–76. https://doi.org/10.1007/s10658-007-9117-9

Tivoli B, Baranger A, Muehlbauer FJ, Cooke BM (2007b) Ascochyta blights of grain legumes. Springer Publishing, 1–141. https://doi.org/10.1007/978-1-4020-6065-6

Tullio V, Banche G, Allizond V, Roana J, Mandras N, Scalas D, Panzone M, Cervetti O, Valle S, Carlone N, Cuffini AM (2010) Non-dermatophyte moulds as skin and nail foot mycosis agents: *Phoma herbarum*, *Chaetomium globosum* and *Microascus cinereus*. Fungal Biology 114: 345–349. https://doi.org/10.1016/j.funbio.2010.02.003

Vaghefi N, Pethybridge SJ, Hay FS, Ford R, Nicolas ME, Taylor PWJ (2016) Revisiting *Stagonosporopsis* species associated with chrysanthemum and pyrethrum ray blight. Australasian Plant Pathology 45: 561–570. https://doi.org/10.1007/s13313-016-0446-z

Vaidya G, Lohman DJ, Meier R (2011) SequenceMatrix: concatenation software for the fast assembly of multi-gene datasets with character set and codon information. Cladistics 27: 171–180. https://doi.org/10.1111/j.1096-0031.2010.00329.x

Valenzuela-Lopez N, Cano-Lira JF, Guarro J, Sutton DA, Wiederhold N, Crous PW, Stchigel AM (2018) Coelomycetous Dothideomycetes with emphasis on the families Cucurbitariaceae and Didymellaceae. Studies in Mycology 90: 1–69. https://doi.org/10.1016/j.simyco.2017.11.003

van Agtmaal M, Straathof A, Termorshuizen A, Teurlincx S, Hundscheid M, Ruyters S, Busschaert P, Lievens B, de Boer W (2017) Exploring the reservoir of potential fungal plant pathogens in agricultural soil. Applied Soil Ecology 121: 152–160. https://doi.org/10.1016/j.apsoil.2017.09.032

Vilgalys R, Hester M (1990) Rapid genetic identification and mapping of enzymatically amplified ribosomal DNA from several *Cryptococcus* species. Journal of Bacteriology 172: 4238–4246. https://doi.org/10.1128/JB.172.8.4238-4246.1990

Vilgalys R, Sun BL (1994) Ancient and recent patterns of geographic speciation in the oyster mushroom *Pleurotus* revealed by phylogenetic analysis of ribosomal DNA sequences. Proceedings of the National Academy of Sciences 91: 4599–4603. https://doi.org/10.1073/pnas.91.10.4599

Voøíšková J, Baldrian P (2012) Fungal community on decomposing leaf litter undergoes rapid successional changes. The International Society for Microbial Ecology Journal 7: 477–486. https://doi.org/10.1038/ismej.2012.116

White TJ, Bruns T, Lee S, Taylor J (1990) Amplification and direct sequencing of fungal ribosomal RNA genes for phylogenetics. In: Innis MA, Gelfand DH, Sninsky JJ, White TJ (Eds) PCR protocols: a guide to methods and applications: 315–322. Academic Press, San Diego, California, USA. https://doi.org/10.1016/B978-0-12-372180-8.50042-1

Woudenberg JHC, Aveskamp MM, de Gruyter J, Spiers AG, Crous PW (2009) Multiple *Didymella* teleomorphs are linked to the *Phoma clematidina* morphotype. Persoonia 22: 56–62. https://doi.org/10.3767/003158509X427808

Yang Y, Dou Y, Huang YM, An SS (2017) Links between soil fungal diversity and plant and soil properties on the Loess Plateau. Frontiers in Microbiology 8: 2198. https://doi.org/10.3389/fmicb.2017.02198

Zhang T, Jia RL, Yu LY (2016a) Diversity and distribution of soil fungal communities associated with biological soil crusts in the southeaster Tengger Desert (China) as revealed by 454 pyrosequencing. Fungal Ecology 23: 156–163. https://doi.org/10.1016/j.funeco.2016.08.004

Zhang XY, Wang GH, Xu XY, Nong XH, Wang J, Amin M, Qi SH (2016b) Exploring fungal diversity in deep-sea sediments from Okinawa Trough using high-throughput Illumina sequencing. Deep Sea Research Part I: Oceanographic Research Papers 116: 99–105. https://doi.org/10.1016/j.dsr.2016.08.004

Zhang ZF, Liu F, Zhou X, Liu XZ, Liu SJ, Cai L (2017) Culturable mycobiota from Karst caves in China, with descriptions of 20 new species. Persoonia 39: 1–31. https://doi.org/10.3767/persoonia.2017.39.01

MycoKeys 65: 101–118 (2020)
doi: 10.3897/mycokeys.65.48660
http://mycokeys.pensoft.net

RESEARCH ARTICLE

A peer-reviewed open-access journal
MycoKeys
Launched to accelerate biodiversity research

Morphological and molecular identification of four new resupinate species of *Lyomyces* (Hymenochaetales) from southern China

Jun-Zhu Chen[1,2,3], Chang-Lin Zhao[1,2,3]

1 *Key Laboratory for Forest Resources Conservation and Utilization in the Southwest Mountains of China, Ministry of Education, Southwest Forestry University, Kunming 650224, China* **2** *College of Biodiversity Conservation, Southwest Forestry University, Kunming 650224, China* **3** *Key Laboratory of Forest Disaster Warning and Control of Yunnan Province, Southwest Forestry University, Kunming 650224, China*

Corresponding author: Chang-Lin Zhao (fungichanglinz@163.com)

Academic editor: Bao-Kai Cui | Received 21 November 2019 | Accepted 4 March 2020 | Published 26 March 2020

Citation: Chen J-Z, Zhao C-L (2020) Morphological and molecular identification of four new resupinate species of *Lyomyces* (Hymenochaetales) from southern China. MycoKeys 65: 101–118. https://doi.org/10.3897/mycokeys.65.48660

Abstract

Four new wood-inhabiting fungal species, *Lyomyces bambusinus*, *L. cremeus*, *L. macrosporus* and *L. wuliangshanensis*, are proposed based on a combination of morphological and molecular evidence. *Lyomyces bambusinus* is characterized by resupinate basidiomata with colliculose to tuberculate hymenial surface and broadly ellipsoid, hyaline, slightly thick-walled, smooth basidiospores. *Lyomyces cremeus* is characterised by resupinate basidiomata with smooth, cream hymenial surface and ellipsoid, hyaline, thin-walled to slightly thick-walled basidiospores. *Lyomyces macrosporus* is characterized by pruinose basidiomata with reticulate hymenial surface, presence of three kinds of cystidia and larger basidiospores (6.7–8.9 × 4.4–5.4 μm). *Lyomyces wuliangshanensis* is characterized by coriaceous basidiomata and ellipsoid, hyaline, slightly thick-walled, smooth basidiospores. The phylogenetic analyses based on molecular data of the internal transcribed spacer (ITS) region sequences revealed that the four new species belonged to *Lyomyces*. *Lyomyces bambusinus* grouped with *L. sambuci*. *Lyomyces cremeus* clade was sister to a clade comprised of *L. microfasciculatus*. *Lyomyces macrosporus* was sister to *L. allantosporus*. *Lyomyces wuliangshanensis* was closely related to *L. mascarensis*.

Keywords

Phylogeny, Schizoporaceae, taxonomy, wood-inhabiting fungi, Yunnan Province

Introduction

Lyomyces P. Karst. typified by *L. sambuci* (Pers.) P. Karst., is a small corticioid genus characterized by resupinate to effused basidiomata with smooth to granular or odontioid hymenophore, a monomitic hyphal system bearing clamp connections, strongly encrusted generative hyphae, the presence of several types of cystidia; clavate to suburniform basidia, and smooth, thin- to slightly thick-walled, cyanophilous basidiospores (Karsten 1881; Bernicchia and Gorjón 2010). The members of *Lyomyces* grow on dead, still-attached or fallen branches of angiosperms, on dead wooden and herbaceous stems, or occasionally on gymnosperm wood (Yurchenko et al. 2017). Twenty-three species are currently known in *Lyomyces* worldwide (Rabenhorst 1851; Karsten 1881, 1882; Peck 1903; Bourdot and Galzin 1911; Cunningham 1959, 1963; Wu 1990; Hjortstam and Ryvarden 2009; Yurchenko et al. 2013, 2017; Gafforov et al. 2017; Riebesehl and Langer 2017) and five species were recorded in China (Xiong et al. 2009; Gafforov et al. 2017; Riebesehl and Langer 2017).

Molecular studies on *Lyomyces* and related genera have been carried out recently (Riebesehl and Langer 2017; Yurchenko et al. 2017; Viner et al. 2018; Riebesehl et al. 2019). Riebesehl and Langer (2017) indicated that *Hyphodontia* s.l. should be divided into several genera: *Hastodontia* (Parmasto) Hjortstam & Ryvarden, *Hyphodontia* J. Erikss, *Kneiffiella* (Pers.) Gray, *Lagarobasidium* Jülich, *Lyomyces* and *Xylodon* (Pers.) Gray and thus 35 new combinations were proposed, including fourteen *Lyomyces* species. The clarification of *Lyomyces sambuci* complex was conducted based on ITS and 28S sequences analyses and four new species of *Lyomyces* were described (Yurchenko et al. 2017). Viner et al. (2018) studied the taxonomy of *Lagarobasidium* and *Xylodon*, and showed that twelve species clustered into *Lyomyces* clade and then grouped with *Xylodon* clade. Phylogenetic and morphological studies on *Xylodon* showed that *Xylodon* was distinct from *Hastodontia*, *Hyphodontia*, *Kneiffiella* and *Lyomyces* and the *Lyomyces* generic species *L. sambuci* was sister to *L. crustosus* (Pers.) P. Karst. formed a single lineage with a high support (Riebesehl et al. 2019).

During investigations on wood-inhabiting fungi in southern China, four additional taxa were found, which could not be assigned to any described species in *Lyomyces*. In this study, the authors expand samplings from previous studies (Gafforov et al. 2017; Riebesehl and Langer 2017) to examine taxonomy and phylogeny of them within *Lyomyces*, based on the internal transcribed spacer (ITS) regions sequences.

Materials and methods

Morphological studies

The specimens studied have been deposited in the herbarium of Southwest Forestry University (SWFC), Kunming, Yunnan Province, P.R. China. Special color terms fol-

low Petersen (1996). Macromorphological descriptions are based on field notes. Micromorphological data were obtained from the dried specimens and observed under a light microscope following Dai (2010) and Cui et al. (2019). The following abbreviations are used: KOH = 5% potassium hydroxide; CB = cotton blue; CB+ = cyanophilous; IKI = Melzer's reagent; IKI– = non-amyloid and non-dextrinoid; L = mean spore length (arithmetic average of all spores); W = mean spore width (arithmetic average of all spores); Q = L/W ratio; n (a/b) = number of spores (a) measured from given number (b) of specimens.

DNA extraction and sequencing

CTAB rapid plant genome extraction kit-DN14 (Aidlab Biotechnologies Co., Ltd, Beijing) was used to obtain genomic DNA from dried specimens, according to the manufacturer's instructions (Han et al. 2016; Song and Cui 2017) . The ITS region was amplified with the primer pair ITS5 and ITS4 (White et al. 1990). The PCR cycling procedure for ITS was as follows: initial denaturation at 95 °C for 3 min, followed by 35 cycles at 94 °C for 40 s, 58 °C for 45 s and 72 °C for 1 min, and a final extension of 72 °C for 10 min followed Shen et al. (2019). The PCR products were purified and directly sequenced at Kunming Tsingke Biological Technology Limited Company, Yunnan Province, P.R.China. All newly generated sequences were deposited in GenBank (Table 1).

Phylogenetic analyses

Sequencher 4.6 (GeneCodes, Ann Arbor, MI, USA) was used to assemble and edit the DNA sequence. Sequences were aligned in MAFFT 7 (https://mafft.cbrc.jp/alignment/server/) using the "G-INS-I" strategy and manually adjusted in BioEdit (Hall 1999). The sequence alignment was deposited in TreeBase (submission ID 25382). Sequences of *Palifer verecundus* (G. Cunn.) Stalpers & P.K. Buchanan and *Xylodon asperus* (Fr.) Hjortstam & Ryvarden obtained from GenBank were used as outgroups to root trees following Yurchenko et al. (2017) in Fig. 1.

Maximum parsimony (MP), Maximum Likelihood (ML) and Bayesian Inference (BI) analyses were applied to the ITS dataset sequences. Approaches to phylogenetic analyses followed Wu et al. (2018) and Zhu et al. (2019) the tree construction procedure was performed in PAUP* version 4.0b10 (Swofford 2002). All characters were equally weighted and gaps were treated as missing data. Trees were inferred using the heuristic search option with TBR branch swapping and 1000 random sequence additions. Max-trees were set to 5000, branches of zero length were collapsed and all most-parsimonious trees were saved. Clade robustness was assessed using bootstrap (BT) analysis with 1000 replicates (Felsenstein 1985). Descriptive

Table 1. List of species, specimens and GenBank accession numbers of sequences used in this study.

Species name	Sample no.	GenBank accession no.	References
		ITS	
Lyomyces allantosporus	KAS-GEL 4933	KY800401	Yurchenko et al. 2017
	FR 0249548	KY800397	Yurchenko et al. 2017
Lyomyces bambusinus	CLZhao 3675	MN945969	Present study
	CLZhao 4808	MN945970	Present study
	CLZhao 4831	MN945968	Present study
	CLZhao 4840	MN945971	Present study
Lyomyces cremeus	CLZhao 2812	MN945973	Present study
	CLZhao 4138	MN945974	Present study
	CLZhao 8295	MN945972	Present study
Lyomyces crustosus	YG-G 39	MF382993	Gafforov et al. 2017
	UC 2022841	KP814310	Rosenthal et al. 2017
Lyomyces erastii	MA-Fungi 34336	JX857800	Gafforov et al. 2017
	YG 022	MF382992	Gafforov et al. 2017
Lyomyces griseliniae	KHL 12971	DQ873651	Larsson et al. 2006
Lyomyces juniperi	KAS-GEL 4940	DQ340316	Yurchenko et al. 2017
	FR 0261086	KY081799	Riebesehl and Langer 2017
Lyomyces macrosporus	CLZhao 4516	MN945977	Present study
	CLZhao 4531	MN945978	Present study
	CLZhao 8605	MN945975	Present study
	CLZhao 3951	MN945976	Present study
Lyomyces mascarensis	KAS-GEL 4833	KY800399	Yurchenko et al. 2017
	KAS-GEL 4908	KY800400	Yurchenko et al. 2017
Lyomyces microfasciculatus	CLZhao 4626	MK343568	Present study
	CLZhao 5109	MN954311	Present study
	TNM F 24757	JN129976	Yurchenko and Wu 2014
Lyomyces organensis	MSK 7247	KY800403	Yurchenko et al. 2017
Lyomyces orientalis	KAS-GEL 3376	DQ340325	Yurchenko et al. 2017
	KAS-GEL 3400	DQ340326	Yurchenko et al. 2017
Lyomyces pruni	Ryberg 021018	DQ873624	Larsson et al. 2006
Lyomyces sambuci	80 SAMHYP	JX857721	Yurchenko et al. 2017
	83 SAMHYP	JX857720	Yurchenko et al. 2017
Lyomyces vietnamensis	TNM F 9073	JX175044	Yurchenko and Wu 2014
Lyomyces wuliangshanensis	CLZhao 4108	MN945980	Present study
	CLZhao 4144	MN945981	Present study
	CLZhao 4167	MN945979	Present study
	CLZhao 4206	MN945982	Present study
	CLZhao 4475	MN945983	Present study
Palifer verecundus	KHL 12261	DQ873642	Larsson et al. 2006
Xylodon asperus	UC 2023169	KP814365	Yurchenko et al. 2017

tree statistics tree length (TL), consistency index (CI), retention index (RI), rescaled consistency index (RC) and homoplasy index (HI) were calculated for each most-parsimonious tree generated.

Sequences were also analyzed using Maximum Likelihood (ML) ML analysis was conducted with RAxML-HPC2 through the Cipres Science Gateway (www.phylo.org; Miller et al. 2009). Branch support (BS) for ML analysis was determined by 1000 bootstrap replicates and evaluated under the gamma model.

MrModeltest 2.3 (Nylander 2004) was used to determine the best-fit evolution model for the data set for Bayesian Inference (BI). Bayesian Inference was performed with MrBayes 3.1.2 with a general time reversible (GTR) model of DNA substitution and a gamma distribution rate variation across sites (Ronquist and Huelsenbeck 2003). Four Markov chains were used in each of 2 runs from random starting trees for 600,000 generations, with trees and parameters sampled every 100 generations. The first quarter of generations were discarded as burn-in. A majority rule consensus tree of all remaining trees and posterior probabilities was calculated. Branches that received bootstrap support for maximum likelihood (BS) ≥75%, maximum parsimony (BP) ≥75%, and Bayesian posterior probabilities (BPP) ≥0.95 were considered significantly supported.

Phylogeny results

The ITS dataset (Fig. 1) included sequences from 39 fungal specimens representing 18 species. The dataset had an aligned length of 608 characters, of which 277 characters were constant and 242 parsimony-informative. MP analysis yielded 8 equally parsimonious trees (TL = 978, CI = 0.523, HI = 0.478, RI = 0.738, RC = 0.385). The best-fit model for ITS alignment estimated and applied in the BI was GTR+I+G. At the end of the BI runs, the average standard deviation of split frequencies was 0.008676. The tree topology obtained by BI and ML was similar to the MP one.

The phylogenetic tree (Fig. 1) demonstrated that all samples grouped into the *Lyomyces* in the present study. *Lyomyces bambusinus* grouped with *L. sambuci*. *Lyomyces cremeus* formed a monophyletic lineage and then grouped with *L. microfasciculatus* (Yurchenko & Sheng H. Wu) Riebesehl & Langer. *Lyomyces macrosporus* was sister to *L. allantosporus* Riebesehl, Yurchenko & Langer. *Lyomyces wuliangshanensis* was closely related to *L. mascarensis* Riebesehl, Yurchenko & Langer.

Taxonomy

***Lyomyces bambusinus* C.L. Zhao, sp. nov.**
Figs 2, 6
MycoBank No: 834036

Holotype. China. Yunnan Province: Puer, Zhenyuan County, Heping Town, Ailaoshan National Nature Reserve, on dead bamboo, 11 January 2018, CLZhao 4831 (SWFC).

Etymology. The epithet *bambusinus* (Lat.): refers to the occurrence on bamboo.

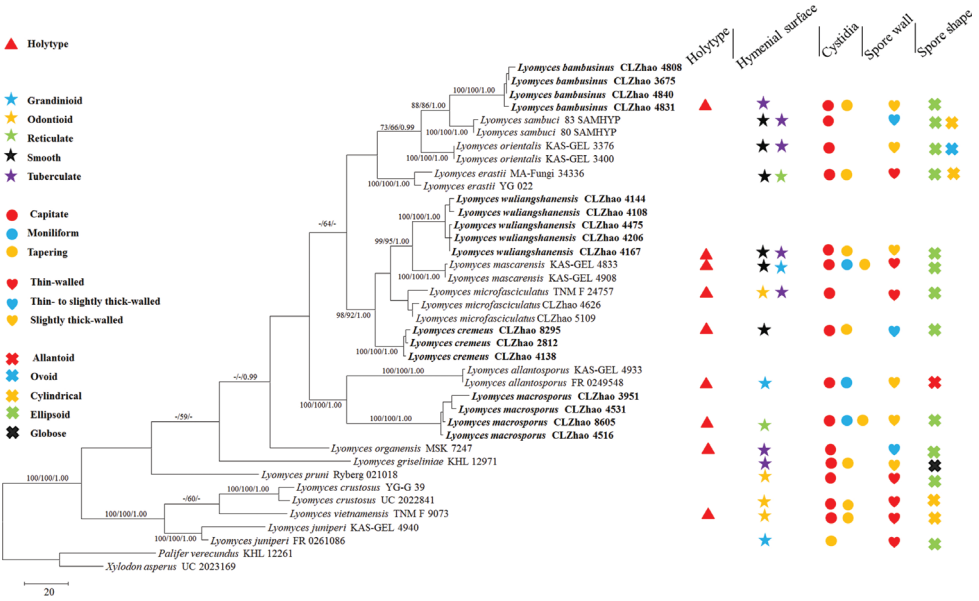

Figure 1. Maximum parsimony strict consensus tree illustrating the phylogeny of four new species and related species in *Lyomyces* based on ITS sequences. Branches are labelled with maximum likelihood bootstrap equal to or higher than 70%, parsimony bootstrap proportions equal to or higher than 50% and Bayesian posterior probabilities equal to or high than 0.95 respectively.

Basidiomata. Annual, resupinate, ceraceous when fresh, becoming brittle and cracking upon drying, up to 20 cm long and 8 cm wide, 100–200 μm thick. Hymenial surface colliculose to tuberculate, white to cream when fresh, turning cream to buff upon drying. Margin narrow, concolorous with hymenial surface.

Hyphal system. Monomitic; generative hyphae with clamp connections, hyaline, thick-walled, branched, 2.5–3.9 μm in diameter, IKI–, cyanophilous; tissues unchanged in KOH. Numerous crystals present among hyphae.

Hymenium. Two kinds of cystidia: 1) capitate, hyaline, thin-walled, 35–55 × 4–7 μm, smooth or slightly encrusted; 2) tapering, hyaline, thin-walled, 40–65 × 4–5.5 μm, smooth or slightly encrusted; cystidioles present, hyaline, thin-walled, 12–17 × 2–3 μm. Basidia clavate, constricted, thin-walled, with four sterigmata and a basal clamp connection, 16.5–35 × 3.5–7 μm.

Spores. Basidiospores broadly ellipsoid, hyaline, slightly thick-walled, smooth, IKI–, cyanophilous, guttulate, (4.5–)4.7–5.9 (–6.2) × (3.4–)3.7–4.6(–4.8) μm, L = 5.31 μm, W = 4.19 μm, Q = 1.23–1.3 (n = 120/4).

Ecology and distribution. On dead bamboo, causing a white rot. China.

Additional specimens examined. China. Yunnan Province: Puer, Jingdong County, Wuliangshan National Nature Reserve, on dead bamboo, 3 October 2017, CLZhao 3675; Zhenyuan County, Heping Town, Ailaoshan National Nature Reserve, on dead bamboo, 11 January 2018, CLZhao 4808, CLZhao 4840 (SWFC).

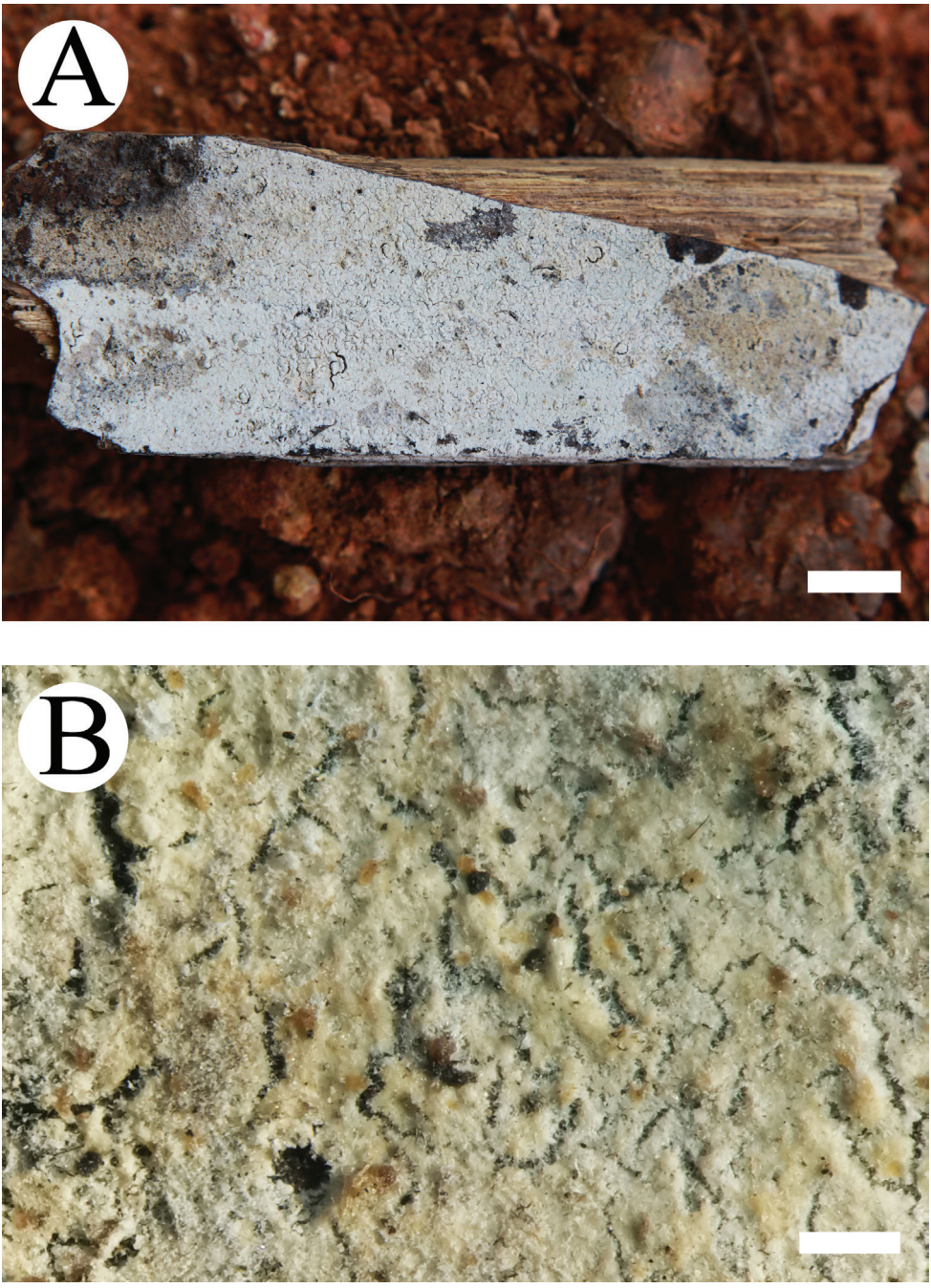

Figure 2. Basidiomata of *Lyomyces bambusinus* (holotype). Scale bars: 1 cm (**A**); 5 mm (**B**).

Lyomyces cremeus **C.L. Zhao, sp. nov.**
Figs 3, 7
MycoBank No: 834037

Holotype. China. Yunnan Province: Jingdong County, Taizhong Town, Ailaoshan Ecological Station, on fallen branch of angiosperm, 23 August 2018, CLZhao 8295 (SWFC).

Etymology. The epithet *cremeus* (Lat.): refers to the cream hymenial surface.

Basidiomata. Annual, resupinate, ceraceous when fresh, becoming membranaceous upon drying, up to 13 cm long and 5 cm wide, 50–100 μm thick. Hymenial surface smooth, pale cream when fresh, turn cream upon drying. Margin narrow, white to cream.

Hyphal system. Monomitic; generative hyphae with clamp connections, hyaline, thick-walled, branched, 3–5 μm in diameter, IKI–, cyanophilous; tissues unchanged in KOH. Numerous crystals present among hyphae.

Hymenium. Two kinds of cystidia: 1) capitate, hyaline, thin-walled, 20–40 × 3–5 μm, smooth or slightly encrusted; 2) tapering, hyaline, thin-walled, 18–35 × 3–4.5 μm, smooth or slightly encrusted; cystidioles present, hyaline, thin-walled, 15–20 × 2.5–4 μm. Basidia clavate, with four sterigmata and a basal clamp connection, 9–18.5 × 3–6 μm.

Spores. Basidiospores ellipsoid, hyaline, thin-walled to slightly thick-walled, smooth, IKI–, cyanophilous, guttulate, 4.5–5.6(–5.8) × 3.3–4.3(–4.5) μm, L = 5.01 μm, W = 3.94 μm, Q = 1.25–1.3 (n = 90/3).

Ecology and distribution. Lignicolous, causing a white rot. China.

Additional specimens examined. China. Yunnan Province: Yuxi, Xinping County, Shimenxia Forestry Park, on fallen branch of angiosperm, 21 August 2017, CLZhao 2812; Puer, Jingdong County, Wuliangshan National Nature Reserve, on fallen branch of angiosperm, 5 October 2017, CLZhao 4138 (SWFC).

Lyomyces macrosporus **C.L. Zhao, sp. nov.**
Figs 4, 8
MycoBank No: 834038

Holotype. China. Yunnan Province: Puer, Jingdong County, Taizhong Town, Ailaoshan National Nature Reserve, on fallen branch of angiosperm, 24 August 2018, CLZhao 8605 (holotype in SWFC).

Etymology. The epithet *macrosporus* (Lat.): refers to the larger basidiospores.

Basidiomata. Annual, resupinate, subceraceous when fresh, becoming pruinose upon drying, up to 22 cm long and 3 cm wide, 100–200 μm thick. Hymenial surface reticulate, cream when fresh, turning cream to buff upon drying. Margin narrow, white to buff.

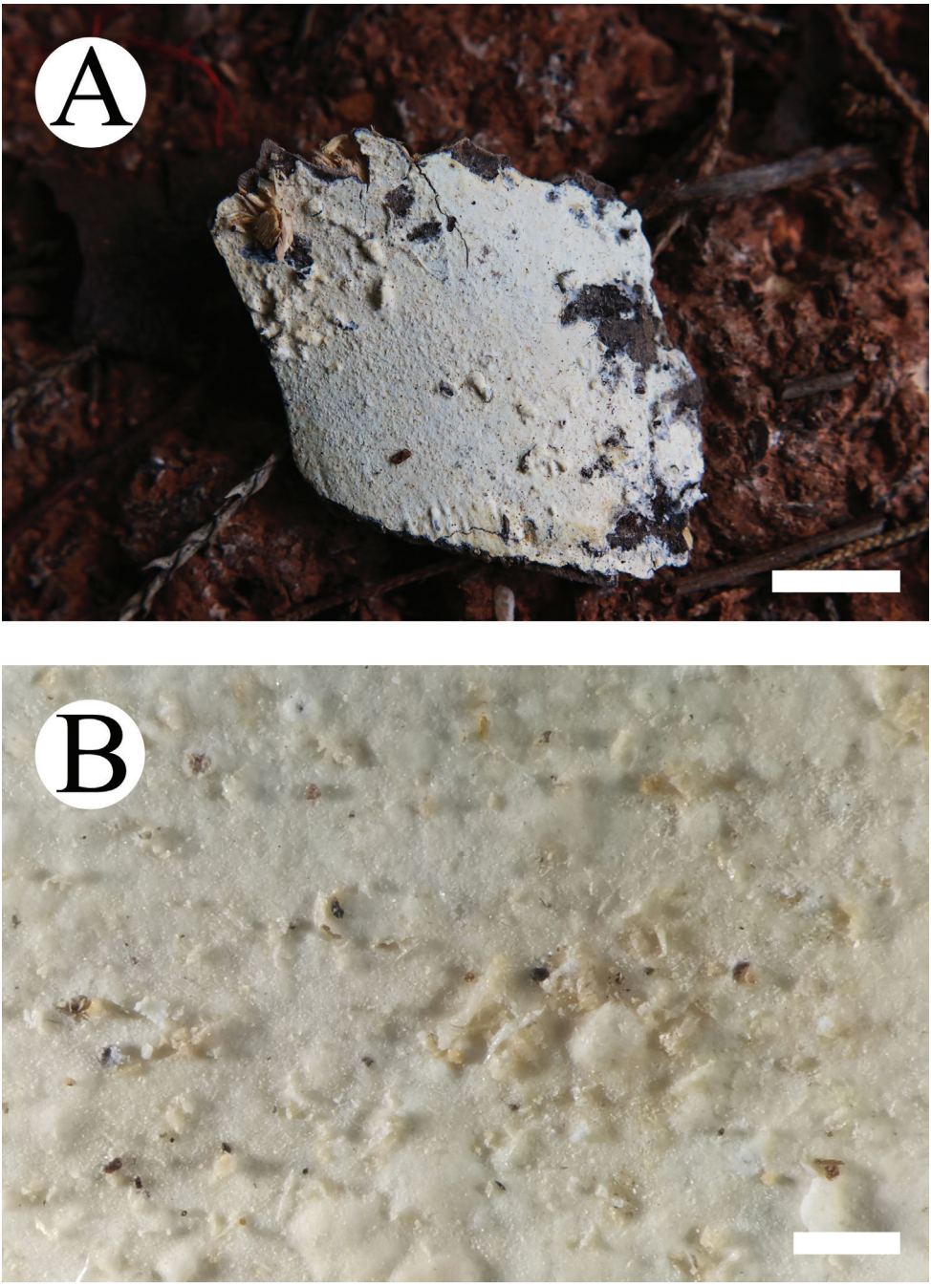

Figure 3. Basidiomata of *Lyomyces cremeus* (holotype). Scale bars: 1 cm (**A**); 5 mm (**B**).

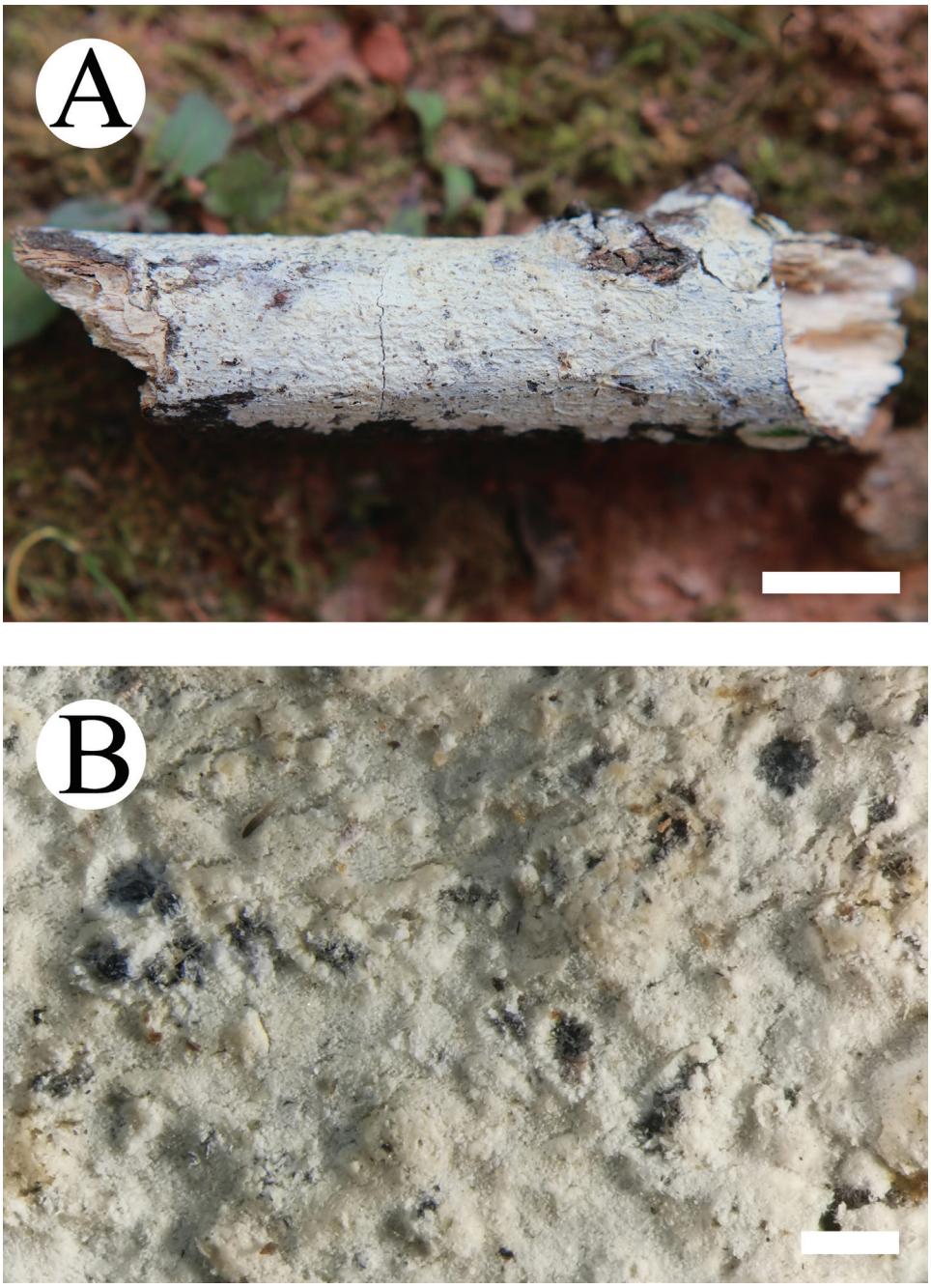

Figure 4. Basidiomata of *Lyomyces macrosporus* (holotype). Scale bars: 1 cm (**A**); 5 mm (**B**).

Hyphal system. Monomitic; generative hyphae with clamp connections, hyaline, thick-walled, branched, 2.5–4 μm in diameter, IKI–, cyanophilous; tissues unchanged in KOH. Numerous crystals present among hyphae.

Hymenium. Three kinds of cystidia: 1) capitate, hyaline, thin-walled, 19–35 × 3–7 μm; 2) tapering, hyaline, thin-walled, 13–20 × 2.5–4 μm; 3) moniliform, hyaline, thin-walled, 15–22 × 4.5–6 μm; fusoid cystidioles present, hyaline, thin-walled, 15–20 × 2.5–4 μm. Basidia subclavate to clavate, constricted, hyaline, thin-walled, with four sterigmata and a basal clamp connection, 22.2–38 × 4.5–7 μm.

Spores. Basidiospores ellipsoid, hyaline, slightly thick-walled, smooth, IKI–, cyanophilous, guttulate, (6.4–)6.7–8.9(–9.1) × 4.4–5.4(–5.7) μm, L = 7.84 μm, W = 4.93 μm, Q = 1.48–1.8 (n = 120/4).

Ecology and distribution. Lignicolous, causing a white rot. China.

Additional specimens examined. China. Yunnan Province: Puer, Jingdong County, Taizhong Town, Ailaoshan National Nature Reserve, on fallen branch of angiosperm, 4 October 2017, CLZhao 3951; Wuliangshan National Nature Reserve, on fallen branch of angiosperm, 6 October 2017, CLZhao 4516, CLZhao 4531 (SWFC).

Lyomyces wuliangshanensis **C.L. Zhao, sp. nov.**
Figs 5, 9
MycoBank No: 834039

Holotype. China. Yunnan Province: Puer, Jingdong County, Wuliangshan National Nature Reserve, on fallen branch of angiosperm, 5 October 2017, CLZhao 4167 (SWFC).

Etymology. The epithet *wuliangshanensis* (Lat.): refers to the locality (Wuliangshan) of the type specimens.

Basidiomata. Annual, resupinate, subcoriaceous when fresh, becoming coriaceous upon drying, up to 15 cm long and 5 cm wide, 50–150 μm thick. Hymenial surface smooth to more or less tuberculate, white to cream when fresh, turning cream to buff upon drying. Margin narrow, concolorous with hymenial surface.

Hyphal system. Monomitic; generative hyphae with clamp connections, hyaline, thick-walled, branched, 2–3 μm in diameter, IKI–, cyanophilous; tissues unchanged in KOH. Numerous crystals present among hyphae.

Hymenium. Two kinds of cystidia: 1) capitate, hyaline, thin-walled, 22–37 × 3–6 μm; 2) tapering, hyaline, thin-walled, 21–35 × 4–6.5 μm; fusoid cystidioles present, hyaline, thin-walled, 16–21 × 2.5–3.5 μm. Basidia clavate, hyaline, thin-walled, with four sterigmata and a basal clamp connection, 12–20 × 3–4.3 μm.

Spores. Basidiospores ellipsoid, hyaline, slightly thick-walled, smooth, IKI–, cyanophilous, guttulate, (3.3–)3.5–5.3(–5.5) × 2.8–4(–4.2) μm, L = 4.3 μm, W = 3.56 μm, Q = 1.22–1.31 (n = 120/4).

Ecology and distribution. Lignicolous, causing a white rot. China.

Additional specimens examined. China. Yunnan Province: Puer, Jingdong County, Wuliangshan National Nature Reserve, on angiosperm trunk, 5 October 2017, CLZhao 4108, CLZhao 4144; on angiosperm stump, 5 October 2017, CLZhao 4206; on fallen branch of angiosperm, 6 October 2017, CLZhao 4475 (SWFC).

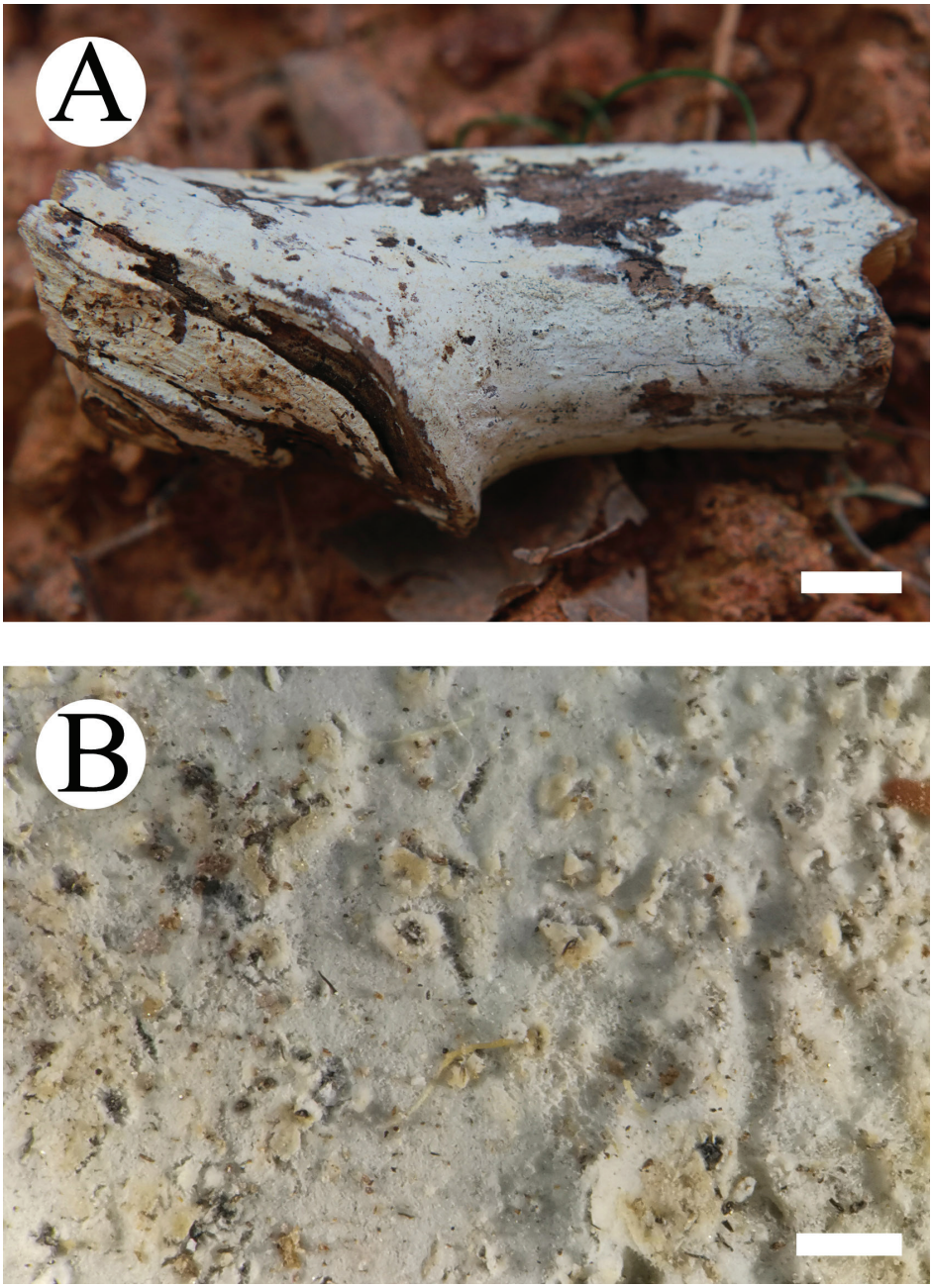

Figure 5. Basidiomata of *Lyomyces wuliangshanensis* (holotype). Scale bars: 1 cm (**A**); 5 mm (**B**).

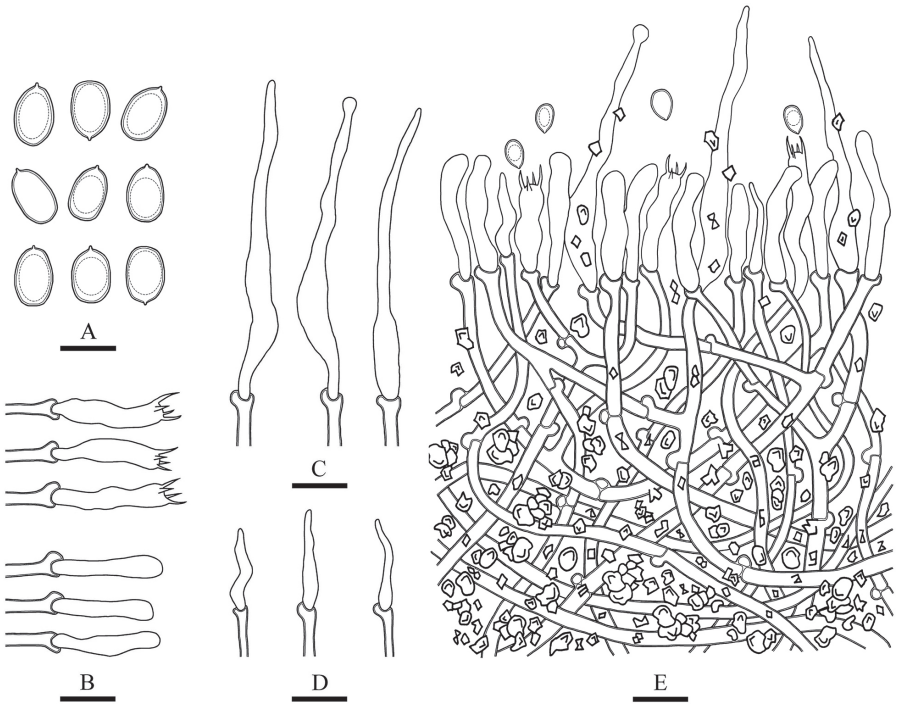

Figure 6. Microscopic structures of *Lyomyces bambusinus* (drawn from the holotype) **A** basidiospores **B** basidia and basidioles **C** cystidia **D** cystidioles **E** a cross section of basidiomata. Scale bars: 5 μm (**A**); 10 μm (**B–E**).

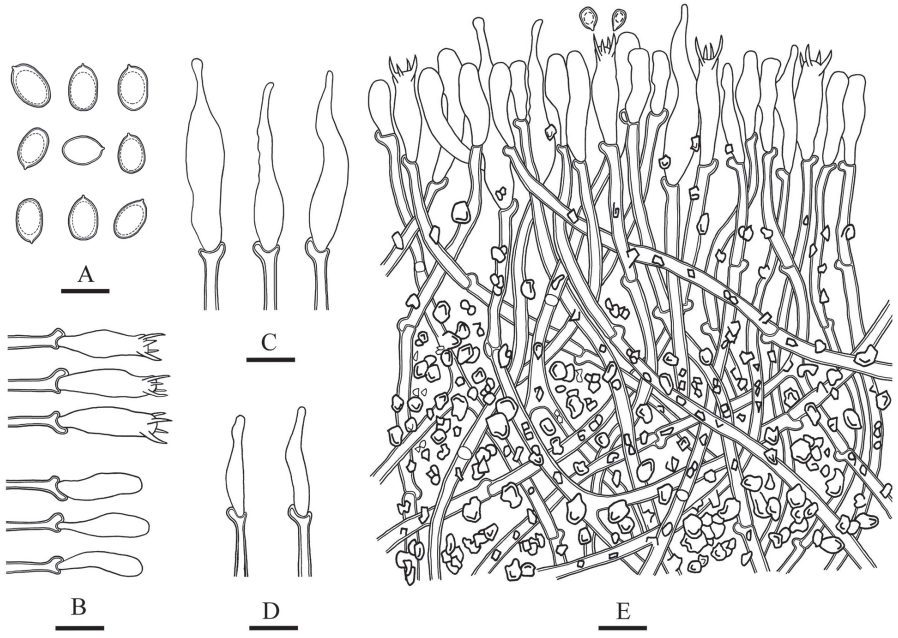

Figure 7. Microscopic structures of *Lyomyces cremeus* (drawn from the holotype) **A** basidiospores **B** basidia and basidioles **C** cystidia **D** cystidioles **E** a cross section of basidiomata. Scale bars: 5 μm (**A**); 10 μm (**B–E**).

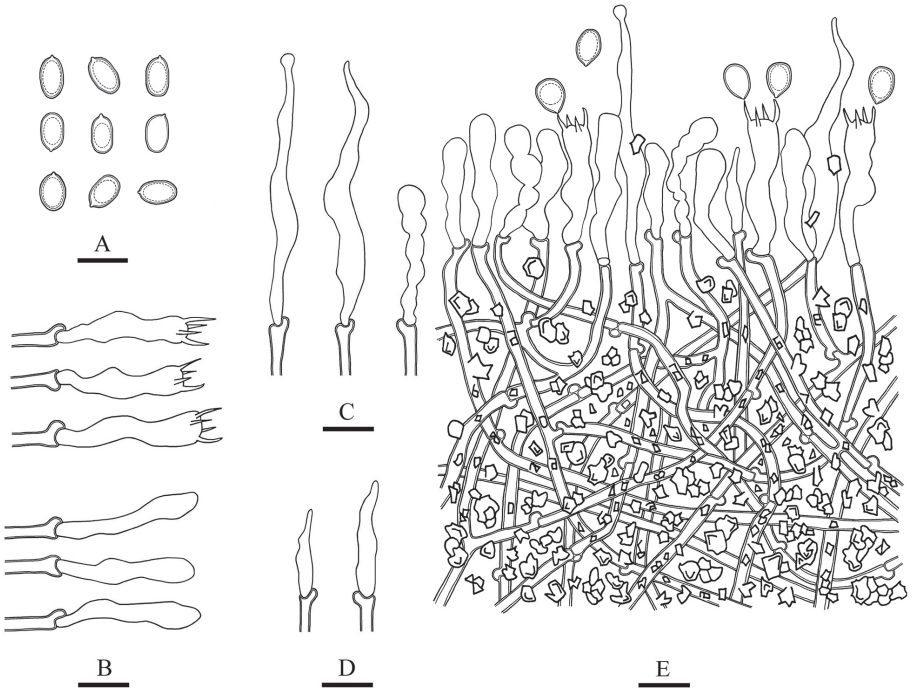

Figure 8. Microscopic structures of *Lyomyces macrosporus* (drawn from the holotype) **A** basidiospores **B** basidia and basidioles **C** cystidia **D** cystidioles **E** a cross section of basidiomata. Scale bars: 10 μm (**A–E**).

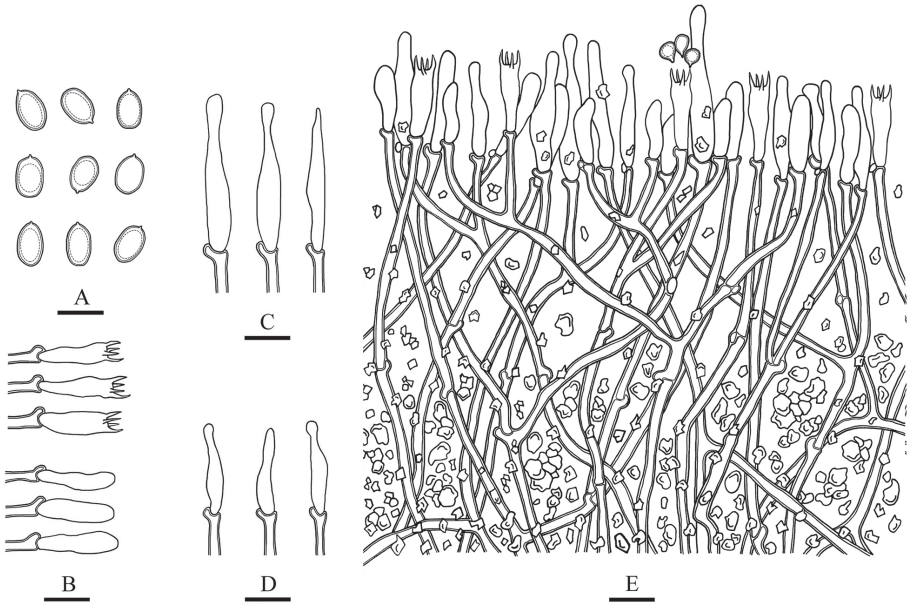

Figure 9. Microscopic structures of *Lyomyces wuliangshanensis* (drawn from the holotype) **A** basidiospores **B** basidia and basidioles **C** cystidia **D** cystidioles **E** a cross section of basidiomata. Scale bars: 5 μm (**A**); 10 μm (**B–E**).

Discussion

Miettinen et al. (2016) analyzed a phylogenetic classification in Phanerochaetaceae (Polyporales, Basidiomycota) and showed that the macromorphology of basidiomata and hymenophore construction did not reflect monophyletic groups. The phylogeny we obtained (Fig. 1) shows that the macromorphological and micromorphological characters are not consistent with monophyletic groups.

In our phylogeny, *Lyomyces bambusinus* was sisiter to *L. sambuci*, but morphologically *L. sambuci* differs from *L. bambusinus* by having ellipsoid to oblong, narrower basidiospores (4.5–6 × 3–3.5 μm, Yurchenko et al. 2017). *Lyomyces cremeus* formed a monophyletic lineage with strong supports (100% BS, 100% BP, 1.00 BPP; Fig. 1) and then was sister to a clade comprised of *L. microfasciculatus*, *L. mascarensis*, and *L. wuliangshanensis*. However *L. microfasciculatus* differs in odontioid hymenophore and presence of minute peg-like fascicles of hyphae (Yurchenko and Wu 2014). *Lyomyces macrosporus* was sister to *L. allantosporus*, but morphologically *L. allantosporus* differs in having porulose hymenophore and suballantoid to allantoid, narrower basidiospores (7–9 × 3–3.8 μm, Yurchenko et al. 2017). *Lyomyces wuliangshanensis* grouped closely with *L. mascarensis*, but *L. mascarensis* differs from *L. wuliangshanensis* by having thin-walled generative hyphae and presence of capitate cystidia (17–38 × 3.5–6 μm, Yurchenko et al. 2017).

Five *Lyomyces* species were reported from China prior to this study, *Lyomyces albus* (Sheng H. Wu) Riebesehl & Langer, *L. capitatocystidiatus* (H.X. Xiong, Y.C. Dai & Sheng H. Wu) Riebesehl & Langer, *L. microfasciculatus*, *L. sambuci* and *L. tenuissimus* (Yurchenko & Sheng H. Wu) Riebesehl & Langer. *Lyomyces albus* differs from four new species by its odontioid hymenophore (Riebesehl and Langer 2017); *L. capitatocystidiatus* by grandinioid hymenophore with arachnoid-farinaceous hymenial surface (Xiong et al. 2009); *L. microfasciculatus* by minutely odontioid hymenial surface and small emerging fascicles of flexuous hyphae (Yurchenko and Wu 2014); *L. tenuissimus* by much thinner basidiomata and non-encrusted, subicular hyphae, shorter cystidia and shorter basidia (Yurchenko et al. 2013).

Hyphodontia s.l. is an extensively studied group of Hymenochaetales (Dai 2012; Viner et al. 2018; Riebesehl et al. 2019), but the Chinese species diversity is still not well known, especially in subtropical and tropical areas. The four new *Lyomyces* species here described are from the subtropics.

Acknowledgements

This research was supported by the National Natural Science Foundation of China (Project No. 31700023), Yunnan Agricultural Foundation Projects (2017FG001-042), and the Key Laboratory of State Forestry Administration for Highly-Efficient Utilization of Forestry Biomass Resources in Southwest China (Southwest Forestry University) (Project No. 2019-KF10).

References

Bernicchia A, Gorjón SP (2010) Fungi Europaei 12: Corticiaceaes l. Edizioni Candusso, Lomazzo, 1–1007.

Bourdot H, Galzin A (1911) Hyménomycètes de France: III. Corticiées: *Corticium*, *Epithele*, *Asterostromella*. Bulletin de la Société Mycologique de France 27: 223–266.

Cui BK, Li HJ, Ji X, Zhou JL, Song J, Si J, Yang ZL, Dai YC (2019) Species diversity, taxonomy and phylogeny of Polyporaceae (Basidiomycota) in China. Fungal Diversity 97: 137–392. https://doi.org/10.1007/s13225-019-00427-4

Cunningham GH (1959) Hydnaceae of New Zealand. Part II. The genus *Odontia*. In Transactions of the Royal Society of New Zealand 86: 65–103.

Cunningham GH (1963) The Thelephoraceae of Australia and New Zealand. Bulletin of the New Zealand Department of Scientific and Industrial Research 145: 1–359.

Dai YC (2010) Hymenochaetaceae (Basidiomycota) in China. Fungal Diversity 45: 131–343. https://doi.org/10.1007/s13225-010-0066-9

Dai YC (2012) Polypore diversity in China with an annotated checklist of Chinese polypores. Mycoscience 53: 49–80. https://doi.org/10.1007/s10267-011-0134-3

Felsenstein J (1985) Confidence intervals on phylogenetics: an approach using bootstrap. Evolution 39: 783–791. https://doi.org/10.2307/2408678

Gafforov Y, Riebesehl J, Ordynets A, Langer E, Yarasheva M, Ghobad-Nejhad M, Zhou LW, Wang XW, Gugliotta ADM (2017) *Hyphodontia* (Hymenochaetales, Basidiomycota) and similar taxa from Central Asia. Botany 95: 1041–1056. https://doi.org/10.1139/cjb-2017-0115

Hall TA (1999) Bioedit: A user-friendly biological sequence alignment editor and analysis program for windows 95/98/NT. Nucleic Acids Symposium Series 41: 95–98.

Han ML, Chen YY, Shen LL, Song J, Vlasák J, Dai YC, Cui BK (2016) Taxonomy and phylogeny of the brown-rot fungi: *Fomitopsis* and its related genera. Fungal Diversity 80: 343–373. https://doi.org/10.1007/s13225-016-0364-y

Hjortstam K, Ryvarden L (2009) A checklist of names in *Hyphodontia* sensu stricto - sensu lato and *Schizopora* with new combinations in *Lagarobasidium*, *Lyomyces*, *Kneiffiella*, *Schizopora*, and *Xylodon*. Synopsis Fungorum 26: 33–55.

Karsten PA (1881) Enumeratio *Thelephorearum* Fr. et *Clavariearum* Fr. *Fennicarum*, systemate novo dispositarum. Revue Mycologique Toulouse 3: 21–23.

Karsten PA (1882) Rysslands, Finlans och den Skandinaviska halföns Hattsvampar. Sednare Delen: Pip-, Tagg-, Hud-, Klubb- och Gelésvampar. Bidrag till Kännedom av Finlands Natur och Folk 37: 1–257.

Larsson KH, Parmasto E, Fischer M, Langer E, Nakasone KK, Redhead SA (2006) Hymenochaetales: a molecular phylogeny for the hymenochaetoid clade. Mycologia 98: 926–936. https://doi.org/10.1080/15572536.2006.11832622

Miettinen O, Spirin V, Vlasák J, Rivoire B, Stenroos S, Hibbett D (2016) Polypores and genus concepts in Phanerochaetaceae (Polyporales, Basidiomycota). MycoKeys 17: 1–46. https://doi.org/10.3897/mycokeys.17.10153

Miller MA, Holder MT, Vos R, Midford PE, Liebowitz T, Chan L, Hoover P, Warnow T (2009) The CIPRES Portals. CIPRES. http://www.phylo.org/sub_sections/portal [2009-08-04. (Archived by WebCite(r) at http://www.webcitation.org/5imQlJeQa]

Nylander JAA (2004) MrModeltest v2. Program distributed by the author. Evolutionary Biology Centre, Uppsala University.

Peck CH (1903) Report of the state botanist. Bulletin of the New York State Museum 67: 1–194.

Petersen JH (1996) Farvekort. The Danish Mycological Society's colour-chart. Foreningen til Svampekundskabens Fremme, Greve, 6.

Rabenhorst GL (1851) Klotzschii herbarium vivum mycologicum sistens fungorum per totam *Germaniam crescentium* collectionem perfectam. Editio prima. Centuria 8: 1501–1600.

Riebesehl J, Langer E (2017) *Hyphodontia* s.l. (Hymenochaetales, Basidiomycota) – 35 new combinations and new keys to currently all 120 species. Mycological Progress 16: 637–666. https://doi.org/10.1007/s11557-017-1299-8

Riebesehl J, Yurchenko E, Nakasone KK, Langer E (2019) Phylogenetic and morphological studies in *Xylodon* (Hymenochaetales, Basidiomycota) with the addition of four new species. MycoKeys 47: 97–137. https://doi.org/10.3897/mycokeys.47.31130

Ronquist F, Huelsenbeck JP (2003) MRBAYES 3: bayesian phylogenetic inference under mixed models. Bioinformatics 19: 1572–1574. https://doi.org/10.1093/bioinformatics/btg180

Rosenthal LM, Larsson KH, Branco S, Chung JA, Glassman SI, Liao HL, Liao HL, Peay KG, Smith DP, Talbot JM, Taylor JW, Vellinga EC, Vilgalys R, Bruns TD (2017) Survey of corticioid fungi in North American pinaceous forests reveals hyperdiversity, underpopulated sequence databases, and species that are potentially ectomycorrhizal. Mycologia 109: 115–127. https://doi.org/10.1080/00275514.2017.1281677

Shen LL, Wang M, Zhou JL, Xing JH, Cui BK, Dai YC (2019) Taxonomy and phylogeny of *Postia*. Multi-gene phylogeny and taxonomy of the brown-rot fungi: *Postia* and its related genera. Persoonia 42: 101–126. https://doi.org/10.3767/persoonia.2019.42.05

Song J, Cui BK (2017) Phylogeny, divergence time and historical biogeography of *Laetiporus* (Basidiomycota, Polyporales). BMC Evolutionary Biology 17: 102. https://doi.org/10.1186/s12862-017-0948-5

Swofford DL (2002) PAUP*: phylogenetic analysis using parsimony (*and other methods). Version 4.0b10. Sinauer Associates, Massachusetts.

Viner I, Spirin V, Zíbarová L, Larsson KH (2018) Additions to the taxonomy of *Lagarobasidium* and *Xylodon* (Hymenochaetales, Basidiomycota). MycoKeys 41: 65–90. https://doi.org/10.3897/mycokeys.41.28987

White TJ, Bruns T, Lee S, Taylor J (1990) Amplification and direct sequencing of fungal ribosomal RNA genes for phylogenetics. In: Innis MA, Gelfand DH, Sninsky JJ, White TJ (Eds) PCR Protocols: a guide to methods and applications. Academic Press, San Diego, 315–322. https://doi.org/10.1016/B978-0-12-372180-8.50042-1

Wu SH (1990) The Corticiaceae (Basidiomycetes) subfamilies Phlebioideae, Phanerochaetoideae and Hyphodermoideae in Taiwan. Acta Botanica Fennica 142: 1–123.

Wu ZQ, Xu TM, Shen S, Liu XF, Luo KY, Zhao CL (2018) *Elaphroporia ailaoshanensis* gen. et sp. nov. in Polyporales (Basidiomycota). MycoKeys 29: 81–95. https://doi.org/10.3897/mycokeys.29.22086

Xiong HX, Dai YC, Wu SH (2009) Three new species of *Hyphodontia* from Taiwan. Mycological Progress 8: 165–169. https://doi.org/10.1007/s11557-009-0587-3

Yurchenko E, Wu SH (2014) Three new species of *Hyphodontia* with peg-like hyphal aggregations. Mycological Progress 13: 533–545. https://doi.org/10.1007/s11557-013-0935-1

Yurchenko E, Riebesehl J, Langer E (2017) Clarification of *Lyomyces sambuci* complex with the descriptions of four new species. Mycological Progress 16: 865–876. https://doi.org/10.1007/s11557-017-1321-1

Yurchenko E, Xiong HX, Wu SH (2013) Four new species of *Hyphodontia* (*Xylodon* Hjortstam & Ryvarden, Basidiomycota) from Taiwan. Nova Hedwigia 96: 545–558. https://doi.org/10.1127/0029-5035/2013/0092

Zhu L, Song J, Zhou JL, Si J, Cui BK (2019) Species diversity, phylogeny, divergence time and biogeography of the genus *Sanghuangporus* (Basidiomycota). Frontiers in Microbiology 10: 812. https://doi.org/10.3389/fmicb.2019.00812

MycoKeys 65: 119–138 (2020)
doi: 10.3897/mycokeys.65.49769
http://mycokeys.pensoft.net

RESEARCH ARTICLE

A peer-reviewed open-access journal
MycoKeys
Launched to accelerate biodiversity research

Lignicolous freshwater ascomycota from Thailand: Phylogenetic and morphological characterisation of two new freshwater fungi: *Tingoldiago hydei* sp. nov. and *T. clavata* sp. nov. from Eastern Thailand

Li Xu[1], Dan-Feng Bao[2,3,4], Zong-Long Luo[2], Xi-Jun Su[2], Hong-Wei Shen[2,3], Hong-Yan Su[2]

1 *College of Basic Medicine, Dali University, Dali 671003, Yunnan, China* **2** *College of Agriculture & Biological Sciences, Dali University, Dali 671003, Yunnan, China* **3** *Center of Excellence in Fungal Research, Mae Fah Luang University, Chiang Rai 57100, Thailand* **4** *Department of Entomology & Plant Pathology, Faculty of Agriculture, Chiang Mai University, Chiang Mai 50200, Thailand*

Corresponding author: Hong-Yan Su (suhongyan16@163.com)

Academic editor: R. Phookamsak | Received 31 December 2019 | Accepted 6 March 2020 | Published 26 March 2020

Citation: Xu L, Bao D-F, Luo Z-L, Su X-J, Shen H-W, Su H-Y (2020) Lignicolous freshwater ascomycota from Thailand: Phylogenetic and morphological characterisation of two new freshwater fungi: *Tingoldiago hydei* sp. nov. and *T. clavata* sp. nov. from Eastern Thailand. MycoKeys 65: 119–138. https://doi.org/10.3897/mycokeys.65.49769

Abstract

Lignicolous freshwater fungi represent one of the largest groups of Ascomycota. This taxonomically highly diverse group plays an important role in nutrient and carbon cycling, biological diversity and ecosystem functioning. The diversity of lignicolous freshwater fungi along a north-south latitudinal gradient is currently being studied in Asia. In this paper, we introduce two novel freshwater taxa viz. *Tingoldiago hydei* **sp. nov.** and *T. clavata* **sp. nov.** which were collected from freshwater substrates in Eastern Thailand. Morphological comparison based on the size of ascomata, asci and ascospores, as well as multi-gene phylogenetic analyses based on LSU, SSU, ITS and TEF1-α DNA sequences, supports their placement in *Tingoldiago* (Lentitheciaceae). Descriptions and illustrations of these two new species are provided.

Keywords

2 new species, Lentitheciaceae, Freshwater fungi, phylogeny, taxonomy

Introduction

Freshwater fungi are those which the whole or part of their life cycle is found in a freshwater habitat (Thomas 1996, Wong et al. 1998) and they are an evolutionary important group (Vijaykrishna et al. 2006). The members of freshwater fungi can be saprobes, parasites, endophytes and mutualistic taxa (Vijaykrishna et al. 2005, Zhang et al. 2008, Swe et al. 2009, Jones et al. 2014, Huang et al. 2018). There is a wide range of organisms that can be freshwater fungi hosts, such as wood, plants, alga, foams, fish etc. (Sparrow 1960, Ellis and Ellis 1985, Jones et al. 2014). However, a lot of studies on freshwater fungi have focused on lignicolous freshwater fungi (Tsui et al. 2000, Cai et al. 2002, Luo et al. 2004, 2018, Jones et al. 2014, Hyde et al. 2016, Yang et al. 2017), which were defined as those fungi that grow on submerged woody debris in freshwater streams, ponds, lakes and tree hollows (Hyde et al. 2016). They also grow on submerged wood in peat swamps and dams (Pinnoi et al. 2006, Pinruan et al. 2007, 2014, Hu et al. 2010). Lignicolous freshwater fungi are a diverse group comprising species from different phyla (Aphelidiomycota, Ascomycota, Basidiomycota, Blastocladiomycota, Chytridiomycota, Monoblepharomycota, Mortierellomycota and Rozellomycota) (Shearer et al. 2007, Kagami et al. 2012, Zhang et al. 2012, Jones et al. 2014, Wijayawardene et al. 2018). The dominant groups of lignicolous freshwater fungi are Dothideomycetes and Sordarialmycets (Jones et al. 2014, Hyde et al. 2016, Wijayawardene et al. 2017, 2018).

We are studying the diversity of lignicolous freshwater fungi in Thailand, in order to establish the phylogenetic relationships of lignicolous freshwater fungi, understanding the natural classification of this group and contributing to the biogeographical diversity of fungi (Hyde et al. 2016). The study on freshwater fungi in Thailand was first investigated by Tubaki et al. (1983) and they reported 40 freshwater fungal species from foam. Subsequently, mycologists started to study lignicolous freshwater fungi in Thailand and several taxa have been reported (Sivichai et al. 1998, 1999, 2000, 2002, 2010, Jones et al. 1999, Marvanová et al. 2000, Hu et al. 2010, Zhang et al. 2013, Luo et al. 2015, 2016, Bao et al. 2018).

Lentitheciaceae was introduced by Zhang et al. (2012) to accommodate *Massarina*-like species in the order Pleosporales. Presently, 13 genera are accepted in this family (Dayarathne et al. 2018, Hyde et al. 2018). Species in this family are widely distributed in the world (China, Egypt, Hungary, Italy, Japan, Russia, Saudi, Thailand, UK, Uzbekistan) and are commonly saprobic on stems and twigs of herbaceous and woody plants in terrestrial or aquatic habitats (Wanasinghe et al. 2014, 2018, Knapp et al. 2015, Wijayawardene et al. 2015, Luo et al. 2016, Tibpromma et al. 2017, Hyde et al. 2018). The genus *Tingoldiago* was established by Hirayama et al. (2010) with a single species *Tingoldiago graminicola* K. Hiray. & Kaz. Tanak, this species being originally treated as *Massarina ingoldiana*. Later, Hirayama et al. (2010) re-assessed the phylogeny of *Massarina ingoldiana* and introduced two new genera *Tingoldiago and Lindgomyces* to accommodate *Massarina ingoldiana sensu lato*, based on phylogenetic analyses. Currently, only one species is accepted in this genus.

In this paper, we introduce two new freshwater species of *Tingoldiago* (Lentitheciaceae), based on morpho-molecular studies. Detailed descriptions and illustrations of these two new species are provided.

Materials and methods

Collection, Isolation and morphological studies

Submerged decaying wood samples were collected from That Phanom, Nakhon Phanom, Thailand and brought to the laboratory in plastic bags. The samples were incubated in plastic boxes lined with moistened tissue paper at room temperature for one week. Specimen observations and morphological studies were conducted, following the protocols provided by Luo et al. (2018).

Pure cultures were obtained by single spore isolation followed by Chomnunti et al. (2014). Germinating ascospores were transferred aseptically to potato dextrose agar (PDA) plates and grown at 16–25 °C in daylight. Colony colour and other characters were observed and measured after three weeks. The specimens were deposited in the herbarium of Mae Fah Luang University (MFLU), Chiang Rai, Thailand. Living cultures are deposited in the Culture Collection of Mae Fah Luang University (MFLUCC). Facesoffungi numbers and Index Fungorum numbers were obtained, following Jayasiri et al. (2015) and Index Fungorum (2019). New species have been established as recommended by Jeewon and Hyde (2016).

DNA extraction, PCR amplification and sequencing

Fungal mycelium was scraped from the surface of colonies grown on a PDA plate or MEA plate at 25 °C for 4 weeks, transferred into a 1.5 ml centrifuge tube and ground using liquid nitrogen. The EZ geneTM fungal gDNA kit (GD2416) was used to extract DNA from the ground mycelium according to the manufacturer's instructions. The gene regions of the large subunit of the nuclear ribosomal DNA (LSU), the internal transcribed spacers (ITS), the small subunit of the nuclear ribosomal DNA (SSU) and the translation elongation factor (TEF1-α) RNA were amplified using the primer pairs LR0R/LR7 (Vilgalys and Hester 1990), ITS5/ITS4, NS1/ NS4 (White et al. 1990) and 983F/2218R (Liu et al. 1999), respectively. The amplification reactions were performed in 25 µl of PCR mixtures containing 9.5 µl ddH_2O, 12.5 µl 2× PCR MasterMix (Tsingke Co., China), 1 µl DNA sample and 1µl of each primer. The PCR thermal cycle programme for LSU, ITS, SSU and TEF1-α amplification were as follows: 94 °C for 3 minutes, followed by 35 cycles of denaturation at 94 °C for 30 seconds, annealing at 56 °C for 50 seconds, elongation at 72 °C for 1 minute and a final extension at 72 °C for 10 minutes and finally kept at 4 °C. PCR amplification was confirmed on 1% agarose electrophoresis gels

stained with ethidium bromide. PCR products were sequenced using the same set of primers used in PCR in Beijing Tsingke Biological Engineering Technology and Services Co. Ltd. (Beijing, P.R. China).

Sequencing and sequence alignment

The sequence was assembled by using BioEdit and sequences with high similarity indices were determined from a BLAST search to find the closest matches with taxa in Lentitheciaceae and from recently published data (Dayarathne et al. 2018). All consensus sequences and the reference sequences were aligned using MAFFT v. 7 (http://mafft.cbrc.jp/alignment/server/index.html) (Katoh and Standley 2013), then checked visually and manually optimised using BioEdit v.7.0.9 (Hall 1999). Ambiguous regions were excluded from the analyses and gaps were treated as missing data. The phylogeny website tool "ALTER" (Glez-Peña et al. 2010) was used to convert the alignment fasta file to Phylip format for RAxML analysis and Clustalx BETA and PAUP 4.0 were used to convert the alignment fasta file to a Nexus file for Bayesian analysis. Phylogenetic analyses were obtained from Maximum Likelihood (ML), Maximum Parsimony (MP) and Bayesian analysis.

Phylogenetic analyses

Maximum likelihood trees were generated using the RAxML-HPC2 on XSEDE (8.2.8) (Stamatakis 2006, Stamatakis et al. 2008) in the CIPRES Science Gateway platform (Miller et al. 2010) using GTR+ I + G model of evolution which was estimated by MrModeltest 2.2 (Nylander et al. 2008). Maximum likelihood bootstrap values (ML), equal to or greater than 75%, are given above each node (Figure 1).

MP analyses were performed using the heuristic search option with 1000 random taxa addition and tree bisection and reconnection (TBR) as the branch-swapping algorithm. All characters were unordered and of equal weight and gaps were treated as missing data. Maxtrees were unlimited, branches of zero length were collapsed and all multiple, equally parsimonious trees were saved. Clade stability was assessed using a bootstrap (BS) analysis with 1000 replicates, each with ten replicates of random stepwise addition of taxa (Hillis and Bull 1993).

The Bayesian analysis was performed with MrBayes v3.2 (Ronquist et al. 2012), with the best-fit model of sequence evolution estimated with MrModeltest 2.2 (Nylander et al. 2008) to evaluate posterior probabilities (PP) (Rannala and Yang 1996, Zhaxybayeva and Gogarten 2002) by Markov Chain Monte Carlo (MCMC) sampling. Six simultaneous Markov chains were run for 10,000,000 generations, trees were sampled every 1000th generation and 1,0000 trees were obtained. Based on the tracer analysis, the first 1,000 trees representing 10% were discarded as the burn-in phase in the analysis. The remaining trees were used to calculate posterior probabilities in the majority rule consensus tree (critical value for the topological convergence diagnostic set to 0.01).

Table 1. Taxa used in this study and their GenBank accession numbers, the newly generated sequences are indicated wirh * and the type strains are indicated in bold.

Taxa	strain	GenBank accession number			
		LSU	SSU	ITS	TEF1
Bambusicola bambusae	**MFLUCC 11–0614**	**JX442035**	**JX442039**	**NR121546**	**KP761722**
B. irregulispora	**MFLUCC 11–0437**	**JX442036**	**JX442040**	**NR121547**	**KP761723**
B. massarinia	**MFLUCC 11–0389**	**JX442037**	**JX442041**	**NR121548**	**–**
Bimuria novaezelandiae	AFTOL ID931	–	–	–	DQ471087
Byssothecium circinans	**CBS67592**	**GU205217**	**GU205235**	**–**	**GU349061**
Corynespora cassiicola	CBS100822	GU301808	GU296144	–	GU349052
C. smithii	CABI5649b	GU323201	–	–	GU349018
Dacampia engeliana	**72868**	**KT383791**	**–**	**–**	**–**
D. hookeri	**74269**	**KT383793**	**–**	**–**	**–**
D. hookeri	**81840**	**KT383795**	**–**	**–**	**–**
Darksidea alpha	**CBS 135650**	**KP184019**	**KP184049**	**NR137619**	**KP184166**
D. beta	**CBS 135637**	**KP184023**	**KP184049**	**NR137957**	**KP184189**
D. delta	**CBS 135638**	**–**	**–**	**NR137075**	**–**
D. epsilon	**CBS 135658**	**KP184029**	**KP184070**	**NR137959**	**KP184186**
D. gamma	**CBS 135634**	**KP184031**	**KP184073**	**NR137587**	**KP184188**
D. zeta	**CBS 135640**	**KP184013**	**KP184071**	**NR137958**	**KP184191**
Falciformispora lignatilis	BCC 21117	GU371826	GU371834	KF432942	GU371819
F. lignatilis	BCC 21118	GU371827	GU371835	KF432943	GU371820
Halobyssothecium obiones	27AV2385	–	–	KX263864	–
H. obiones	MFLUCC 15–0381	MH376744	MH376745	MH377060	MH376746
Helicascus nypae	**BCC36752**	**GU479789**	**GU479755**	**–**	**GU479855**
Kalmusia scabrispora	KT2202	AB524594	AB524453	–	AB539107
Karstenula rhodostoma	CBS69094	GU301821	GU296154	–	GU349067
Katumotoa bambusicola	**KT1517a**	**AB524595**	**AB524454**	**LC014560**	**AB539108**
Keissleriella breviasca	KT649	AB807588	AB797298	–	AB808567
K. culmifida	KT2642	AB807592	AB797302	LC014562	**–**
K. gloeospora	KT829	AB807589	AB797299	LC014563	–
K. poagena	CBS136767	KJ869170	–	KJ869112	–
K. quadriseptata	KT2292	AB807593	AB797303	AB811456	AB808572
K. taminensis	KT571	AB807595	AB797305	LC014564	AB808574
K. trichophoricola	CBS 136770	KJ869171	–	KJ869113	–
Lentithecium clionina	KT1149A	AB807540	AB797250	LC014566	AB808515
L. fluviatile	**CBS 123090**	**FJ795450**	**FJ795492**	**–**	**–**
L. pseudoclioninum	KT1111	AB807544	AB797254	AB809632	AB808520
Massarina cisti	**CBS 266 62**	**FJ795447**	**FJ795490**	**LC014568**	**AB808514**
M. eburnea	CBS 473 64	GU301840	GU296170	–	GU349040
Montagnula opulenta	AFTOLID1734	DQ678086	AF164370	–	–
Morosphaeria ramunculicola	**JK5304B**	**GU479794**	**GU479760**	**–**	**–**
Murilentithecium clematidis	IT1078	KM408758	KM408760	KM408756	–
M. clematidis	MFLUCC 14–0562	KM408759	KM408761	KM408757	KM454445
Neoophiosphaerella sasicola	KT1706	AB524599	AB524458	LC014577	AB539111
Palmiascoma gregariascomum	MFLUCC 11–0175	KP744495	KP753958	KP744452	–
Paraconiothyrium brasiliense	CBS100299	JX496124	AY642523	JX496011	**–**
Paraphaeosphaeria michotii	MFLUCC 13–0349	KJ939282	KJ939285	KJ939279	–
P. minitans	CBS122788	EU754173	EU754074	–	GU349083
Phaeodothis winteri	CBS18258	–	GU296183	–	–
Phragmocamarosporium platani	MFLUCC 14–1191	KP842915	KP842918	–	–

Taxa	strain	GenBank accession number			
		LSU	SSU	ITS	TEF1
Pleurophoma ossicola	CBS139905	KR476769	–	KR476736	–
P. ossicola	**CPC24985**	**KR476770**	**–**	**NR137992**	**–**
Pleurophoma pleurospora	CBS130329	JF740327	–	–	–
Poaceascoma aquaticum	**MFLUCC 14–0048**	**KT324690**	**KT324691**	**–**	**–**
P. halophila	**MFLUCC 15–0949**	**MF615399**	**MF615400**	**–**	**–**
P. helicoides	**MFLUCC 11–0136**	**KP998462**	**KP998463**	**KP998459**	**KP998461**
Pseudomurilentithecium camporesii	**MDLUCC 14-1118**	**MN638846**	**MN638850**	**MN638861**	**–**
Setoseptoria arundinacea	KT600	AB807575	AB797285	LC014595	AB808551
S. magniarundinacea	KT1174	AB807576	AB797286	LC014596	AB808552
S. phragmitis	**CBS 114802**	**KF251752**	**–**	**KF251249**	**–**
S. scirpi	**MFUCC 14–0811**	**KY770982**	**KY770980**	**MF939637**	**KY770981**
Stagonospora macropycnidia	CBS 114202	GU301873	GU296198	–	GU349026
Tingoldiago graminicola	KH155	AB521745	AB521728	LC014599	AB808562
T. graminicola	KH68	AB521743	AB521726	LC014598	AB808561
T. graminicola	KT891	AB521744	AB521727	–	AB808563
****T. hydei***	**MFLUCC 19-0499**	**MN857177**	**–**	**MN857181**	**–**
****T. clavata***	**MFLUCC 19-0496**	**MN857178**	**MN857186**	**MN857182**	**–**
**T. clavata*	MFLUCC 19-0498	MN857179	MN857187	MN857183	–
**T. clavata*	MFLUCC 19-0495	MN857180	MN857188	MN857184	–
Towyspora aestuari	**MFLUCC 15–1274**	**KU248852**	**KU248853**	**NR148095**	**–**
Trematosphaeria pertusa	**CBS 122368**	**FJ201990**	**FJ201991**	**NR132040**	**KF015701**
Trematosphaeria pertusa	CBS 122371	GU301876	GU348999	KF015669	KF015702

The phylograms were visualised in FigTree 1.4.2 (Rambaut 2014) and made in Adobe Illustrator CS5 (Adobe Systems Inc., USA). All newly generated sequences of this study have been submitted in GenBank.

Results

Phylogenetic analyses

The aligned sequence matrix comprises LSU, SSU, ITS and TEF1-α sequence data for 69 taxa, with *Corynespora smithii* and *Corynespora cassiicola* as out-group taxa. The dataset comprises 3334 characters after alignment including gaps (LSU: 1–897; SSU: 898–1920; ITS: 1921–2522; TEF1-α: 2523–3479). The topologies of RAxML, MP and Bayesian are similar and the bootstrap support values for Maximum Likelihood (ML), Maximum Parsimony (MP) higher than 75% and Bayesian posterior probabilities (PP) greater than 0.95 are given above the nodes. Maximum parsimony analyses indicated that 2,442 characters were constant, 232 variable characters parsimony uninformative and 805 characters are parsimony-informative. The RAxML analysis of the combined dataset yielded the best scoring tree (Figure 1) with a final ML optimisation likelihood value of -21568.713178. The matrix had 1322 distinct alignment patterns,

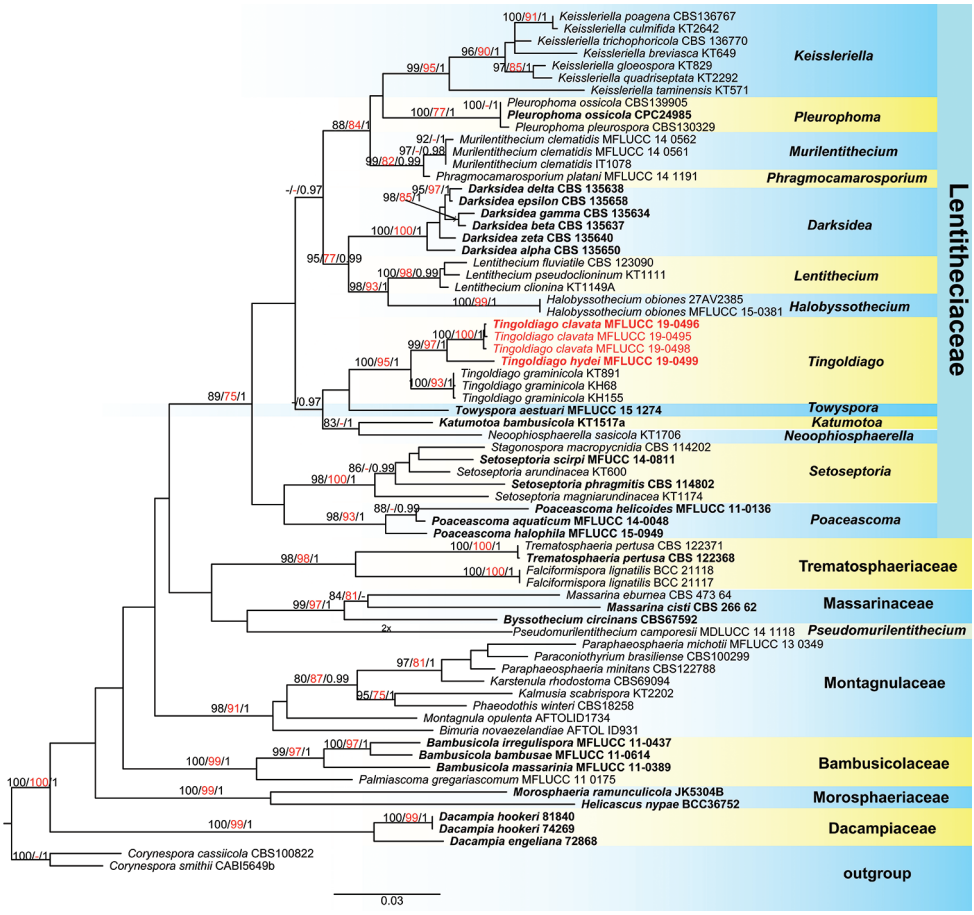

Figure 1. Phylogenetic tree based on RAxML analyses of combined LSU, SSU, ITS and TEF1-α sequence data. Bootstrap support values for maximum likelihood (ML, black) and maximum parsimony (MP, red) higher than 75% and Bayesian posterior probabilities (PP, black) greater than 0.95 are indicated above the nodes as MP / ML /PP. The ex-type strains are in bold and the newly obtained isolates are in red. The tree is rooted at *Corynespora smithii* (CABI5649b) and *Corynespora cassiicola* (CBS100822).

with 30.89% undetermined characters or gaps. Estimated base frequencies were as follows: A = 0.238228, C = 0.248262, G = 0.272670, T = 0.240839; substitution rates AC = 1.161111, AG = 2.490274, AT = 1.596115, CG = 1.194931, CT = 7.261814, GT = 1.000000; gamma distribution shape parameter α = 0.183824.

The novel species *Tingoldiago hydei* and *T. clavata*, introduced in this paper, are supported by multi-phylogenetic analyses. Four newly generated strains clustered together within *Tingoldiago* with strong statistical support (100 ML/95 MP/1.00 PP, Figure. 1). Three strains of *T. clavata* clustered together and sister to *T. hydei* with strong bootstrap support (99 ML/97 MP/1 PP, Figure 1).

Taxonomy

Tingoldiago hydei **D.F. Bao, Z.L. Luo & H.Y. Su, sp. nov.**
Index Fungorum No: IF557047
Facesoffungi No: FoF07082
Figure 2

Etymology. Referring to Kevin D. Hyde for his contributions in fungal taxonomy.

Holotype. Thailand, That Phanom, Nakhon Phanom, on submerged decaying wood, 13 November 2018, D.F. Bao, B-126 (MFLU 19–2842, holotype), ex-type living culture, MFLUCC 19–0499.

Description. *Saprobic* on submerged decaying wood. ***Sexual morph:*** *Ascomata* 180–280 × 330–470 μm ($\overline{x}$ = 400 × 420 μm, n = 10), immersed to semi-immersed, erumpentia, gregarious, scattered, depressed globose to conical with a flattened base, dark brown to black, as dark spots on host surface. *Ostioles* central, papillate, short, crest-like, dark brown. *Peridium* 33.5–50 μm wide, comprising 4–6 layers, brown to dark brown cells of *textura anngularis*. *Hamathecium* comprising 2–2.5 μm (n = 30) wide, numerous, branched, septate, hyaline, cellular pseudoparaphyses. *Asci* 95–164 × 18–22 μm ($\overline{x}$ = 129 × 20 μm, n = 20), 8-spored, bitunicate, fissitunicate, cylindrical-clavate, rounded at apex, with a short pedicellate. *Ascospores* 37.5–42 × 7.5–9 μm ($\overline{x}$ = 40 × 8 μm, n = 30), overlapping, 2–3-seriate, clavate with round ends, straight, uniseptate, deeply constricted at septum, with broad and short upper cells 17.5–20 × 7–8.7 μm ($\overline{x}$ = 18.7 × 7.9 μm, n = 30), narrow and long lower cells 20.6–23.3 × 5.9–7.4 μm ($\overline{x}$ = 21.9 × 6.7 μm, n = 30), tapering towards the end, with short appendages at the septum, hyaline, guttulate, smooth, surrounded by a fusiform gelatinous sheath. ***Asexual morph:*** Undetermined.

Culture characteristics. Ascospores germinating on PDA within 24 hours. Colonies on MEA effuse, greyish-white to dark brown from above and below, reaching 3–4 cm diameter within 30 days at room temperature under natural light, composed of subhyaline to pale brown, septate, smooth hyphae.

Notes. Phylogenetic analysis showed that *Tingoldiago hydei* is related to *T. clavata*; however, they are in different lineages with significant support (99 ML/97 MP/1.00 PP, Figure 1). *Tingoldiago hydei* resembles *T. clavata* in having bitunicate, cylindrical-clavate asci and clavate, hyaline, uniseptate, ascospores with broad and short upper cells, narrow and long lower cells, tapering towards the end, surrounded by a gelatinous sheath. However, *Tingoldiago hydei* can be distinguished from *T. clavata* in having longer and narrower asci (95–164 × 18–22 vs. 110–148 × 20–27 μm) and smaller ascospores (37.5–42 × 7.5–9 vs. 48–51 × 7.5–8.5 μm). Moreover, ascospores of *T. clavata* have longer appendages at the septum, while the appendages of *T. hydei* are much shorter than *T. hydei*.

Tingoldiago clavata is similar to the type species, *T. raminicola* in having immersed to semi-immersed, depressed globose to conical ascomata with flattened base, bitunicate, fissitunicate, cylindrical-clavate asci and clavate, straight, uniseptate ascospores.

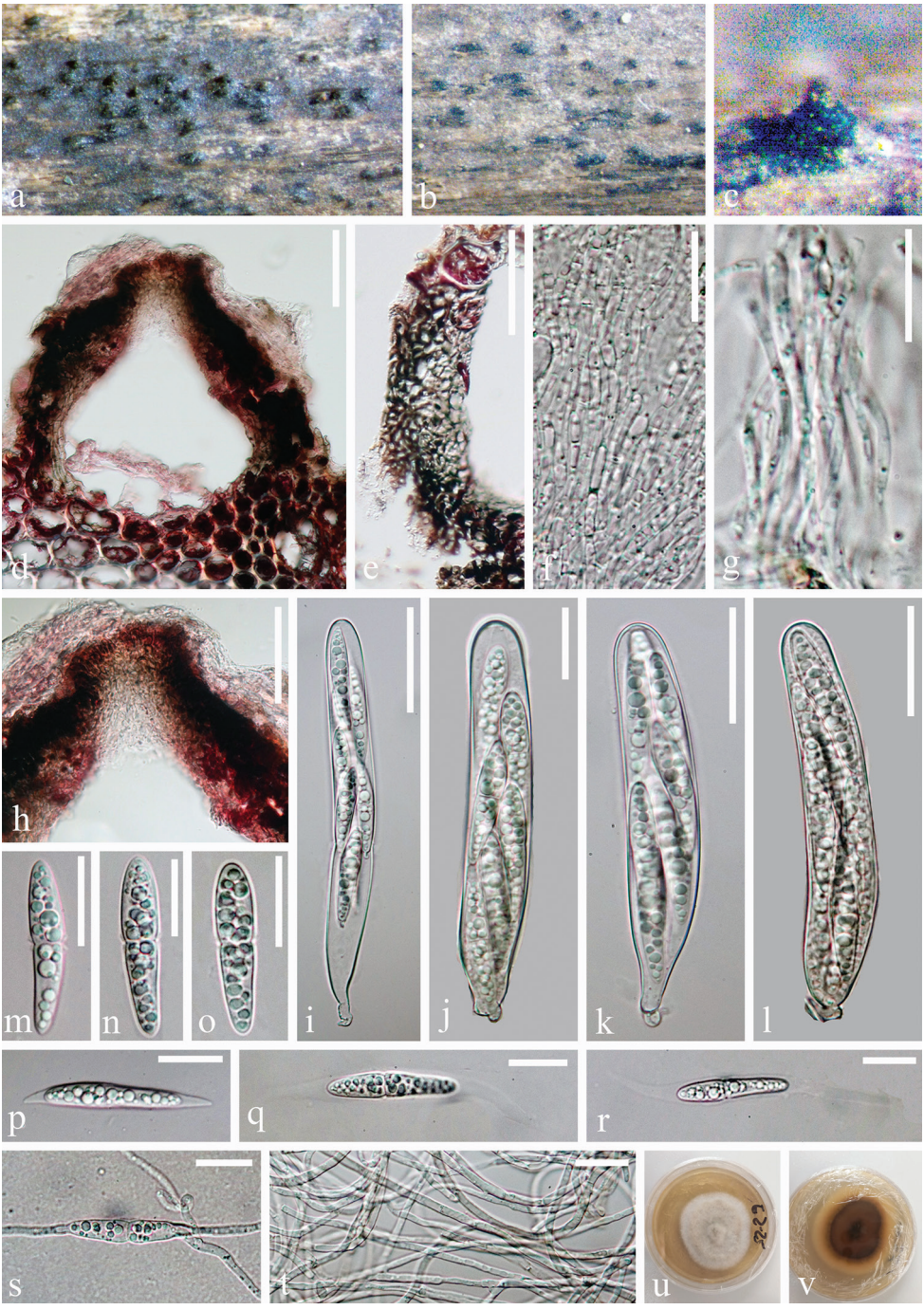

Figure 2. *Tingoldiago hydei* (MFLU 19–2842, holotype). **a–c** Ascomata on wood **d** section of ascoma **e** peridium **f, g** pseudoparaphyses **h** ostiole **i–l** asci **m–r** ascospores **s** germinating ascospore **t** vegetative hyphae in culture **u, v** culture on PDA from surface and reverse. Scale bars: 50 μm (**d, e, h**), 20 μm (**f–g, m–t**), 30 μm (**i–l**).

However, *T. clavata* differs from *T. raminicola* in having longer asci (95–164 × 18–22 vs. 87.5–122 × 18.25–25 μm) and smaller ascospores (37.5–42 × 7.5–9 vs. 43.5–53 × 7.5–11 μm). Moreover, ascopores of *T. clavata* have short appendages at the septum while ascospores of *T. raminicola* lack appendages. In addition, we compared the base pairs of ITS regions between these two species and there were 25 base pairs without gaps (5.1%) differences. Therefore, we introduce our isolate as a new species based on both phylogeny and morphological characters.

Tingoldiago clavata **D.F. Bao, L. Xu & H.Y. Su, sp. nov.**
Index Fungorum No: IF557048
Facesoffungi No: FoF07083
Figure 3

Etymology. Referring to the clavate ascospores of this fungus.

Holotype. Thailand, That Phanom, Nakhon Phanom, on submerged decaying wood, 13 November 2018, D.F. Bao, B-161 (MFLU 19–2843, holotype), ex-type culture, MFLUCC 19–0496.

Description. *Saprobic* on submerged decaying wood. ***Sexual morph*****:** *Ascomata* 145–210 × 145–195 μm ($\overline{x}$ = 175 × 169 μm, n = 10), immersed to semi-immersed, gregarious, scattered, erumpentia, depressed globose to conical with a flattened base, dark brown to black, as dark spots on host surface. *Ostiole* central, round to papillate, short, crest-like, dark brown. *Peridium* 28–47 μm wide, comprising several layers, pale brown to brown cells of *textura anngularis*. *Hamathecium* comprising 1.5–2.0 μm (n = 30) wide, numerous, branched, septate, hyaline, cellular pseudoparaphyses. *Asci* 110–148 × 20–27 μm ($\overline{x}$ = 129 × 23 μm, n = 20), 8-spored, bitunicate, fissitunicate, cylindrical-clavate, rounded at apex, with a short pedicellate. *Ascospores* 48–51 × 7.5–9 μm ($\overline{x}$ = 50.5 × 8.5 μm, n = 30), overlapping, 2–3-seriate, clavate, with round ends, straight, uniseptate, deeply constricted at septum, hyaline, with broad and short upper cells 16.6–18.9 × 7.8–9.0 μm ($\overline{x}$ = 17.7 × 8.4 μm, n = 30), narrow and long lower cells 30–32.9 × 6.5–8.0 μm ($\overline{x}$ = 31.5 × 7.3 μm, n = 30), tapering towards the end, guttulate, smooth, 2–4 equatorial appendages at the septum and surrounded by a fusiform gelatinous, sheath. ***Asexual morph*****:** Undetermined.

Culture characteristics. Ascospores germinating on PDA within 24 hours. Colonies on MEA effuse, velvety, greyish-white to dark brown from above and below, reaching 2.5–3 cm diameter within 30 days at room temperature under natural light, composed of subhyaline to brown, septate, smooth hyphae.

Additional specimens examined. Thailand, That Phanom, Nakhon Phanom, on submerged decaying wood, 13 November 2018, D.F. Bao, B160 (paratype: MFLU 19–2844; living culture, MFLUCC 19–0498); Thailand, That Phanom, Nakhon Phanom, on submerged decaying wood, 13 November 2018, D.F. Bao, B136 (paratype: MFLU 19–2845; living culture, MFLUCC 19–0495)

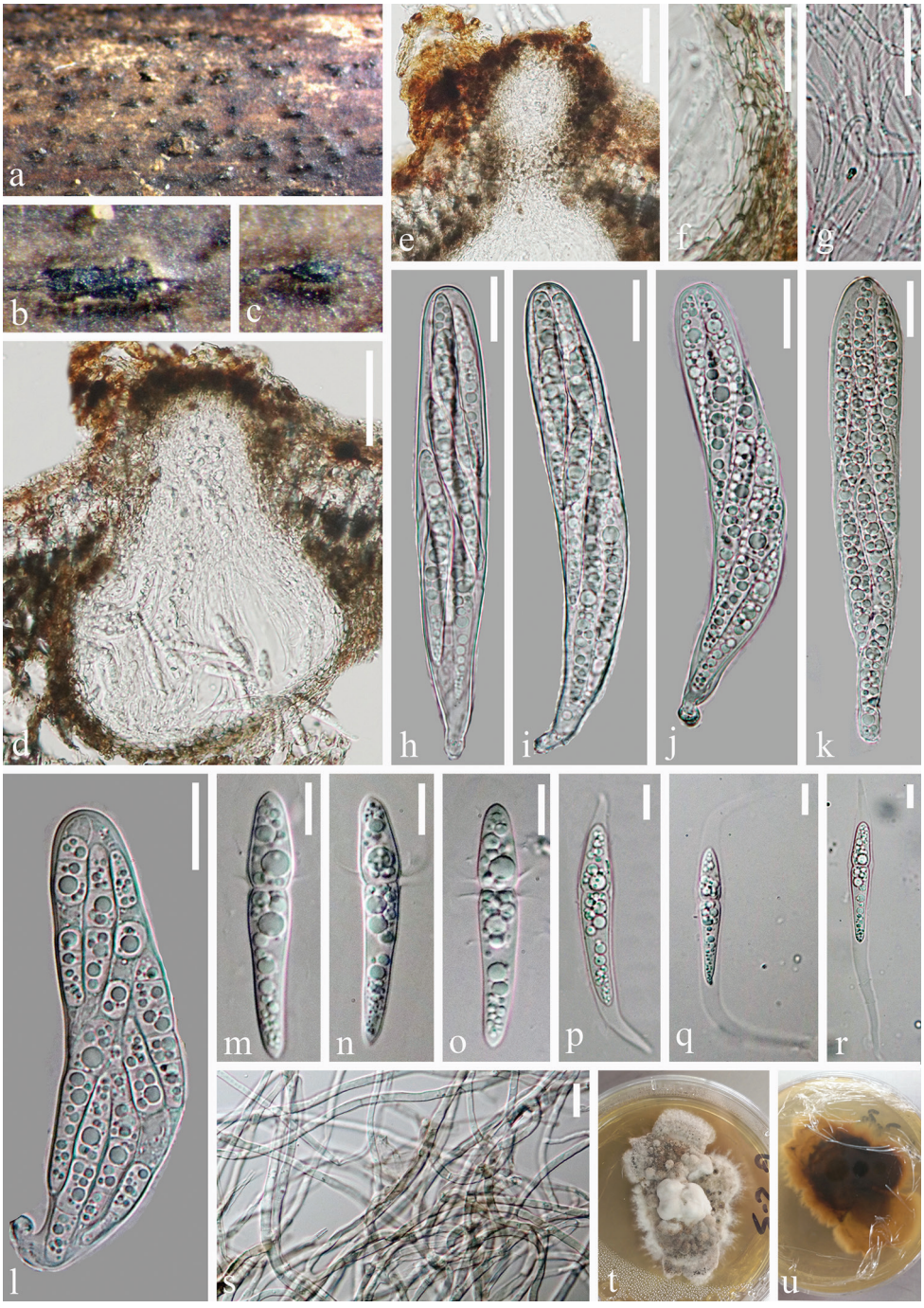

Figure 3. *Tingoldiago clavata* (MFLU 19–2843, holotype). **a–c** ascomata on wood **d** section of ascoma **e** ostiole **f** peridium **g** pseudoparaphyses **h–l** asci **m–r** ascospores **s** vegetative hyphae in culture **t, u** culture on PDA from surface and reverse. Scale bars: 50 µm (**d, e**), 20 µm (**f–l**), 10 µm (**m–s**).

Notes. *Tingoldiago clavata* resembles the type species, *T. graminicola* in having bitunicate, cylindrical-clavate asci with a short pedicellate and clavate, hyaline, 1-septate, ascospores with broad upper cells, narrow lower cells. However, we can distinguish them by the size of ascomata and asci and the colour, septate and appendages of ascospores. *Tingoldiago clavata* has smaller ascomata (110–148 ×145–195 vs. 150–250 × 250–450 μm) and larger asci (110–148 × 20–27 vs. 87.5–122 × 18.25–25 μm). Moreover, ascopsores of *T. clavata* are hyaline, uniseptate, with 2–4 equatorial appendages at the septum, while ascopspores of *T. graminicola* are brown and 3-septate at maturity and lacking appendages at the septum. In addition, a comparison of the 491 nucleotides across the ITS gene region of *T. clavata* and *T. graminicola* reveals 25 base-pair differences and therefore provides further evidence to introduce *T. clavata* as a new species as recommended by Jeewon and Hyde (2016).

Discussion

During the last decade, freshwater fungi in Thailand have been mainly reported from north, south and northeast of Thailand (Jones et al. 1999, Marvanová and Hywel-Jones 2000, Sivichai and Boonyuen 2010, Sivichai and Hywel-Jones 1999, Sivichai et al. 1998, 2000, Sri-indrasutdhi et al. 2010). No freshwater fungi from Eastern Thailand have been reported so far. In this study, two new freshwater species, viz. *Tingoldiago hydei* and *T. clavata* from Eastern Thailand, are introduced, based on morphology and phylogeny. *Tingoldiago hydei* and *T. clavata* satisfied the generic concept of the genus *Tingoldiago* (Hirayama et al. 2010). They comprise globose to conical, immersed to erumpent ascomata, cellular pseudoparaphyses, bitunicate, fissitunicate asci and clavate ascospores with a median primary septum and a large fusiform gelatinous sheath around the ascospore (Hirayama et al. 2010). Morphologically, *T. hydei* and *T. clavata* are quite similar as they have similar shape of asci and ascospores; however, we can distinguish them by the size of ascomata, asci and ascospores (Table 2). In addition, we also compared the morphological differences of these two species with the type species, *T. graminicola*. Ascopores of *T. hydei* and *T. clavata* are hyaline, uniseptate, with appendages at the septum and the upper cells are broader and shorter than the lower cells, while the ascopsores of *T. graminicola* are hyaline, uniseptate, but becoming brown and 3-septate with age, lacking appendages at the septum, upper cells and lower cells are similar lengths. Phylogenetic analyses showed that our two new isolates clustered together and are sister to the type species, *Tingoldiago graminicola* with strong bootstrap support (100 ML/92 MP/1.00 PP). This evidence strongly supports our two isolates to be the new species.

Hyde et al. (2020) introduced a new genus, *Pseudomurilentithecium* in Lentitheciaceae. In their phylogenetic analysis, *Pseudomurilentithecium* clustered with *Poaceascoma* and was basal to Lentitheciaceae. However, in our phylogenetic analysis, *Pseudomurilentithecium* grouped with the members of Massarinaceae, rather than Lentitheciaceae. Therefore, further investigation is required to confirm the placement of the genus.

Table 2. The morphological comparisons of *Tingoldiago* species discussed in this study.

Taxa	Distribution	Ascomata (µm)	Pseudoparaphyses (µm)	Asci (µm)	Ascospores (µm)	References
Tingoldiago graminicola	Japan, UK	150–250 × 250–450	1.5–4	87.5–122 × 18.25–25	43.5–53 × 7.5–11	Hirayama et al. 2010
T. hydei	Thailand	180–280 × 330–470	1.8–2.5	95–164 × 18–22	37.5–42 × 7.5–9	This study
T. clavata	Thailand	145–210 × 145–195	1.4–2.0	110–148 × 20–27	48–51 × 7.5–8.5	This study

Tingoldiago is a well-resolved genus in this family with a stable clade within Lentitheciaceae. The genus can be distinguished from other genera in this family by having hyaline, uniseptate, upper cells are broad and basal cells are narrow ascospores with a large fusiform gelatinous sheath. The sheath is considered to be an adaptation by the genus that enables ascospores to attach to the substrates in moving water (Shearer 1993, Hyde and Goh 2003, Jones 2006, Devadatha et al. 2019). It is reported that the genus *Tingoldiago* is exclusively found in freshwater habitats (Hirayama et al. 2010) and our two new species were collected from lotic habitats of Mekong River.

Acknowledgements

We would like to thank the National Natural Science Foundation of China (NSFC 31860006, 31660008) and the Fungal Diversity Conservation and Utilization Innovation team of Dali University (ZKLX2019213) for financial and laboratory support. Dan-Feng Bao thanks Shaun Pennycook from Landcare Research, Auckland, New Zealand, for advising on the taxon names. Wen-Li Li and Yan-Mei Zhang are acknowledged for their help on DNA extraction and PCR amplification.

References

Bao DF, Luo ZL, Jeewon R, Nalumpang S, Su HY, Hyde KD (2018) *Neoastrosphaeriella aquatica* sp. nov. (Aigialaceae), a new species from freshwater habitat in southern Thailand. Phytotaxa 391: 197–206. https://doi.org/10.11646/phytotaxa.391.3.3

Cai L, Tsui CKM, Zhang KQ, Hyde KD (2002) Aquatic fungi from Lake Fuxian, Yunnan, China. Fungal Diversity 9: 57–70.

Dayarathne MC, Hyde KD, Wanasinghe DN, Jones EBG, Chomnunti P (2018) A novel marine genus, *Halobyssothecium* (Lentitheciaceae) and epitypification of *Halobyssothecium obiones* comb. nov. Mycological Progress 17: 1161–1171. https://doi.org/10.1007/s11557-018-1432-3

Devadatha B, Sarma VV, Jeewon R, Hyde KD, Jones EBG (2019) *Morosphaeria muthupetensis* sp.nov. (Morosphaeriaceae) from India: Morphological characterisation and multigene phylogenetic inference. Botanica Marina 61: 395–405. https://doi.org/10.1515/bot-2017-0124

Ellis MB, Ellis JP (1985) Microfungi on Land Plants: An Identification Handbook (1st ed.). Macmillan Pub Co.

Glez-Peña D, Gómez-Blanco D, Reboiro-Jato M, Fdez-Riverola F, Posada D (2010) ALTER: program-oriented conversion of DNA and protein alignments. Nucleic Acids Research 38: 14–18. https://doi.org/10.1093/nar/gkq321

Hall TA (1999) BioEdit: a user-friendly biological sequence alignment editor and analysis program for Windows 95/98/NT. Nucleic Acids Symposium Series 41: 95–98. https://doi.org/10.1093/nar/gkq321

Hillis DM, Bull JJ (1993) An empirical test of bootstrapping as a method for assessing confidence in phylogenetic analysis. Systematic Biology 42: 182–192. https://doi.org/10.1093/sysbio/42.2.182

Hirayama K, Tanaka K, Raja HA, Miller AN, Shearer CA (2010) A molecular phylogenetic assessment of *Massarina ingoldiana sensu lato*. Mycologia 102: 729–746. https://doi.org/10.3852/09-230

Hu DM, Cai L, Chen H, Bahkali AH, Hyde KD (2010) Fungal diversity on submerged wood in a tropical stream and an artificial lake. Biodiversity and Conservation 19: 3799–3808. https://doi.org/10.1007/s10531-010-9927-5

Hyde KD (1995) Tropical Australia freshwater fungi VII. New genera and species of ascomycetes. Nova Hedwigia 61: 119–140.

Hyde KD, Chaiwan N, Norphanphoun C, Boonmee S, Camporesi E, Chethana KWT, Dayarathne MC, de Silva NI, Dissanayake AJ, Ekanayaka AH, Hongsanan S, Huang SK, Jayasiri SC, Jayawardena RS, Jiang HB, Karunarathna A, Lin CG, Liu JK, Liu NG, Lu YZ, Luo ZL, Maharachchikumbura SSN, Manawasinghe IS, Pem D, Perera RH, Phukhamsakda C, Samarakoon MC, Senwanna C, Shang QJ, Tennakoon DS, Thambugala KM, Tibpromma S, Wanasinghe DN, Xiao YP, Yang J, Zeng XY, Zhang JF, Zhang SN, Bulgakov TS, Bhat DJ, Cheewangkoon R, Goh TK, Jones EBG, Kang JC, Jeewon R, Liu ZY, Lumyong S, Kuo CH, Mckenzie EHC, Wen TC, Yan JY, Zhao Q (2018) Mycosphere notes 169–224. Mycosphere 9(2): 271–430. https://doi.org/10.5943/mycosphere/9/2/8

Hyde KD, Fryar S, Tian Q, Bahkali AH, Xu JC (2016) Lignicolous freshwater fungi along a north-south latitudinal gradient in the Asian/Australian region; can we predict the impact of global warming on biodiversity and function? Fungal Ecology 19: 190–200. https://doi.org/10.1016/j.funeco.2015.07.002

Hyde KD, Goh TK (2003) Adaptations for dispersal in filamentous freshwater fungi. Fungal Diversity 10: 231–258.

Hyde KD, Jones EBG, Liu JK, Ariyawansa H, Boehm E, Boonmee S, Braun U, Chomnunti P, Crous PW, Dai DQ, Diederich P, Dissanayake A, Doilom M, Doveri F, Hongsanan S, Jayawardena R, Lawrey JD, Li YM, Liu YX, Lücking R, Monkai J, Muggia L, Nelsen MP, Pang KL, Phookamsak R, Senanayake IC, Shearer CA, Suetrong S, Tanaka K, Thambugala KM, Wijayawardene NN, Wikee S, Wu HX, Zhang Y, Aguirre-Hudson B, Alias SA,

Aptroot A, Bahkali AH, Bezerra JL, Bhat DJ, Camporesi E, Chukeatirote E, Gueidan C, Hawksworth DL, Hirayama K, Hoog SD, Kang JC, Knudsen K, Li WJ, Li XH, Liu ZY, Mapook, A, McKenzie EHC, Miller AN, Mortimer PE, Phillips AJL, Raja HA, Scheuer C, Schumm F, Taylor JE, Tian Q, Tibpromma S, Wanasinghe DN, Wang Y, Xu JC, Yacharoen S, Yan JY, Zhang M (2013) Families of Dothideomycetes. Fungal Diversity 63: 1–313. https://doi.org/10.1007/s13225-013-0263-4

Hyde KD, Dong Y, Phookamsak R, Jeewon R, Bhat DJ, Jones EBG, Liu NG, Abeywickrama PD, Mapook A, Wei DP, Perera RH, Manawasinghe IS, Pem D, Bundhun D, Karunarathna A, Ekanayaka AH, Bao DF, Li JF, Samarakoon MC, Chaiwan N, Lin CG, Phutthacharoen K, Zhang SN, Senanayake IC, Goonasekara ID, Thambugala KM, Phukhamsakda C, Tennakoon DS, Jiang HB, Yang J, Zeng M, Huanraluek N, Liu JK, Wijesinghe SN, Tian Q, Tibpromma S, Brahmanage RS, Boonmee S, Huang SK, Thiyagaraja V, Lu YZ, Jayawardena LS, Dong W, Yang EF, Singh SK, Singh SM, Rana S, Lad SS, Anand G, Devadatha B, Niranjan M, Sarma VV, Liimatainen K, Aguirre-Hudson B, Niskanen T, Overall A, Alvarenga RLM, Gibertoni TB, Pliegler WP, Horváth E, Imre A, Alves AL, Santos ACDS, Tiago RV, Bulgakov TS, Wanasinghe DN, Bahkali AH, Doilom M, Elgorban AM, Maharachchikumbura SSN, Rajeshkumar KC, Haelewaters D, Mortimer PE, Zhao Q, Lumyong S, Xu JC, Sheng J (2020) Fungal diversity notes 1151–1276: taxonomic and phylogenetic contributions on genera and species of fungal taxa. Fungal Diversity In press.

Huang SK, Jeewon R, Hyde KD, Bhat JD, Wen TC (2018) Novel taxa within Nectriaceae: *Cosmosporella* gen. nov. and *Aquanectria* sp. nov. from freshwater habitats in China. Crytogamie Mycologie 39: 169–192. https://doi.org/10.7872/crym/v39.iss2.2018.169

Jayasiri SC, Hyde KD, Ariyawansa HA, Bhat DJ, Buyck B, Cai L, Dai YC, Abd-Elsalam KA, Ertz D, Hidayat I, Jeewon R, Jones EBG, Bahkali AH, Karunarathna SC, Liu JK, Luangsaard JJ, Lumbsch HT, Maharachchikumbura SSN, McKenzie EHC, Moncalvo JM, Ghobad-Nejhad M, Nilsson H, Pang KA, Pereira OL, Phillips AJL, Raspé O, Rollins AW, Romero AI, Etayo J, Selçuk F, Stephenson SL, Suetrong S, Taylor JE, Tsui CKM, Vizzini A, Abdel-Wahab MA, Wen TC, Boonmee S, Dai DQ, Daranagama DA, Dissanayake AJ, Ekanayaka AH, Fryar SC, Hongsanan S, Jayawardena RS, Li WJ, Perera RH, Phookamsak R, de Silva NI, Thambugala KM, Tian Q, Wijayawardene NN, Zhao RL, Zhao Q., Kang JC, Promputtha I (2015) The faces of fungi database: fungal names linked with morphology, phylogeny and human impacts. Fungal Diversity 74: 3–18. https://doi.org/10.1007/s13225-015-0351-8

Jeewon R, Hyde KD (2016) Establishing species boundaries and new taxa among fungi: recommendations to resolve taxonomic ambiguities. Mycosphere 7: 1669–1677. https://doi.org/10.5943/mycosphere/7/11/4

Jones EBG (2006) Form and function of fungal spore appendages. Mycoscience 47: 167–183. https://doi.org/10.1007/S10267-006-0295-7

Jones EBG, Hyde KD, Pang KL (2014) Freshwater Fungi and Fungal-like Organisms. De Gruyter, Germany. https://doi.org/10.1515/9783110333480

Jones EBG, Wong SW, Sivichai S, Au DWT, Hywel-Jones NL (1999) Lignicolous freshwater ascomycota from Thailand: *Micropeltopsis quinquecladiopsis* sp. nov. Mycological Research 103: 729–735. https://doi.org/10.1017/S0953756298007618

Kagami M, Amano Y, Ishii N (2012) Community structure of planktonic fungi and the impact of parasitic chytrids on phytoplankton in Lake Inba, Japan. Microbial Ecology 63: 358–368. https://doi.org/10.1007/s00248-011-9913-9

Katoh K, Standley DM (2013) MAFFT multiple sequence alignment software version 7: improvements in performance and usability. Molecular Biology and Evolution 30: 772–780. https://doi.org/10.1093/molbev/mst010

Knapp DG, Kovács GM, Zajta E, Groenewald JZ, Crous PW (2015) Dark septate endophytic pleosporalean genera from semiarid areas. Persoonia 35: 87–100. https://doi.org/10.3767/003158515X687669

Liu YJ, Whelen S, Hall BD (1999) Phylogenetic relationships among ascomycetes: evidence from an RNA polymerase II subunit. Molecular Biology and Evolution 16: 1799–1808. https://doi.org/10.1093/oxfordjournals.molbev.a026092

Luo J, Yin JF, Cai L, Zhang KQ, Hyde K D (2004) Freshwater fungi in Lake Dianchi, a heavily polluted lake in Yunnan, China. Fungal Diversity 16: 93–112.

Luo ZL, Maharachchikumnura SSN, Liu XY, Li SH, Chen LJ, Su HY, Zhou DQ, Hyde KD (2015) *Annulatascus saprophyticus* sp. nov. and *Pseudoannulatascus* gen. nov. to accommodate *Annulatascus biatriisporus* (Annulatascales Sordariomycetes) from Thailand. Phytotaxa 239(2): 174–182. https://doi.org/10.11646/phytotaxa.239.2.6

Luo ZL, Bahkali AH, Liu XY, Phookamsak R, Zhao YC, Zhou DQ, Su HY, Hyde KD (2016) *Poaceascoma aquaticum* sp. nov. (Lentitheciaceae), a new species from submerged bamboo in freshwater. Phytotaxa 253(1): 71–80. https://doi.org/10.11646/phytotaxa.253.1.5

Luo ZL, Hyde KD, Liu JK, Bhat DJ, Bao DF, Li WL, Su HY (2018) Lignicolous freshwater fungi from China II: Novel *Distoseptispora* (Distoseptisporaceae) species from northwestern Yunnan Province and a suggested unified method for studying lignicolous freshwater fungi. Mycosphere 9: 444–461. https://doi.org/10.5943/mycosphere/9/3/2

Marvanová L, Hywel-Jones NL (2000) *Sigmoidea conforta* sp. nov. and two rare hyphomycete species from streams in Thailand. Cryptogamie Mycologie 21: 13–26. https://doi.org/10.1016/S0181-1584(00)00101-9

Miller MA, Pfeiffer W, Schwartz T (2010) Creating the CIPRES Science Gateway for inference of large phylogenetic trees. Proceedings of the 2010 Gateway Computing Environments Workshop (GCE): 1–8. https://doi.org/10.1109/GCE.2010.5676129

Nylander JAA, Wilgenbusch JC, Warren DL, Swofford DL (2008) AWTY (are we there yet?): a system for graphical exploration of MCMC convergence in Bayesian phylogenetics. Bioinformatics 24: 581–583. https://doi.org/10.1093/bioinformatics/btm388

Pinnoi A, Lumyong S, Hyde KD, Jones EBG (2006) Biodiversity of fungi on the palm *Eleiodoxa conferta* in Sirindhorn peat swamp forest, Narathiwat, Thailand. Fungal Diversity 22: 205–218.

Pinruan U, Lumyong S, Hyde KD, Jones EBG (2007) Occurrence of fungi on tissues of the peat swamp palm *Licuala longecalycata*. Fungal Diversity 25: 157–173.

Pinruan U, Lumyong S, Hyde KD, Jones EBG (2014) Tropical peat swamp fungi with special reference to palms. In: Jones EBG, Hyde KD, Pang KL (Eds) Freshwater Fungi. De Gruyter, Germany, 371–388. https://doi.org/10.1515/9783110333480.371

Rambaut A (2014) FigTree v1.4: tree figure drawing tool. http://tree.bio.ed.ac.uk/software/figtree/

Rannala B, Yang Z (1996) Probability distribution of molecular evolutionary trees: a new method of phylogenetic inference. Journal of Molecular Evolution 43(3): 304–311. https://doi.org/10.1007/BF02338839

Ronquist F, Teslenko M, van der Mark P, Ayres DL, Darling A, Höhna S, Larget B, Liu L, Suchard MA, Huelsenbeck JP (2012) MrBayes 3.2: efficient Bayesian phylogenetic inference andmodel choice across a large model space. Systematic Biology 61(3): 539–542. https://doi.org/10.1093/sysbio/sys029

Sheaer CA (1993) The freshwater ascomycetes. Nova Hedwigia 56: 1–33.

Shearer CA, Descals E, Kohlmeyer B, Kohlmeyer J, Marvanová L, Padgett D, Porter D, Raja HA, Schmit JP, Thorton HA, Voglmayr H (2007) Fungi biodiversity in aquatic habitats. Biodiversity and Conservation 16: 49–67. https://doi.org/10.1007/s10531-006-9120-z

Sivichai S, Boonyuen N (2010) *Jahnula morakotii* sp. nov. and *J. appendiculata* from a peat swamp in Thailand. Mycotaxon 112: 475–481. https://doi.org/10.5248/112.475

Sivichai S, Hywel-Jones N (1999) *Biflagellospora* (aero-aquatic hyphomycetes) from submerged wood in Thailand. Mycological Research 103: 908–914. https://doi.org/10.1017/S0953756298007928

Sivichai S, Hywel-jones NL, Jones EBG (1998) Lignicolous freshwater Ascomycota from Thailand: 1. *Ascotaiwania sawada* and its anamorph state Monotosporella. Mycoscience 39: 307–311. https://doi.org/10.1007/BF02464013

Sivichai S, Hywel-jones NL, Somrithipol S (2000) Lignicolous freshwater Ascomycota from Thailand: *Melanochaeta* and *Sporoschisma anamorphs*. Mycological Research 104: 478–485. https://doi.org/10.1017/S0953756299001604

Sivichai S, Jones EBG, Hywel-Jones NL (2000) Fungal colonisation of wood in a freshwater stream at Khao Yai National Park, Thailand. Fungal Diversity 5: 71–88.

Sivichai S, Jones EBG, Hywel-Jones NL (2002) Fungal colonisation of wood in a freshwater stream at Tad Ta Phu, Khao Yai National Park, Thailand. Fungal Diversity 10: 113–129.

Sparrow FK (1960) Aquatic Phycomycetes (Second Rev). The University of Michigan Press, Ann Arbor. https://doi.org/10.5962/bhl.title.5685

Sri-indrasutdhi V, Boonyuen N, Suetrong S, Chuaseeharonnachai C, Sivichai S, Jones EBG (2010) Wood-inhabiting freshwater fungi from Thailand: *Ascothailandia grenadoidia* gen. et sp. nov., *Canalisporium grenadoidia* sp. nov. with a key to *Canalisporium* species (Sordariomycetes, Ascomycota). Mycoscience 51: 411–420. https://doi.org/10.1007/S10267-010-0055-6

Stamatakis A (2006) RAxML-VI-HPC: maximum likelihood-based phylogenetic analyses with thousands of taxa and mixed models. Bioinformatics 22(21): 2688–2690. https://doi.org/10.1093/bioinformatics/btl446

Stamatakis A, Hoover P, Rougemont J (2008) A rapid bootstrap algorithm for the RAxML web servers. Systematic Biology 57: 758–771. https://doi.org/10.1080/10635150802429642

Swe A, Jeewon R, Pointing SB, Hyde KD (2009) Diversity and abundance of nematode-trapping fungi from decaying litter in terrestrial, freshwater and mangrove habitats. Biodiversity and Conservation 18: 1695–1714. https://doi.org/10.1007/s10531-008-9553-7

Thomas K (1996) Australian freshwater fungi. In: Grgurinovic CA (Ed.) Introductory Volume to the Fungi (Part2). Fungi of Australian. Canberra, Australia: Australian Biological Resources Study 1–37.

Tibpromma S, Hyde KD, Jeewon R, Maharachchikumbura SSN, Liu JK, Bhat DJ, Jones EBG, McKenzie EHC, Camporesi E, Bulgakov TS, Doilom M, de Azevedo Santiago ALCM, Das K, Manimohan P, Gibertoni TB, Lim YW, Ekanayaka AH, Thongbai B, Lee HB, Yang JB, Kirk PM, Sysouphanthong P, Singh SK, Boonmee S, Dong W, Raj KNA, Latha KPD, Phookamsak R, Phukhamsakda C, Konta S, Jayasiri SC, Norphanphoun C, Tennakoon DS, Li JF, Dayarathne MC, Perera RH, Xiao Y, Wanasinghe DN, Senanayake IC, Goonasekara ID, de Silva NI, Mapook A, Jayawardena RS, Dissanayake AJ, Manawasinghe IS, Chethana KWT, Luo ZL, Hapuarachchi KK, Baghela A, Soares AM, Vizzini A, Meiras-Ottoni A, Mešić A, Dutta AK, de Souza CAF, Richter C, Lin CG, Chakrabarty D, Daranagama DA, Lima DX, Chakraborty D, Ercole E, Wu F, Simonini G, Vasquez G, da Silva GA, Plautz HL, Ariyawansa HA, Lee H, Kušan I, Song J, Sun JZ, Karmakar J, Hu K, Semwal KC, Thambugala KM, Voigt K, Acharya K, Rajeshkumar KC, Ryvarden L, Jadan M, Hosen MI, Mikšík M, Samarakoon MC, Wijayawardene NN, Kim NK, Matočec N, Singh PN, Tian Q, Bhatt RP, de Oliveira RJV, Tulloss RE, Aamir S, Kaewchai S, Marathe SD, Khan S, Hongsanan S, Adhikari S, Mehmood T, Bandyopadhyay TK, Svetasheva TY, Nguyen TTT, Antonín V, Li WJ, Wang Y, Indoliya Y, Tkalčec Z, Elgorban AM, Bahkali AH, Tang AMC, Su HY, Zhang H, Promputtha I, Luangsaard J, Xu JC, Yan JY, Kang JC, Stadler M, Mortimer PE, Chomnunti P, Zhao Q, Phillips AJL, Nontachaiyapoom S, Wen T-C, Karunarathna SC (2017) Fungal diversity notes 491–602: taxonomic and phylogenetic contributions to fungal taxa. Fungal Diversity 83(1): 1–261. https://doi.org/10.1007/s13225-017-0378-0

Tsui CKM, Hyde KD, Hodgkiss IJ (2000) Biodiversity of fungi on submerged wood in Hong Kong streams. Aquatic Microbial Ecology 21: 289–298. https://doi.org/10.3354/ame021289

Tubaki K, Watanabe K, Manoch L (1983) Aquatic hyphomycetes from Thailand. Transactions of the Mycological Society of Japan 24: 451–457. https://doi.org/10.3354/ame021289

Vilgalys R, Hester M (1990) Rapid genetic identification and mapping of enzymatically amplified ribosomal DNA from several Cryptococcus species. Journal of Bacteriology 172: 4238–4246. https://doi.org/10.1128/JB.172.8.4238-4246.1990

Vijaykrishna D, Jeewon R, Hyde KD (2005) *Fusoidispora aquatica*: New freshwater ascomycetes from Hong Kong based on morphology and molecules. Sydowia 57: 267–280.

Vijaykrishna D, Jeewon R, Hyde KD (2006). Molecular taxonomy, origins and evolution of freshwater ascomycetes. Fungal Diversity 23: 367–406.

Wanasinghe DN, Jones EBG, Camporesi E, Boonmee S, Ariyawansa HA, Wijayawardene NN, Hyde KD (2014) An Exciting Novel Member of Lentitheciaceae in Italy from Clematis Vitalba. Cryptogamie Mycologie 35(4): 323–337. https://doi.org/10.7872/crym.v35.iss4.2014.323

Wanasinghe DN, Phukhamsakda C, Hyde KD, Jeewon R, Lee HB, Jones EG, Tibpromma S, Tennakoon DS, Dissanayake AJ, Jayasiri SC, GafforovErio Y, Camporesi E, Bulgakov TS, Ekanayake AH, Perera RH, Samarakoon SC, Goonasekara ID, Mapook A, Li WJ, Senanayake IC, Li JF, Norphanphoun C, Doilom M, Bahkali AH, Xu JC, Mortimer PE, Tibell L, Tibell S, Karunarathna SC (2018) Fungal diversity notes 709–839: taxonomic and phylogenetic contributions to fungal taxa with an emphasis on fungi on Rosaceae. Fungal Diversity 89(1): 1–236. https://doi.org/10.1007/s13225-018-0395-7

White TJ, Bruns T, Lee S, Taylor J (1990) Amplification and direct sequencing of fungal ribosomal RNA genes for phylogenetics. In: Innis GM, Shinsky D, White T (Eds) PCR protocols: a guide to methods and applications. Academic, New York, 315–322. https://doi.org/10.1016/B978-0-12-372180-8.50042-1

Wijayawardene NN, Hyde KD, Bhat DJ, Goonasekara ID, Nadeeshan D, Camporesi E, Schumacher RK, Yong W (2015) Additions to Brown Spored Coelomycetous Taxa in Massarinae, Pleosporales: Introducing *Phragmocamarosporium* gen. nov. and *Suttonomyces* gen. nov. Cryptogamie Mycologie 36: 213–224. https://doi.org/10.7872/crym/v36.iss2.2015.213

Wijayawardene NN, Hyde KD, Rajeshkumar KC, Hawksworth DL, Madrid H, Kirk PM, Braun U, Singh RV, Crous PW, Kukwa M, Lűcking R, Kurtzman CP, Yurkov A, Haelewaters D, Aptroot A, Lumbsch HT, Timdal E, Ertz D, Etayo J, Phillips AJL, Groenewald JZ, Papizadeh M, Selbmann L, Dayarathne MC, Weerakoon G, Jones EBG, Suetrong S, Tian Q, Castanéda-Ruiz RF, Bahkali AH, Pang KL, Tanaka K, Dai DQ, Sakayaroj J, Hujslová M, Lombard L, Shenoy BD, Suija A, Maharachchikumbura SSN, Thambugala KM, Wanasinghe DN, Sharma BO, Gaikwad S, Pandit G, Zucconi L, Onofri S, Egidi E, Raja HA, Kodsueb R, Cáceres MES, Pérez-Ortega S, Fiuza PO, Monteiro JS, Vasilyeva LN, Shivas RG, Prieto M, Wedin M, Olariaga I, Lateef AA, Agrawal Y, Fazeli SAS, Amoozegar MA, Zhao GZ, Pfliegler WP, Sharma G, Oset M, Abdel MA, Takamatsu S, Bensch K, Silva NI, De Kesel A, Karunarathna A, Boonmee S, Pfister DH, Lu YZ, Luo ZL, Boonyuen N, Daranagama DA, Senanayake IC, Jayasiri SC, Samarakoon MC, Zeng XY, Doilom M, Quijada L, Rampadarath S, Heredia G, Dissanayake AJ, Jayawardana RS, Perera PH, Tang LZ, Phukhamsakda C, Hernández-Restrepo M, Ma XY, Tibpromma S, Gusmao LFP, Weerahewa D, Karunarathna SC (2017) Notes for genera: Ascomycota. Fungal Diversity 86: 1–594. https://doi.org/10.1007/s13225-017-0386-0

Wijayawardene NN, Pawłowska J, Letcher PM, Kirk PM, Humber RA, Schüßler A, Wrzosek M, Muszewska A, Okrasińska A, Istel Ł, Gęsiorska A, Mungai P, Lateef AA, Rajeshkumar KC, Singh RV, Radek R, Walther G, Wagner L, Walker C, Wijesundara DSA, Papizadeh M, Dolatabadi S, Shenoy BD, Tokarev YS, Lumyong S, Hyde KD (2018) Notes for genera: basal clades of Fungi (including Aphelidiomycota, Basidiobolomycota, Blastocladiomycota, Calcarisporiellomycota, Caulochytriomycota, Chytridiomycota, Entomophthoromycota, Glomeromycota, Kickxellomycota, Monoblepharomycota, Mortierellomycota, Mucoromycota, Neocallimastigomycota, Olpidiomycota, Rozellomycota and Zoopagomycota). Fungal Diversity 92: 43–129. https://doi.org/10.1007/s13225-018-0409-5

Wong MKM, Goh TK, Hodgkiss IJ, Hyde KD, Ranghoo VM, Tsui CKM, Ho WH, Wong WSW, Yuen TK (1998) Role of fungi in freshwater ecosystems. Biodiversity and Conservation 7: 1187–1206. https://doi.org/10.1023/A:1008883716975

Yang J, Liu JK, Hyde KD, Jones EBG, Liu Z (2017) Two new species in Fuscosporellaceae from freshwater habitat in Thailand. Mycosphere 8: 1893–1903. https://doi.org/10.5943/mycosphere/8/10/12

Zhang H, Jones EBG, Zhou DQ, Bahkali AH, Hyde KD (2011) Checklist of freshwater fungi in Thailand. Cryptogamie, Mycologie 32: 199–217. https://doi.org/10.7872/crym.v32.iss2.2011.199

Zhang H, Hyde KD, Abdel-Wahab MA, Abdel-Aziz F A, Ariyawansa HA, KoKo TW, Zhao RL, Alias SA, Bahkali AH, Zhou DQ (2013) A modern concept for *Helicascus* with a *Pleurophomopsis*-like asexual state. Sydowia 65: 147–166.

Zhang Y, Jeewon R, Fournier J, Hyde KD (2008) Multi-gene phylogeny and morphotaxonomy of *Amniculicola lignicola*: novel freshwater fungus from France and its relationships to the Pleosporales. Fungal Biology 112: 1186–1194. https://doi.org/10.1016/j.mycres.2008.04.004

Zhang Y, Crous PW, Schoch CL, Hyde KD (2012) Pleosporales. Fungal Diversity 53: 1–221. https://doi.org/10.1007/s13225-011-0117-x

Zhaxybayeva O, Gogarten JP (2002) Bootstrap, Bayesian probability and maximum likelihood mapping: exploring new tools for comparative genome analyses. BMC Genomics 3: 4. https://doi.org/10.1186/1471-2164-3-4